PHYTOCHEMISTRY AND ANTIMYCOBACTERIAL ACTIVITIES OF THE LEAF EXTRACTS OF *Pavetta crassipes* K. SCHUM

BY

NNEKA NWAMAKA IBEKWE

Matric no: 136990

B.Sc (Hons), Industrial Chemistry (University of Nigeria, Nsukka)

M.Sc, Pharmaceutical Chemistry (University of Nigeria, Nsukka)

A Thesis in the Department of Chemistry

Submitted to the Faculty of Science

In partial fulfillment of the requirements for the Degree of

DOCTOR OF PHILOSOPHY

of the

UNIVERSITY OF IBADAN

October 2012

TITLE PAGE

PHYTOCHEMISTRY AND ANTIMYCOBACTERIAL ACTIVITIES OF THE LEAF EXTRACTS OF *Pavetta crassipes* K. SCHUM

BY

NNEKA NWAMAKA IBEKWE

Matric no: 136990

B.Sc (Hons), Industrial Chemistry (University of Nigeria, Nsukka)

M.Sc, Pharmaceutical Chemistry (University of Nigeria, Nsukka)

A Thesis in the Department of Chemistry

Submitted to the Faculty of Science

In partial fulfillment of the requirements for the Degree of

DOCTOR OF PHILOSOPHY

of the

UNIVERSITY OF IBADAN

October, 2012

ABSTRACT

Tuberculosis (TB), an infectious disease mainly caused by *Mycobacterium tuberculosis* is the second greatest contributor among infectious diseases to adult mortality, causing approximately two million deaths annually worldwide. Effective treatment of TB has been hampered by the emergence of drug resistant strains of *M. tuberculosis*. There is therefore an increasing need for the development of new antituberculosis drugs to combat this disease. *Pavetta crassipes* (Rubiaceae) is a plant which has been claimed as a traditional cure for TB and other respiratory diseases in Northern Nigeria. The aims of this study were to isolate, identify the constituents responsible for the reported biological activities of *P. crassipes* leaves against *M. tuberculosis* and subsequently evaluate the activity of the pure isolated compounds against this organism.

Pavetta crassipes leaf was collected at Suleja and its identity was confirmed in the herbarium of the National Institute for Pharmaceutical Research and Development, Abuja. Cold maceration was employed in the successive extraction of air-dried leaves of *P. crassipes* using hexane, ethyl acetate and methanol. Separation and isolation of the plant constituents were achieved by column chromatography, preparative high performance liquid chromatography and preparative thin layer chromatography. Structures of the isolated compounds were established by spectroscopic methods (infra-red spectroscopy, ultraviolet spectroscopy, mass spectrometry, 1D and 2D- nuclear magnetic resonance spectroscopy) and chemical methods. The antimycobacterial activity of *P. crassipes* extracts, fractions and constituents was determined against *M. tuberculosis* $H_{37}Rv$ using the broth microdilution method, with isoniazid as the reference compound. Isolated compounds were also tested for antimycobacterial activity using the green fluorescence reporter assay method.

Ursolic acid, β-sitosterol, 3-caffeoyl 1-ethyl quinate, 3-caffeoyl 1-methyl quinate, quercetin 3-O-β-rutinoside, D-mannitol and a novel monoterpene iridoid glucoside, pavetoside were isolated and structurally elucidated. The ethyl acetate and methanol extracts exhibited antimycobacterial activities with Minimum Inhibitory Concentration (MIC) of 250 and 521 µg/mL, respectively against *M. tuberculosis*. Ursolic acid, 3-caffeoyl 1-methyl quinate, and 3-caffeoyl 1-ethyl quinate were found active against *M. tuberculosis* with MIC of 200, 100, and 50 µg/mL, respectively. β-

sitosterol, quercetin 3-O-β-rutinoside, D-mannitol and pavetoside did not exhibit any significant activity against *M. tuberculosis*.

The antimycobacterial activity of *Pavetta crassipes* was attributed to ursolic acid, 3-caffeoyl 1-ethyl quinate, and 3-caffeoyl 1-methyl quinate. The presence of antimycobacterial terpenoid and quinate esters in leaves of *Pavetta crassipes* provides scientific evidence for the ethnomedicinal use of this plant as a traditional antituberculosis remedy.

Keywords: *Pavetta crassipes*, *Mycobacterium tuberculosis*, Quinate esters, Ursolic acid, Pavetoside

Word count: 389

ACKNOWLEDGEMENTS

It has been quite a journey, a thesis such as this has been one with a lot of test of emotions and character; happiness, anger, frustrations, patience, perseverance, hardwork, discipline, will power, friendship, love, mentorship and support. Like the sayings go, "Nothing good comes easy" and "If it were easy, anyone would do it."

I would start by appreciating my supervisors, Professor A.A. Adesomoju, Professor J.I. Okogun and Dr C.E. Barry III. I consider it a great privilege to be trained and mentored by these great scientists. The passion for meticulous and quality science, the open door policies and leadership qualities have taught me a lot about mentorship and good leadership. I am immensely grateful for the roles you have played in modeling me to a good scientist.

I sincerely thank the Division of Acquired Immunodeficiency Syndrome (DAIDS), National Institute of Allergy and Infectious Diseases (NIAID), National Institute of Health, Maryland for the PhD fellowship. Funding for this program was provided (in part) by the Division of Intramural Research of the NIAID, National Institutes of Health (NIH). This afforded me a great opportunity to do some good science and provided me with all the materials and the environment to achieve that. I also thank the Oak Ridge Institute for Science and Education, Tennessee, USA, for administering the program. I specially acknowledge William Rosa, Barbara Dorsey, Lise Neiler and Norma Faulkner, whom I had direct contacts with in the course of the sponsorship and who saw to my welfare especially on my visits to the United States of America.

I also acknowledge and thank the management and staff of the National Institute for Pharmaceutical Research and Development (NIPRD), under the leadership of Professor K.S. Gamaniel, for the support given to me in the course of this program. My thanks also go to Dr. U.S. Inyang, the immediate past Director-General, for his encouragements during and after his tenure.

I thank the staff and fellow colleagues of the Department of Chemistry, University of Ibadan, under the headship of Prof R.A. Oderinde, for their encouragements and contributions. I specially thank Dr. Olapeju O. Aiyeelagbe, Dr. Patricia A. Onocha and Dr. I. A. Oladosu, who always offered genuine advice on how to go about my project.

This thesis was borne out of a collaborative project, the NIH/NIPRD/UI project on TB drug discovery. I must acknowledge the contributions of my other team members; Prof Kolo Ibrahim, Dr. Abayomi Orishadipe, Dr. Helena Boshoff, Peters Oladosu, Dogonyaro Bege, John Nvau, Auwal Usman, Matthew Tsado and Uduak Nssien. I also acknowledge and thank Katherine Perry, the project manager, for steering the wheel of this project.

A good measure of this work was carried out at National Institute of Allergy and Infectious diseases (NIAID), NIH. I sincerely thank Michael Goodwin for training me on the HPLC and also for his help with acquiring some spectral data. Many thanks to Noel Whitaker of National Institute of Diabetes Diseases and Kidney (NIDDK), NIH, for acquiring the mass spectral data. Additionally, I thank Katie and Ben, for running the bioassays on the samples. I also thank Dr. G. Ellestad (Columbia University, USA) and Joaquin Randle (Acorn, USA) for acquiring the NMR data of my compounds, and also for their patience with me on my numerous questions and e-mails. I acknowledge my other friends in the laboratory especially Eu gene and Jacquie.

It is very important that I express my gratitude to four traditional medicine practitioners (TMPs), Isa Mai Maigani and Rabiu Sule from Zaria in Kaduna state and Azijah Oyhu and Haruna Mary from Jos in Plateau state. These TMPs provided the title plant during an ethnobotanical survey of Nigerian medicinal plants used in the treatment of tuberculosis, as one of the components of their herbal recipes as used by the indeginous people. My thanks also go out to two of my colleagues at NIPRD, Muazzam Ibrahim, an ethnobotanist, who collected the plant, and to Jemilat Ibrahim, a taxonomist, who identified the plant.

I must also acknowledge my professional colleagues of the Department of Medicinal Chemistry and Quality Control, NIPRD. I thank Dr. Oby Obodozie, for always urging me on and for her belief in my abilities. I also thank the Head of the Department, Dr. S. J. Ameh and other colleagues; Dr. Bola Mustapha, Rukaiyatu, Florence, Theresa, Martha, Cordelia, Ache and Cecilia.

This program would not have been possible without the solid foundation my parents laid for me. I specially and sincerely thank my parents, Mr. and Mrs. I.A. Ibekwe, for the education they gave me. Thanks also to my siblings; my sister, Ada and my four brothers, Emeka, Okey, Osinachi and Anieto. You have always showed me your love and support. I also specially acknowledge my aunty, Chibuogu Agu, who helped with the care of my daughter while I was running this program.

To my friends and colleagues who have believed in my abilities, and continually encouraged me, I thank you all; Mercy Ezeunala, Omoregie Egharevba, Dr. Philip Builders, Gloria Ajoku, Dr. Martins Emeje, Ogadi Emenyeonu, Iheanyi Mboma, Roseline Oroh and Esther Owolabi. I specially thank my friend and sister, Ifesi Emeka-Osisioma, who at different occasions during this program, showed me the true meaning of friendship. I also acknowledge a good friend of mine, TJ. Those constant words of yours "Keep at it, you'll get by" were always in my head. Thanks for your encouragement.

Very importantly, I must thank my beautiful daughter, Ifunanya, who even though tender, quite understood that her mother was in some academic pursuit. You would help me fill out my details on my notebooks and you were first to refer to me as a doctor, without any prior discussion on that. It was a hard task combining raising you and running this program, but it's been worth it. I love you so dearly!

My ultimate thanks remains to my heavenly Father who makes all things possible, and from whom all good things come!!!

CERTIFICATION PAGE

I certify that this work was carried out by Miss Nneka Nwamaka Ibekwe in the Department of Chemistry, University of Ibadan, Nigeria.

Supervisor

……

A.A. Adesomoju

B.Sc, Ph.D (Ibadan)

Professor of Chemistry

University of Ibadan

Nigeria

Supervisor

……

J.I. Okogun

B.Sc Special (London), Ph.D (London), DIC (London), FAS

Professor of Chemistry

Special Consultant, NIPRD

Abuja, Nigeria

Supervisor

……

C. E. Barry III

B.Sc, Ph.D (Cornell University, USA)

Chief, Tuberculosis Research Section

NIAID, NIH

Bethesda, Maryland, USA

DEDICATION

To my daughter

Ifunanyachukwu

My priceless jewel

Table of Contents

LIST OF FIGURES

LIST OF TABLES

LIST OF ABBREVIATIONS

^{13}C {^{1}H}-spectrum	^{13}C {^{1}H} broadband decoupled NMR
APCI	atmospheric pressure chemical ionisation
API	atmospheric pressure ionisation
BCG	bacille Calmette-Guérin
CapNMR	capillary NMR
CD_3OD	deuterated methanol
$CDCl_3$	deuterated chloroform
CID	collision-induced dissociation
COSY	correlated spectroscopy
DAD	photo diode array detection
DBE	double bond equivalence
DEPT	distortionless enhancement by polarization transfer
DMSO-d_6	deuterated dimethyl sulphoxide
ESI	electrospray ionisation
$H_{37}Ra$	*Mycobacterium tuberculosis* $H_{37}Ra$ strain
$H_{37}Rv$	*Mycobacterium tuberculosis* $H_{37}Rv$ strain
HMBC	heteronuclear multiple bond correlation
HPLC	high-performance liquid chromatography
HRESIMS	high resolution electrospray ionization mass spectrometry
HRMS	high resolution mass spectrometry
HSQC	heteronuclear single quantum correlation
IR	infrared
J (Hz)	coupling constant (hertz)
LC	liquid chromatography
LORA	low oxygen recovery assay
MIC	minimum inhibitory concentration
mp	melting point
MS	mass spectrometry

MS-MS	tandem mass spectrometry
MS^n	multiple-stage mass spectrometry
MTB	*Mycobacterium tuberculosis*
MABA	microplate alamar blue assay
NI	negative ion
NIAID	National Institute of Allergy and Infectious Diseases
NIDDK	National Institute of Diabetes and Digestive and Kidney diseases
NIH	National Institutes of Health
NIPRD	National Institute for Pharmaceutical Research and Development
NMR	nuclear magnetic resonance spectroscopy
PCE	*Pavetta crassipes* ethyl acetate extract
PCH	*Pavetta crassipes* hexane extract
PCM	*Pavetta crassipes* methanol extract
PI	positive ion
*R*f	retardation factor
SPE	solid-phase extraction
TB	tuberculosis
TOF	time of flight
UV	ultraviolet
WHO	World Health Organisation

CHAPTER ONE

INTRODUCTION

1.1 Tuberculosis: An Overview

Tuberculosis (TB) is a contagious, infectious disease mainly caused by *Mycobacterium tuberculosis* in humans. It is an aerobic pathogenic bacterium that establishes its infection usually in the lungs, a condition known as pulmonary tuberculosis (PTB). Progression of TB infection is fundamentally regulated by host's immune system integrity which may succeed through microbial immediate elimination and/or latency conditioning, or fail resulting in development of active disease. Tuberculosis may also occur in the bones, meninges, joints, genito-urinary tract, liver, kidneys, intestines and heart. These other forms of the disease are referred to as extra-pulmonary tuberculosis (Ducati *et al*., 2006).

Tuberculosis is spread by aerosol transmission from the lungs of one sick patient to other persons and the most important source is by coughing. Coughing produces tiny infectious droplet nuclei which are particles of respiratory secretions usually less than 5µm in diameter and containing tubercule bacilli. Other sources of infection are sneezing, talking, spitting or singing. Direct sunlight kills tubercle bacilli in 5 minutes, but they can survive in the dark for long periods. Thus, transmission generally occurs indoors (WHO, 2004).

Tuberculosis is the second greatest contributor among infectious diseases to adult mortality causing approximately two million deaths per year globally. It is estimated that one-third of the world's population is infected with the tubercule bacillus (Dye *et al*., 1999).

1.1.1 Physiology and Etiology of *Mycobacterium tuberculosis*

Mycobacterium tuberculosis is an obligate, aerobic, rod-shaped, slow growing pathogenic bacterial species. It is the main causative agent of tuberculosis. It belongs to the genus *Mycobacterium* which has more than 60 species (Heifets, 1997). Its physiology is that of a waxy coating on its cell wall (primarily mycolic acid) and also highly aerobic, requiring high volumes

of oxygen. The microbe's width and height vary from 0.3–0.6 and 1 to 4 µm, respectively and it presents a complex cellular envelope, slow growth, and genetic homogeneity (Ducati *et al*, 2006). The generation time is around 24 hours in both synthetic medium and on infected animals. *M. tuberculosis* does not stain well with the Gram stain due to the waxy outer layer of its cell wall, and, consequently requires the use of the Ziehl-Nielsen or fluorochrome stains (Peloquin and Ebert, 1999).

The *Mycobacterium* genus is divided into the fast-growing species (which are usually saprophytic) and the slow-growers (generally pathogenic). The fast-growing species are usually not pathogenic but some species may cause opportunistic infections in humans and animals such as *M. fortuitum* which can be responsible for pyogranulomas in the skin of human and other mammals. These species include *M. intracellulare, M. africanum, M. smegmatis, M. kansaii, M. fortuitum* and *M. avium* complex. The *M. tuberculosis* complex consists of the pathogenic species, namely *M. tuberculosis, M. bovis, M. africanum, M. microti* and *M. canetti*. These "tubercle bacilli" cause tuberculosis in humans and animals. *Mycobacterium tuberculosis, M. africanum* and *M. canetti* are human pathogens while *M. microti* causes disease in rodents (McGaw *et al*., 2008a).

1.1.2 Pathogenesis of Tuberculosis

1.1.2.1 Primary Infection

Primary infection occurs in people who have not had any previous exposure to tubercule bacilli. Droplet nuclei, which are inhaled into the lungs, are so small that they avoid the mucociliary defences of the bronchi and lodge in the terminal alveoli of the lungs. The main determinants of risk of infection are the concentration of bacilli in an exhaled particle from a source, its aerodynamic features, the ventilation rate, and the exposure period. Infection begins with multiplication of tubercule bacilli in the lungs. The resulting lesion is the Ghon focus. Lymphatics drain the bacilli to the hilar lymph nodes. The Ghon focus and related hilar lymphadenopathy form the primary complex. Bacilli may spread in the blood from the primary complex throughout the body. The immune response (delayed hypersensitivity and cellular immunity) develops about 4-6 weeks after the primary infection. The size of the infecting dose of bacilli and the strength of the immune response determine what happens next. However, a few

dormant bacilli may persist. A positive tuberculin purified protein derivative (PPD) skin test would be the tool for diagnosis of infection. In a few cases the immune response is not strong enough to prevent multiplication of bacilli, and disease occurs within a few months (WHO, 2004; Bloom and Murray, 1992; Ducati *et al.*, 2006).

1.1.2.2 Post-primary TB

Post-primary TB occurs after a latent period of months or years following primary infection. It may occur either by reactivation of the dormant turbercle bacilli acquired from a primary infection or by reinfection (WHO, 2004). Reactivation means that dormant bacilli persisting in tissues for months or years after primary infection start to multiply. This may be in response to a trigger, such as weakening of the immune system by HIV infection. Reinfection means a repeat infection in a person who has previously had a primary infection. Tuberculosis is a state in which one or more organs of the body become diseased shown by clinical symptoms and signs. This is because the tubercle bacilli in the body have started to multiply and become numerous enough to overcome the body's defenses.

The immune response of the patient results in a pathological lesion that is characteristically localized, often with extensive tissue destruction and cavitation. Post primary TB usually affects the lungs but it can involve any part of the body. The characteristic features of post-primary PTB are the following: extensive lung destruction with cavitation; positive sputum smear; upper lobe involvement and usually no intrathoracic lymphadenopathy. Patients with these lesions are the main transmitters of infection in the community (WHO, 2004).

Approximately 15% of the patients with the active disease present extra-pulmonary TB, caused by granuloma evolution due to excessive bacterial growth, invading the blood stream and disseminating the bacilli to various parts of the body. Also called miliary TB, it frequently occurs in the pleura, lymph nodes, liver, spleen, bones and joints, heart, brain, genital-urinary system, meningis, peritoneum, and skin. (Ducati *et al*., 2006).

Considering that post-primary tuberculosis accounts for most cases of active disease in both developing and developed countries, identifying the source of reactivation tuberculosis has once again surfaced as a central issue for tuberculosis control (Bishai, 2000). There are however,

controversies about the source of reactivation tuberculosis. In addition to the conventional wisdom that latent bacilli reside in granulomatous pulmonary lesions (granuloma), Hernandez-Pando *et al*., (2000), in their study, observed that in some instances mycobacterial DNA was present in cells other than macrophages, such as type II pneumocytes, endothelial cells, and fibroblasts. New strategies for the eradication of latent organisms are required, and this will involve a better understanding of the mechanism by which the tubercule bacilli persist.

1.1.3 Epidemiologic History and Control of Tuberculosis in sub-Saharan Africa

Tuberculosis was essentially unknown in sub-Saharan Africa as late as the beginning of the 20th century, though it was already commonly known in Europe and North America, as early as the seventeenth century (Daniel *et al*., 1994). By the beginning of the 90's, there was a sharp rise in incident cases of TB in Africa (Murray, 2004). It was thought to be endemic due to the dense population, poor nutrition and poor sanitary conditions. About 80% of individuals newly diagnosed with the disease every year live in the 22 most populous countries (Dye, 2006).

In 2000 there was an estimated 8.3 million new cases of TB worldwide. Ninety five percent of TB cases and 98% of TB deaths were in developing countries. Seventy five percent of TB cases in developing countries were in the economically productive age group (15–50 years). The highest TB incidence rate (290/100,000 per year) and the highest annual rate of increase of cases (6%) were recorded in sub-Saharan Africa in 2000. In the same period, there were 1.8 million deaths, with 226,000 of this number attributable to HIV (12%). Generally, TB deaths comprise 25% of all avoidable adult deaths in developing countries (WHO, 2004).

The World Health Organisation statistical data revised in 2006 indicated that in the year 2004, Africa had the second largest incidence of tuberculosis (29% of global total) and the highest TB mortality rate (81 per 10000 pop). This was attributed to the spread of HIV being the single most important factor determining the increased incidence of TB in the past 10 years. Also according to Dye *et al*., (2005), much of the increase in global tuberculosis incidence seen since 1980 is attributable to the spread of HIV in Africa. The trajectory of TB for 9 different regions of the world is shown in Figures 1.1 and 1.2.

Though tuberculosis is profoundly affected by HIV infection, other risk factors need to be given attention (Corbett *et al*., 2006). These include diabetes, under nutrition and respiratory illnesses caused by tobacco and air pollution.

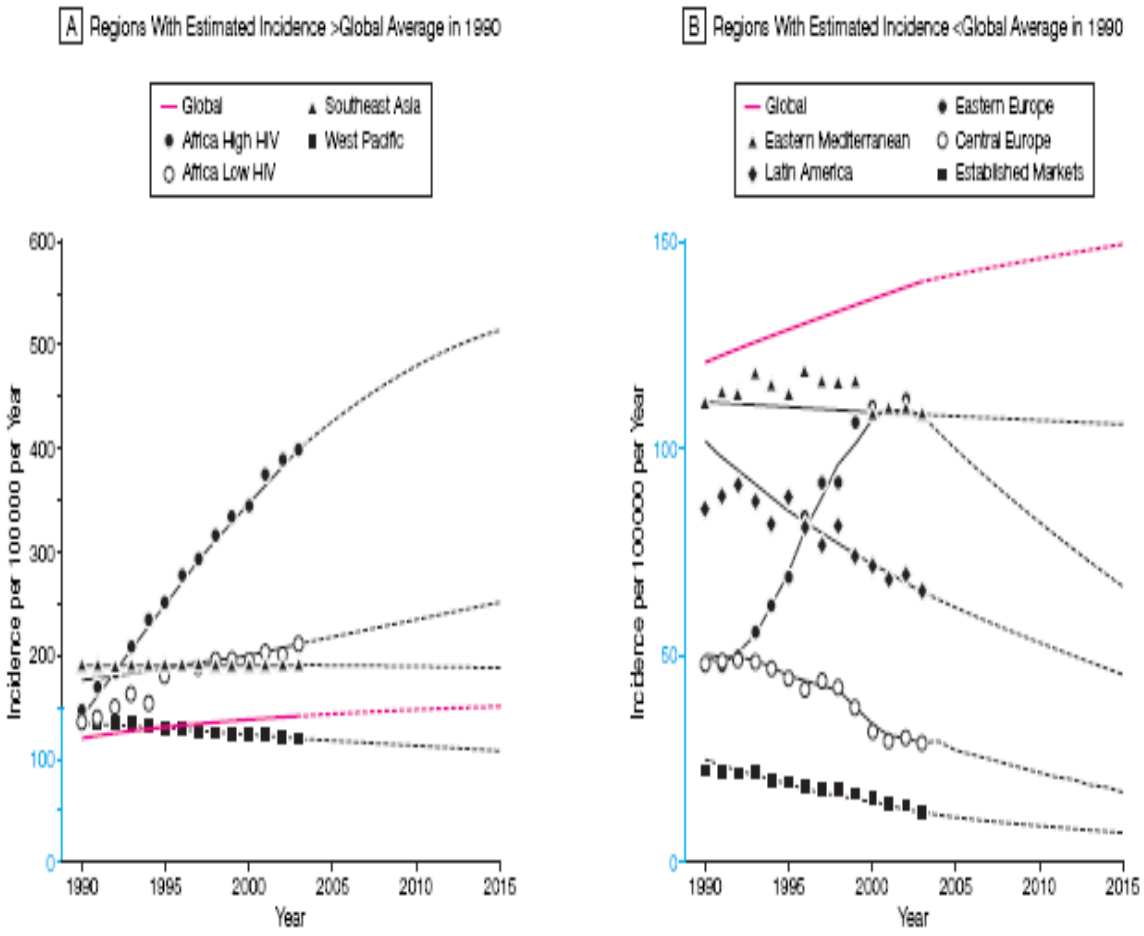

Figures 1.1. and 1.2. Trajectories of the Tuberculosis Epidemic for 9 Epidemiologically Different Regions of the World (Dye *et al*., 2005)

1.1.4 Tuberculosis in Nigeria

Nigeria has the world's fifth largest tuberculosis burden, with nearly 311,000 estimated cases annually (WHO, 2008).

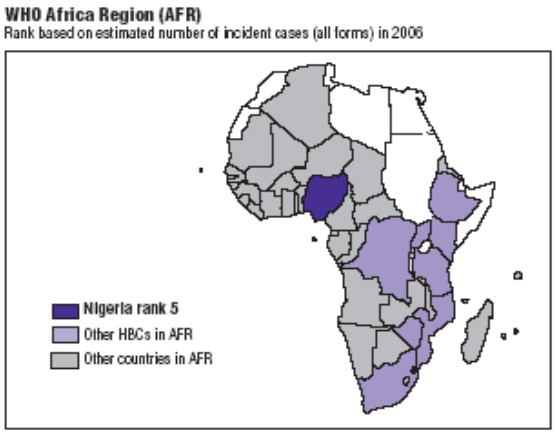

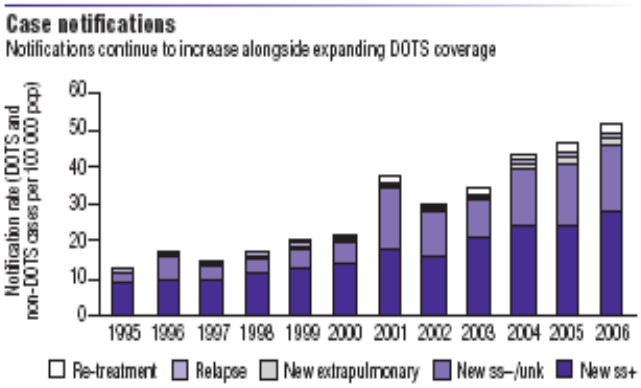

Figures 1.3. and 1.4. Map of African region showing Nigeria with its TB burden ranking and the case notifications between the period 1995 and 2006 (WHO, 2008)

The bar graph shows that on the average, the case notifications have progressively increased from the period 1995- 2006. Table 1.1 shows the estimates of the burden in 2006.

Table 1.1. Estimates of epidemiological burden of TB in Nigeria as at 2006, with a population (in thousands) of 144,720 (WHO, 2008)

Incidence (all cases /100,000 pop a year)	311
Trend in incidence rate (% yr, 2005-2006)	**-1.3**
Incidence (ss +/ 100,000 pop/yr)	137
Prevalence (all cases /100,000 pop/)2	**616**
Mortality (deaths/ 100,000 pop/yr)	**81**
Of new TB cases , % HIV	9.6
Of new TB cases , % MDR-TB	1.9
Of previously treated TB cases, % MDR-TB	9.3

1.1.5 Directly Observed Treatment Short Course Control Strategy

The World Health Organisation came up, in 1995, with a more standardized control strategy called DOTS (Directly Observed Treatment Short Course), also endorsed by the International Union against Tuberculosis and Lung Diseases (IUATL), to detect and cure TB (WHO, 1996).

The five elements of DOTS are summarized as:

1. Political commitment with increased and sustained financing
2. Case detection through quality-assured bacteriology
3. Standardized treatment, with supervision and patient support
4. An effective drug supply and management system
5. Monitoring and evaluation system, and impact measurement

Despite the implementation of this strategy, the incidence, prevalence and mortality rates of TB in Africa have continued to be on the increase, and this trend is forecasted to continue to 2015 (Dye *et al*., 2005). Co-infection of HIV with tuberculosis has challenged DOTS as a sole tuberculosis control strategy for Africa (Corbett *et al*., 2006; De Cock and Chaisson, 1999).

However, in the year 2006, the World Health Organisation launched the new Stop TB Strategy, a 10 year plan for the control of TB (WHO, 2006). The core of this strategy is still DOTS.

1.1.6 Current Antituberculosis Drugs

The principal objective of chemotherapy in TB patients is the eradication of the whole bacilliary load. Chemotherapy of tuberculosis evolved in the 1940s. Some of the agents discovered since then include para-aminosalicylic acid (**1**), isoniazid (**2**), pyrazinamide (**3**), cycloserine (**4**), ethionamide (**5**), rifampicin (**6**), and ethambutol (**7**). A majority of these drugs were discovered through broad random sampling. These drugs are grouped into first and second line drugs (Table 1.2). First line drugs are mainly bactericidal, and combine a high degree of efficacy with a relative toxicity to the patient during treatment. Second-line drugs are mainly bacteriostatic, which have a lower efficacy and are usually more toxic. The antituberculosis agents currently in use, their mechanism of action, toxicity and side effects have been discussed (Tripathi *et al*., 2005; Chhabria *et al*., 2009).

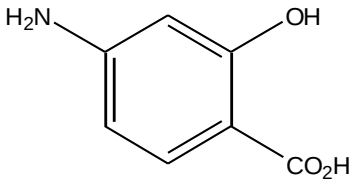

1

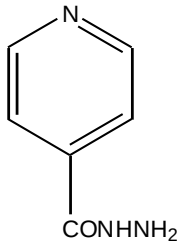

2

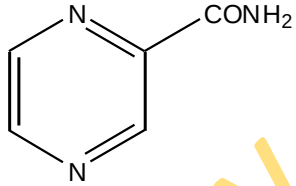

3

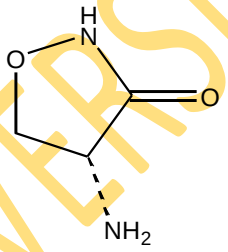

4

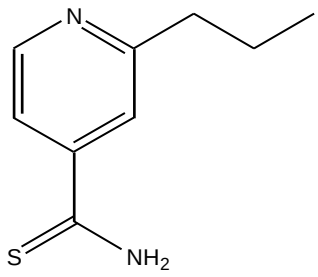

5

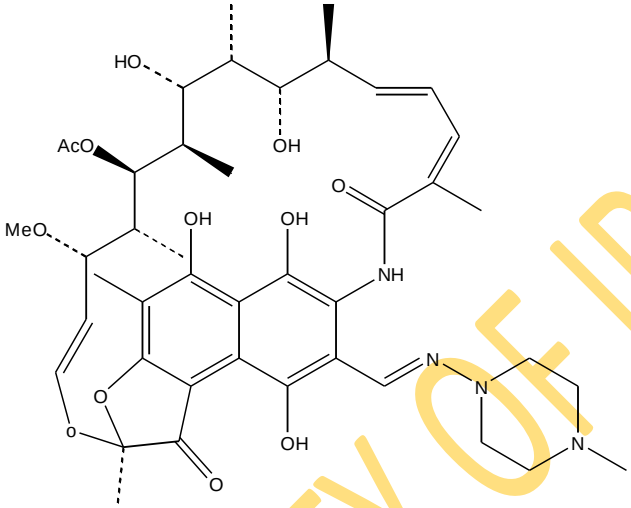

6

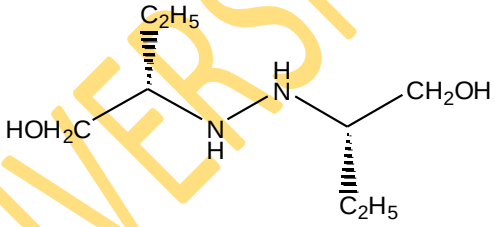

7

Table 1.2. **Drugs used for the treatment of tuberculosis (Davies, 1999)**

First line drugs		**Second line drugs**	
Essential	**Others**	**Old**	**New**
Isoniazid	Pyrazinamide	Ethionamide	Quinolones
Rifampicin	Ethambutol	Cycloserine	Ofloxacin
	Streptomycin	Capreomycin	Ciproflaxin
		Amikacyn	Sparfloxacin
		Kanamycin	
		Para-aminosalicylic acid	Macrolides
			Clarithromycin
			Clofazimine
			Amoxycillin
			Clavulanic acid
New			
Rifamycins			
Rifabutin			
Rifapentine			

There are two states of TB, the active state and the latent state. The standard treatment for active TB is a regimen of isoniazid, rifampicin and pyrazinamide for two months, followed by isoniazid and rifampin for four additional months. This is conveniently abbreviated to 2HRZ/4HR. Ethambutol is usually added as a first line regimen when drug resistant TB is a possibility and for areas with high prevalence of resistance (Forget and Menzies, 2006).

1.1.7 Drug Resistant Strains of *Mycobacterium tuberculosis*

Resistance to one or several forms of treatment occurs when the bacteria develop the ability to withstand antibiotic attack and relay that ability to newly produced bacteria. Since that entire strain of bacteria inherits this capacity to resist the effects of the various treatments, resistance can spread from one person to another.

Inadequate, incomplete, or improperly supervised treatment regimen, wrong prescription, and co-infection with HIV have caused the emergence of resistant strains of *M. tuberculosis* (MTB). A particularly dangerous form of drug resistant TB is multidrug-resistant TB (MDR-TB), which is defined as a specific form of drug-resistant TB due to a bacillus resistant to at least isoniazid and rifampicin (first line drugs), the two most powerful anti-TB drugs. It takes longer to treat with second line drugs, which are more expensive and have more side-effects. Even more recently there have been reports on the emergence of extensively drug-resistant tuberculosis (XDR-TB), which is TB resistant to at least rifampicin and isoniazid from among the first line drugs in addition to resistance to any fluoroquinolone, and one of three injectable second-line anti-TB drugs used in TB treatment (capreomycin, kanamycin, amikacin) (CDC, 2006).

1.1.8 The need for TB Drug Discovery and Development

With the emergence of these drug resistant and new strains of TB, side effects and length of treatment regimen of existing ones and also the influence of HIV, it becomes imperative that there is an urgent need for the discovery and development of new anti-tuberculosis agents (Newton *et al*., 2000). Pauli *et al*., (2005) also mentioned the need for novel anti-tubercular agents acting on a different site from the existing ones. More recent technologies in molecular biology employ the use of the *M. tuberculosis* genome sequence to choose novel drug targets and to facilitate the identification and validation of new drug targets essential for tubercule bacilli, both *in vitro* and *in vivo* (Chhabria *et al*., 2009).

1.2 Objectives of the Study

Pavetta crassipes is an ethnomedicinal Nigerian plant used locally in the formulation of traditional medicinal recipes for the treatment of tuberculosis or tuberculosis- related symptoms

such as cough, chest pain and other upper respiratory infections. The objectives of the study seek to:

1. Isolate, identify the constituents responsible for the reported biological activities of *P. crassipes* leaves against *M. tuberculosis* and subsequently evaluate the activity of the compounds against MTB.
2. To characterize other isolated constituents of the plant.

CHAPTER TWO

LITERATURE SURVEY

2.1 Natural Products Research

2.1.1 Secondary Metabolism

Natural products are defined as secondary metabolites, usually of relatively complex structure, which are of more restricted distribution and more characteristic of specific botanical sources than are compounds produced by primary metabolic processes (Geismann and Crout, 1969). Secondary metabolites are not necessarily produced under all conditions, and in a vast majority of cases, the functions of these compounds and their benefit to the organism are not yet known. Some are produced as toxic materials for providing defence against predators, as volatile attractants towards the same or other species, or as colouring agents to attract or warn other species, but they all play some vital role for the well being of the producer. It is this area of secondary metabolism that provides most of the pharmacologically active natural products (Dewick, 2009).

2.1.2 Biosynthesis of Secondary Metabolites

2.1.2.1 Building Blocks

The building blocks for secondary metabolism are derived from primary metabolism, which involves the processes involved in synthesizing carbohydrates, proteins, fats and nucleic acids, found to be essentially the same in all organisms (Clayden *et al*., 2001). The most important building blocks employed in the biosynthesis of secondary metabolites are derived from the intermediates acetyl coenzyme A (acetyl-CoA), shikimic acid, mevalonic acid, and methylerythritol phosphate (Fig 2.1). These are utilized, respectively in the acetate, shikimate, mevalonate, and methylerythritol phosphate pathways (Dewick, 2009).

Secondary metabolites can be synthesized by combining several building blocks of the same type, or by using a mixture of different building blocks. This expands structural diversity and, consequently, makes subdivisions based entirely on biosynthetic pathways rather more difficult.

A typical natural product might be produced by combining elements from the acetate, shikimate, and methylerythritol phosphate pathways, for example.

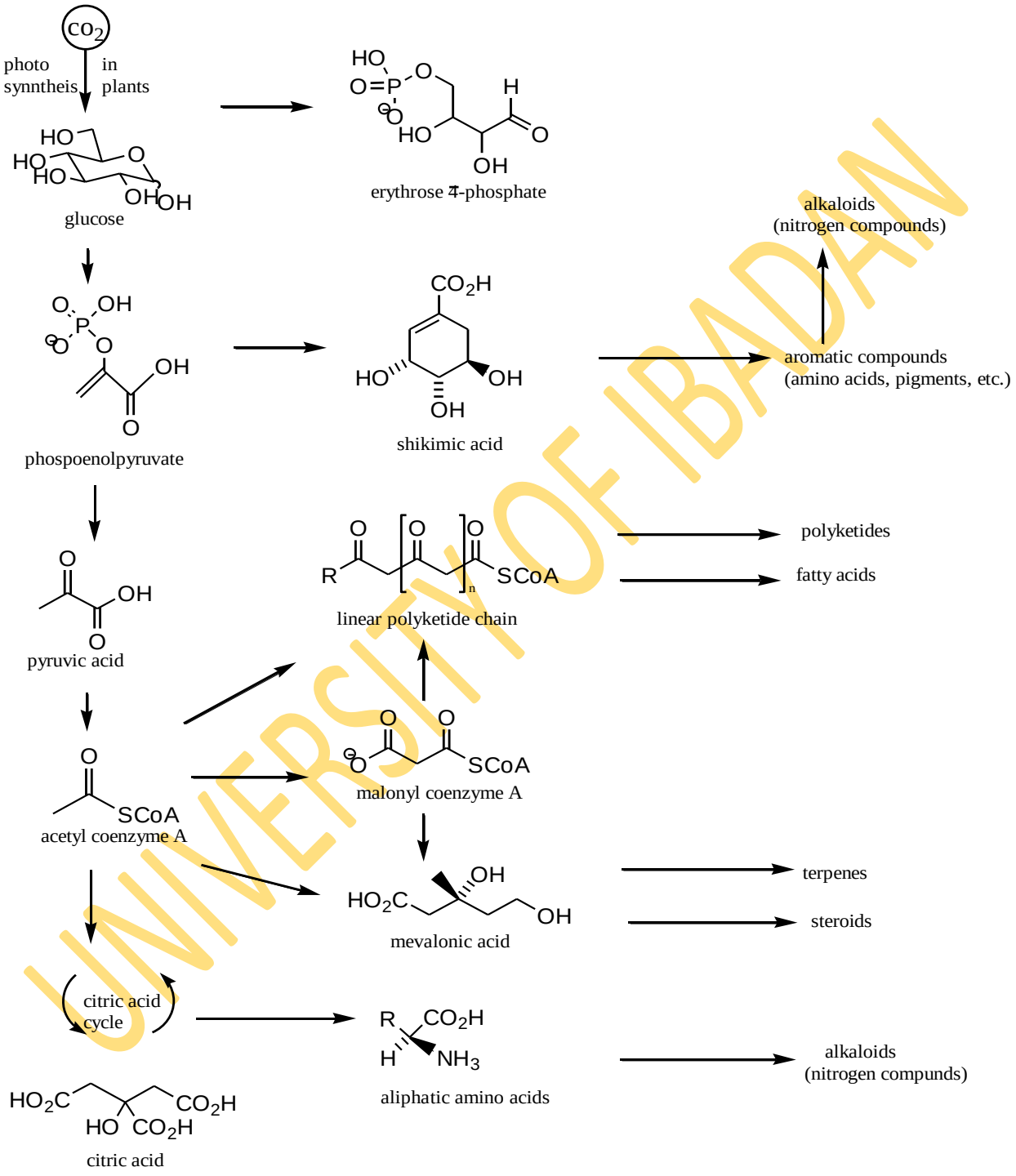

Figure 2.1. Secondary metabolism pathways

2.1.2.2 Biosynthetic Pathways

A biosynthetic pathway is a sequence of chemical transformations; with a few exceptions, each of these reactions is catalyzed by an enzyme. Chemical modification of a substrate depends upon the binding properties conferred by a particular combination of functional groups in the constituent amino acids of the protein. The main thrust of biosynthetic research has been in delineating the sequence of reactions and characterizing the enzymes involved (Dewick, 2009).

Any biosynthetic study begins with speculation, comparing structurally related compounds from the same or different organisms, and suggesting possible interrelationships based on known chemical reactions, i.e. application of 'paper chemistry'. This usually entails feeding an isotopically labeled compound to a plant, microorganism, animal tissue, etc, that produces the required metabolite. For success, it is an absolute requirement that the organism is actively synthesizing the compound during the feeding period. The metabolite is then isolated, purified, and analysed to detect the presence of the isotope. The formation of a labeled product is cautiously interpreted as a demonstration of the precursor-product relationship, though it should be confirmed that the position of labeling in the product is the same as that in the precursor; organisms can degrade an introduced chemical to smaller portions and utilize it in their general metabolism. Examples of isotopes used are ^{3}H, ^{14}C and ^{13}C. The natural abundance of ^{13}C is 1.1%, and modern NMR spectrometers can detect this in relatively small samples of a compound. Hence, any biosynthetic enrichment can be detected simply by an enhancement of the natural abundance signal. Furthermore, the position of labeling is immediately established from the spectrum via the assignment of the enhanced signal. This has made a huge impact on biosynthetic methodology (Dewick, 2009).

2.1.3 Biosynthetic Pathways of Selected Groups of Natural Products

2.1.3.1 Simple Benzoic Acids

The shikimate pathway provides an alternative route to aromatic compounds. It begins with a coupling of phosphoenolpyruvate (PEP) from the glycolytic pathway and D-erythrose 4-phosphate from the pentose phosphate cycle to give the seven-carbon 3-deoxy-D-arabino-heptulosonic acid 7-phosphate (DAHP; Fig 2.2). Elimination of phosphoric acid from DAHP followed by an intramolecular aldol reaction generates the first carbocyclic intermediate 3-

dehydroquinic acid. Reduction of 3-dehyroquinic acid leads to quinic acid. Shikimic acid is formed from 3-dehydroquinic acid via 3-dehydroshikimic acid through dehydration (3-dehydrogenase and reduction (shikimate dehydrogenase) steps. The simple phenolic acids protocatechuic acid (3,4-dihydroxybenzoic acid) and gallic acid (3,4,5-trihydroxybenzoic acid) can be formed by branchpoint reactions from 3-dehyroshikimic acid which involve dehydration and enolization, or, in the case of gallic acid, dehydrogenation and enolization (Dewick, 2009).

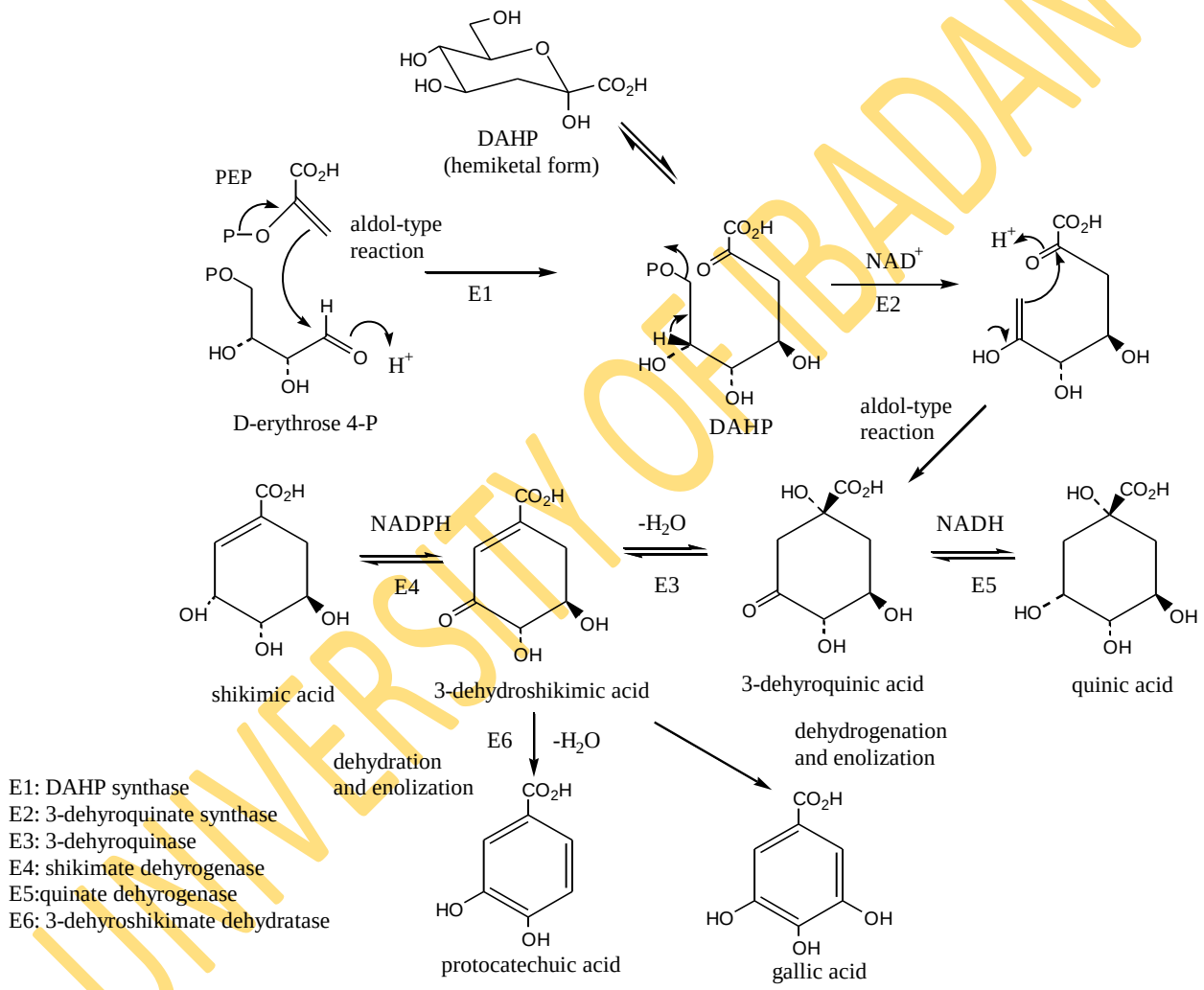

Figure 2.2. Biosynthetic pathway of shikimic acid and simple benzoic acids

2.1.3.2 Phenylpropanoids; Cinnamic Acids and Esters

L-Phenylalanine and L-tyrosine, as C_6C_3 building blocks, are precursors for cinnamic acids and their derivatives. A frequent first step is the elimination of ammonia from the side-chain to generate the appropriate *trans* (*E*) cinnamic acid. In the case of phenylalanine, this would give cinnamic acid, whilst tyrosine could yield 4-coumaric acid (*p*-coumaric acid; Fig 2.3). Other cinnamic acids are obtained by further hydroxylation and methylation reactions, sequentially building up substitution patterns typical of the shikimate pathway metabolites, i.e. an ortho oxygenation pattern. Some of the more common natural cinnamic acids are 4-coumaric, caffeic, ferulic, and sinapic acids. These can be found in plants in free form and in a range of esterified forms, e.g. with quinic acid as in chlorogenic acid (3-O-caffeoylquinic acid; Fig 2.4; Dewick, 2009)

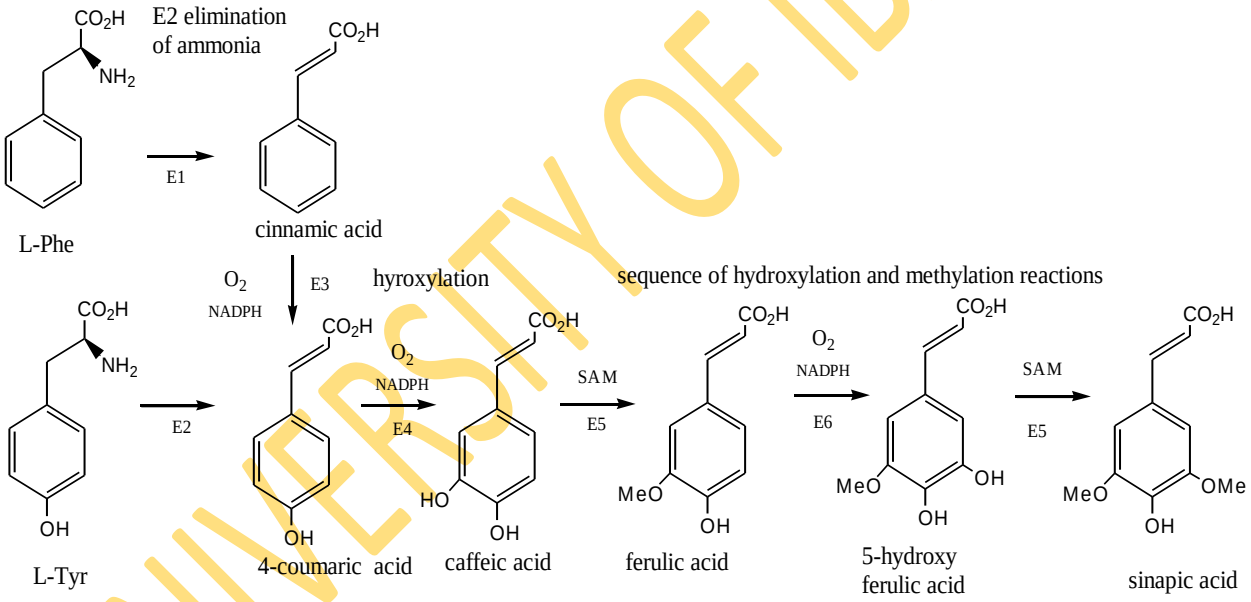

E1: phenylalanine ammonia lyase (PAL)
E2: tyrosine ammonia lyase (TAL)
E3: cinnamate 4-hyroxylase
E4: p-coumarate 3-hyroxylase
E5: caffeic acid *O*-methyltransferace

Figure 2.3. Biosynthetic pathway of cinnamic acid and derivatives

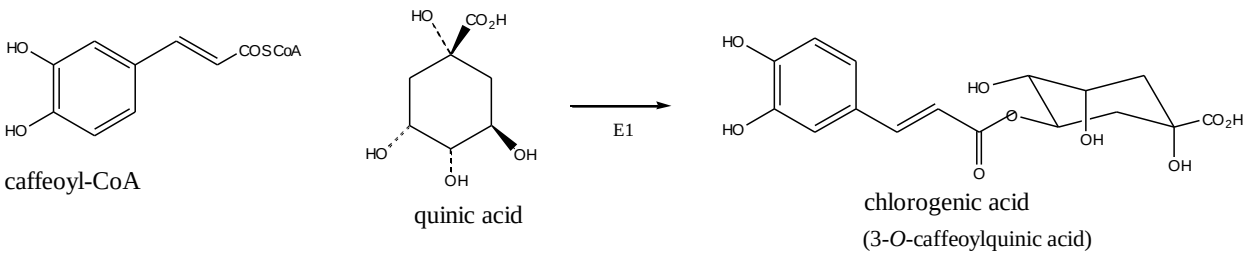

E1: quinnate *O*-hydroxycinnanoyltransferase

Figure 2.4. Esterification reaction between caffeic acid and quinic acid

2.1.3.3 Aromatic Polyketides; Flavonoids and Stilbenes

Flavonoids (and stilbenes) are synthesized in plants via the phenylpropanoid and acetate-malonate metabolic pathway. They are products from a cinnamoyl-CoA starter unit, with chain extension using three molecules of acetyl-CoA, to give initially a polyketide which can be folded in two different ways. Depending on the folding system, these allow aldol or Claisen-like reactions to occur, generating stilbenes or chalcones as end products formed by enzymes stilbene synthase and chalcone synthase, respectively (Fig 2.5; Dewick, 2009). Both structures nicely illustrate the different characteristic oxygenation patterns in the two aromatic rings derived from the acetate or shikimate pathways.

With the stilbenes, the terminal ester function is no longer present, therefore, hydrolysis and decarboxylation have also taken place during this transformation. A Michael-type nucleophilic attack of the phenolic group to the α, β-unsaturated ketone gives rise to chalcones which act as precursors for a vast range of flavonoid derivatives such as flavones, flavonols, anthocyanidins, and catechins (Dewick, 2009).

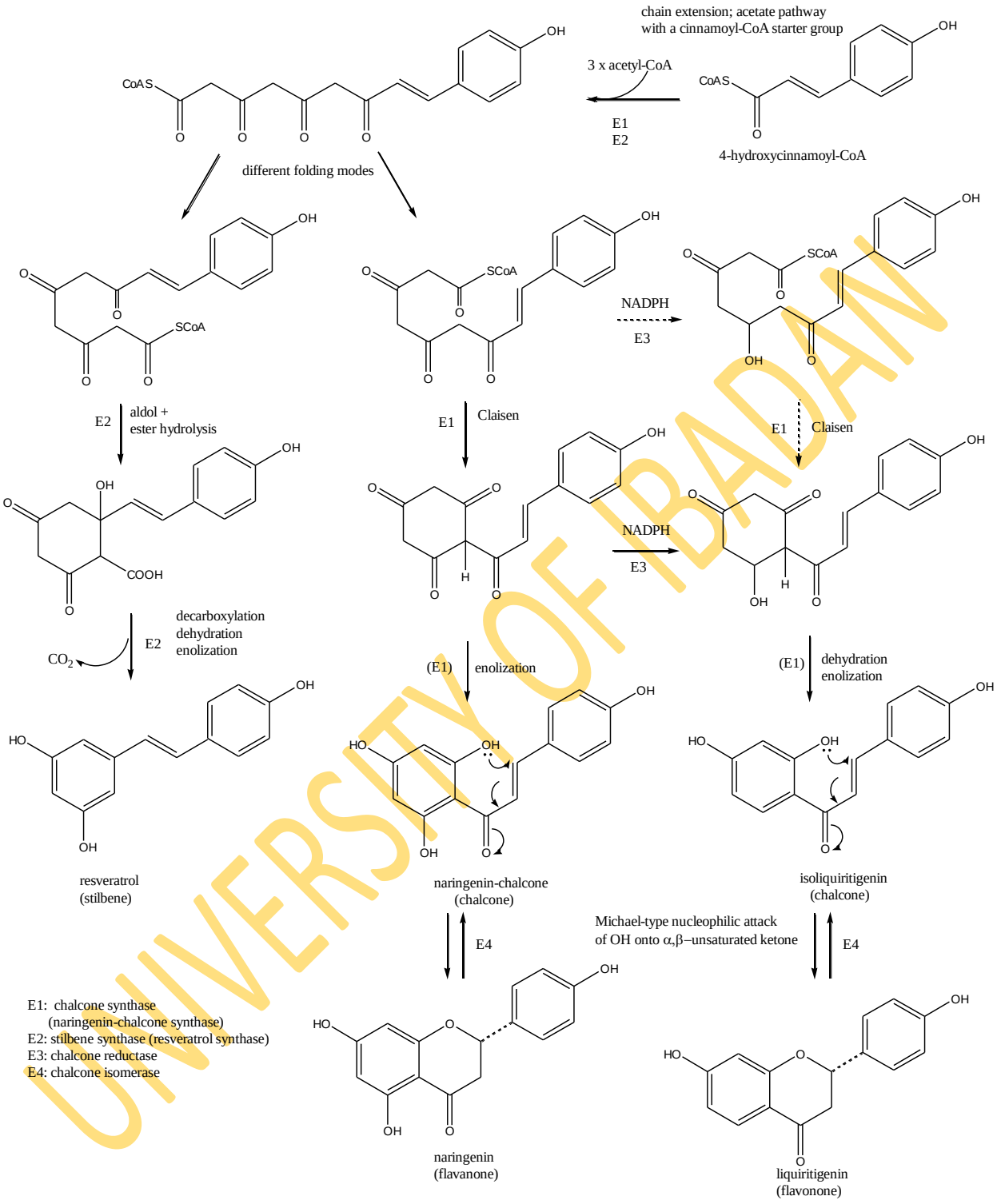

Figure 2.5. Biosynthetic pathway of flavonoids and stilbenes

2.1.3.4 Terpenoids and Steroids

Terpenoids and steroids form a large and structurally diverse family of natural products derived from C_5 isoprene units joined in a head-to-tail fashion. The biosynthesis of terpenoids was thought to originate from the mevalonate pathway, until the methylerythritol phosphate pathway was also elucidated (Rohdich *et al*., 2003). The biochemically active isoprene units are the diphosphate (pyrophosphate) esters; dimethylallyl diphosphate (DMAPP) and isopentenyl diphospate (IPP). These units may be derived by two pathways: by way of intermediates mevalonic acid (MVA) or methylerythritol phosphate (MEP) (Dewick, 2009). A representation of these isoprene units in different structures are classified as hemiterpenes, monoterpenes, sequisterpenes, diterpenes, sesterterpenes, triterpenes and tetraterpenes (Fig 2.6).

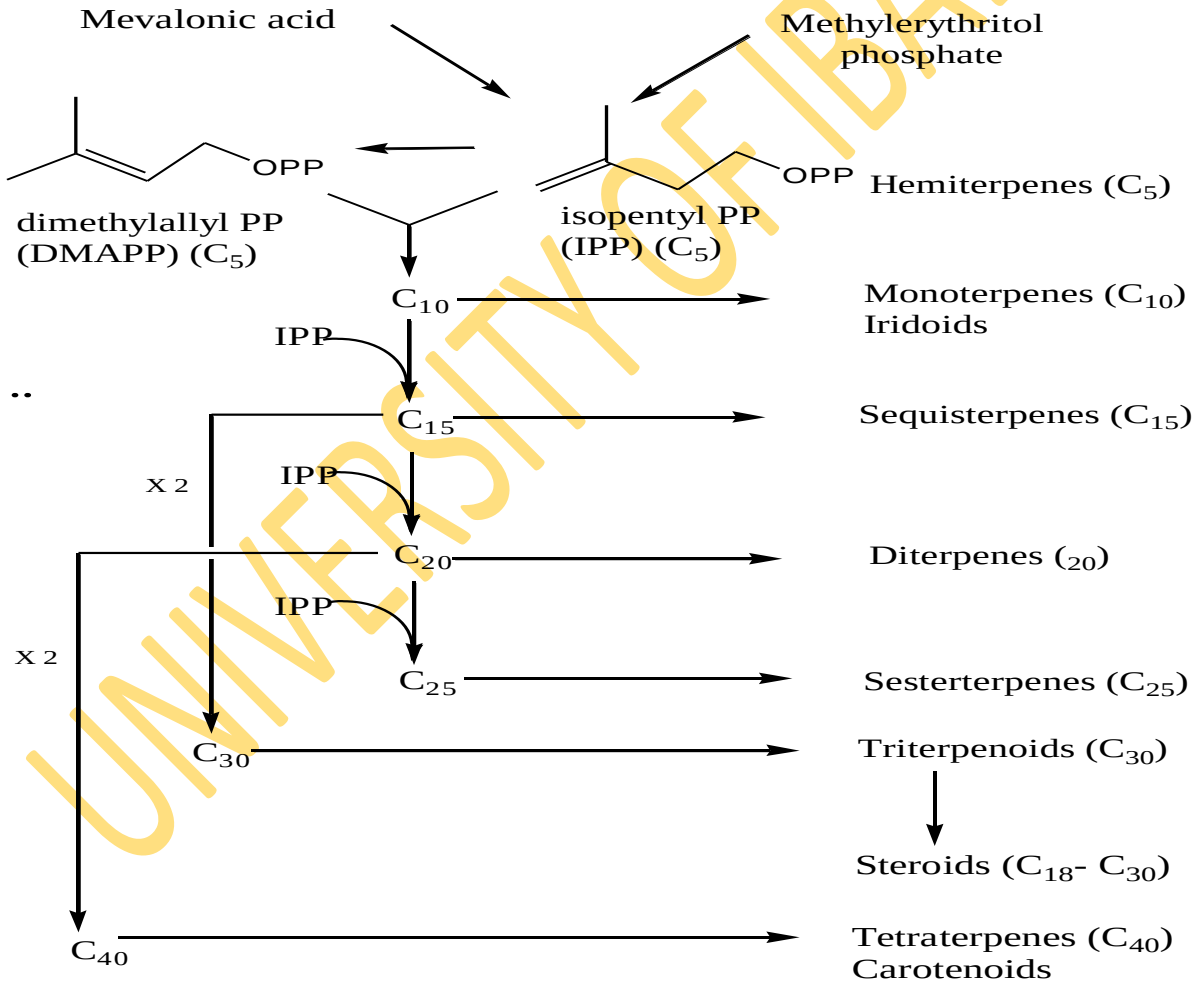

Figure 2.6. General biosynthetic pathways of different classes of terpenoids

2.1.3.4.1 Iridoids

Iridoids are secondary metabolites of terrestrial and marine flora and fauna and are found in a large number of plant families usually as glycosides. Structurally, they are cyclopenteno [c] pyran monoterpenoids and biogenetically and chemotaxonomically, they provide a structural link between terpenes and alkaloids. Iridoids contain a cyclopentane ring which is usually fused to a six-membered oxygen heterocycle. Cleavage of the cyclopentane ring produces seco-iridoids, while cleavage of the pyran ring produces iridoid derivatives, hence the cyclopentane ring is known as the basic skeletal ring in iridoids (Dewick, 2009; Dinda *et al*., 2007).

The iridoid system arises from geranoil by a type of folding (Fig 2.7). The fundamental cyclization to iridodial is formulated as attack of hydride on the dialdehyde, produced by a series of hydroxylation and oxidation reactions on geraniol. Further oxidation gives iridotrial, in which hemiacetal formation then leads to production of the heterocyclic ring. A large number of iridoids are found as glycosides, e.g loganin; glycosylation effectively transforms the hemicacetal linkage into an acetal. The pathway to loganin involves, in addition, a sequence of reactions in which the remaining aldehyde group is oxidized to the acid and methylated, and the cyclopentane ring is hyroxylated. Loganin, in further metabolism, cleaves to give secologanin, representative of the secoiridoids (Dewick, 2009).

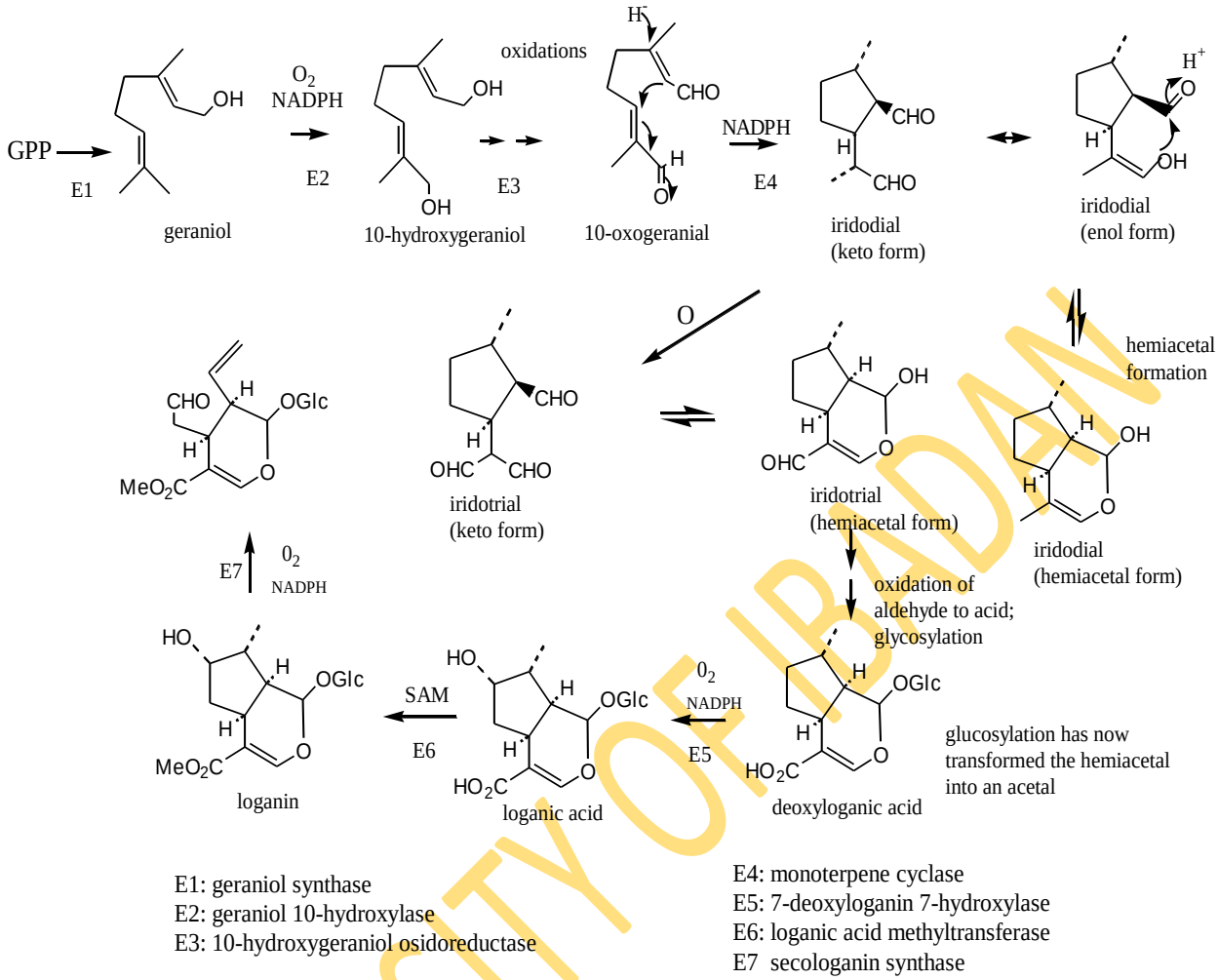

Figure 2.7. Biosynthetic pathway of iridoids

2.1.3.4.2 Triterpenes

Triterpenes, which comprise a broad chemical group, are abundantly found in nature. Approximately 200 different triterpenoid skeletons are known (Connolly and Hill, 2007). Squalene is the precursor of triterpenes and steroids. Squalene is formed from two molecules of farnesyl diphosphate (FPP), (Fig 2.8). Cyclization of squalene is via an intermediate 2,3-oxidosqualene (squalene-2,3- oxide). Most natural triterpenes and steroids contain a 3-hydroxy group, the original epoxide oxygen from oxidosqualene. Depending on the folding pattern of this intermediate, two conformations; a *chair- boat- chair- boat* conformation or a *chair- chair- chair- boat* conformation is possible. These produce a transient protosteryl cation and a dammarenyl cation, respectively with these conformational characteristics. These cations undergo further carbocation- promoted cyclizations and/or Wagner-Meeriwein rearrangements to give the cucurbitacins and euphol (stereoisomer of lanosterol; Fig 2.9). Wherein the Wagner-Meerwein rearrangements do not take place, the dammarenyl cation could be quenched with water to give dammarenediols. Alternatively, further migration and cyclization reactions lead to the formation of β-amyrin, α-amyrin (and/or taraxasterol) and lupeol, representing the oleanane, ursane and lupane type triterpenes, respectively (Fig 2.10; Dewick, 2009).

Hopanoids, another triterpene type skeleton, are characteristic in ferns. They arise from squalene by a similar carbocation cyclization mechanism, but do not involve the initial epoxidation to oxidosqualene. Cyclization is initiated by protonation of double bond to give tertiary cation, followed by carbocation promoted cyclizations to give hopanoyl cation which is quenched with water to give hopan-22-ol or loss of proton to give hopene (Dewick, 2009). The biosynthesis of hopanoids is summarized in Fig 2.11.

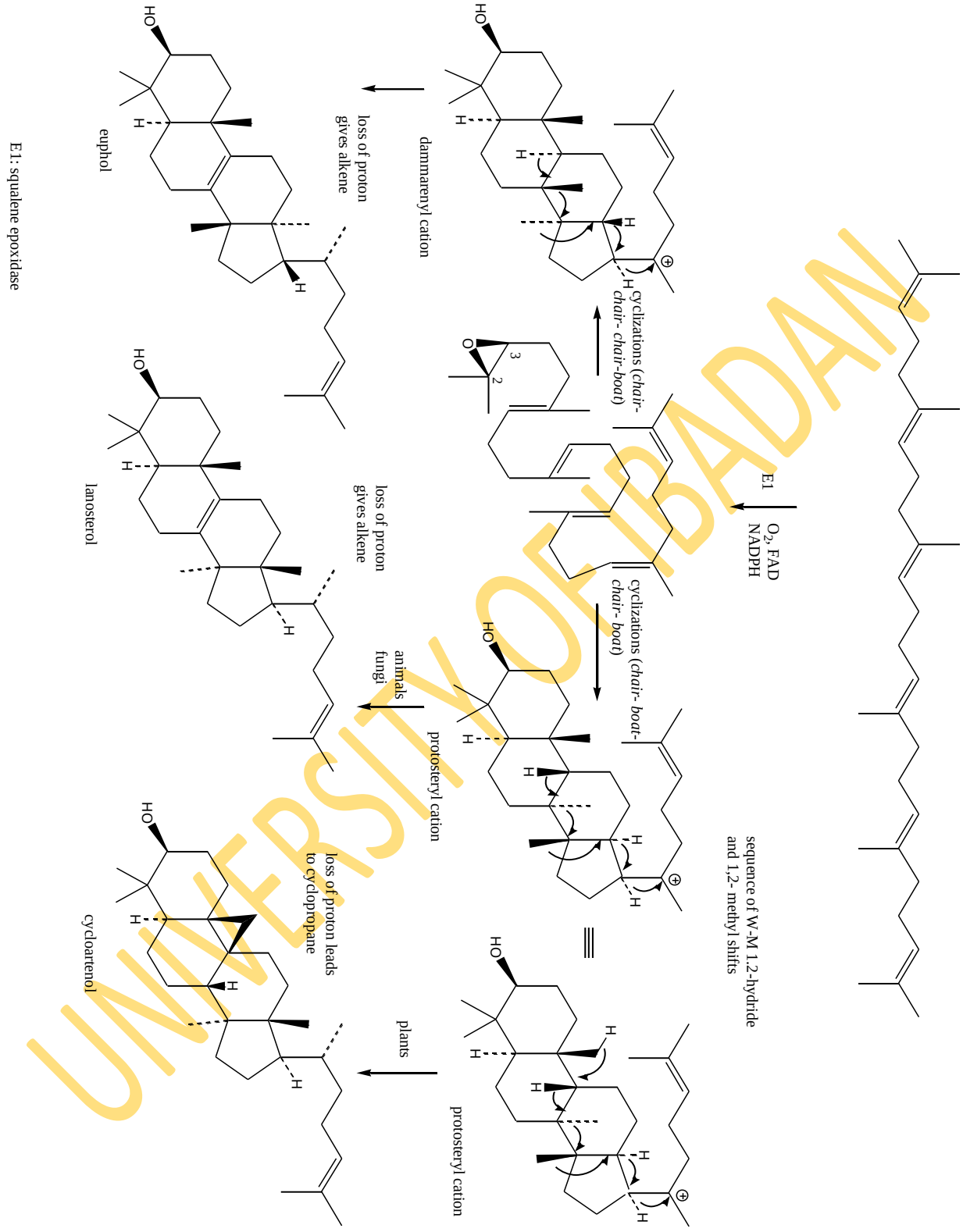

Figure 2.8. Cationic intermediates in plant triterpenoid biosynthesis

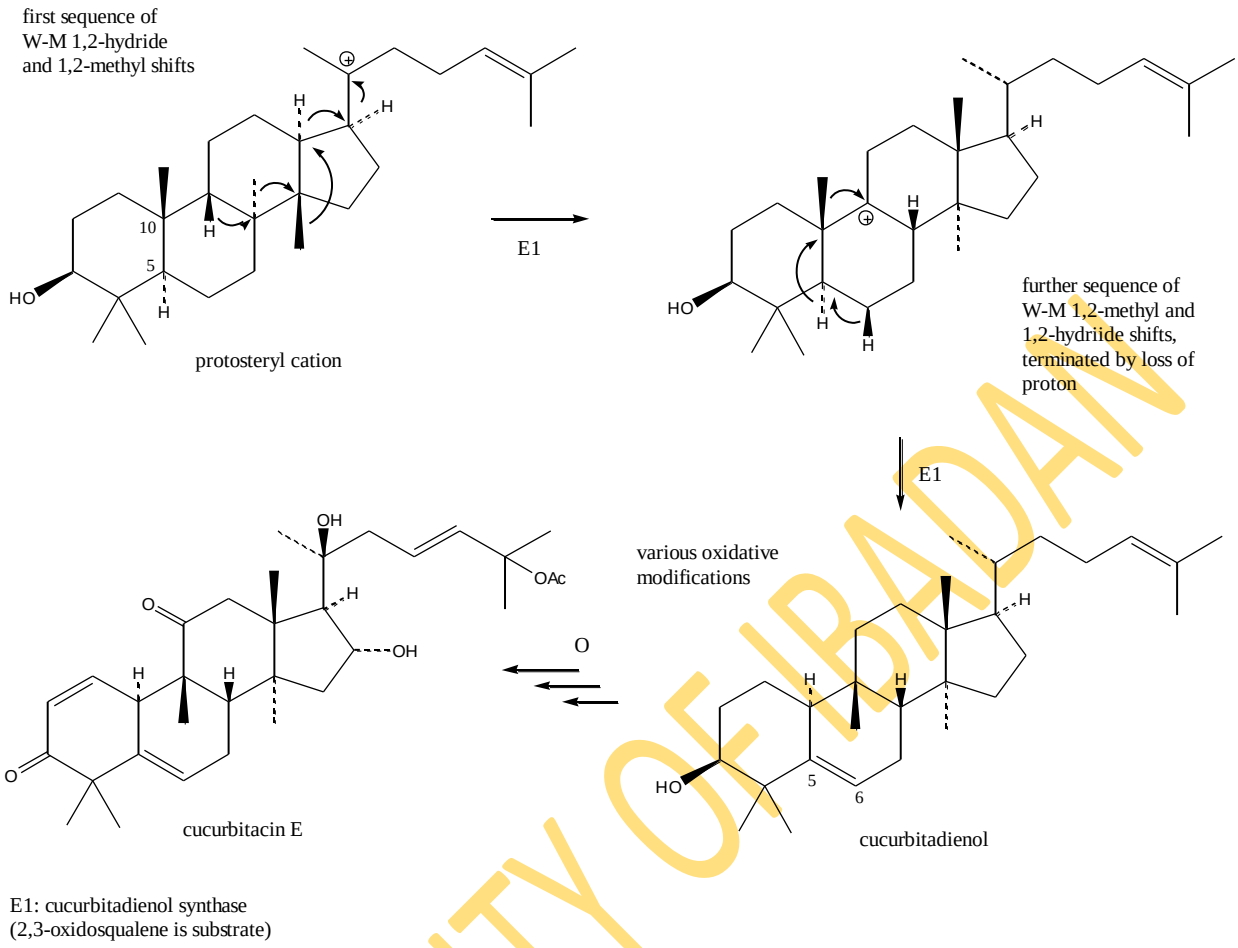

Figure 2.9. Biosynthetic pathway of cucurbitacins

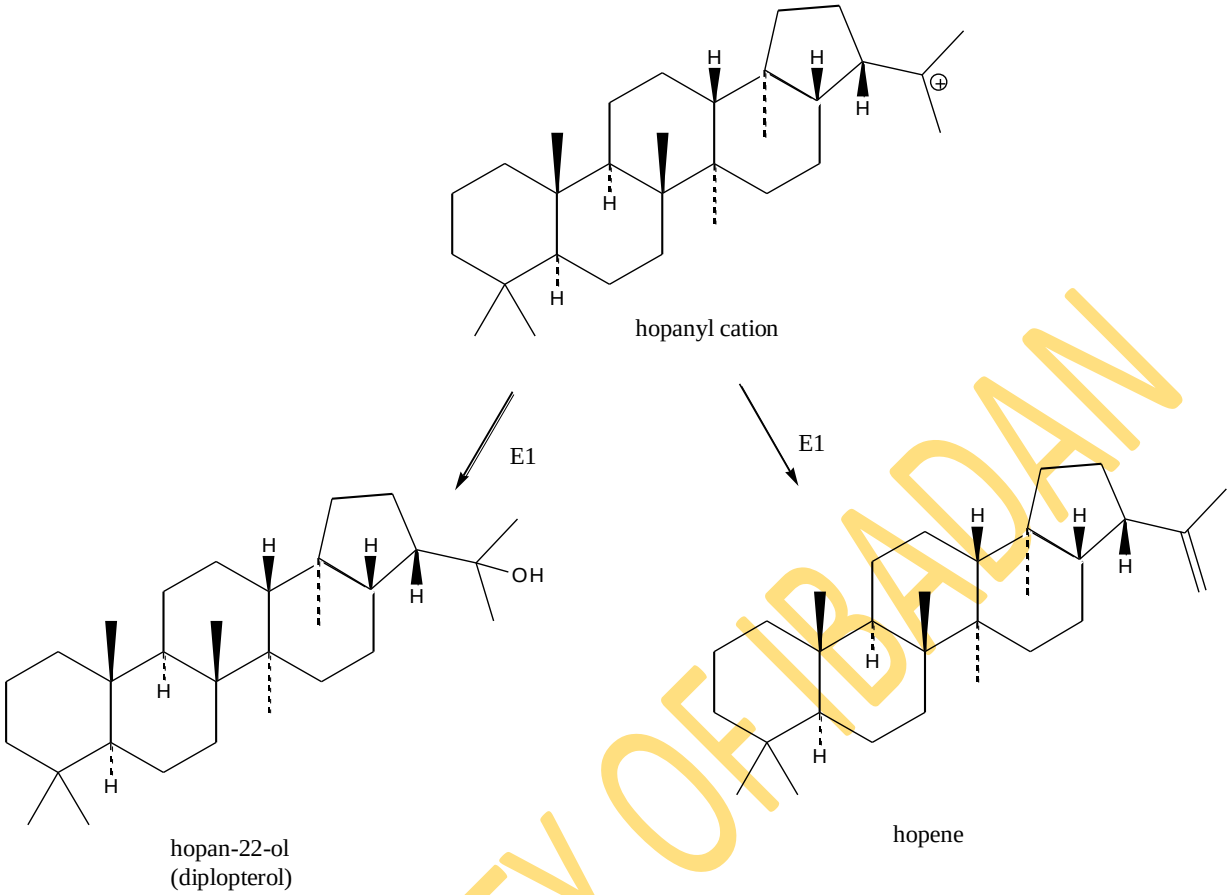

Figure 2.10. Biosynthetic pathway of hopanoids

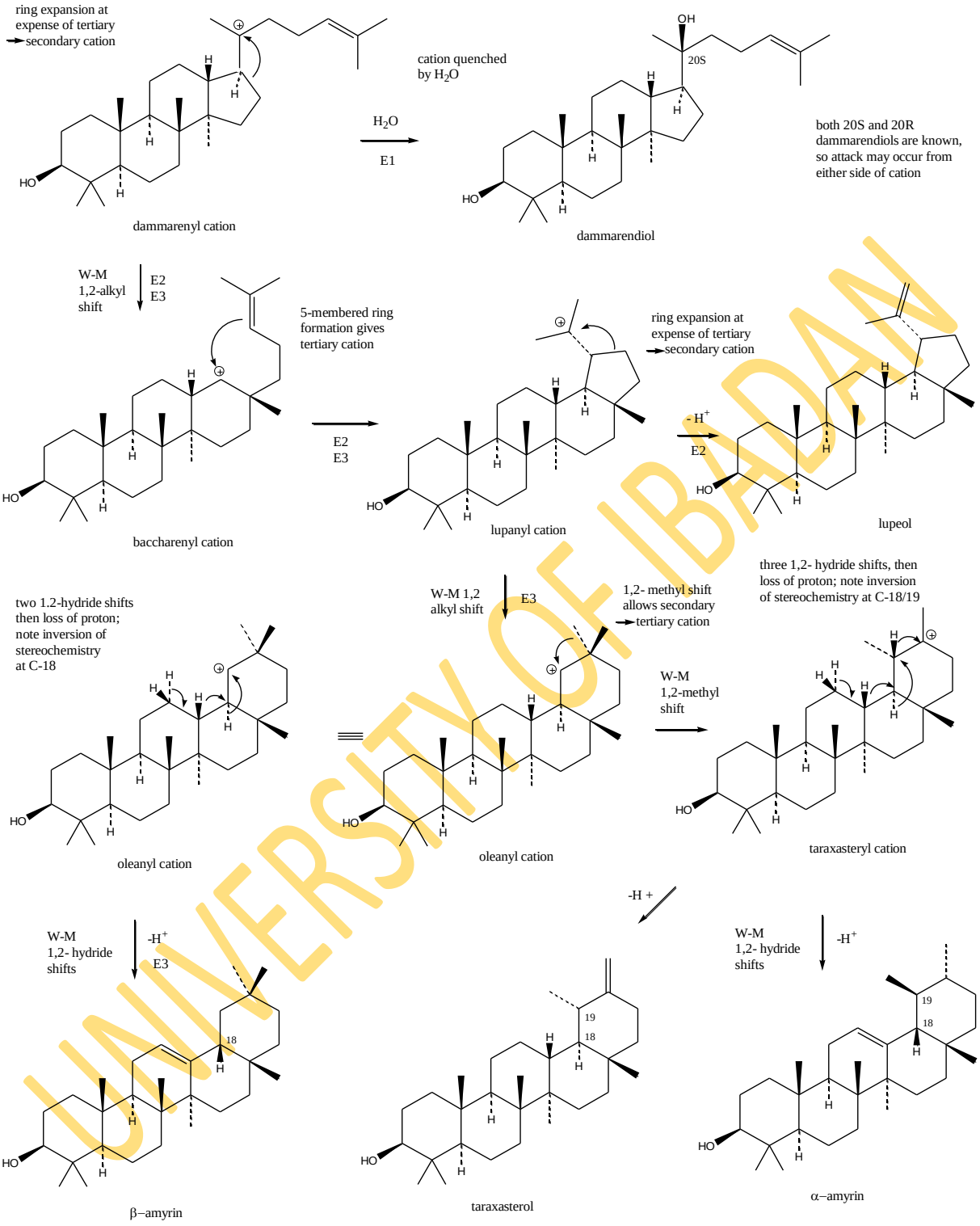

Figure 2.11. Biosynthetic pathway of oleanane, ursane and lupane type triterpenoids

2.1.3.4.3 Steroids

Steroids are modified triterpenes containing a tetracyclic ring, but lacking the three methyl groups at C-4 and C-14. Many steroids exist in nature as sterols, steroidal saponins, cardioactive glycosides, bile acids, corticosteroids and mammalian sex hormones. Many synthetic and semi-synthetic steroidal compounds are routinely used in medicine. The different biological activities observed resulting from compounds containing a common structural skeleton are in part ascribed to the functional groups attached to the steroid nucleus, and in part to the overall shape conferred on this nucleus by the stereochemistry of ring fusions (Dewick, 2009).

In plants, fungi and algae, the major steroids are found as sterols characterized by an extra one-carbon or two-carbon substituents on the side chain, attached at C-24. They include campesterol, sitosterol, stigmasterol, fucosterol and ergosterol. These sterols, termed phytosterols, are structural components of membranes in plants, algae, and fungi and affect the permeability of these membranes. They also appear to play a role in cell proliferation. (Dewick, 2009).

The biosynthesis of these phytosterols involves a series of reactions such as alkylation, reduction and dehydrogenation as summarized in Fig 2.12, via cycloartenol as the substrate in plants and algae, and lanosterol in fungi (Dewick, 2009).

Figure 2.12. Biosynthetic pathway of some common sterols

2.1.3.5 Alkaloids

Alkaloids are nitrogen containing compounds found in about 20% of plant species. Over 27000 different alkaloid structures have been characterized, with 21000 from plants. Alkaloids contain one or more nitrogen atoms, typically as primary, secondary, or tertiary amines, and this usually confers basicity on them, facilitating isolation and purification, since water-soluble salts can be formed in the presence of mineral acids. Alkaloids containing quaternary amines are also found in nature. The biological activity of many alkaloids is often dependent on the amine function being transformed into a quaternary system by protonation at physiological pH values. The potent biological activity of some alkaloids has also led to their uses as pharmaceuticals, stimulants, narcotics, and poisons. Examples of plant-derived alkaloids currently in clinical use include the analgesics, morphine and codeine, the anti-cancer agents, vinblastine and taxol, the antibiotic, sanguinarine, and the sedative, scopolamine (Dewick, 2009).

Alkaloids are often classified according to the nature of the nitrogen-containing structure (e.g pyrrolidine, piperidine, quinoline, isoquinoline, indole), though the structural complexity of some examples rapidly expands the number of subdivisions. The nitrogen atoms in alkaloids originate from an amino acid, and, in general, the carbon skeleton of the particular amino acid precursor is also largely retained intact in the alkaloid structure, though the carboxylic acid carbon is often lost through decarboxylation. Accordingly, subdivision of alkaloids into groups based on amino acid precursors forms a rational and often illuminating approach to classification. Relatively few amino acid precursors are actually involved in alkaloid biosynthesis, the principal ones being ornithine, lysine, nicotinic acid, tyrosine, tryptophan, anthranilic acid, and histidine. Building blocks from the acetate, shikimate, or methylerythritol phosphate pathways are also frequently incorporated into the alkaloid structures. However, a large group of alkaloids are found to acquire their nitrogen atoms via transamination reactions, incorporating only the nitrogen from an amino acid, whilst the rest of the molecule may be derived from acetate or shikimate; others may be terpenoids or steroid in origin. The term ‘pseudoalkaloid’ is sometimes used to distinguish this group (Dewick, 2009).

2.2 Natural Products in Drug Discovery of Pharmaceuticals

Natural products have played and continue to play a significant role in the drug discovery process. For a long period of mankind existence, natural products were the only therapy available to humans. Drugs of natural origin have been classified as natural products, products derived semi-synthetically from natural products, or synthetic products based on natural product models (Cragg *et al*., 1997). Natural product chemistry and organic synthesis are powerful tools for optimising leads and for generating new diversity from natural scaffolds. The amalgamation of both is an important strategy in rational drug design.

Statistics from the studies carried out by different workers continue to emphasize the potentials and untapped reservoir of molecules with therapeutic interest. Eighty percent of the world's population depends mainly on natural products for their health care and sixty percent of the orthodox drugs used have their origin from natural products (Cragg and Newman, 2005). Newman and co-workers (2003) have reported that 61% of the 877 small molecule new chemical entities registered as drugs worldwide during the period of 1981-2002 were or have been inspired by natural products. Farnsworth *et al*. (1985) have reported that at least 119 compounds derived from 90 plant species can be considered as important drugs currently in use in one or more countries, with 77% of these being derived from plants used in traditional medicine. In a similar study, Fabricant and Farnsworth (2001) identified 122 compounds from 94 plant species, which are used globally as drugs, with 80% of these having an ethnomedical use identical or related to the current use of the active elements of the plant. Further evidence of the importance of natural products is provided by the fact that close to half of the bestselling pharmaceuticals in 1991 were either natural products or their derivatives (O'Neill and Lewis, 1993).There is an urgent need to identify novel, active chemotypes as leads for effective drug development, and, as was dramatically illustrated by the discovery of the "wonder" antibiotics of the 1940s and 1950s, nature is the prime source of such lead discoveries. It has however been estimated that only 5-15% of the approximately 250 000 species of higher plants have been systematically investigated for the presence of bioactive compounds (Balandrin *et al*., 1993). Dr. Norman Farnsworth stated in his closing remarks in his guest editorial on "An old source for new drugs" in the August 1995 issue of *Pharmaceutical Technology* that "the world of plants represents a virtually untapped reservoir of novel drugs awaiting imaginative and progressive organisations"(Farnsworth, 1995).

The success of natural products in drug discovery can be attributed to their high chemical diversity, biochemical specificity, greater number of chiral centres and increased steric complexity than either synthetic drugs or combinatorial libraries, and the effects of evolutionary pressure to create biologically active molecules by interactions with different proteins and biological targets (Wolfender, 2009; Queiroz *et al*., 2009). Some excellent examples of the potentials of natural products are as seen in the isolation of taxol, the anti-cancer agent from the Yew tree, *Taxus brevifolia* L. (Taxaceae) and artimisinin , the anti-malarial from *Artemisia annua* L. (Asteraceae). Other important natural product pharmaceuticals include quinine and quinidine from *Cinchona* spp., atropine from *Atropa belladonna*, vincristrine and vinblastine from *Catharanthus roseus*, digoxin from *Digitalis* spp. and morphine and codeine from *Papaver somniferum*.

2.3 Plants and Plant Metabolites with Antimycobacterial Activity World-wide

The use of plants and plant preparations for the treatment of diseases has been in existence since prehistory. There has been tremendous research all over the world in the search for novel antituberculosis agents. Natural plant products are potential antituberculosis agents. However, none of the drugs currently used as first or second line drugs in the chemotherapy of tuberculosis has its origin from plant natural products.

A guided methodological approach to the discovery of plant based drugs involves the following steps:

- Taxonomic identification of the plant
- Collection and drying of the vegetable material, precautions need to be taken to avoid the formation of artifacts
- Extraction of plant materials using different solvents
- Fractionation of the extracts
- Analysis of extracts and fractions by a combination of chromatographic methods
- Purity control of the isolated compounds
- Structure elucidation of the constituents by a combination of diverse spectroscopic techniques (UV/VIS, IR spectrophotometry, carbon and proton nuclear magnetic resonance, mass

spectroscopy), X-ray diffraction and chemical techniques (hydrolysis, formation of derivatives, degradation reaction etc)

- *In vitro* and/or *in vivo* screening model
- Pharmacological and toxicological assays (pre-clinical assays) (Queiroz *et al*., 2009; Hostettmann *et al*., 1997)

Many groups have taken to this research area with screening of plant extracts as a preliminary step towards discovering new antituberculosis compounds. Several literature reports on *in vitro* inhibition of different strains of *M. tuberculosis* by plant extracts are documented. In some review articles earlier published, several plants with antimycobacterial activity against tuberculosis were reported (Newton *et al*., 2000; Lall and Meyer, 1999; Gautam *et al*., 2007 and McGaw *et al*., 2008a).

Some excellent review articles have also been published on the classes of compounds with antimycobacterial activity. These compounds were grouped under different classes, such as alkaloids, terpenoids, coumarins/chromones, peptides and phenolics (Okunade *et al*., 2004; Copp, 2003; Copp and Pearce, 2007 and Cantrell *et al*., 2001).

A few of these plant metabolites are discussed below. These will be grouped into four broad classes;

1. Alkanes, alkenes, alkynes and simple aromatics
2. Phenolics and acetogenic quinines
3. Alkaloids
4. Terpenes and steroids

2.3.1 Alkanes, Alkenes, Alkynes and simple aromatics

i. Five monocyclo-pentenyl compounds with long alkyl side chains, isolated from the non polar extracts of the seeds of *Hydnocarpus anthminthica* were found to be active against BCG and *M. tuberculosis*. These compounds given the trivial names anthelminthicin A (**8**), anthelminthicin B (**9**), anthelminthicin C (**10**), chaulmoogric acid (**11**) and ethyl chaumoograte (**12**), were all active against both organisms at ≤ 16.8 µg/mL. Anthelminthicin C **(10)** was also found to inhibit the pathway between chorismate and para-aminobenzoic acid (PABA) with an MIC of 11.3 µM,

representing a new example of PABA inhibitor isolated from a natural source (Wang *et al*., 2010).

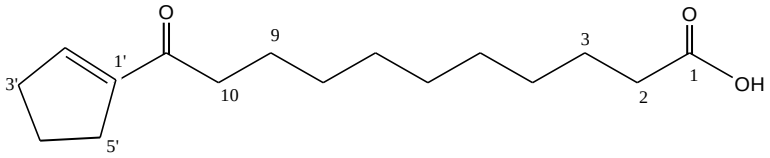

8

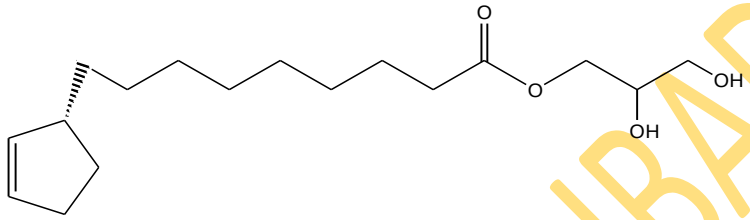

9

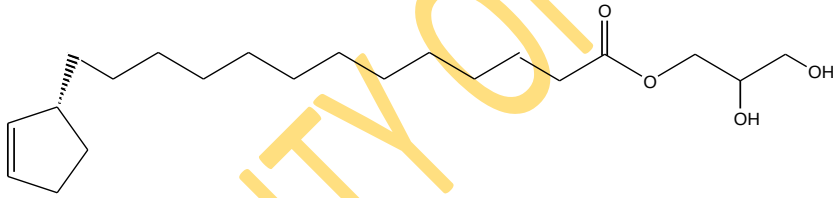

10

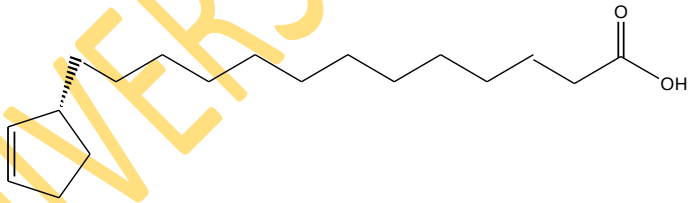

11

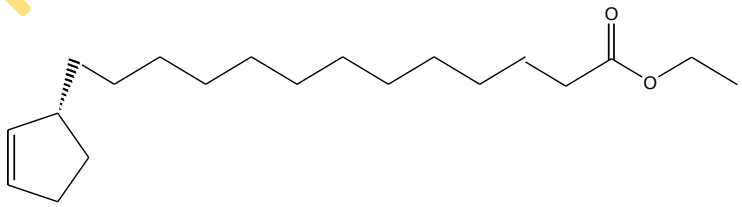

12

ii. Phytochemical investigations of the petroleum ether and chloroform extracts of the roots of *Angelica sinensis* led to the isolation and identification of five polyenes including fulcarindiol (**13**) and 9Z,17-octadecadiene-12,14-diyne-1,11,16-triol,1-acetate (**14**). These polyenes exhibited antituberculosis activity against two pathogenic strains of *M. tuberculosis* (Erdman and $H_{37}Rv$) *in vitro* in a Microplate Alamar Blue Assay (MABA). Compounds **13** and **14** were found to be most potent with MICs between 1.4 - 26.7 µg/mL against both strains (Deng *et al*., 2008).

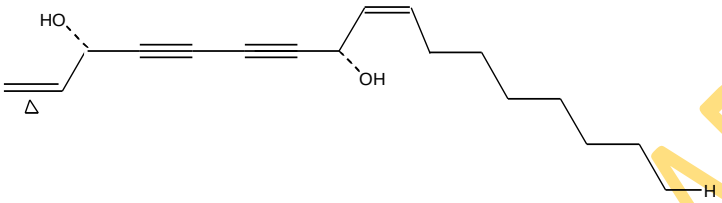

13

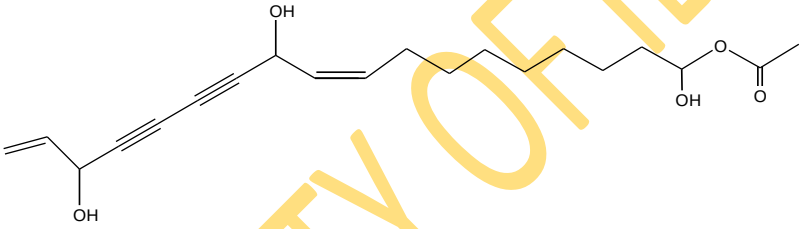

14

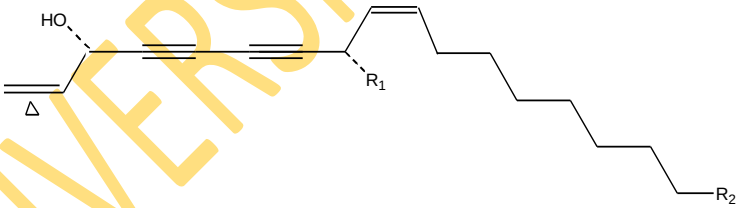

15 $R_1 = R_2 = H$

16 $R_1 = OH$, $R_2 = CH_2OAc$

17 $R_1 = OH$, $R_2 = H$, Δ saturated

18 $R_1 = OH$, $R_2 = CH_2OAc$, Δ saturated

Similarly, bio-assay guided fractionation of *Oplopanax horridus* (Devil's club), a medicinal plant of North America, led to the isolation of five polyynes including known falcarindiol (**13**) and falacrinol (**15**), and three new analogues (**16, 17** and **18**). All compounds were active against *M. tuberculosis* and an isoniazid resistant *M. avium*, at 10 µg/disc in a disc diffusion assay (Kobaisy *et al*., 1997). In a related study, Inui and co-workers (2007) investigated the synergistic

effects of the selected active regions of the crude extract of *O. horridus*, from Alaska. Using Counter Current Chromatography (CCC) as their isolation technique and MABA as the *in vitro* bioassay method, they observed significant synergist effects for the recombined fractions.

iii. A simple diyne (**19**), isolated from *Solidago canadensis* was found to inhibit *M. tuberculosis* $H_{37}Rv$ with an MIC of 25 µg/mL. A radiorespirometry bioassay was used in the evaluation (Lu *et al*., 1998).

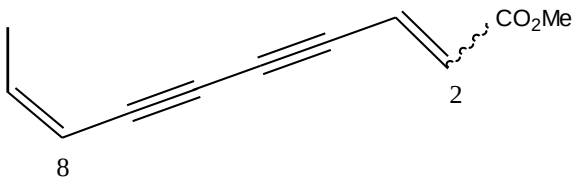

19

iv. *Cinnamomum kotoense*, a tree endemic to Taiwan, was shown to have antituberculosis activity and bio-guided fractionation of the active chloroform extract led to the isolation of active compounds, isoobtusilactone A (**20**) and lincomolide B (**21**) with MICs of 22.48 and 10.16 µg/mL, respectively. Agar dilution was employed as the method for bioassay. Rifampin was used as a positive control (Chen *et al*., 2005).

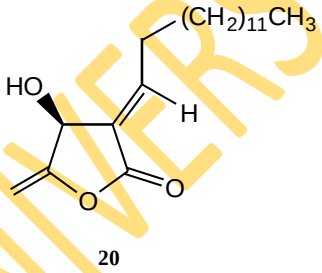

20

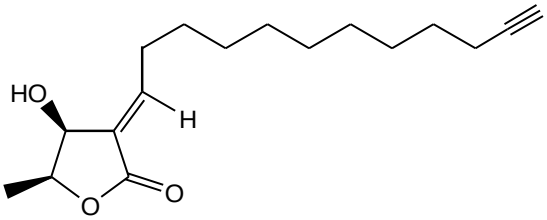

21

v. From the wood oil of a traditional Japanese tree *Chamaecyparis obtuse*, a simple di-α,β-unsaturated ketone (4,4-dimethyl-6-methylene-2-cyclohexen-1-one), yoshixol (**22**) was isolated and had activity against *M. chelonei* at an unspecified potency (Koyama *et al*., 1997).

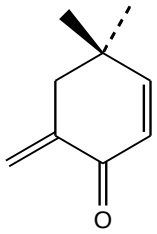

22

vi. Ma and co-workers (2005), in their study, isolated five new compounds, from the dichloromethane (CH_2Cl_2) extract of the stem bark of *Micromelum hirsutum*, a tree in Vietnam. One of the compounds isolated, a lactone, (-)-Z-9-octadecenel-4-olide (**23**), showed high *in vitro* activity against $H_{37}Rv$, with an MIC of 1.5 µg/mL. This compound also exhibited activity against the Erdman strain of *M. tuberculosis* with an MIC of 5.6 µg/mL. The bioassay method used was fluorometric microplate Alamar assay. It was also found to be mildly cytotoxic towards Vero cell line with an IC_{50} of 95 µg/mL.

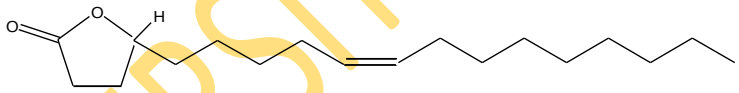

23

vii. The stem bark of *Mitrephora celebica*, a plant native to North Sulawesi, was evaluated for antituberculosis activity. Polyacetylene carboxylic acids, 13, 14-dihydrooropheic acid (**24**) and oropheic acid (**25**) were isolated and shown to be active against *M. smegmatis* with an MIC of 12.5 µg/mL (Zgoda *et al*., 2001).

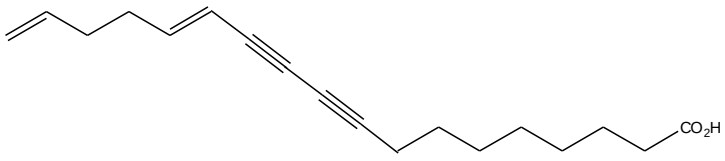

24

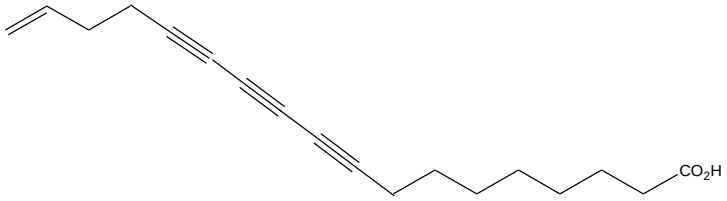

25

viii. Two phenylpropanoids (**26** and **27**) were isolated from *Pimpinella sp*, a Turkish plant and inhibited the growth of some *mycobacterium* species comprised of *M. intracellulare*, *M. smegmatis*, *M. aurum* and *M. phlei* with MICs between 1.25-10 µg/mL (Tabanca *et al*., 2005).

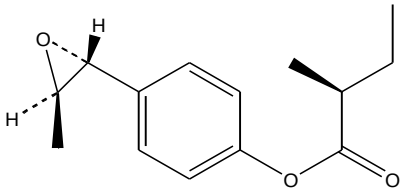

26

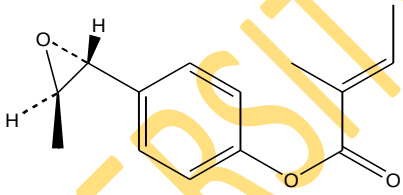

27

ix. The antimycobacterial activities of resin glycosides which occur in plants in the Convolvulaceae family have been reported. Chemically, these glycolipids are composed of a linear tetra- or pentaglycosidic oligosaccharide unit and one or more fatty acids. Sometimes, the carboxylic acid function of the fatty acid attacks the hydroxyl group of another sugar to generate a macrocyclic lactone structure. The oligosaccharide moiety often bears acylations with a wide range of organic acids. Four new partially acylated tetrasaccharides of 11-hydroxyhexadecanoic acid (**28**-**31**) were isolated from a methanol extract of *Ipomoea tyrianthina*. All compounds were active against H_{37}Rv strain of *M. tuberculosis* with an MIC of 25 µg/mL. MABA was employed in the bioassay technique (León-Rivera et *al*., 2008). In another related study, resin glycosides and other

metabolites isolated from *Scrophularia cryptophila* were screened for antimycobacterial activities, but did not have any significant activities (≥100 µg/mL) (Tasdemir *et al*., 2008).

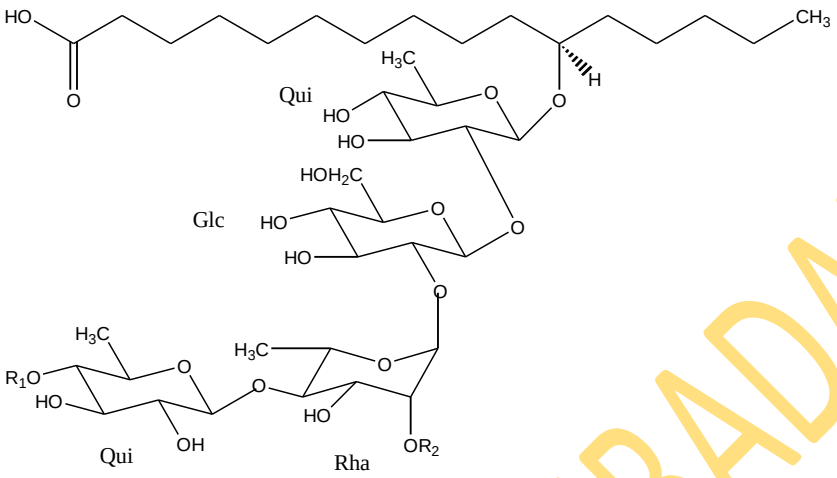

28 R_1 = nil, R_2 = mba

29 R_1 = tig, R_2 = mba

mba= 2-methylbutanoyl, nil= 2-methyl-3-hydroxybutanonyl, tig= 2-methylbutenoyl

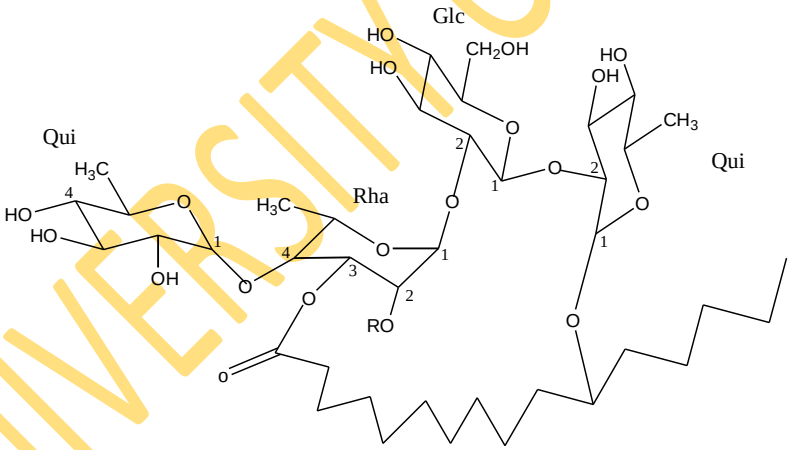

30 R = 2-methylbutenoyl

31 R = propanoyl

2.3.2 Phenolics and Quinones

i. The ethyl acetate and methanol extracts of *Butea monosperma* were found to be active against *M. tuberculosis* H_{37}Ra, using MABA as the screening technique. Twelve flavonoids were isolated, subjected to antimycobacterial evaluation and chalcone butein (**32**) exhibited the highest activity with an MIC of 12.5 µg/mL. The activity of other flavonoids was between 25 and 100 µg/mL.

The assay results indicated that the presence of glucosidic moiety tended to decrease the activity of the flavonoid aglycone and also, the absence of α, β olefinic system decreased the biological activity (Chokchaisiri *et al*., 2009).

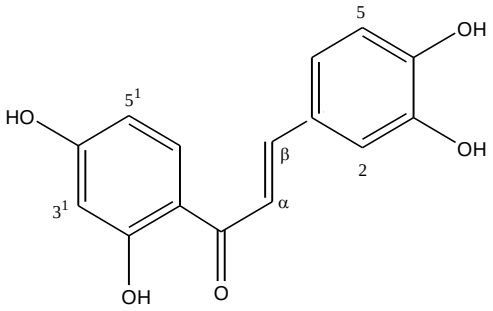

32

ii. Six structurally diverse phenolic compounds were isolated from the root bark of *Artocarpus rigidus*. All were active against *M. tuberculosis* at ≤ 100 µg/mL. However, the most active was a flavonoid, Artonin F (**33**) with an MIC of 6.25 µg/mL. This compound was also found not cytotoxic when screened against three different human cell lines (Namdaung *et al*., 2006).

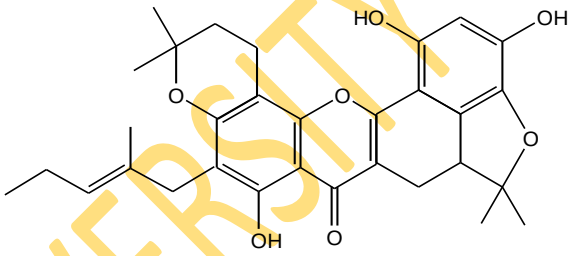

33

iii. Three acylphenols; malabaricone A (**34**), dodecanoylphloroglucinol (**35**) and 1-(2,4,6-trihydroxyphenyl)-9-phenylnonan-1-one (**36**), isolated from *Knema glauca*, a tropical tree native to Thailand, were found to be active *in vitro* against $H_{37}Ra$ strain of *M. tuberculosis* with MIC values of 25, 50 and 100 µg/mL, respectively. MABA was employed as the bioassay technique, with isoniazid and kanamycin sulfate used as positive control (Rangkaew *et al*., 2009).

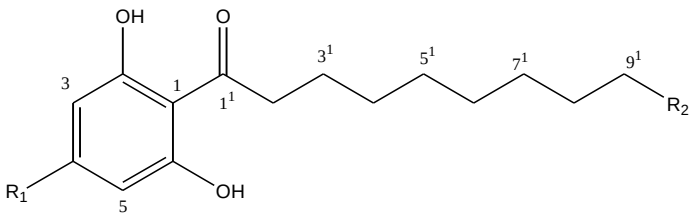

34 R_1 = H, R_2 = 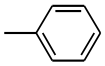

35 R_1 =OH, R_2 = $-CH_2CH_2CH_3$

36 R_1 = OH, R_2 = 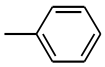

iv. Bioassay-guided fractionation of the ethyl acetate and methanol extracts from the flowers of *Goniothalamus laoticus*, a Thai medicinal plant, led to the isolation of some bioactive compounds including three styryllactone derivatives; gonotriol (**37**), (+)-altholactone (**38**) and howiinin A (**39**). These compounds exhibited antimycobacterial activity against *M. tuberculosis* H_{37}Ra at 100, 6.25 and 6.25 µg/mL, respectively. MABA was the technique of assay (Lekphrom *et al*., 2009).

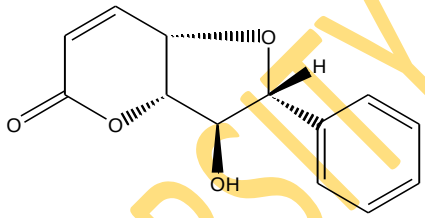

37

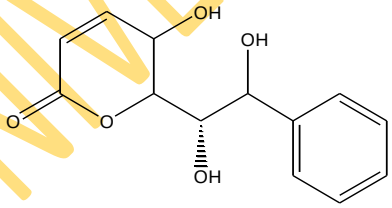

38

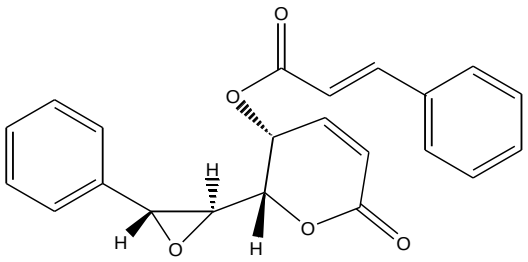

39

v. Agrawal and co-workers (2008), in their studies on the rhizomes of *Curcuma longa*, an ethnomedicinal plant used in India, identified demethoxycurcumin (**40**) as the compound responsible for the antituberculosis activity of the extracts. It was found to be active at 200 µg/mL when screened for *in vitro* antituberculosis activity employing the BACTEC 460 radiometric susceptibility assay against *M. tuberculosis* $H_{37}Rv$. Semi-synthetic modifications of demethoxycurcumin yielded a novel lipophilic analogue, 4-{4-[7-(3-methoxy-4-methylphenyl)-3,5-dioxohepta-1,6-dienyl]-phenoxy}-but-2-enoic acid ethyl ester (**41**), which was twenty five times more active at 7.8 µg/mL. The objective of the synthesis was to increase the lipophilicity of the compound by attaching fatty acid ester chains at the phenolic hydroxyl groups. This further suggested that lipophilicity aided the transport of compounds across the outer lipid layer of mycobacteria.

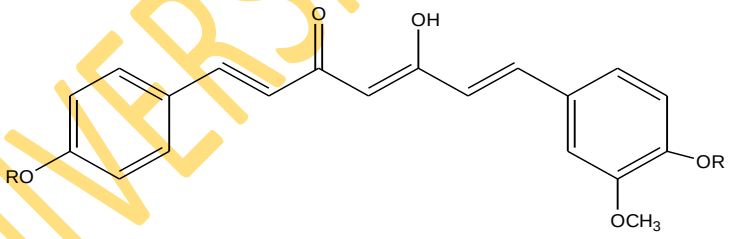

40 R = H

41 R = CH_2-CH=CH-$COOCH_2CH_3$

vi. Bio-assay guided fractionation of the ethanolic extract of *Nuclea natelensis*, using bio-autobiographic TLC assay led to the isolation of shinanolone (**42**), as the active principle against a drug sensitive strain of *M. tuberculosis* (MRC strain no. $H_{37}Rv$ ATCC27294). However, it was only found to be sensitive at 0.1 mg/mL (Weigenand *et al*., 2004).

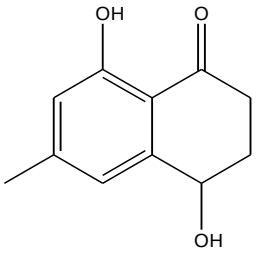

42

In a similar study, Mcgaw *et al*. (2008b), isolated four naphthoquinones and a triterpenoid from the roots of *Nuclea natalensis*. The naphthoquinones; shinanolone (**42**), diospyrin (**43**), nordiospyrin (**44**) and 7-methyljuglone (**45**) showed activities against five different fast and slow growing *mycobacterium* species screened. 7-methyljulone was the most active with MICs of 1.71, 2.44, 41.67, 33.69 and 8 µg/mL against *M. bovis*, *M. smegmatis*, *M. fortuitum*, *M. bovis* BCG and *M. tuberculosis*, respectively. MTT based microtitre plate assay was used for screening the compounds.

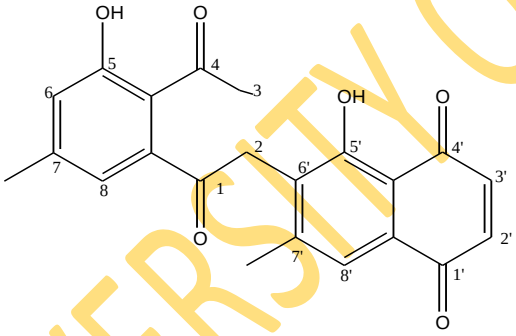

43

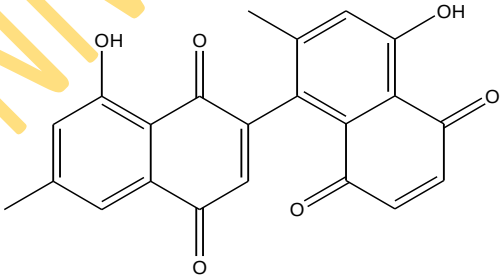

44

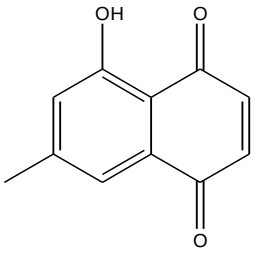

45

vii. An isoflavanquinone, abruquinone B (**46)**, was isolated from the aerial parts of *Abrus precatorius*, and inhibited *M. tuberculosis*, $H_{37}Ra$, at a concentration of 12.5 µg/mL. MABA was the technique, and isoniazid and kanamycin sulphate were the reference compounds for antimycobacterial assay. This was the first report of the antituberculosis activities of isoflavanquinones (Limmatvapirat *et al*., 2004).

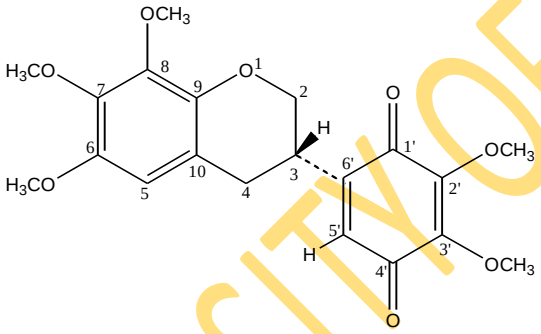

46

viii. The n-hexane and dichloromethane extracts of the above-ground biomass and roots of *Valeriana laxiflora*, collected in Chile, led to the isolation of nine compounds of which seven compounds including three known flavones showed antituberculosis activity against *M. tuberculosis* $H_{37}Rv$. The flavones, 5,7-dihydroxy-3,6,4´-trimethoxyflavone (**47**), tricin (**48**), and 5,7,3´-trihydroxy-4´-methoxyflavone (**49**) had MIC values of 46.2, 58.5 and >128 µg/mL, respectively. The bioassay method was MABA. Rifampicin was used as a positive control. However, the most active compounds in the assay were also cytotoxic to the Vero cells (Gu *et al*., 2004).

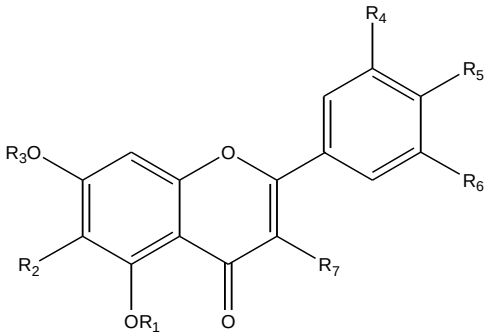

47 R_1 = H, R_2 = OMe, R_3 = H, R_4 = H, R_5 = OMe, R_6 = H, R_7 = OMe

48 R_1 = R_2 = R_3 = H, R_4 = OMe, R_5 = OH, R_6 = OMe, R_7 = H

49 R_1 = R_2 = R_3 = R_4 = H, R_5 = OMe, R_6 = OH, R_7 = H

ix. Studies on the rhizome of *Zingiber officinale* led to the isolation of three bioactive gingerol analogues, 6-gingerol (**50**), 8-gingerol (**51**) and 10-gingerol (**52**) with the latter two being more active with MIC values of 25-50 µg/mL against *M. tuberculosis* and *M. avium* (Hiserodt *et al*., 1998).

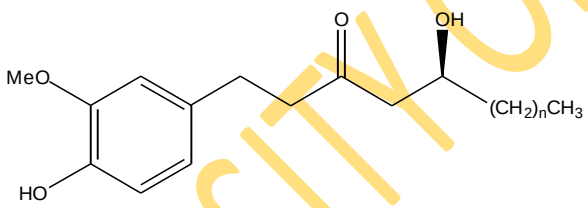

50 n=4

51 n=6

52 n=8

x. Licochalcone A (**53**), a compound isolated from Chinese licorice roots, showed promising *in vitro* inhibitory effect against human pathogenic strains of *mycobacterium* species including *M. tuberculosis*, *M. bovis* and BCG within the range of 5-20 µg/mL. It was however less active against other *M. tuberculosis* complex species (*M. avium* and *M. intracellulare*) within the range of 20-80 µg/mL (Friis-Møller *et al*., 2002).

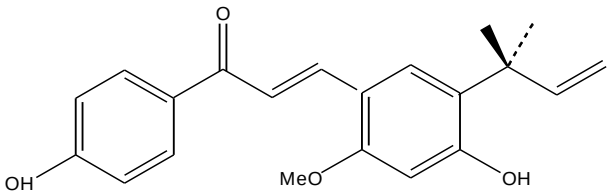

53

xi. Four isoflavonoids were isolated from the root bark of *Erythrina indica* and screened against *M. smegmatis*. One of the novel compounds, a 3-phenylcoumarin metabolite, named indicanine B (**54**) inhibited the growth of *M. smegmatis* with an MIC of 18.5 µg/mL (Waffo *et al*., 2000).

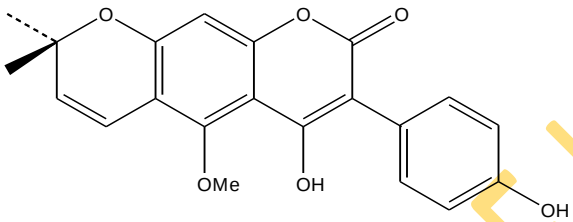

54

xii. Studies on *Erythrina gibbosa*, a Panamanian plant also led to the isolation of two bioactive flavonoids, paseollidin (**55**) and erythrabyssin II (**56**), which exhibited activity against *M. tuberculosis* within the MIC range of 8-25 µg/mL (Mitscher and Baker, 1998a).

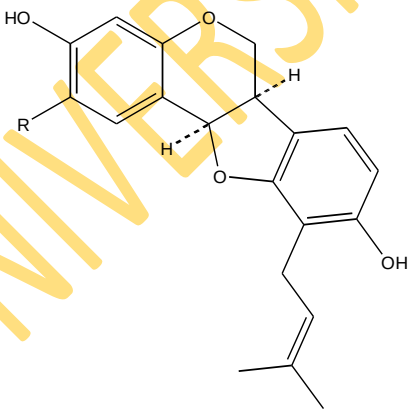

55 R = H

56 R = 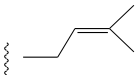

xiii. Of several antimycobacterial compounds isolated in a vast study on some Mexican plants, four phenolics (**57-60**) isolated from *Iostephane heterophylla* (**57**), *Rumex hymenosepalus* (**58** and **59**), and *Larrea divaricata* (**60**) were active against *M. tuberculosis* $H_{37}Rv$ at 16, 128, 128 and 50 µg/mL, respectively in a radiorespirometric assay. The enhanced bioactivity (MIC 32 µg/mL) of the semi-synthetic 4-acetoxy derivative of **58** was presumably due to better cell membrane penetration resulting from increased lipophilicity (Rivero-Cruz *et al*., 2005).

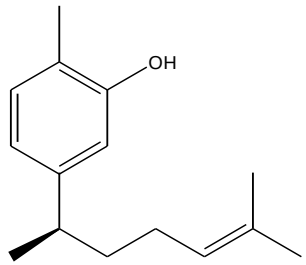

57

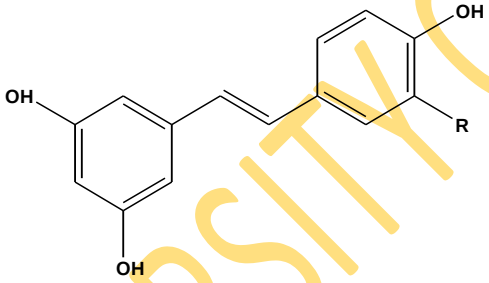

58 R = H

59 R = OH

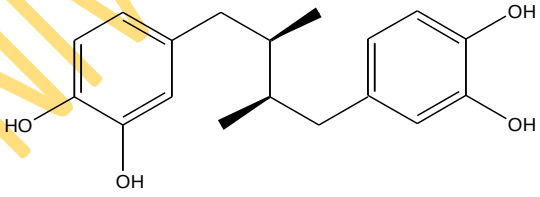

60

In the same study, two flavonoid compounds (**61** and **62**) isolated from *Larrea divaricata* recorded some activity towards *M. tuberculosis* $H_{37}Rv$ at 50 µg/mL (Rivero-Cruz *et al*., 2005). Related analogues (**63** – **65**) isolated from the crude extracts of *Haplopappus sonorensis*, also

showed activity against *M. tuberculosis* $H_{37}Rv$. 5-hydroxy-3,7,4'-trimethoxyflavone (**63**), 5,7-dihydroxy-3,4'-dimethoxyflavone (**64**) and 5,4'-dihydroxy-3,7-dimethoxyflavone (**65**) were identified as the antimycobacterial principles by assay-guided fractionation. Compound **64** was the most active compound, inhibiting the organism at 98% at a concentration of 100 µg/mL (Murillo *et al*., 2003).

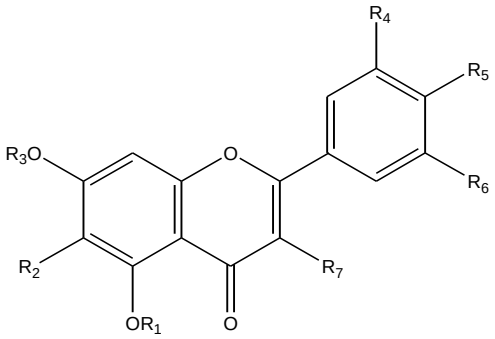

61 $R_1 = R_2 = R_3 = R_4$, R_5 = OMe, R_6 = H, R_7 = OMe

62 R_1 = H, R_2 = OH, $R_3 = R_4$ =H, R_5 = OMe, R_6 = H, R_7 = OMe

63 $R_1 = R_2$ =H, R_3 = Me, R_4 = H, R_5 =OMe, R_6 = H, R_7 = OMe

64 $R_1 = R_2 = R_3 = R_4$ =H, R_5 =OMe, R_6 = H, R_7 = OMe

65 $R_1 = R_2$ = H, R_3 = Me, R_4 = H, R_5 = OH, R_6 = H, R_7 = OMe

xiv. Investigations on the antimycobacterial properties of *Senna oblique*, a shrub located in Ecuador and Peru led to the bio-assay guided fractionation of the methanol extracts of the stem and fruits. Quinquangulin (**66**) and rubrofasarin (**67**), two known tricyclic naphthopyrones were isolated and reported to be active against *M. tuberculosis* in a radiometric culture at 12 µg/mL. This was the first report of naphthopyrones associated with this activity (Graham *et al*., 2004).

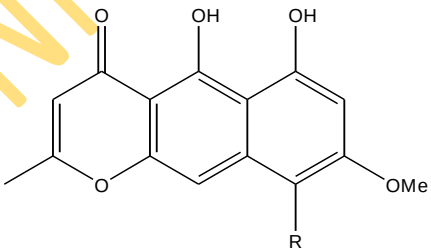

66 R = Me

67 R = H

xv. Combretastatins D-3 (**68**), a macrocyclic lactone was isolated from the dichloromethane extract of the stems of *Getonia floribunda*, a woody climber commonly found in Thailand. It was found to be active against *M. tuberculosis* $H_{37}Ra$ with an MIC of 100 µg/mL employing MABA technique (Vongvanich *et al*., 2005).

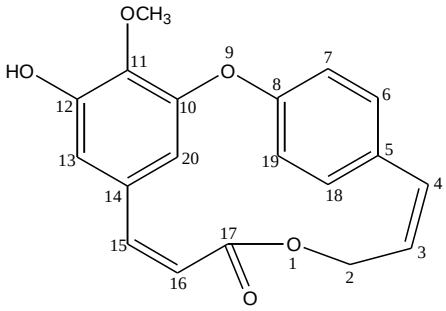

68

xvi. *Eriosema chinense* (leguminosae-Papilionoideae) is a plant of the only species of its genus found in Thailand. The roots were investigated for phytochemical profile and biological activities. Fourteen prenylated flavonoids were isolated and evaluated for antimycobacterial activity against *M. tuberculosis* $H_{37}Rv$ employing MABA as the choice of bioassay. Four of the isolates, three flavanones and one flavonol (**69**-**72**), were found most active with MICs of 12.5 µg/mL. One of the flavanones (**69**), with a linear pyrano ring, was found more cytotoxic against two human cell lines than **72**, its regioisomer with an angular pyrano ring (Sutthivaiyakit *et al*., 2009).

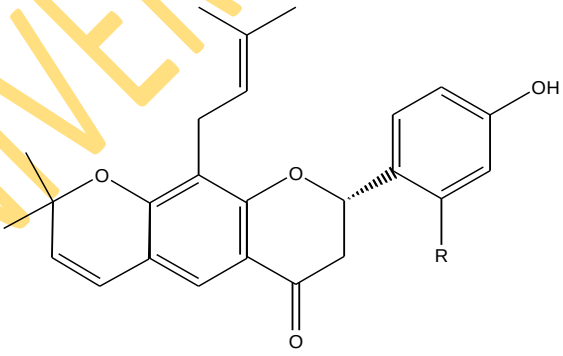

69 R = OH

70 R = H

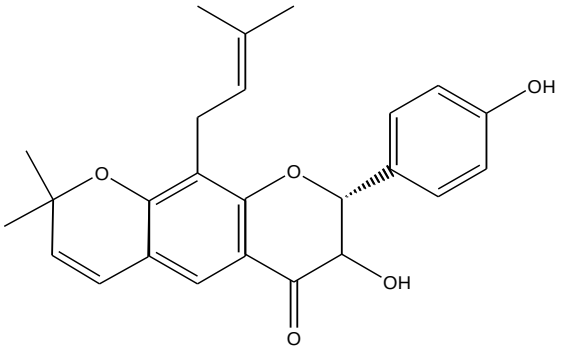

71

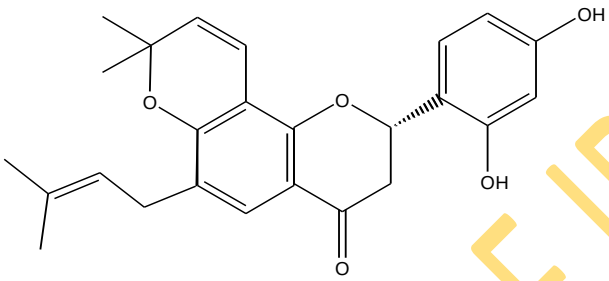

72

xvii. The stem bark of *Combretum molle*, a tree with a reputation in Ethiopian traditional medicine but widespread throughout tropical Africa southwards to South Africa and also Yemen, was extracted using acetone as one of the solvents. The extract showed inhibitory activity against *M. tuberculosis* at concentrations higher than 1.0 mg/mL. Further purification led to the isolation of punicalagin (**73**), a known tannin, as the active compound against *M. tuberculosis*. This compound inhibited two strains of *M. tuberculosis*, ATCC 27294 and a patient strain at concentrations higher than 600 µg/mL and 1.2 mg/mL, respectively. This was supposedly the first report of a tannin exhibiting antimycobacterial activity (Asres *et al*., 2001).

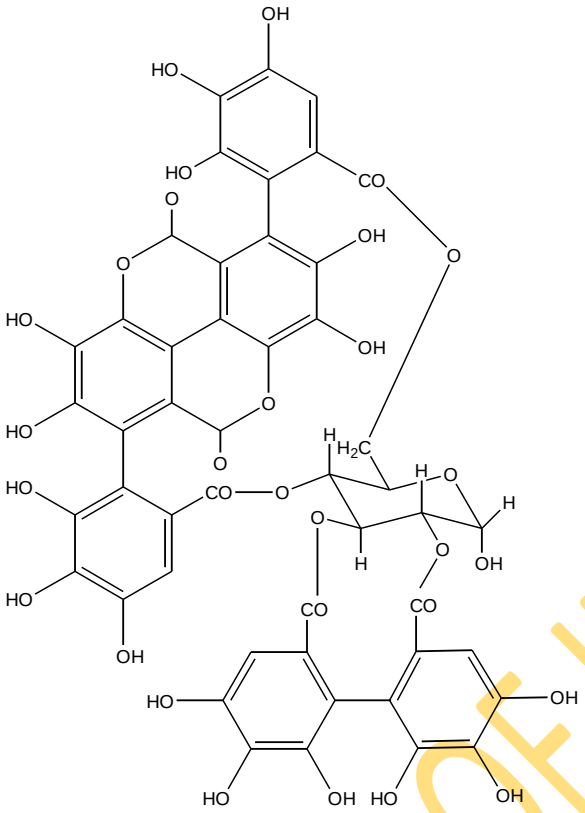

73

2.3.3 Alkaloids

i. A pentacyclic alkaloid, (-)nordicentrine (**74**) was one of the compounds isolated from the flowers of *Goniothalamus laoticus* in a bioassay-guided fractionation of the ethyl acetate and methanol extracts. It was found to be active against *M. tuberculosis* H_{37}Ra at 12.5 µg/mL (Lekphrom *et al*., 2009).

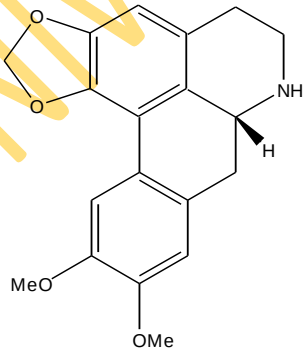

74

ii. Bioassay-directed fractionation of the organic extract of the whole plant *Xanthorhiza simplicissima* led to the isolation of the known alkaloid, berberine (**75**) as the major active antimycobacterial component against *M. intracellularae* with an MIC of 0.78-1.56 µg/mL (Okunade et *al*., 1994). Similarly, berberine was shown to inhibit *M. smegmatis* and *M. tuberculosis* with an MIC of 25 µg/mL (Gentry *et al*., 1998; Mitscher and Baker, 1998b).

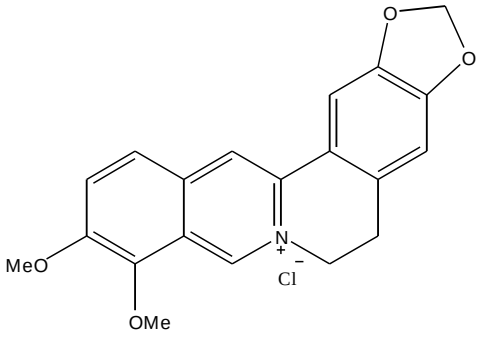

75

iii. Five quinolone alkaloids (**76-80**), isolated from unripe fruit of *Evodia rutaecarpa*, were shown to be active against some fast-growing mycobacteria (*M. fortuitum*, *M. smegmatis*, and *M. phlei*) with MICs of 2-32 µg/mL (Adams *et al*., 2005).

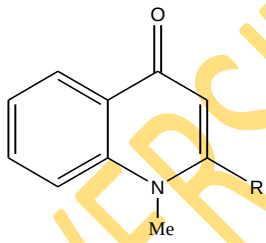

76 R = n-$CH_{11}H_{23}$

77 R =

78 R =

79 R =

80 R =

iv. Out of the fourteen compounds isolated from the stem and leaves of *Piper sanctum*, three tetracyclic alkaloids, cepharanone B (**81**), piperolactam A (**82**) and cepharadione B (**83**)

exhibited good activity against *M. tuberculosis* $H_{37}Rv$, with MICs of 12, 8 and 32 µg/mL, respectively using the MABA assay (Mata *et al*., 2004).

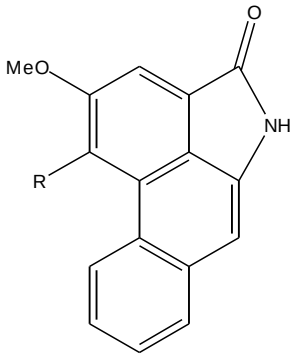

81 R = OMe

82 R = OH

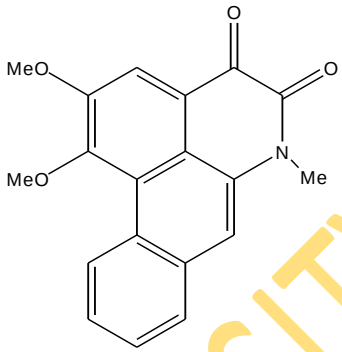

83

v. Six known carbazoles were isolated from the roots and rhizomes of *Clausena excavata* and showed activity against *M. tuberculosis* with MICs ≤ 100 µg/mL. The most active carbazole was 3-methoxycarbonylcarbazole (**84**) with an MIC of 50 µg/mL (Sunthitikawinsakul *et al*., 2003). In a similar study, six out of the seven compounds isolated from the dichloromethane extract of *Micromelum hirsutum* were substituted carbazoles, of which four (**85-88**) were active against *M. tuberculosis* within the MIC range of 14.3-42.3 µg/mL. **85**, **86** and **87** were also found to be moderately selective against the Vero cell line (Ma *et al*., 2005).

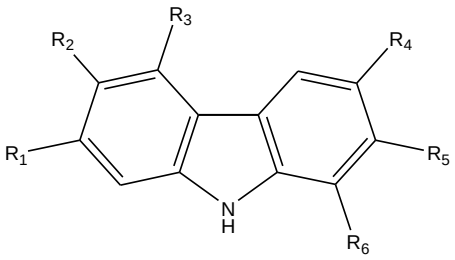

84 $R_1 = R_2 = R_3 = H$, $R_4 = CO_2Me$, $R_5 = R_6 = H$

85 $R_1 = H$, $R_2 = OH$, $R_3 =$ prenyl, $R_4 = CHO$, $R_5 = R_6 = H$

86 $R_1 = H$, $R_2 = OMe$, $R_3 = H$, $R_4 = CHO$, $R_5 = OH$, $R_6 = H$

87 $R_1 = R_2 = R_3 = H$, $R_4 = CHO$, $R_5 = R_6 = H$

88 $R_1 = H$, $R_2 = OMe$, $R_3 = H$, $R_4 = CHO$, $R_5 = R_6 = H$

vi. A pyrole alkaloid, solsodomine A (**89**), isolated from the fresh berries of *Solanum sodomaeum*, was found to be active against *M. intracellulare* with an MIC of 10 µg/mL (El sayed *et al*., 1998).

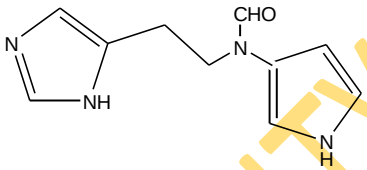

89

2.3.4 Terpenes

Terpenoids constitute a major class of natural products isolated from higher plants. In their review of antimycobacterial plant terpenoids, Cantrell *et al*. (2001), observed some structural similarities that were important for high activity. Under the different classes of terpenes, lipophilic compounds were found to be more active than the more polar ones. This was attributed to the fact that these compounds being of moderate to high lipophilicity will permeate the lipid mycobacterial cell wall more easily.

2.3.4.1 Monoterpenes

Pyrethrin I (**90**) and II (**91**) were isolated through the bioassay-directed fractionation of the organic extracts of a Kenyan collection of *Chrysanthemum cinerariaefolium*, as the major antimycobacterial constituents. The compounds exhibited growth inhibition of *M. tuberculosis* $H_{37}Rv$ with MIC values of 64 and 32 µg/mL, respectively (Rugutt *et al*., 1999).

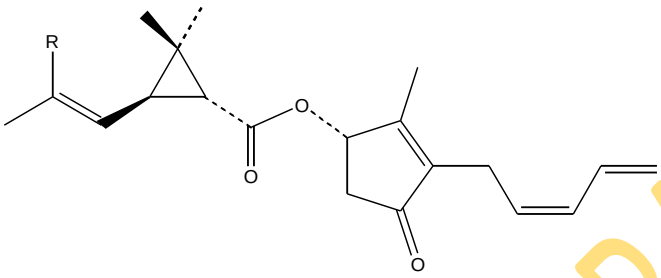

90 R = Me

91 R = CO_2Me

2.3.4.2 Sequisterpenes

i. Bioassay guided fractionation of the active crude extract of *Warburgia salutaris* yielded a fraction that showed enhanced antimycobacterial activity as well as inhibitory activity against purified, recombinant mycobacterial arylamine N-acetyltransferase (NAT), an enzyme involved in mycobacterial cell wall lipid synthesis. The strains used were *M. tuberculosis* $H_{37}Rv$ and *M. bovis* Pasteur. Further purification resulted in the isolation of a major component in the fraction, a novel drimane sequisterpenoid lactone, 11α-hydroxycinnamosmolide (**92**). However, the activity of the compound could not account for the overall activity of the antimycobacterial fraction (Clarkson *et al*., 2007).

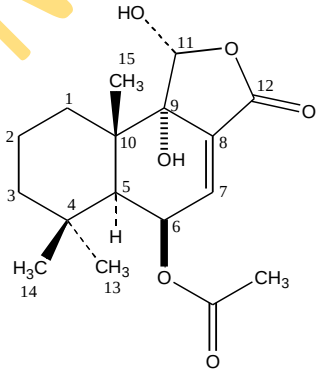

92

ii. The roots and aerial parts of *Juniperus communis* were investigated for antimycobacterial activity and the activities of the n-hexane extracts were attributed to three terpenoids including a sequisterpene identified as longifolene (**93**). The bioassay techniques used were MABA and LORA (Gordien *et al*., 2009).

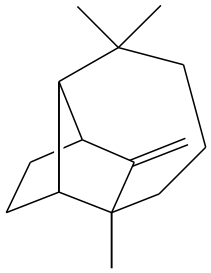

93

2.3.4.3 Diterpenes

i. E-phytol (**94**), of terpenoid origin, was isolated from the methanol extract of a Kenyan shrub, *Leucas volkensii* and the hexane extract of a Philippines collection of *Morinda citrifolia* as one of the antituberculosis components with MICs of 2 and 32 µg/mL, respectively. Semi-synthetic analogues were also made and tested for their antimycobacterial activity. It was shown that the Δ^2 unsaturation may not be necessary for activity, but the overall polarity of the molecule was clearly important (Rajab *et al*., 1998; Saludes *et al*., 2002). In another related study, the phytochemical investigation of the leaves of *Pourthiaea lucida*, a tree endemic to Taiwan, led to the isolation of thirteen compounds of which (E)-phytol was found to be the most active against $H_{37}Rv$ at 12.5 µg/mL. The agar dilution method was employed in the biological assay (Chen *et al*., 2010).

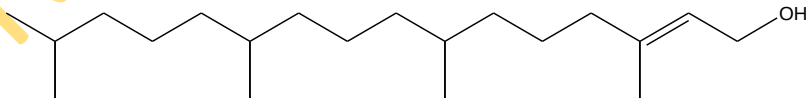

94

ii. *Sapium haematospermum* Mull (Euphorbiaceae), a plant native to the drier regions of South America, was extracted with dichloromethane: methanol (1:1), and bio-assay directed fractionation of the extract led to the isolation of fourteen compounds, out of which two were

diterpenes, lecheronol A (**95**) and B (**96**). These diterpenes exhibited activity against *M. tuberculosis* with MIC's of 4 and 128 µg/mL, respectively (Woldemichael *et al*., 2004).

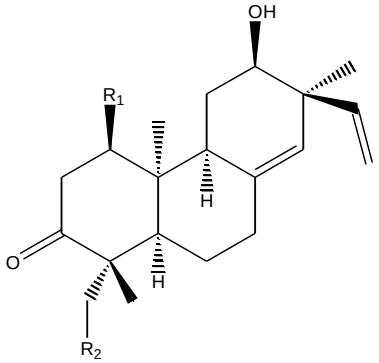

95 R_1 = OH, R_2 = H

96 R_1 = H, R_2 = OH

iii. *Juniperus communis* is a coniferous shrub distributed throughout the Artic and temperate zones of the Northern hemisphere. In the investigations of the roots and aerial parts for antimycobacterial activity, the activities of the n-hexane extracts were attributed to a sequisterpene identified as longifolene (**93**) and two diterpenes, characterized as totarol (**97**) and trans-communic acid (**98)**. *In vitro* bioassays were carried out against different types of mycobacteria; non-tuberculous mycobacteria, *M. tuberculosis* H_{37}Rv and drug resistant variants, and non-replicating persistent *M. tuberculosis* H_{37}Rv. Totarol was found to be most active against all mycobacteria with activities ranging between 2 and 23.9 µg/mL. However, cytotoxicity studies carried out showed it to be relatively toxic towards mammalian cells with a selectivity index calculated to be < 10. The authors confirmed their initial assumption that active metabolites could be produced as defensive agents due to evolutionary pressures in the unique ecosystem in which mycobacteria thrive (Gordien *et al*., 2009).

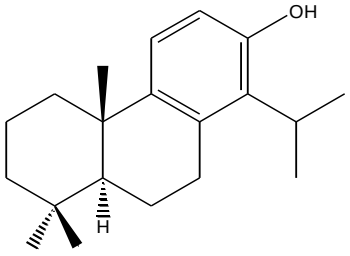

97

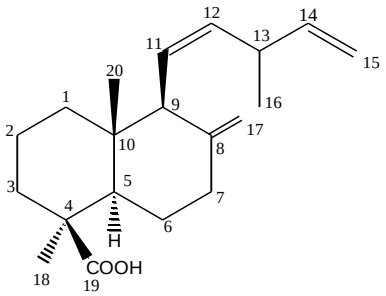

98

iv. A diterpene acid, kaurenoic acid (**99**), was isolated from the leaves of *Pleurothyrium cinereum*, a plant native to Columbia, and was found active against *M. tuberculosis* H_{37}Rv employing MABA as the assay method. It induced 91.3% and 88.6% growth inhibition at 50 µg/mL and 25 µg/mL, respectively (Coy *et al.*, 2009).

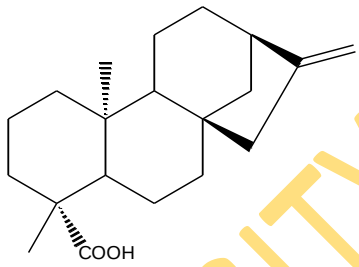

99

v. Seven new diterpenoids isolated from the roots of *Salvia multicaulis*, a plant endemic to the Middle East were tested against *M. tuberculosis* H_{37}Rv using the broth microdilution method. All compounds; multicaulin (**100**), 12-demethylmulticaulin (**101**), multiorthoquinone (**102**) , 2-demethylmultiorthoquinone (**103**), 12-methyl-5-dehydrohorminone (**104**), 12-methyl-5-dehydroacetylhorminone (**105**) and salvipimarone (**106**) were significantly active with MICs between 0.46 and 5.6 µg/mL, comparative to the standard first line drugs, such as rifampicin, streptomycin and ethambutol. 12-demethylmulticauline (**101**) was the most active with an MIC of 0.46 µg/mL (Ulubelen *et al.*, 1997).

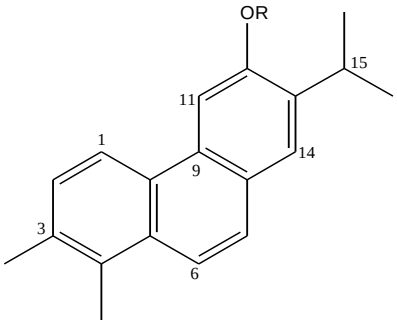

100 R = Me

101 R = H

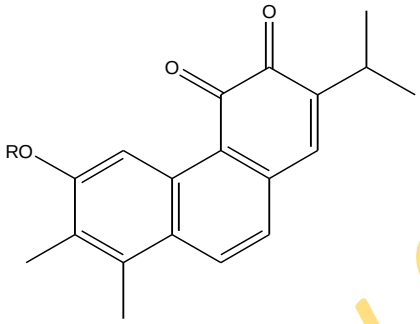

102 R= Me

103 R = H

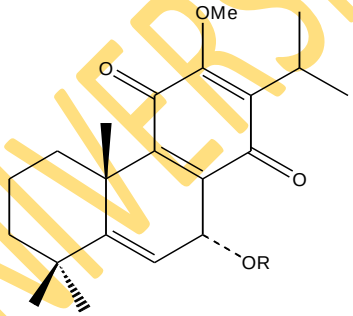

104 R = H

105 R = Ac

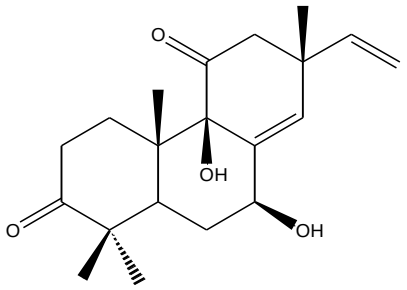

106

2.3.4.4 Triterpenes and Sterols

i. Zeorin (**107**), a triterpenoid of the hopane series, was isolated from the plant *Sarmienta scandens* and inhibited *M. tuberculosis* $H_{37}Rv$ with an MIC of 8 µg/mL. The regioisomeric 7β, 22-diol (**108**) and monoacetate (**109**) were found inactive (MIC > 128 µg/mL) in the same assay (Wächter *et al*., 1999).

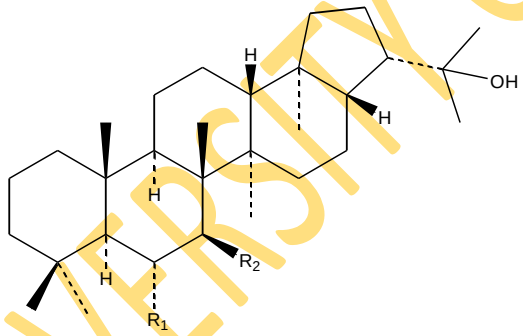

107 R_1 = OH, R_2 = H

108 R_1 = H, R_2 = OH

109 R_1 = H, R_2 = OAc

ii. Lupane type triterpenoids have also been reported to exhibit antimycobacterial activity. Betulin (**110**) *and* betulinic acid (**111**) isolated from *Valeriana laxiflora* (Gu *et al*., 2004), and analogue (**112**) isolated from *Sapium haematospermum* possessed varying degrees of activity towards *M. tuberculosis* with MICs of 30.0, 62.1 and 13.4 µg/mL, respectively (Woldemichael *et al*., 2004).

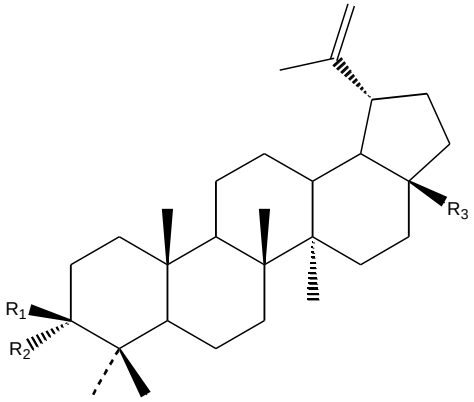

110 R_1 = OH, R_2 = H, R_3 = CH_2OH

111 R_1 = OH, R_2 = H, R_3 = COOH

112 R_1 = H, R_2 = OH, R_3 = Me

iii. The ubiquitous oleanane triterpenoids have been reported from many sources to exhibit antimycobacterial activity. Oleanolic acid (**113**) has been isolated from *Junellia tridens* (Caldwell *et al*., 2000), Latin American *Valeriana laxiflora* (Gu *et al*., 2004), Mexican *Lantana hispida* (Jiménez-Arellanes *et al*., 2007) and South African *Buddleja saligna* (Bamuamba *et al*., 2008) and reported as inhibiting the growth of *M. tuberculosis* with MICs of 50 µg/mL, 50 µg/mL, 25 µg/mL and 5 µg/disk, respectively. Related known oleanolic acid analogues (**114-117**), isolated from *Sapium haematospermum* also exhibited variable activity towards *M. tuberculosis* with MIC values of 12.2, 64, >128 and >128 µg/mL, respectively (Woldemichael *et al*., 2004). Other oleanane type triterpenoids, isolated from *Junellia tridens* were also reported to be active against *M. tuberculosis* (Caldwell *et al*., 2000). This compound and its derivatives also showed good selectivity against Chinese Hamster Ovarian (CHO) cell line suggesting their potential pharmaceutical value (Bamuamba *et al*., 2008).

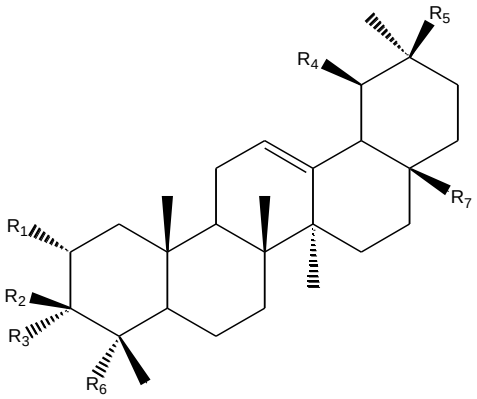

113 R_1 = H, R_2 = OH, R_3 = R_4 = H, R_5 = R_6 = Me, R_7 = COOH

114 R_1 = R_2 = H, R_3 = OH, R_4 =H, R_5 = R_6 = R_7 = Me

115 R_1 = H, R_2 = OH, R_3 = R_4 = H, R_5 = R_6 = R_7 = Me

116 R_1 = R_2 = H, R_3 = OH, R_4 = Me, R_5 = H, R_6 = R_7 = Me

117 R_1 = R_2 = OH, R_3 = R_4 = R_5 = H, R_6 = CH_2OH, R_7 = COOH

Two other oleanane derivatives were also isolated from the hexane extract of *Lantana hispida*. These compounds characterized as 3-acetoxy-22β-(2[1]-methyl-2Z-butenoyloxy)-12-oleanene-28-oic acid (**118**) and 3-hydroxy-22β-(2[1]-methyl-2Z-butenoyloxy)-12-oleananen-28-oic acid (**119**), were both active against H_{37}Rv strain of *M. tuberculosis* with MICs of 50 µg/mL. The compounds were also active against the first line resistant strains of *M. tuberculosis* (Jiménez-Arellanes *et al*., 2007).

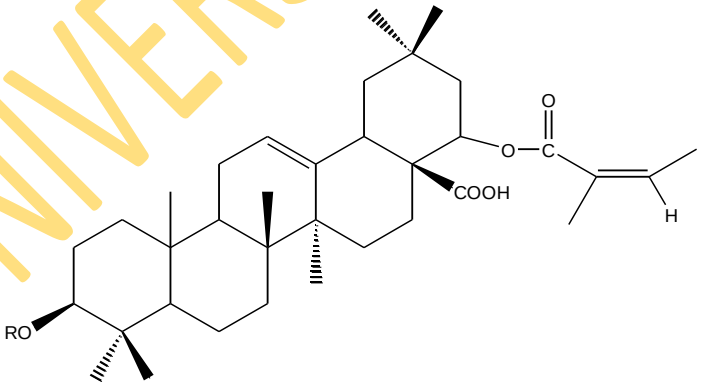

118 R = $COCH_3$

119 R = H

iv. Ursane type skeleton of triterpenoids are found in many plants. They have also been reported to exhibit antimycobacterial activity. Ursolic acid (**120**) was isolated from South African *Leyssera gnaphaloides* with MIC of 5µg/disc in a disc diffusion method (Bamuamba *et al*., 2008), and also with its analogue, 24-hydroxyursolic acid (**121**), isolated from *Valeriana laxiflora* (Gu *et al*., 2004), with MICs of 41.9 and 15.5 µg/mL, respectively.

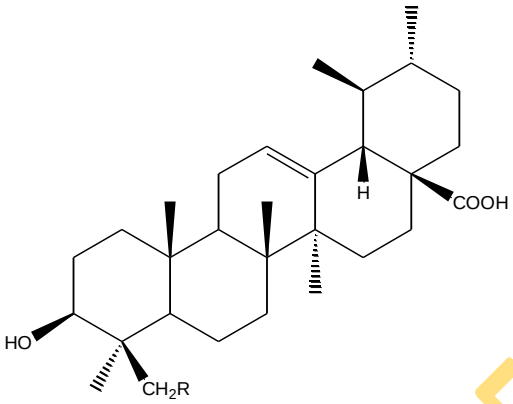

120 R = H

121 R = OH

v. From the leaves of *Elatoriospermum tapos* (Euphorbiaceae), a Southeast Asian rainforest tree, a novel seco-terpenoid amongst other compounds, was isolated and screened for activity against *M. tuberculosis* using MABA. This compound, 2,3-secotaraxer-14-ene-2,3,28-trioc acid 2,3-dimethyl ester (**122**) was found to be active against $H_{37}Ra$ with an MIC of 4.13 µg/mL. It was however also cytotoxic against two cell lines, NCI-H187 and BC, with IC_{50} values of 4.65 and 7.08 µg/mL, respectively (Pattamadilok and Suttisri, 2008).

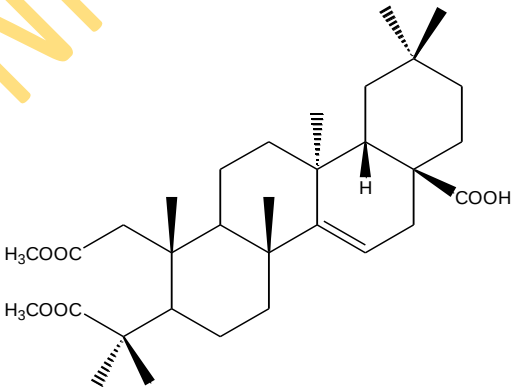

122

vi. Two jujubogenin saponin triterpenoids were isolated from the plant *Colubrina retusa* and the saponins (**123** and **124**) were active against *M. intracellulare* with MIC values of 50 and 10 µg/mL, respectively, but the hydrolysis product (**125**) was completely devoid of biological activity (ElSohly *et al*., 1999).

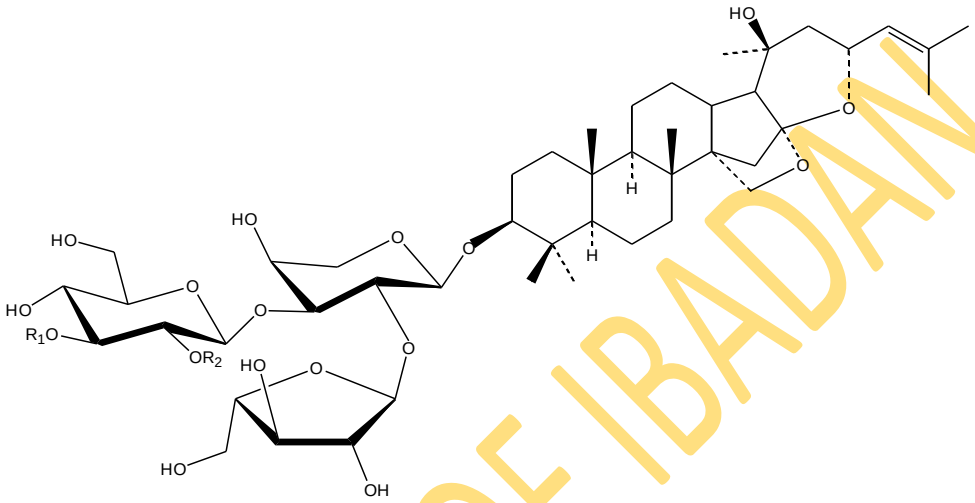

123 R_1 = H, R_2 = *p*-coumaroyl

124 R_1 = *p*-coumaroyl, R_2 = H

125 $R_1 = R_2$ =H

vii. Ergosterol-5,8-endoperoxide (**126**) was isolated as an antimycobacterial component of the plant *Ajuga remota* and exhibited an MIC of 1 µg/mL against *M. tuberculosis* H_{37}Rv. The more non-polar 3-acetate derivative (**127**) was less potent with an MIC of 8 µg/mL (Cantrell *et al*., 1999).

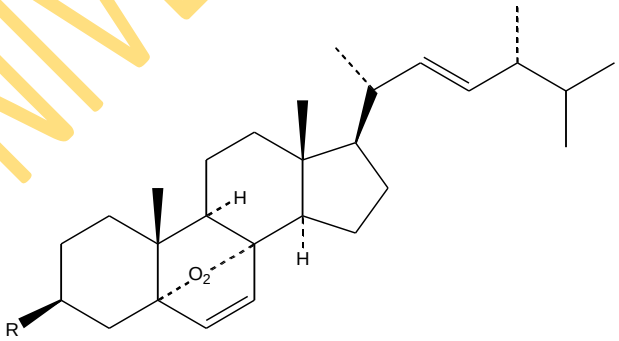

126 R = OH

127 R = OAc

viii. Bioassay guided fractionation of the active dichloromethane-methanol extract of *Thalia multiflora* led to the isolation of four active sterols stigmast-5-en-3β-ol-7-one (**128**), stigmast-4-ene-6β-ol-3-one (**129**), stigmasta-5,22-dien-3β-ol-7-one (**130**) and stigmasta-4,22-dien-6β-ol-3-one (**131**) with MIC values of 1.98, 4.2, 1.0 and 2.2 µg/mL, respectively against *M. tuberculosis* $H_{37}Rv$. Besides being lipophilic compounds, oxidation of carbons 6 or 7 or the presence of α, β unsaturated ketone either on ring A or B, was thought to increase activity significantly. More interestingly, these compounds were evaluated for their toxicity and found not to be cytotoxic at a concentration of 102 µg/mL (Gutierrez-Lugo *et al*., 2005). Also in their studies, Chen *et al*. (2010) isolated amongst other compounds, stigmasta-5-en-3β-ol-7-one (**128**) with an MIC of 55 µg/mL against $H_{37}Rv$.

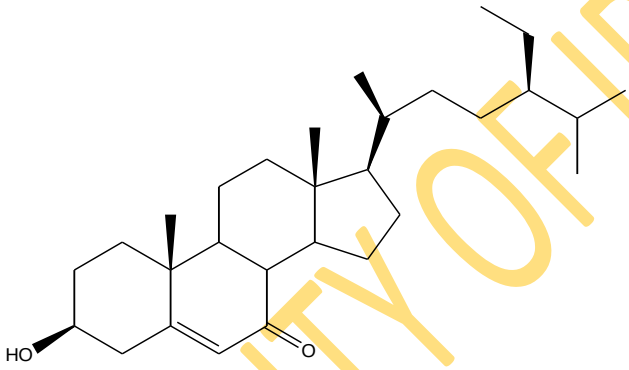

128

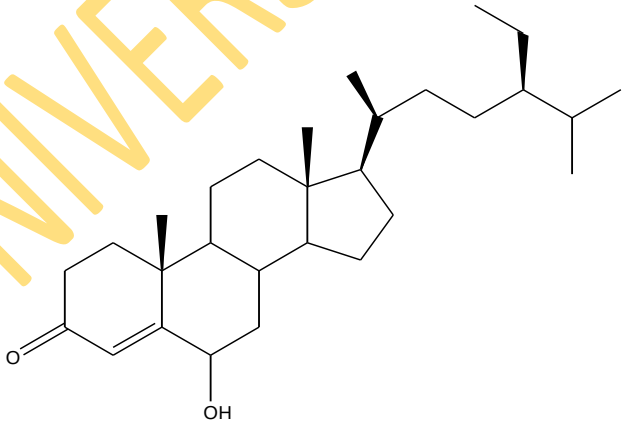

129

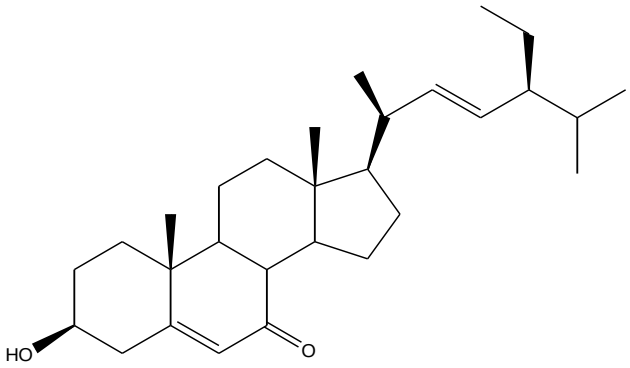

130

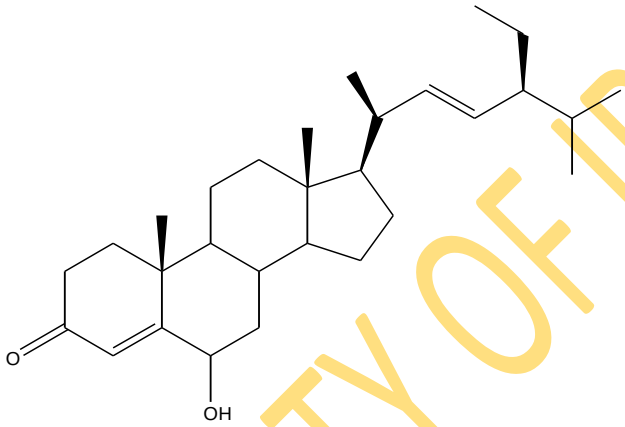

131

In conclusion, plants belonging to different families and genera were investigated phytochemically and for their antimycobacterial activities. Noteworthy is the ethnomedicinal use of most of the investigated plants in various societies for the treatment of tuberculosis or related symptoms such as cough and other respiratory diseases This survey extensively reviewed the different types of plant metabolites that have exhibited potential antimycobacterial activities. Though these compounds are structurally diverse, they are useful templates for discovery of new pharmaceuticals for the treatment of tuberculosis. The presence or absence of certain functional groups or moieties has been shown to either increase or decrease bioactivity. Some workers have also carried out structural activity relationships (SAR) by synthesizing derivatives of the parent compounds With the development of new molecular targeted bioassays such as mycolic acid biosynthesis or cell wall biosynthesis, it will be easier to draw conclusions on structural relationships. It was also observed that different assay techniques were employed in the *in vitro*

screening against different species of mycobacteria but most workers employed MABA, a technique based on a resazurin based oxidation-reduction indicator, as the method of choice for drug susceptibility testing of *M. tuberculosis* species. This may be due to considerations of rapidity, low technology requirements and low cost. First line drugs especially isoniazid and rifampicin were mostly used as reference compounds in the screening assays.

2.4 Plants with Antimycobacterial Activity in Nigeria

Some plants were attributed to being components of traditional antituberculosis recipes in Nigeria. Adeleye and co-workers (2008) evaluated the ethanolic and aqueous extracts of twelve Nigerian medicinal plants for antimycobacterial activity. The study revealed that four of the plant extracts (*Allium cepa*, *Allium ascalonicum*, *Terminalia glaucescens* and *Securidaca longepedunculata*) as well as the wonder cure concoction (Epa-ijebu) showed activity on both the culture isolate and the control strain ($H_{37}Rv$) at 0.5 mg/mL. Mann *et al*. (2008), in evaluating some Nigerian medicinal plants for antimycobacterial activity, found four plants to have antimycobacterial activity at $\leq$ 1250 µg/mL. These plants were *Anogeissus leocarpus*, *Terminalia avicennoides*, *Combretum spp* and *Capparis brassii*. Despite these studies, there seems to be no thorough investigations to identify the active constituents.

The biodiversity of the Nigerian flora portends great possibilities in the search for novel antituberculosis compounds. A good number of plants are used locally in the treatment of tuberculosis, but have not been investigated for their anti-tuberculosis properties. Nigeria has a tropical climate with sharp regional variances depending on rainfall. Based on the rainfall distribution, with a wet south and a dry northern half, and also factors such as soil, elevation, and human impact on the environment, there are two broad vegetation types; forests and savanna. Nigerian ecology varies from a tropical forest in the south to dry savanna in the far north, yielding a diverse mix of plant and animal life (Microsoft Encarta Encyclopedia, 2006).

2.5 Current Trends in Natural Products Isolation and Structural Elucidation

The armory of a natural products chemist in isolation usually involves some form of chromatography. In the older days, when spectroscopy was at its infancy, chemists had a tough time determining the structures of even very simple compounds. Physical properties such as boiling point, melting point, refractive index were used to get some preliminary structural

information. This was then compared to similar structures in literature to determine if there were any close matches. Where more than one existed, these compounds were converted to a known derivative and properties tested and compared.

However with the advent of spectroscopy (NMR, IR, UV) and spectrometry (mass spec), an organic natural product chemist is equipped with the technology to identify these metabolites. These classical instrumental techniques though, present their limitations. The constraints with these conventional methods of structural elucidation include:

a) Small sample size: These conventional spectroscopic methods, particularly NMR, usually require more than 1 mg of compound in order to obtain the prerequisite spectra. So whereas microgram quantities of material may be sufficient for assaying for biological activity, milligram quantities are required for structural elucidation.
b) Instability of bioactive compounds: Some bioactive compounds occur as epimers and cis/trans isomers. In some cases, these compounds even when well resolved using the classical chromatographic methods, become unstable on drying (Cogne *et al*., 2003). This may lead to artifact formation or even the complete destruction of the compound. This therefore poses a problem with the traditional approach to structural elucidation.
c) Environmental hazards: In some natural products, it is the minor compounds that are biologically active. To isolate these compounds in even milligram quantities, large amounts of plant material, 10 kg or more, are often extracted. This invariably leads to deforestation and worse still, extinction of some rare medicinal plants.
d) Dereplication: One major drawback of conventional method/strategy is the frequent isolation of known metabolites. For drug discovery purposes, this heightens the overall efforts especially in bioassay-guided fractionation, since some common or ubiquitous compounds may confuse the natural products chemist in his search for new compounds. Natural products dereplication is an attempt to minimize effort by using that which is already known.
e) Sample handling, time consumption and cost of solvents/resources.

2.5.1 Hyphenated Techniques in Isolation and Structural Elucidation

These are methods combining two or more analytical techniques (usually a separation and a spectroscopic technique) into one integrated technique described by the use of a hyphen e.g. LC-MS, LC-NMR, and LC-UV-DAD. The combination of the high separation efficiency of HPLC

with these different detectors has made possible the acquisition of on-line complementary spectroscopic data on an LC peak of interest (Figure 2.13).

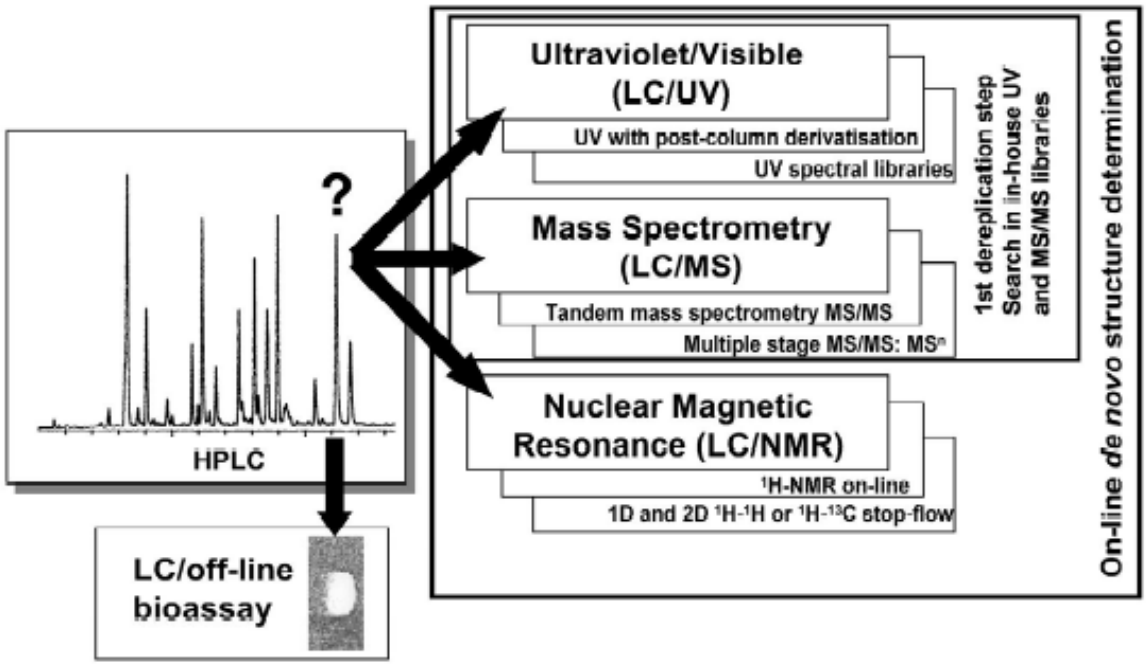

Figure 2.13. Type of information that can be obtained on a given LC peak with different LC-hyphenated techniques available (Wolfender *et al*., 2003).

Advantages:

a) Identification of known compounds present in an extract prior to their isolation (dereplication). Chemical screening using hyphenated techniques such as LC-UV, LC-MS and LC-NMR rapidly provides plenty of structural information, leading to a partial or a complete on-line de novo structure determination of the natural products of interest. This allows for the concentration of resources on the elucidation of novel chemical entities.

b) Less tedious and saves more time.

c) Makes the production and analysis of large natural product libraries more efficient in practical applications.

d) Comprehensive metabolite profiling especially in the ongoing field of plant metabolomic research. Metabolite profiling refers to the detection and identification of plant metabolites. A metabolite database employing LC-MS was used in determining the metabolomics of tomato fruit, *Solanum lycopersicum* (Moco *et al*., 2006). This way, several novel compounds not previously reported for tomato fruit were identified in this manner and added to the database.

e) Compounds with very similar polarity can be more easily separated and identified which would otherwise be more tedious if preparative purification of individual components on a sufficient scale for bioactivity testing was to be achieved by employing the traditional approach (Clarkson *et al*., 2007).

f) Structural investigation of labile or unstable natural products. A typical example is the investigation of the methanol extract of an African Scrophulariaceae species *Jamesbrittenia fodina*. In this study, one of the fractions contained two isomeric peaks in the same proportions, suggesting that the constituents were probably unstable upon drying of the fraction. This was analyzed using stop-flow LC/^{1}H- NMR (Cogne *et al*., 2003). In another study, Schaller *et al*. (2001) employed the on-flow and stop-flow LC-NMR to isolate two unstable diterpenes from a Zimbabwean tree, *Bobgunnia madagascariensis* and study their interconversion reactions.

The next section attempts a general review on these methods, their successes and their intrinsic limitations.

2.5.2 HPLC

In isolating natural products from complex crude extracts, a lot of pre-fractionation and fractionation techniques are employed, sometimes yielding very little success. To achieve efficient isolation of natural products from these complex matrices without the need for complex sample preparation, the high performance liquid chromatography (HPLC) has become one of the most versatile techniques used in this regard. It is routinely used in phytochemistry to pilot the preparative isolation of natural products and to control the final purity. The advantages over most other separation techniques include convenience, speed, choice of column stationary phases, high sensitivity, applicability to a broad variety of sample matrices and ability to hyphenate the chromatographic method to spectroscopic detectors (Wolfender, 2009).

Over the years, there have been improvements on the performance of the HPLC in terms of resolution, speed and reproducibility. This is attributed to technological advances in some basic conditions for the operation of the HPLC. The stationary phase (normal or reverse phase); the length, internal diameter and particle size of the column contribute quite significantly to the resolution of the analytes. Most separations of natural products are carried out in the reverse-phase chromatography especially on C-18 columns, eluting with a solvent system of CH_3CN-H_2O and MeOH-H_2O, usually in the gradient mode. Usually, a modifier is added to the mobile phase to improve the resolution. Other important factors include the flow rate of the pressure pumps, the temperature of the instrument and the detection methods.

The development of measurement techniques coupled (hyphenated) to HPLC has provided powerful tools such as LC-UV-photo diode array detection (LC-UV-DAD), LC-mass spectrometry (LC-MS), LC-multiple stage MS (LC-MS"), LC-nuclear magnetic spectrophotometry (LC-NMR) and LC- infrared spectrophotometry (LC-IR). These hyphenated systems generate multi-dimensional data (chromatographic and spectroscopic) for online identification and dereplication purposes.

2.5.3 LC/UV-DAD

Photo diode array detection provides UV spectra directly online and is particularly useful for the detection of natural products with characteristic chromophores. Combined with post-column addition of UV shift reagents classically used for the structural characterization of flavonoids, more information is obtained on the precise localization of the hydroxyl groups on the polyphenols because they possess characteristic chromophores. This is achieved by comparing the genuine and shifted online DAD spectra online (Wolfender, 2009; Hostettmann *et al*., 1997; Queiroz *et al*., 2009).

LC/UV-DAD can provide spectral libraries and used for dereplication, however, the compounds being analyzed must be subjected to the same HPLC conditions, as the composition of the mobile phase may affect the UV bands slightly (Wolfender, 2009). In their study, Politi *et al*. (2004) employed the HPLC-UV/PAD for the partial dereplication of vismiones, anthraquinones, flavonoids , benzoquinones and xanthones and partial identification of two new bianthrones from the leaf and root extracts of *Vismia guineensis*. In another approach, the structures of three C-

glycosyl flavones were determined on-line by LC/UV/APCI-MS^n analysis of the crude extract of *Gnidia involucrate* (Ferrari *et al*., 2000)

2.5.4 LC-MS, LC-MS-MS^n

Mass spectrometry is one of the most sensitive methods of molecular analysis. It also has the ability to determine the molecular weight and to obtain structural information of the analyte. Due to its high power of mass separation, very good selectivities can be obtained. The coupling between LC and MS had been difficult because of the incompatibilities between HPLC and mass spectrometry (MS), but to overcome these challenges, different LC-MS interfaces were developed (Hostettmann, 1997).

The most popular interfaces used in LC-MS are based on atmospheric pressure ionization (API) techniques and the two most commonly used are electrospray ionization (ESI) and atmospheric pressure chemical ionization (APCI). Some combination of high voltage and heat is used to provide the ionization that is needed to produce the ions that are assayed by the MS system. These API techniques produce mainly a soft ionization of the analytes. Thus, molecular ion species are mainly recorded in the form of either protonated molecules $[M+H]^+$ (positive-ion mode, PI) or deprotonated molecule $[M-H]^+$ (negative-ion mode, NI) when only restricted fragment information is provided. Different adducts (e.g., $[M + Na]^+$ (PI) or $[M + HCOO]^-$ (NI) are also produced, depending on the solutes and the modifiers used. Analyte ionization is largely compound dependent and is governed mainly by proton affinity. As a rule of thumb for a good approximation, acidic molecules (e.g., carboxylic acids or phenolics) will produce mainly $[M - H]^-$ in NI, while bases (e.g., alkaloids, amines) will generate $[M + H]^+$ in PI. Compounds such as glycosides will have a high affinity for salts and will tend to form sodium adducts in PI (Wolfender, 2009).

Complimentary structural information on the molecular fragmentation can be generated by in-source collision-induced dissociation (CID) in HPLC-MS-MS or MS^n experiments. The generated CID spectra are, however, not comparable to those recorded by EI, and this hampers a direct use of the standard EI-MS natural products libraries for dereplication purposes. For performing automated dereplication procedures, specific LC/ MS-MS libraries have to be built based on standards available in a given laboratory, which consequently limits this approach (Wolfender, 2003)

Several types of mass spectrometers are used in the HPLC-MS application. These include those of low resolution, such as the single quadrupole (Q) mass spectrometers, those giving high resolution and exact mass capabilities, such as time-of-flight (TOF) instruments, the triple-quadruple (QQQ) MS-MS systems for measuring structurally relevant fragments or for very specific detection and the ion-trap (IT) mass spectrometers which have the unique capability of producing multiple stage MS-MS (MS^n) data that may be essential for structural elucidation purposes (Wolfender, 2009).

In their study, Fu *et al*. (2010) applied a combination of HPLC/ESI-TOF-MS and HPLC/ESI-IT-MS^n to the screening of phenolic and other polar compounds in olive leaf extracts, allowing for high resolution acquirements, accurate mass measurements and complimentary structural information. Also in an integrated approach, a chemical screening by LC with online UV photodiode array detection (LC-UV) and thermospray (TSP) mass spectrometric detection (LC-TSP-MS) allowed for the identification of six xanthones and secoiridoids (Rodriguez et *al*., 1995).

2.5.5 LC-NMR

The coupling of high liquid chromatography with nuclear magnetic resonance, LC-NMR is one of the most powerful techniques in the isolation and structural elucidation of unknown compounds in crude mixtures (Wolfender *et al*., 2001). It represents a potentially interesting complementary technique to LC-UV-MS for detailed on-line structural investigation of compounds presenting original structural features or displaying interesting activities after LC-bioassays. Integration of LC-NMR with other known LC-coupled techniques provides a powerful tool for on-line de novo elucidation of compounds of interest (Wolfender *et al*., 2005). However, LC-NMR does have its drawbacks and these include:

a) The lower sensitivity of the NMR detector. This renders the on-flow measurements of minor products impossible and also hampers the direct observation of ^{13}C-NMR information, an important element for natural product identification. In some cases, the column must be overloaded in order to increase the signal-to-noise ratio, and this indirectly causes peak broadening and loss of resolution.

b) The difficulty of observing analyte resonances in the presence of the much larger resonances of the mobile phase, thus the need for elaborate solvent suppression.

c) High cost of deuterated solvents.

d) Limitations in the acquisition of two dimensional NMR data which are essential in the structural elucidation of novel compounds.

Due to some of these challenges, there have been advances in the development of hyphenated NMR technique. The first is the use of solid phase extraction (SPE) interface between the NMR spectrometer and the chromatograph, which enables analyte focusing, change from a nondeuterated HPLC solvent to a deuterated NMR solvent, and multiple SPE trapping for increasing sensitivity. The other development is that of new miniaturized probe technologies, with the aim of increasing sensitivity and reducing costs (Hu *et al*., 2005). This was exemplified in the investigations on the crude extract of *Thapsia garganica* employing the offline combination of HPLC-SPE and CapNMR (Lambert *et al*., 2007). Five sequisterpene lactones and four phenylpropanoids were isolated and characterized by this technique.

In conclusion, chemical screening of crude extracts using hyphenated techniques allows for the efficient targeted isolation of new types of constituents with potential activities as a complimentary approach to bioassay-guided fractionation. These hyphenated methods provide some good preliminary information on the nature of constituents of the extract. With this structural information, once the novelty or utility of a given constituent is established, a scale up of the chromatographic process of fraction can then be done to obtain a good yield of the constituent for full structure elucidation, biological and pharmacological testing. This way, the isolation of common compounds of little interest is avoided.

2.6 Biological Evaluation of Antimycobacterial Activities of Crude Extracts, Fractions and Compounds

A major aim of investigations into plants is to ascertain the biological or pharmacological effects and this requires suitable bioassays for monitoring these effects. In considering the various assay methods available, the guiding factors should be systems that are simple, rapid, reproducible, and inexpensive. For compounds with very low yields, the bioassay has to be sensitive enough for their detection. The number of false positives should also be reduced to a minimum.

The complexity of the bioassay has to be designed as a function of the facilities, resources, and personnel available. These factors are however determined by the choice of the target organism, depending on its virulence. *Mycobacterium tuberculosis* $H_{37}Rv$ available from the American Type Culture Collection (ATCC 27294) is the organism of choice for antimycobacterial investigations as it has a drug susceptibility profile fairly representative of most drug susceptible clinical isolates. The practicability of working with such a pathogenic organism though, makes this option difficult in many laboratories. This is because there are specific biosafety guidelines that demand the use of laminar-flow hoods and level 3 facility equipment for *M. tuberculosis* laboratorial work. Alternative to this strain, are other slow avirulent strains, *M. tuberculosis* $H_{37}Ra$ and *M. bovis* BCG which are closely related in terms of genetic composition and drug susceptibility profiles to *M. tuberculosis* $H_{37}Rv$. Many researchers prefer to work with the rapidly growing, avirulent, saprophytic, surrogate *mycobacterium* species which include *M. smegmatis, M. fortuitum* and *M. aurum* (McGaw *et al*., 2008a)

Plants contain a cocktail of many compounds and targeting the bioactive molecule can be a tedious task. To this end, the concept of "bioactive fractionation" was developed to target the isolation of these molecules. The means of isolation and identification of biologically active compounds from natural sources is referred to as bioassay-guided fractionation (BGF). This methodology involves alternating chromatographic fractionation of extracts and *in vitro* biological testing against a biological target such as the *M. tuberculosis*. Using this method, three potent antimycobacterial compounds were isolated from *Dracaena angustifolia* (Case *et al*., 2007). Results of these bioassays are interpreted as the minimum inhibitory concentration in terms of µg/mL. Minimum inhibitory concentration (MIC) is defined as the lowest concentration of an antimicrobial that will inhibit the visible growth of a micro organism (Andrews, 2001).

Different *in vitro* biological assay methods are used in the biological testing of the efficacy of plant extracts, fractions and compounds against *M. tuberculosis*. These methods include agar/disc diffusion, micro and macro agar dilution, microbroth dilution, radiorespirometry, reporter gene assays and low oxygen bioassays. Pauli *et al*. (2005) and McGaw *et al*. (2008a) evaluated each of the methods and discussed their limitations.

2.7 Chemistry, Biology and Pharmacology of Plants in the *Pavetta* genus.

The genus *Pavetta* L. belongs to the family Rubiaceae, subfamily Ixoroideae, and tribe Pavettae. It is a genus of flowering shrubs and trees comprising about 400 species occurring in the Old World tropics (tropical and subtropical Africa, Asia and tropical Australia) with about 24 species found in Southern Africa (Bridson, 2003).

In the findings of Bremekamp (1939), a *Pavetta* has terminal or long pedunculate axillary inflorescences, tetramerous, exclusively hermaphrodite flowers; a bilocular ovary (ovules one or, very rarely, two in each cell); very short stigma; on one side deeply concave seed and an entire endosperm. One of the plausible explanations for the name *Pavetta* is derived from pavitmentum, a Latin word describing a pavement of bricks or stones, thus a mosaic of bricks or stones, possibly referring to the scattered bacterial nodules in the leaves (Van Wyk, 1974).

The genus *Pavetta* has some economic values as some of the species are edible and eaten as vegetable. Some others have ornamental values, as the flowers are used in flower arrangements. Some of the species of the genus *Pavetta* have also been investigated and are reported as having different biological and pharmacological activities.

2.7.1 Pavetta owariensis

The schistosomicidal effects of *Pavetta owariensis* were assessed in mice infected with *Schistosoma mansoni*. Both the ethanol and acetone extracts caused a reduction in size of peiovular granuloma formation in the liver (Balde *et al.*, 1989).

Investigations on the hexane extract of the stem bark of *Pavetta owariensis* resulted in the isolation of the trans and cis isomers of five ferulic acid esters; octadecanyl ferulate (**132**), cosanyl ferulate (**133**), docosanyl ferulate (**134**), nonadecanyl ferulate (**135**) and hemicosanyl ferulate (**136**) (Balde *et al.*, 1991a).

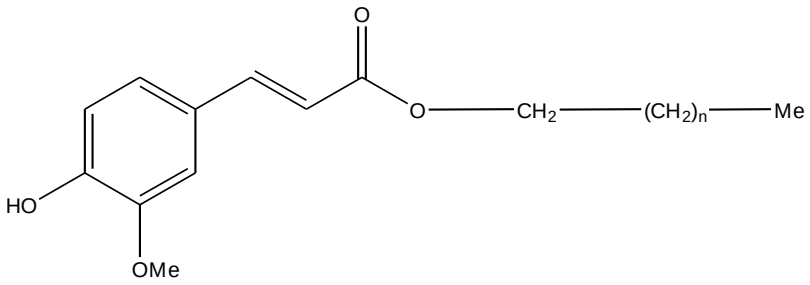

132 n =16

133 n=18

134 n=20

135 n=17

136 n=19

In a related study on the stem bark of *Pavetta owariensis*, proanthocyanidins were found to be responsible for the anthelmintic activities on known anthelmintics. In their investigations on the active components of *P. owariensis*, three monomeric flavan-3-ols and three dimeric proanthocyanidin A-type compounds were isolated. The monomeric flavan-3-ols were characterized and identified as (+)-catechin, (-)-epicatechin, (+)-epicatechin, structured as compound **137**, except for differences in configuration. The dimeric proanthocyanidins were epicatechin-(4β→8,2β→*O*→7)-epicatechin, epicatechin-(4β→8,2β→*O*→7)-(+)-catechin and (+)-epicatechin-(4α→8,2α→*O*→7)-(+)-catechin, structured as compound **138**. These compounds also majorly differed in the configurations at the C2-C7 ether linkage, C4-C7 carbon-carbon linkage and C-3 hydroxyl group (Balde *et al*, 1991b).

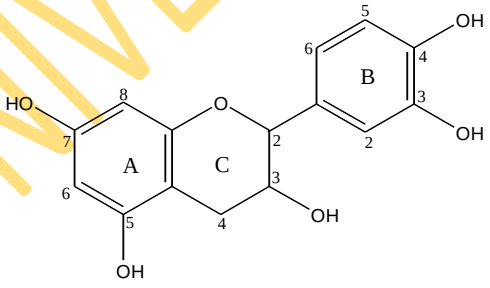

137

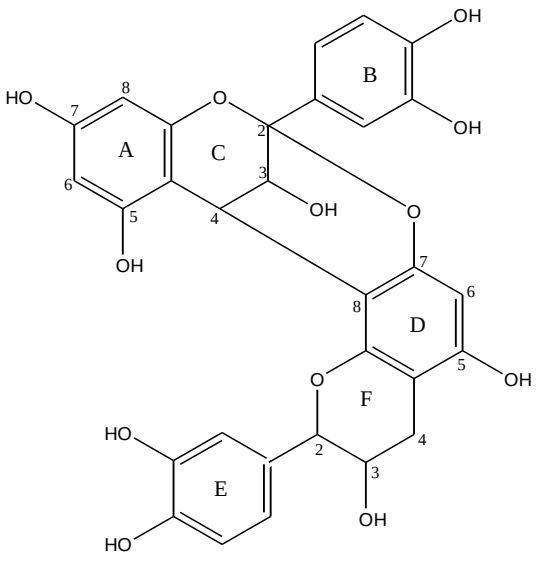

138

Similar investigations on the stem bark of *Pavetta owariensis* led to the isolation of five trimeric proanthocyanidins trivially named cinnamtannin B1, pavetannin B1, pavetannin B3, pavetannin B5 and pavetannin B4. These compounds were grouped into two skeletal types based on the C-4 carbon-carbon linkage. Cinnamtannin B1 (epicatechin-(4β→8, 2β→*O*→7)-epicatechin-(4α→8)-epicatechin) and pavetannin B1 (epicatechin-(4β→8, 2β→*O*→7)-epicatechin-(4α→8)-(+)epicatechin), had C4-C8 linkages (**139**) while pavetannin B3 (epicatechin-(4β→6, 2β→*O*→7)-epicatechin-(4α→8)-epicatechin), pavetannin B5 (epicatechin-(4β→6, 2β→*O*→7)-catechin-(4α→8)-epicatechin) and pavetannin B4 (epicatechin-(4β→6, 2β→*O*→7)-(+) epicatechin-(4β→8)-epicatechin) had C4-C6 linkages (**140**). Other differences were based on the configurations at the carbon-carbon linkages or the ether linkages (Balde *et al*., 1993).

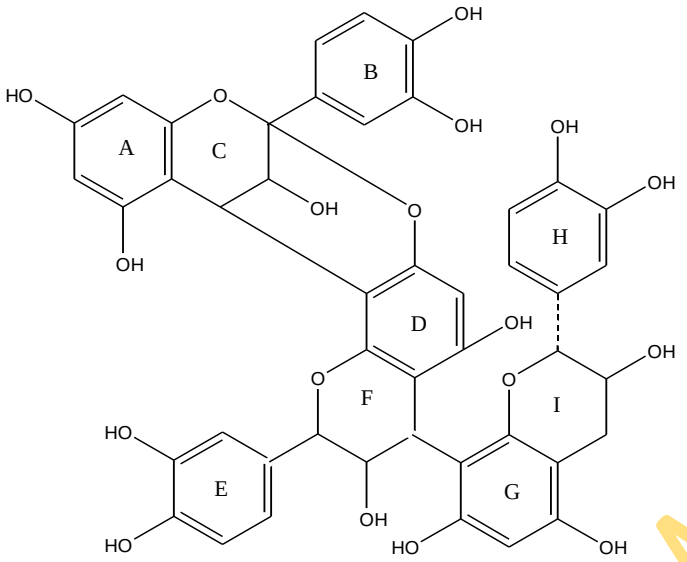

139

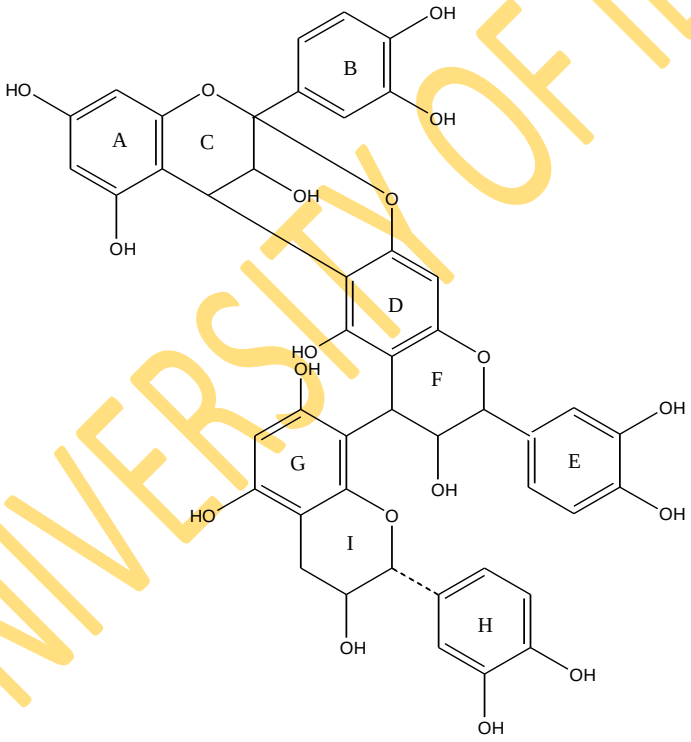

140

2.7.2 Pavetta harborii

Pavetta harborii was investigated and the crude extracts and dried plant material were found to have cardiotoxic effects on rats and sheep. The active principle, pavetamine (**141**) significantly

reduced systolic function and body mass in treated rats, indicating its potential to induce heart failure in the animal model (Hay *et al.*, 2008).

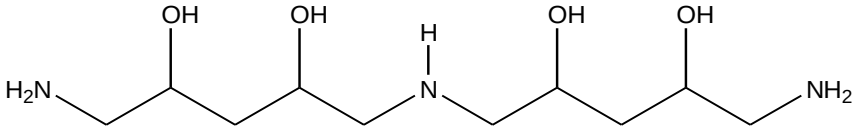

141

2.7.3 Pavetta longiflora

In screening some Yemeni medicinal plants for their inhibitory effects against neutral endopepdidase (NEP), the aqueous extract of *Pavetta longiflora* significantly inhibited the activity of NEP at a concentration of 50 µg/mL (Alasbahi and Melzig, 2008)

2.7.4 Pavetta indica

The *in vivo* anti-inflammatory potential of the methanol extract of *Pavetta indica* leaves was evaluated against different models of inflammation in rats. The extract showed inhibitions that were comparable with a standard drug (Mandal *et al.*, 2003).

2.8 *Pavetta crassipes* K. Schum

Pavetta crassipes is a member of the family Rubiaceae. It is a glabrous shrub to 6m high, trunk to 30 cm girth, of the savanna (Burkill, 1997). It has stout squarish branchlets covered with pale corky bark which splits and falls off; leaves often in threes; flowers greenish-white and fruits black (Fig 2.14)

Figure 2.14. Whole plant (flowering) of *Pavetta crassipes*

Pavetta crassipes is widely distributed in the West African sub-region. The leaf is traditionally used in Nigeria for the management of respiratory disorders and hypertension in ethnobotanical practice. *Pavetta crassipes* leaves, locally known as Gadu in Northern Nigeria, are typically eaten as food or used for the treatment of fever, schistosomisasis, mental illness, convulsion, malaria, hookworms (Amos *et al*., 1998) and pains (Abubakar *et al*., 2007). More recently, it has been reported as one of the plants commonly used in the treatment of chronic joint pains in Kenya (Wambugu *et al*., 2011). The following pharmacological activities have been reported on the plant; anti-plasmodial/ malarial activity (Sanon *et al*., 2003), hypotensive activity (Amos *et al*., 2003), inhibitory effects on gastrointestinal and uterine smooth muscles (Amos *et al*., 1998) and *in vitro* antiprotozoal, antimicrobial and antitumor activities (Balde *et al*., 2010).

CHAPTER THREE

MATERIALS AND METHODS

3.1 General Experimental Procedures/ Analytical Procedures

3.1.1 Solvents, Reagents and Standards

Analytical grades of organic solvents; hexane, ethyl acetate, methanol, butanol, acetone, ethanol (Sigma-Aldrich) were used for extraction, isolation and purification.

Reagents were freshly prepared according to standard procedures.

Ursolic acid (≥ 90% purity; Sigma-Aldrich, USA) was used as standard.

3.1.2 Nuclear Magnetic Resonance (NMR)

Both ^{1}H- (400 MHz) and ^{13}C-NMR (100 MHz) spectral data were recorded in deuterated $CDCl_3$, DMSO-d_6, D_2O or CD_3OD, on a Bruker AMX 400 at Acorn NMR Inc, Carlifornia, USA and Columbia University, USA. The NMR spectrometer chemical shifts were expressed in parts per million (δ) relative to tetramethylsilane (TMS) and the coupling constants were given in Hertz (Hz). Standard pulse sequences were employed for the measurement of 2D NMR spectra (^{1}H-^{1}H COSY, HSQC and HMBC)

3.1.3 Mass Spectra (MS)

High Resolution Mass Spectra (HRMS) were determined on a q-TOF Waters LCT Premier Mass Spectrometer with an electrospray ionization (ESI) or atmospheric pressure ionization (API) source and in the positive or negative mode, at NIH/NIDDK, Bethesda, Maryland, USA.

3.1.4 Ultra-violet Spectra (UV)

Ultra-violet spectra of isolated compounds were run on a Varian Cary 300 Bio UV-Visible Spectrophotometer at NIH/NIAID, Bethesda, Maryland, USA. The UV spectra were recorded between 200 and 500 nm. Wavelengths (λ in nm) are given.

3.1.5 Infrared Spectra (IR)

IR spectra (υ in cm^{-1}) were recorded with a Perkin Elmer Spectrum one FT-IR Spectrophotometer at NIH/NIDDK, Bethesda, Maryland, USA.

3.1.6 Melting Points

Melting points (uncorrected) were determined with a Barnstead Electrothermal 9100 apparatus at NIPRD, Idu, Abuja, Nigeria.

3.1.7 Thin Layer Chromatography (TLC) and Preparative Thin Layer Chromatography (PTLC)

Thin layer chromatographic analysis of extracts, fractions and compounds was carried out using silica 60 F_{254} pre-coated glass plates (0.25 mm, 20 x 20 cm; Merck, Darmstadt, Germany). Spots were detected on TLC plates under short (λ=254 nm) and long (λ=366 nm) UV light and/or visualized by spraying with vanillin-sulphuric acid, followed by charring at 110^{o}C for 5 minutes.

Pre-coated preparative TLC glass plates- Kieselgel 60 F_{254} (0.5 mm, 20 x 20 cm; Analtech Inc, USA), were used for the isolation of compounds.

3.1.8 Open Column Chromatography and High Performance Liquid Chromatography

Open flash column chromatography was performed using silica gel Merck 230-400 µm mesh, 60Å, for the fractionation of extracts.

Preparative HPLC on a Phenomenex system (Varian Pro Star Model 218 coupled to a Varian fraction collector model 701) using a reverse phase column at NIAID/NIH, Bethesda, Maryland, USA, was used for the isolation of compounds, HPLC conditions; flow rate, 25 mL/ min; column temperature 40^{o}C.

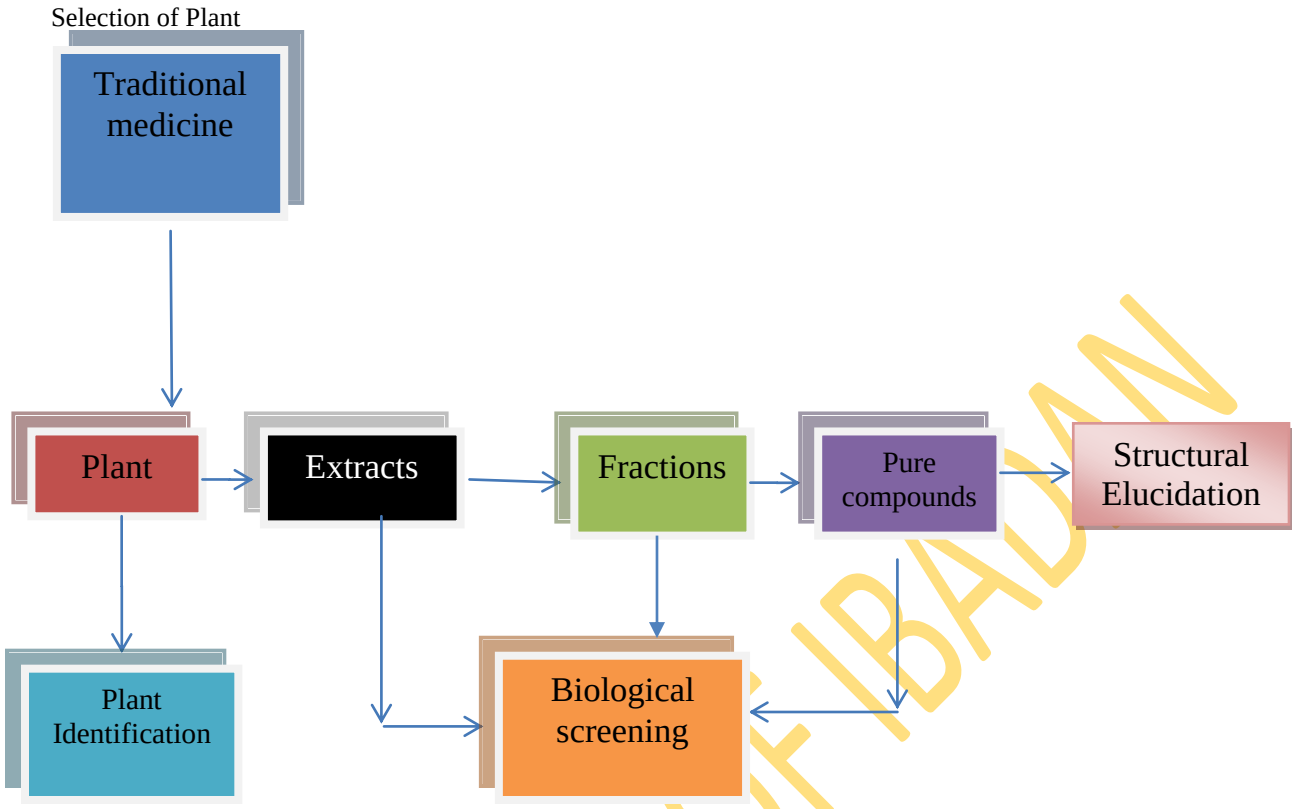

Figure 3.1. Flow chart of isolation of bioactive compounds from *Pavetta crassipes*

3.2 Collection and Authentication of Plant Material

The fresh leaves of *Pavetta crassipes* were collected from Suleja, Niger state, in July 2009 and identified by Jemilat Ibrahim. A labeled voucher specimen, NIPRD/H/6241 was deposited in the herbarium of the National Institute for Pharmaceutical Research and Development, Idu-Abuja (Fig 3.2).

Figure 3.2. Herbarium specimen of *Pavetta crassipes*

3.3 Extraction of Plant

The air-dried leaves of *Pavetta crassipes* (1 kg) was finely ground and extracted successively by maceration with n-hexane, EtOAc and MeOH, at room temperature for 24 h respectively. The hexane, EtOAc and MeOH extracts were evaporated under reduced pressure at 40^{o}C using a rotary evaporator.

3.4 Fractionation of Hexane Extract

The hexane extract (5 g) was fractionated using silica gel column chromatography (250 g). This was eluted with n-hexane, n-hexane-EtOAc and EtOAc (hexane-EtOAc, 90:10, to hexane-EtOAc, 0:100) using gradient elution. The eluates were examined by TLC and combined to give 8 major fractions, PCH_1-PCH_8. Fraction PCH_5 (eluted with 20% EtOAc in hexane), was rechromatographed, (silica gel, hexane-EtOAc, 95:5, to hexane-EtOAc, 80:20), to give 5 combined subfractions, $PCH_{5.1}$-$PCH_{5.5}$. Subfraction $PCH_{5.4}$ (eluted with 10-15% EtOAc in hexane) was recrystallized from methanol to yield **NN03**. Fraction PCH_6, eluted with 30% EtOAc in hexane, was rechromatographed (silica gel, hexane-EtOAc, 95:5, to hexane-EtOAc, 50:50), to obtain 6 combined subfractions, $PCH_{6.1}$-$PCH_{6.6}$. Crystallization of $PCH_{6.5}$ (eluted with 30-50% EtOAc in hexane) from ethanol, yielded **NN05**.

3.5 Fractionation of the Ethyl Acetate Extract

The ethyl acetate extract (9 g) was fractionated using silica gel column chromatography (400 g), with gradient elution of n-hexane, EtOAc and MeOH (hexane-EtOAc, 90:10 to hexane-EtOAc, 0:100 to EtOAc-MeOH, 90:10) to obtain 14 major fractions, PCE_1-PCE_{14}. Fractions PCE_5 and PCE_6, eluted with 20% and 30% EtOAc in hexane, respectively, had similar TLC profiles as fractions PCH_5 and PCH_6 (of the hexane extract). These were rechromatographed under similar conditions and using the same solvent systems as in the hexane extract to give additional quantitities of **NN03** and **NN05**, respectively. Fraction $PCE_{14,}$ eluted with 100% EtOAc-10% MeOH in EtOAc, was chromatographed on a prep-HPLC c18 column 250 x 21.20 mm i.d (5µm, 100A). The separations were monitored at 220 nm, and the fractions were separated with a MeOH-H_2O gradient in 0.01% formic acid starting from MeOH-H_2O 5:95 solvent A to MeOH-H_2O 95:5 solvent B in 50 minutes. A flow rate of 25 mL/min was used. Fractions with similar retention time peaks were pooled. Subfractions $PCE_{14.25}$-$PCE_{14.30}$ and $PCE_{14.31}$-$PCE_{14.32}$ eluted

with MeOH-H_2O 80:20, and MeOH-H_2O 84:16, respectively were pooled. This procedure was repeated twice to obtain sufficient amounts. Subfractions $PCE_{14.(25-30)}$ and $PCE_{14.(31-32)}$ were further purified on a prep TLC plate developed with a solvent system of $CHCl_3$-MeOH 9:1. The compound rich sorbents (fractions) were suspended in methanol for 30 min, filtered under suction while washing with more of the solvent, and the solution evaporated under vacuum, to yield **NN06** and **NN07**, respectively.

3.6 Fractionation of the Methanol Extract

The methanol extract (10 g) was fractionated using silica gel column chromatography (500 g), with a gradient elution of n-hexane, EtOAc, and MeOH (hexane-EtOAc, 90:10 to hexane-EtOAc, 0:100 to EtOAc-MeOH, 50:50). Thirteen major fractions, PCM_1-PCM_{13} were collected based on similarities of their TLC profiles. Compound **NN01** precipitated out on standing from fraction PCM_{10} (eluted with 20% MeOH in EtOAc), as a yellow powder and was further purified by washing with EtOAc. Fraction PCM_{10} was further rechromatographed on a HPLC system using the methodology described earlier for it (see Section 3.5). Similar time peak subfractions, $PCM_{10.17}$- $PCM_{10.19}$, eluted with MeOH-H_2O 20:80 and $PCM_{10.25}$-$PCM_{10.30}$, eluted with MeOH-H_2O 80:20, were pooled. Purification of $PCM_{10.(17-19)}$ was done on a prep TLC plate, developed with solvent system $CHCl_3$-MeOH 4:1. Recovery of compound was as described in section 3.5. This yielded **NN04**. Purification of $PCM_{10.(25-30)}$ was carried out on a prep-TLC plate developed with $CHCl_3$-MeOH 9:1, and recovered from methanol as in section 3.5. This gave an additional quantity of compound **NN06**. Fraction PCM_{11} which was eluted with 50% MeOH in EtOAc, yielded light brown crystals on standing. Further purification by crystallizing from methanol yielded **NN02**, a white solid.

Characterization of Isolated Compounds

In the structural elucidation of the compounds isolated from *P.crassipes*, basic information on the molecule was obtained from a combination of physical and spectral data. Through a combination of experimental chemical shift values from the ^{13}C-NMR spectra and the quasimolecular or pseudomolecular ions from the mass spectra, a potential molecular formula was identified. After the proposal of a structure, extensive literature search was also conducted to compare spectral data and confirm the structure. In cases where the isolated compound was

commercially available, spectral data of the commercial compound were compared to those of the isolate to confirm the structure. Also, some chemical reactions were carried out and the spectral analysis of reaction products was useful in establishing the structures of the isolated compound

3.7 Spectral Data of NN03, Compound 142 (β-sitosterol)

IR ν_{max} (cm^{-1}): 3356 (O-H), 2959, 2933 (C-H), 1464, 1378, 1214, 1060 (C-O)

TOF-ES-MS *m/z*; 397.4 $[M - H_2O]^+$ (calculated for $C_{29}H_{50}O$)

^1H NMR (400 MHz, $CDCl_3$) δ_H (ppm): 5.34 (1H, d, H-6), 3.52 (1H, dddd, H-3), 0.82 (3H, d, H-26), 0.80 (3H, d, H-27), 1.00 (3H, s, H-19), 0.91 (3H, d, J = 6 Hz, H-21), 0.84 (3H, t, *J* = 8.4 Hz, H-29), 0.67 (3H, s, H-18)

^{13}C NMR (100 MHz, $CDCl_3$) δ_C (ppm): 140.7 (C-5), 121.7 (C-6) ,72.0 (C-3), 56.7 (C-14), 56.0 (C-17), 50.1 (C-9), 45.9 (C-24), 42.3 (C-13), 40.4 (C-12), 39.8 (C-4), 37.2 (C-1), 36.5 (C-10), 36.1 (C-20), 33.9 (C-22), 31.9 (C-7), 31.6 (C-8), 29.7 (C-2), 29.1 (C-25), 28.2 (C-16), 26.0 (C-23), 24.3 (C-15), 23.0 (C-28), 21.1 (C-11), 19.8 (C-26), 19.3 (C-27), 19.0 (C-19), 18.7 (C-21), 12.0 (C-29), 11.8 (C-18)

3.8 Spectral Data of NN05, Compound 120 (ursolic acid)

IR ν_{max} (cm^{-1}): 3673 (O-H), 1688 (C=O)

TOF-ES-MS *m/z*; 457.4 $[M + H]^+$, 439.4 $[M - H_2O]^+$ (calculated for $C_{30}H_{48}O_3$)

^1H NMR (400 MHz, DMSO-d_6) δ_H (ppm): 11.92 (1H, s, OH-28), 5.12 (1H, t, H-12), 4.27 (1H, d, OH-3), 2.99 (1H, m, H-3α), 2.09 (1H, d, H-18), 1.03 (3H, s, H-27), 0.90 (3H, d, H-30), 0.89 (3H, s, H-23), 0.86 (3H, s, H-25), 0.81 (3H, d, H-29), 0.74 (3H, s, H-26), 0.67 (3H, s, H-24)

^{13}C NMR (100 MHz, DMSO-d_6) δ_C (ppm): 178.2 (C-28), 138.1 (C-13), 124.5 (C-12), 76.8 (C-3), 54.7 (C-5), 52.3 (C-18), 46.9 (C-9), 46.7 (C-17), 41.6 (C-14), 38.8 (C-8), 38.47 (C-19), 38.40 (C-20), 38.3 (C-4), 38.2 (C-1), 36.5 (C-10), 36.2 (C-22), 32.6 (C-7), 30.1 (C-21), 28.2 (C-

23), 27.5 (C-2), 26.9 (C-15), 23.7 (C-16), 23.2 (C-27), 22.8 (C-11), 21.0 (C-30), 17.9 (C-6), 16.9 (C-26), 16.8 (C-29), 16.0 (C-24), 15.2 (C-25)

3.9 Spectral Data of NN07, Compound 143 (ethyl chlorogenate)

UV (MeOH) λ_{max} (nm): 218, 330

TOF-ES-MS, positive ion, *m/z* 405.1 $[M + Na]^+$, 383.1 $[M + H]^+$ (calculated for $C_{18}H_{22}O_9$)

^{1}H NMR (400 MHz, DMSO-d_6) δ_H (ppm): 7.38 (1H, d, *J* = 15.9 Hz, H-7'), 7.01(1H, d, *J* = 2.0 Hz, H-2'), 6.95 (1H, dd, *J* = 2.0 Hz, 8.1 Hz, H-6'), 6.76 (1H, d, *J* = 8.1 Hz, H-5'), 6.10 (1H, d, *J* = 15.9 Hz, H-8'), 5.01 (1H, m, H-3), 4.01 (2H, m, H-8), 3.86 (1H, m, H-5), 3.56 (1H, dd, H-4), 1.91-2.10 (2H, m, H-2), 1.75-2.10 (2H, m, H-6), 1.12 (3H, t, H-9)

^{13}C NMR (100 MHz, CD_3OD) δ_C (ppm): 175.0 (C-7), 168.3 (C-9'), 149.7 (C-3'), 147.2 (C-7'), 146.9 (C-4'), 127.7 (C-1'), 123.0 (C-6'), 116.5 (C-5'), 115.16 (C-2'), 115.11 (C-7'), 75.8 (C-1), 72.7 (C-4), 72.2 (C-3), 70.4 (C-5), 62.5 (C-8), 38.0 (C-2), 37.8 (C-6), 14.3 (C-9)

3.10 Spectral Data of NN06, Compound 144 (methyl chlorogenate)

UV (MeOH) λ_{max} (nm): 218, 330

TOF-ES-MS, positive ion, *m/z* 391.1 $[M + Na]^+$, 369.1 $[M + H]^+$, (calculated for $C_{17}H_{20}O_9$)

^{1}H NMR (400 MHz, CD_3OD) δ_H (ppm): 7.52 (1H, d, *J* = 15.9 Hz, H-7'), 7.03 (1H, d, *J* = 2.0 Hz, H-2'), 6.94 (1H, dd, *J* = 2.0 Hz, 8.1 Hz, H-6'), 6.78 (1H, d, *J* = 8.1 Hz, H-5'), 6.21 (1H, d, *J* = 15.9 Hz, H-8'), 5.27 (1H, m, H-3), 4.13 (1H, m, H-5), 3.72 (1H, dd, *J* = 3.2 Hz, 6.8 Hz, H-4), 3.69 (3H, s, OCH_3, H-8), 1.98-2.22 (4H, m, H-2, 6)

^{13}C NMR (100 MHz, CD_3OD) δ_C (ppm): 175.0 (C-7), 168.3 (C-9), 149.7 (C-3'), 147.2 (C-7'), 146.9 (C-4'), 127.7 (C-1'), 123.0 (C-6'), 116.5 (C-5'), 115.18 (C-2'), 115.11 (C-7'), 75.9 (C-1), 72.6 (C-4), 72.1 (C-3), 70.4 (C-5), 53.0 (C-1), 38.1 (C-2), 37.8 (C-6)

3.11 Spectral Data of NN01, Compound 145 (rutin)

UV (MeOH) λ_{max} (nm): 257, 358

IR ν_{max} (cm^{-1}): 3337 (O-H), 2943, 2833 (C-H), 1655 (C=O), 1606 (C=C, aromatic), 1448, 1361, 1306, 1202, 1170

TOF-ES-MS, positive ion, *m/z* 633.1 $[M + Na]^+$, 611.1 $[M + H]^+$, 465.1 $[M + H - 146]^+$, 449 .1 $[M + H - 162]^+$ (calculated for $C_{27}H_{30}O_{16}$)

^{1}H NMR (400 MHz, CD_3OD): δ_H (ppm): 7.66 (d, *J* = 2.0 Hz, H-2'), 7.62 (dd, *J* = 2.0, 8.0 Hz, H-6'), 6.85 (d, *J* = 8.0 Hz, H-5'), 6.39 (d, *J* = 2.0 Hz, H-8), 6.20 (d, *J* = 2.0 Hz, H-6). Glucosyl protons: 5.11 (1H, d, *J* = 7.6 Hz, H-1'), 3.80 (1H, dd, H-6$^{a'}$), 3.44 (1H, t, *J* = 3.2 Hz, H-2"), 3.38 (1H, dd, H-6$^{b'}$). Rhamnosyl protons: 4.51 (1H, d, *J* = 1.6 Hz, H-1"), 1.12 (3H, d, *J* = 6 Hz, H-6"), other glycosidic protons; 3.24 - 3.49 (multiplet)

^{13}C NMR (100 MHz, CD_3OD) δ_C (ppm): Aglycone: 179.4 (C-4), 166.0 (C-7), 162.9 (C-5), 159.3 (C-2), 158.5 (C-9), 149.8 (C-4'), 145.8 (C-3'), 135.6 (C-3), 123.5 (C-6'), 123.1 (C-1'), 117.6 (C-2'), 116.0 (C-5'), 105.6 (C-10), 99.9 (C-6), 94.8 (C-8), Glucose and rhamnose; 104.7 (C-1"), 102.4 (C-1'"), 75.7 (C-2"), 68.5 (C-6"), 17.8 (C-6'"), other glycosidic carbons (69.7, 71.3, 72.1, 72.2, 73.9, 77.2 and 78.1)

3.12 Spectral Data of NN04, Compound 147 (pavetoside)

UV (MeOH) λ_{max} (nm): 218

IR ν_{max} (cm^{-1}): 3357 (O-H), 2921 (C-H), 1677 (C=O), 1628 (C=C), 1407, 1070, 1055 (C-O)

TOF-ES-MS, positive ion, *m/z*: 411.1 $[M + Na]^+$, 406.1 $[M + NH_4]^+$. TOF-ES-MS, negative ion, *m/z*; 387.1 $[M - 1]^-$, 343.1 $[M - CO_2]^-$; HRESIMS [M + Na]+, *m/z* 411.0909 (calcd for $C_{16}H_{20}0_{11}Na$, 411.0896).

^{1}H NMR (400 MHz, DMSO-d_6) δ_H (ppm): 7.32 (1H, s, H-3), 6.75 (1H, br s, H-8), 5.80 (1H, s, H-1), 4.42 (1H, d, *J* = 7.6 Hz, H-1'), 3.65 (1H, dd, *J* = 1.6, 12 Hz, H-6^{b}), 3.45 (1H, dd, *J* = 4.8, 12 Hz, H-6^{a}), 3.16 (1H, H-5), 3.16 (1H, H-7), 2.94 (1H, t, H-2'), 2.77 (1H, m, H-6^{b}), 2.38 (1H, dd, *J* = 18.4, 2.4 Hz, H-6^{a}), other glucosidic protons (H-3', H-4', H-5'), 3.0 - 3.3 (multiplet)

^{13}C NMR (100 MHz, DMSO-d_6) δ_C (ppm): 167.7 (C-10), 165.5 (C-11), 157.1 (C-3), 145.5 (C-8), 134.5 (C-9), 111.2 (C-4), 98.8 (C-1'), 93.2 (C-1), 72.9 (C-2'), 76.9, 76.6, 69.7 (glucosidic carbons C3' - C5'), 60.8 (C-6'), 46.3 (C-7), 38.1 (C-6), 32.1 (C-5)

3.13 Spectral Data of NN02, Compound 148 (D-mannitol)

IR ν_{max} (cm^{-1}): 3329 (O-H), 2989 (C-H), 2108, 1637, 1394, 1250, 1066 (C-O)

TOF-AP-MS, positive ion, *m/z* 183.1 $[M + 1]^+$, 165.1 $[M + 1 – H_2O]^+$, 147.1 $[165.1 - H_2O]^+$, 129.1 $[147.1 - H_2O]^+$, 111 $[129.1 - H_2O]^+$, (calculated for $C_6H_{14}O_6$)

^{1}H NMR (400 MHz, D_2O) δ_H (ppm): 3.75 (2H, dd, *J* = 2.4, 11.7 Hz, H-1, 6), 3.68 (2H, d, *J* = 8.6 Hz, H-3, 4), 3.64 (2H, m, H-2, 5), 3.56 (2H, dd, *J* = 6, 11.7 Hz, H-1, 6)

^{13}C NMR (100 MHz, CD_3OD) δ_C (ppm): 70.8 (C-2, 5), 69.2 (C-3, 4) and 63.2 (C-1, 6)

3.14 Acid Hydrolysis of NN01

NN01 (10mg) was dissolved in 1 mL of methanol with concentrated HCl (0.5 mL) and the solution was kept under reflux for 5 h at 70^{o}C. After removal of MeOH by rotary evaporation, the residue was partitioned between n-butanol and H_2O. The butanol (lower) layer was removed, dried over anhydrous Na_2CO_3 and concentrated under reduced pressure, to afford 3 mg of **NN01a**. UV, MS, ^{1}H and ^{13}C experiments were run to confirm the structure of this compound (**146**);

UV (MeOH) λ_{max} (nm): 257, 358

TOF-MS-API, positive ion, *m/z* 303.1 $[M + H]^+$, (calculated for $C_{15}H_{10}O_7$)

^{1}H NMR (400 MHz, CD_3OD): δ_H (ppm): 7.69 (d, *J* = 2.0 Hz, H-2'), 7.64 (dd, *J* = 2.0, 8.0 Hz, H-6'), 6.9 (d, *J* = 8.0 Hz, H-5'), 6.41 (d, *J* = 2.0 Hz, H-8), 6.23 (d, *J* = 2.0 Hz, H-6)

^{13}C NMR (100 MHz, CD_3OD) δ_C (ppm): 175.9 (C-4), 164.1 (C-7), 161.1 (C-5), 156.8 (C-9), 147.3 (C-4'), 146.5 (C-2), 144.8 (C-3'), 135.8 (C-3), 120.2 (C-6'), 122.7 (C-1'), 114.8 (C-2'), 114.5 (C-5'), 103.1 (C-10), 97.8 (C-6), 92.9 (C-8)

3.15 Acetylation of NN01

NN01 (10 mg) was dissolved in 2 mL of acetic anhydride/pyridine (1:1) with stirring at room temperature for 24 h. Progress of the reaction was monitored by TLC, EtOAc: Hex (3:1). The reaction mixture was then poured into ca. 20 mL of icy water. Further partitioning was done with ethyl acetate, followed by washing with aq. $CuSO_4$ and water. The organic layer was then dried with anhydrous sodium sulphate, filtered and concentrated under reduced pressure to yield **NN01b**, TOF-AP-MS, positive ion, *m/z* 1031.2 $[M + H]^+$.

3.16 Antimycobacterial assays

Following the extractions and chromatographic separations, extracts, fractions and compounds were tested against *Mycobacterium tuberculosis.* Bioassays were conducted on drug sensitive H_{37}Rv ATCC 27294 (American Type Culture collection) and BCG. *Mycobacterium tuberculosis* was grown in 7H9-medium which consisted of Middlebrook 7H9 broth base supplemented with 0.5 % (w/v) Albumin, 0.2 % (w/v) glucose, 0.2% (v/v) glycerol, 0.08% (w/v) NaCl and 0.05 % (v/v) Tween 80. The Green Fluorescent Protein Reporter Microplate Assay (GFPMA; Collins *et al*., 1998) and the Broth Microdilution Method (BMM; Coban *et al*., 2004) were employed in the assessment of antimycobacterial activity. Isoniazid was used as positive control.

The broth dilution method was employed for screening *M. tuberculosis* (at NIH) or BCG (at NIPRD). *Mycobacterium tuberculosis* was grown in 7H9-medium to an optical density (OD) 650 nm of 0.2-0.3 after which cells were diluted 1000-fold in 7H9-medium. Organic extracts and fractions for the antimycobacterial assay were prepared at varying concentrations in 100% DMSO while pure compounds were prepared in a concentration of 10 mg/mL in 100% DMSO. 40 µL of the stock solution was taken into 460 µL of 7H9-medium. Susceptibility testing was performed in clear 96-well round-bottom microtitre plates containing 50 µL of 7H9 medium in each well except the first well. The drug solution (100 μL) was transferred into the first well of the microplate and 50 μL taken from it and dispensed into the second well. Similar two-fold dilutions were made in other wells. The last well in each row was used for bacterial controls. Fifty µL of cells (inocula) was added to each of the wells causing a further two-fold dilution and a final volume of 100 µL per well. The plates were sealed in plastic (zip-lock) bags to prevent evaporation from the wells and incubated at 37 °C in a humid atmosphere for 7-10 days.

Growth was visually scored using an inverted mirror. Lack of growth inhibition resulted in a clearly visible pellet (5 mm in diameter) due to the fact that the lack of agitation of the plates caused cells to sink to the bottom of the wells. Growth inhibition by isoniazid or an active compound resulted in either no growth with no visible cell pellet or a concentration-dependent decrease in cell pellet size. The minimum inhibitory concentration (MIC) was taken as the lowest concentration that completely inhibited all growth as evidenced by lack of a visible cell pellet. In addition, some extracts and fractions were associated with considerable evidence of precipitation of material in the wells. In these cases, the well in which total growth inhibition occurred could not always be assigned with certainty. In cases where cell extracts with precipitating material contained a potent inhibitor, precipitation occurred in the first wells followed by one or more wells of no precipitated material and no growth which enabled simple determination of the MIC. When the plates were returned to the incubator for further growth of the organism, the pellet size of wells containing actively growing cells increased whereas the pellets due to precipitated material in wells did not increase in size.

Preliminary antimycobacterial assays of compounds were carried out utilizing a constitutive Green Fluorescence Protein (GFP) expression vector direct readout of fluorescence as a measure of bacterial growth. *Mycobacterium tuberculosis* H_{37}Rv with a constitutive GFP plasmid was used as a test strain. Compounds were prepared in 100 % DMSO at an initial stock concentration of 10 mg/mL. Serial dilutions of the compounds were prepared in the same solvent and added to the wells of a black clear-bottom 384-well plate (in order to minimize background fluorescence) at 2 µL volume compound per well. 48 µL of H_{37}Rv-GFP bacterial suspension was then added to the diluted compound resulting in a final volume of 50 µL in 384-well microtiter plates. Plates were incubated at 37 ^{o}C for 5 days. Mycobacterial growth was determined by measuring GFP fluorescence using a multilabel reader. The increase in fluorescence indicated growth of the GFP-expressing strain whereas a lack of increase of fluorescence readout or even a decrease in fluorescence relative to the day 0 fluorescence value, indicated growth inhibition. The disadvantage of using the Green Flourescence Protein (GFP) strain as readout is that any compound with fluorescence excitation and emission wavelengths close to the excitation and emission spectrum of GFP would lead to interference in this assay leading to potentially false

negative results although this was overcome by reading the fluorescence of the plates on day 0. In addition, fluorescence quenching compound would similarly result in false negative values.
All the bioassay experiments were done in duplicates and assay results were reported in the form of MIC values.

CHAPTER FOUR

RESULTS AND DISCUSSION

4.1 Plant Extraction

One kilogram of air-dried ground leaves of *Pavetta crassipes* yielded 10.4 g of hexane extract, 16.8 g of ethyl acetate extract and 131.7 g of methanol extract, representing an extraction yield of 1.04%, 1.68% and 13.2% respectively.

4.2 Isolation of Compounds

4.2.1 Isolation of NN03

Compound **NN03** was obtained as impure dark green crystals from the column chromatography of the hexane and ethyl acetate extracts of *P. crassipes*. Recrystallization from methanol yielded white crystalline solid (22 g, 15 g), respectively, with an *R*f of 0.4 (silica gel; Hex: EtOAc, 5:1).

4.2.2 Isolation of NN05

Compound **NN05** was obtained as light green solid from the column chromatography of the hexane and ethyl acetate extracts of *P. crassipes*. Recrystallization from ethanol yielded white solid (15 mg, 102 mg), respectively with an *R*f of 0.51 (silica gel; Hex: EtOAc, 3:1).

4.2.3 Isolation of NN07

Compound **NN07** was obtained as yellow solid from HPLC chromatography of the ethyl acetate extracts of *P. crassipes*. Purification on prep TLC yielded amorphous yellow solid (18 mg) with an *R*f of 0.35 (silica gel; $CHCl_3$: MeOH, 9:1).

4.2.4 Isolation of NN06

Compound **NN06** was obtained as yellow solid from HPLC chromatography of the ethyl acetate and methanol extracts of *P. crassipes*. Purification on prep TLC yielded amorphous yellow solid (8 mg, 12 mg), respectively with an *R*f of 0.33 (silica gel; $CHCl_3$: MeOH, 9:1).

4.2.5 Isolation of NN01

NN01 was obtained as a yellow precipitate from the column chromatography of the methanol extract of *P.crassipes*. Purification by washing with ethyl acetate yielded amorphous yellow solid (56 mg) with and *R*f of 0.3 (silica gel; $CHCl_3$: MeOH: CH_3COOH, 7:3:0.5).

4.2.6 Isolation of NN04

NN04 was obtained from the column chromatography of the methanol extract of *P.crassipes*. Purification by prep TLC yielded pale yellow solid (15 mg), respectively with an *R*f of 0.56 (silica gel; $CHCl_3$: MeOH, 4:1).

4.2.7 Isolation of NN02

NN02 was obtained as light brown precipitate from the column chromatography of the methanol extract of *P.crassipes*. Recrystallization from methanol yielded white solid.

4.3 Characterization of Isolated Compounds

4.3.1 Characterization of NN03

NN03 had a melting point of 133-135^{o}C. The IR spectrum (Fig 4.1) indicated the presence of a hydroxyl group at 3356 cm^{-1}. The positive ion mode TOF-ESI mass spectrum (Fig 4.2) showed a pseudomolecular $[M + H]^+$ ion at *m/z* 397.4 corresponding to $C_{29}H_{50}O$ – $[H_2O + H]$. The information from the mass spectrum, together with the number of carbon signals in ^{13}C NMR at 29 (Figs 4.3 and 4.4), led to the determination of the molecular formula as $C_{29}H_{50}O$ (DBE = 5).

The ^{1}H NMR spectra (Figs 4.5 and 4.6) allowed for quick identification of **NN03** as a steroid or terpenoid based on the collection of signals between 2.5 and 0.5 ppm. A diagnostic signal was located at δ_H 5.34 (1H, d). This signal was deduced to be a trisubstituted olefinic proton and assigned to position H-6. The typical seven line dddd signal at δ_H 3.52 was recognized as the proton of a 3-H function (1H, dddd). Other defined signals were two tertiary methyl groups at δ_H 0.67 (3H, s, H-18), 1.00 (3H, s, H-19), three secondary methyl groups at δ_H 0.80 (3H, d, H-27), 0.82 (3H, d, H-26) and 0.91 (3H, d, H-21) and one primary methyl group at δ_H 0.84 (3H, t, H-29). Most other methine and methylene signals had broad multiplets between δ_H 1.07 and 2.26.

In the ^{13}C spectrum (Fig 4.5), 29 signals were observed, which was also suggestive of a steroidal ring. Of these, two olefinic carbons δ_C 140.7 (qC, C-5) and 121.7 (CH, C-6) and a hydroxyl bearing methine δ_C 72.01 (CH-OH, C-3) were revealed.

Analysis of the available data and comparison with data in existing literature (Lee *et al*., 2003) led to full proton and assignments (Table 4.1).

Table 4.1. **^{1}H and ^{13}C spectroscopic data of compound** NN03 **in $CDCl_3$**

Position C/H Atom	**δ_H**	**^{1}H multiplicity**	**δ_C**	**DEPT**	**β-Sitosterol ($CDCl_3$) Lee *et al*. (2003)**
1		m	37.2	CH_2	37.2
2		m	29.7	CH_2	29.7
3	3.52	dddd	72.0	CH	71.8
4		m	39.8	CH_2	39.7
5	5.34	-	140.7	qC	140.7
6		m	121.7	CH	121.7
7		m	31.9	CH_2	31.8
8		m	31.6	CH	31.6
9		m	50.1	CH	50.1
10		-	36.5	qC	36.5
11		m	21.1	CH_2	21.1
12		m	40.4	CH_2	40.5
13		-	42.3	qC	42.3
14		m	56.7	CH	56.8
15		m	24.3	CH_2	24.3
16		m	28.2	CH_2	28.3
17		m	56.0	CH	56.0
18	0.67	s	11.8	CH_3	12.0
19	1.00	s	19.0	CH_3	19.0
20		m	36.1	CH	36.1
21	0.91	d	18.7	CH_3	18.8
22		m	33.9	CH_2	33.9
23		m	26.0	CH_2	26.0
24		m	45.9	CH	45.8
25		m	29.1	CH	29.1
26	0.82	d	19.8	CH_3	19.8
27	0.80	d	19.3	CH_3	19.4
28		m	23.0	CH_2	23.1
29	0.84	t	12.0	CH_3	12.2

Compound **NN03** was deduced as 22, 23-dihydrostigmasterol (β-sitosterol; **142**).

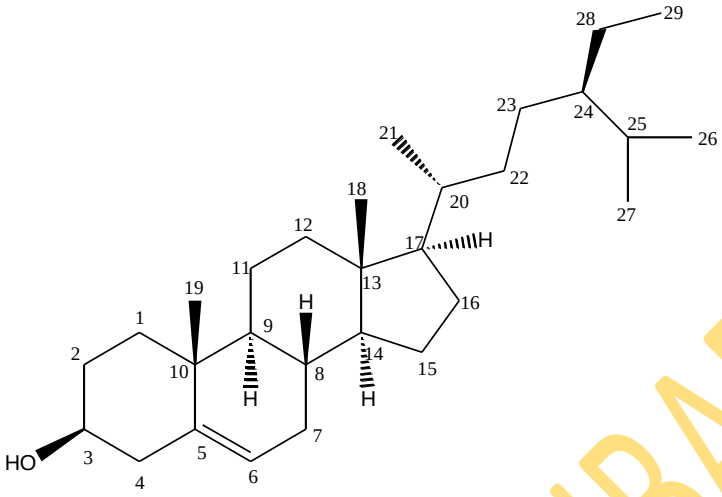

142

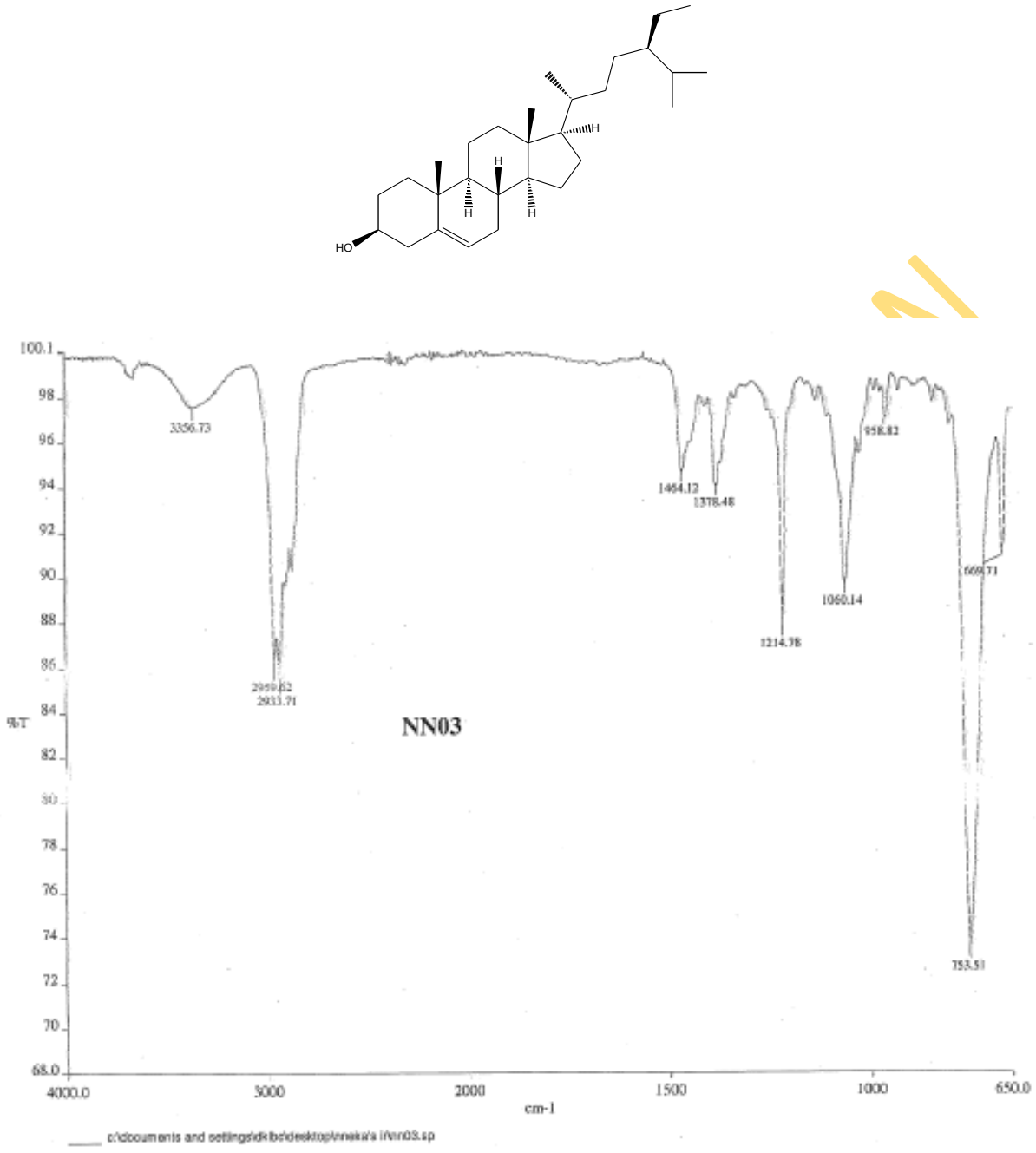

Figure 4.1. Compound NN03 (β-sitosterol) IR spectrum

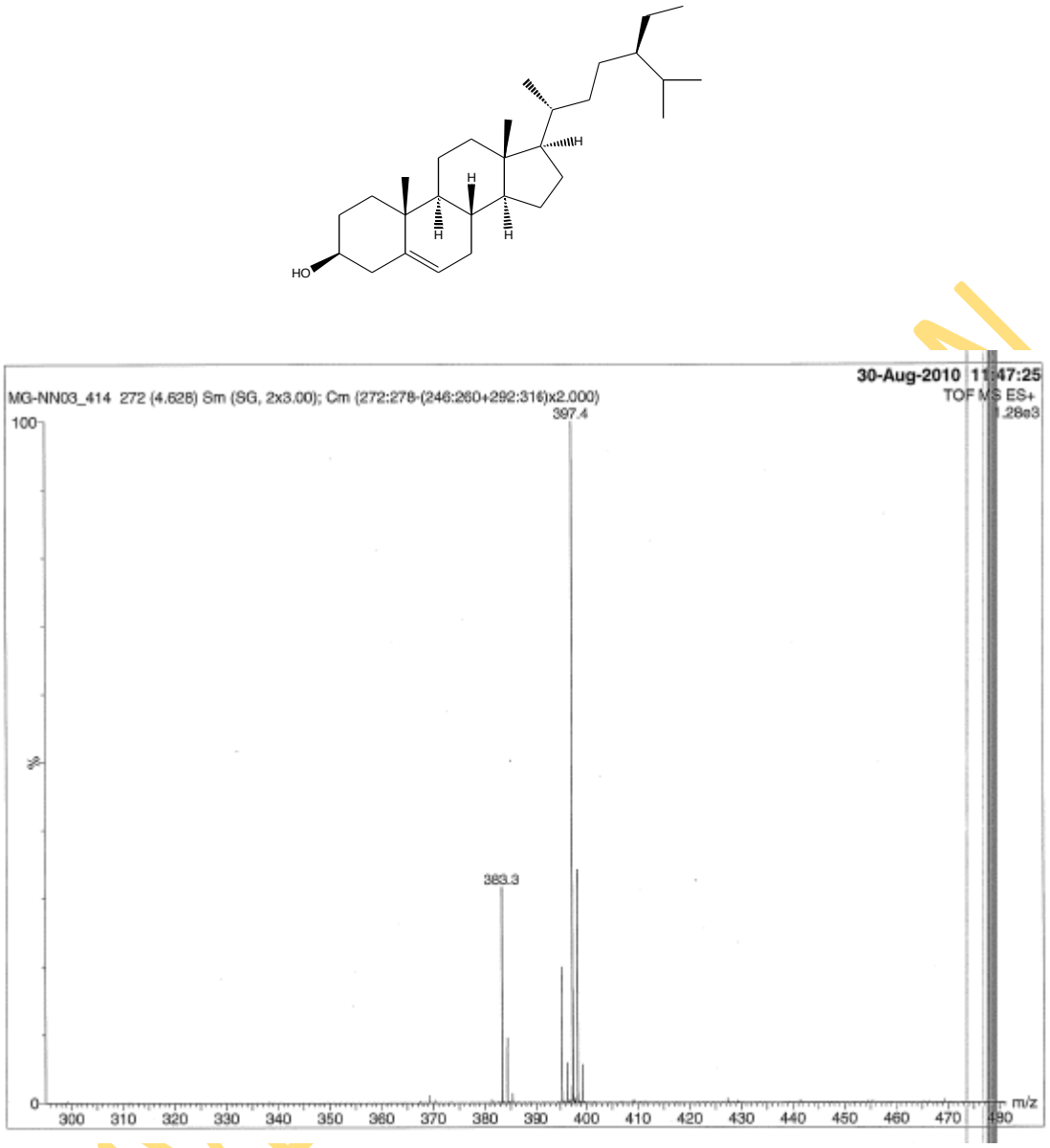

Figure 4.2. Compound NN03 (β-sitosterol) ES-MS-TOF spectrum

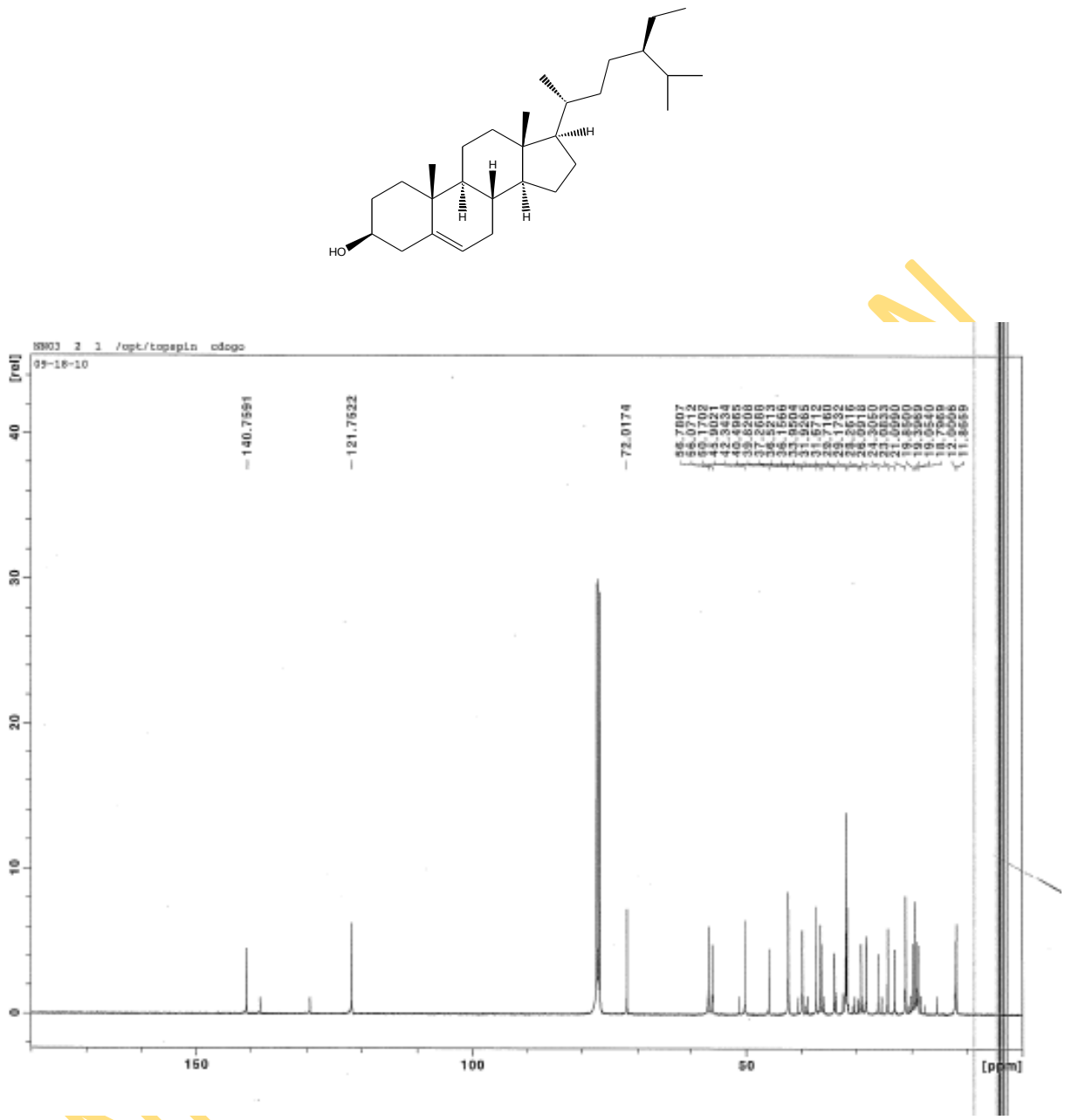

Figure 4.3. Compound NN03 (β-sitosterol) 100 MHz ^{13}C spectrum in $CDCl_3$

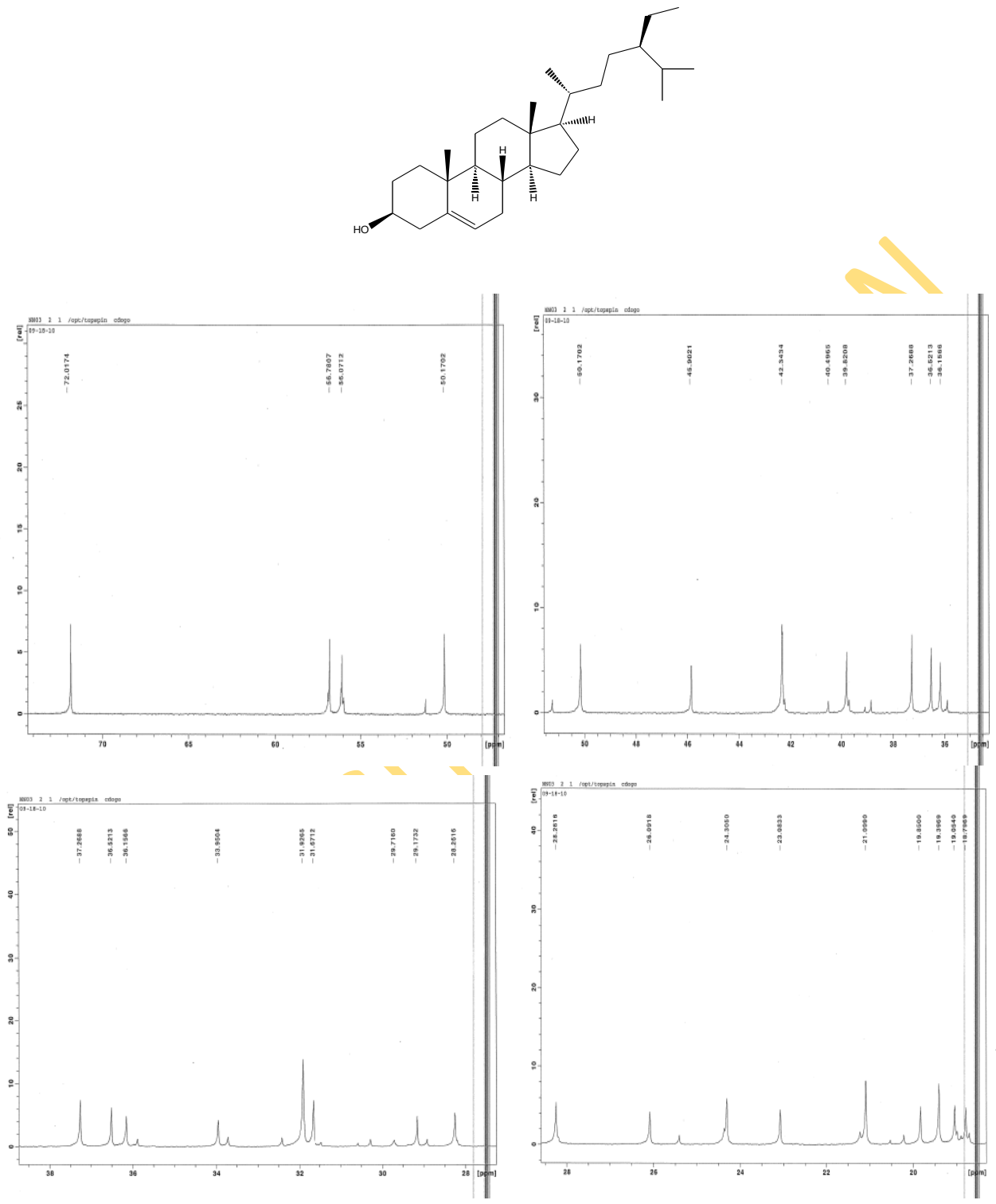

Figure 4.4. Compound NN03 (β-sitosterol) 100 MHz ^{13}C spectrum in $CDCl_3$ (expanded regions)

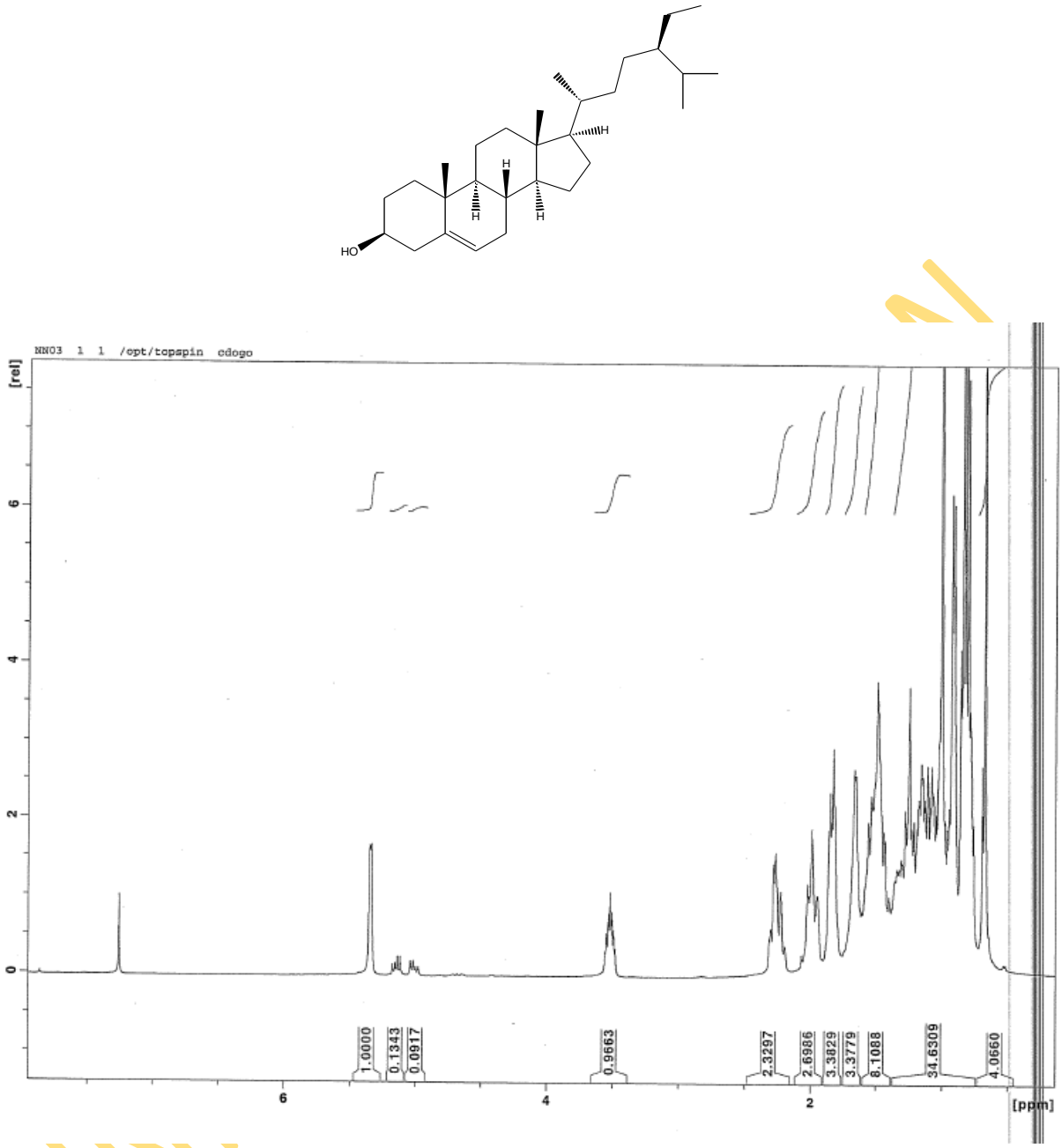

Figure 4.5. Compound NN03 (β-sitosterol) 400 MHz ^{1}H spectrum in $CDCl_3$

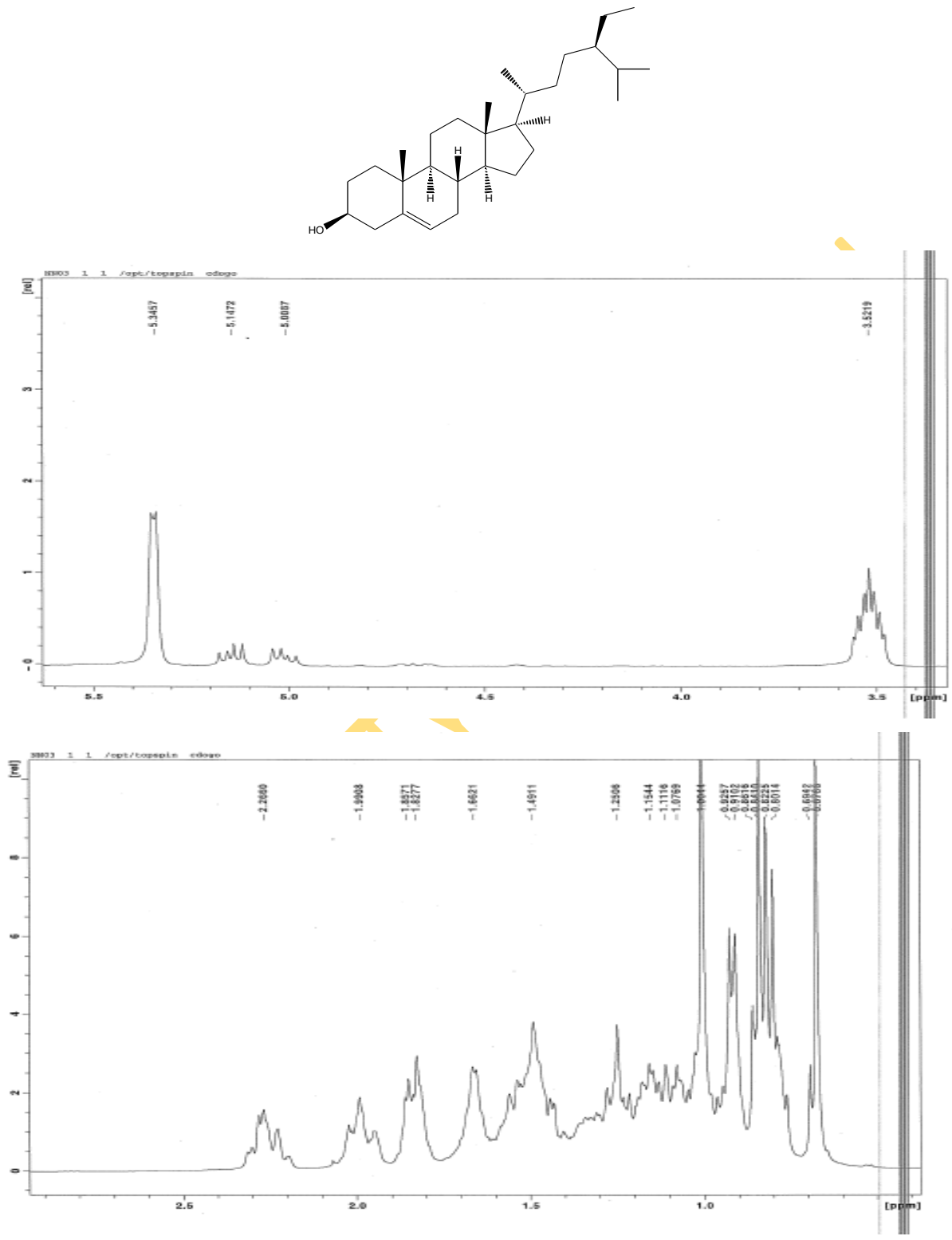

Figure 4.6. Compound NN03 (β-sitosterol) 400 MHz ^{1}H spectrum in $CDCl_3$ (expanded regions)

4.3.2 Characterization of NN05

The melting point of **NN05** was obtained to be 284-286^{o}C. The IR spectrum (Fig 4.7) suggested the presence of a carbonyl group (1688 cm^{-1}) and a hydroxyl group (3673 cm^{-1}). The positive ion mode ESI-TOF mass spectrum (Fig 4.8) showed a pseudomolecular $[M + H]^+$ ion at *m/z* 439.4 corresponding to $C_{30}H_{48}0_3$ – $[H_2O + H]$. Analyses of ^{13}C-NMR, DEPT spectra (Figs 4.9 and 4.10) and ESI-TOF-MS data (Fig 4.8) established the molecular formula as $C_{30}H_{48}O_3$ (DBE = 7).

The ^{1}H NMR spectra (Figs 4.11and 4.12) revealed signals due to a carboxylic proton δ_H 11.92 (1H, s, 17-COOH), a trisubstituted olefinic proton δ_H 5.12 (1H, t, H-12), a hydroxyl proton δ_H 4.27 (1H, d, 5.2 Hz, 3-OH), and two methine protons at δ_H 2.99 (1H, m, H-3) and δ_H 2.09 (1H, d, 12 Hz, H-18). Other signals were due to five tertiary methyl groups at δ_H 1.03 (3H, s, H-27), 0.89 (3H, s, H-23), 0.86 (3H, s, H-25), 0.74 (3H, s, H-26) and 0.67 (3H, s, H-24) and two secondary methyl groups δ_H 0.90 (3H, d, 8 Hz, H-30) and 0.81 (3H, d, 6.4 Hz, H-29). This was suggestive of a pentacyclic triterpenoid with an ursane skeleton. The remaining signals were broad multiplets resonating between δ_H 1.23 and 1.85, most of which were diasterostopic CH_2 groups.

The ^{13}C NMR spectra (Figs 4.9 and 4.10) obtained with the aid of DEPT spectral analysis, revealed 30 carbon signals comprising 7 methyls, 9 methylenes, 7 methines and 7 quartenary carbons. This included a carbonyl carbon δ_C 178.2 (qC, C-28), two olefinic carbons δ_C 138.1 (qC, C-13) and 124.5 (CH, C-12) and a hydroxyl bearing methine δ_C 76.8 (CH-OH, C-3).

Common long range correlations observed in the HMBC spectrum (Fig 4.13) between δ_H 0.89 (3H, s, H-23), 0.67 (3H, s, H-24) and δ_C 76.8 (C-3) and 54.7 (C-2) supported the dimethyl substitution on C-4 of the ring. Direct correlations between protons were done using ^{1}H-^{1}H COSY spectrum (Figs 4-14) while protonated carbons were assigned by HSQC (Fig 4.15). Analysis of available data and comparison with literature data (Seebacher *et al*., 2003) was useful in assigning proton and carbon positions as seen in Table 4.2:

Table 4.2. ^{1}H and ^{13}C NMR spectroscopic data of compound **NN05** in DMSO-d_6

Position C/H Atom	**δ_H, multiplicity (*J* in Hz)**	**δ_C**	**DEPT**	**δ_C ursolic acid (pyridine-d_6) Seebacher *et al*. (2003)**
1		38.2	CH_2	39.2
2		27.5	CH_2	28.2
3	2.99, m 4.27, d (5.2, 3-OH)	76.8	CH	78.2
4		38.3	qC	39.6
5		54.7	CH	55.9
6		17.9	CH_2	18.8
7		32.6	CH_2	33.7
8		38.8	qC	40.1
9		46.9	CH	48.1
10		36.5	qC	37.5
11		22.8	CH_2	23.7
12	5.12, t	124.5	CH	125.7
13		138.1	qC	139.3
14		41.6	qC	42.6
15		27.5	CH_2	28.8
16		23.7	CH_2	25.0
17		46.7	qC	48.1
18	2.09, d (12)	52.3	CH	53.6
19		38.47	CH	39.5
20		38.40	CH	39.4
21		30.1	CH_2	31.1
22		36.2	CH_2	37.4
23	0.89, s	28.2	CH_3	28.8
24	0.67, s	16.0	CH_3	16.5
25	0.86, s	15.2	CH_3	15.7

26	0.74, s	16.9	CH_3	17.5
27	1.03, s	23.2	CH_3	24.0
28		178.2	qC	179.7
29	0.81, d (6.4)	16.8	CH_3	17.5
30	0.90, d (8)	21.0	CH_3	21.4

Given all the data and analysis described above, **NN05** was identified as 3β-hydroxyurs-12-en-28-oic acid (ursolic acid; **120**). This was confirmed from the comparison done on the ^{1}H and ^{13}C spectra of the isolate and an authentic, commercial sample of ursolic acid (Sigma-Aldrich; Figs 4.16 and 4.17). The spectra compared very well except for slight impurities observed in the ^{13}C at δ_C 30.67 (**NN05**) due to acetone, and at δ_C 56 and 18.5 (Sigma-Aldrich) due to ethanol.

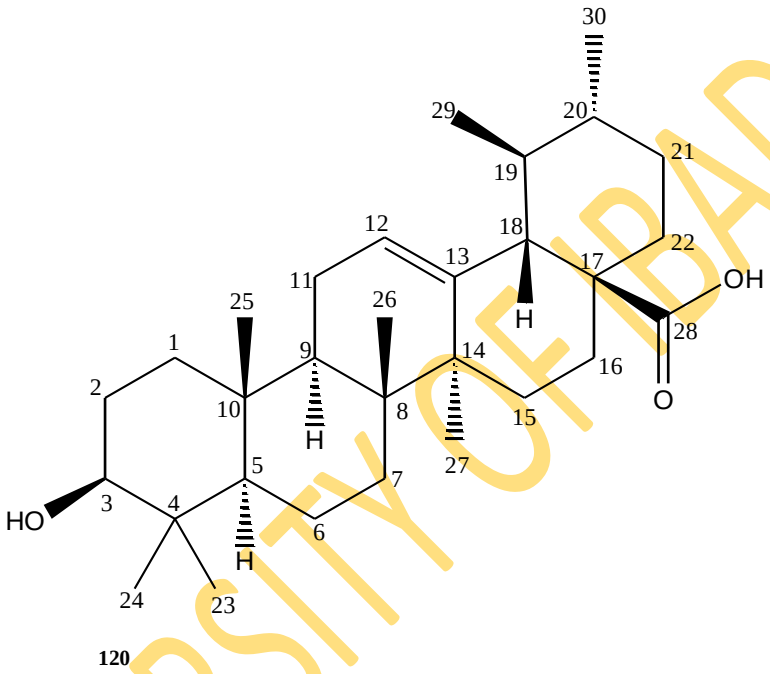

120

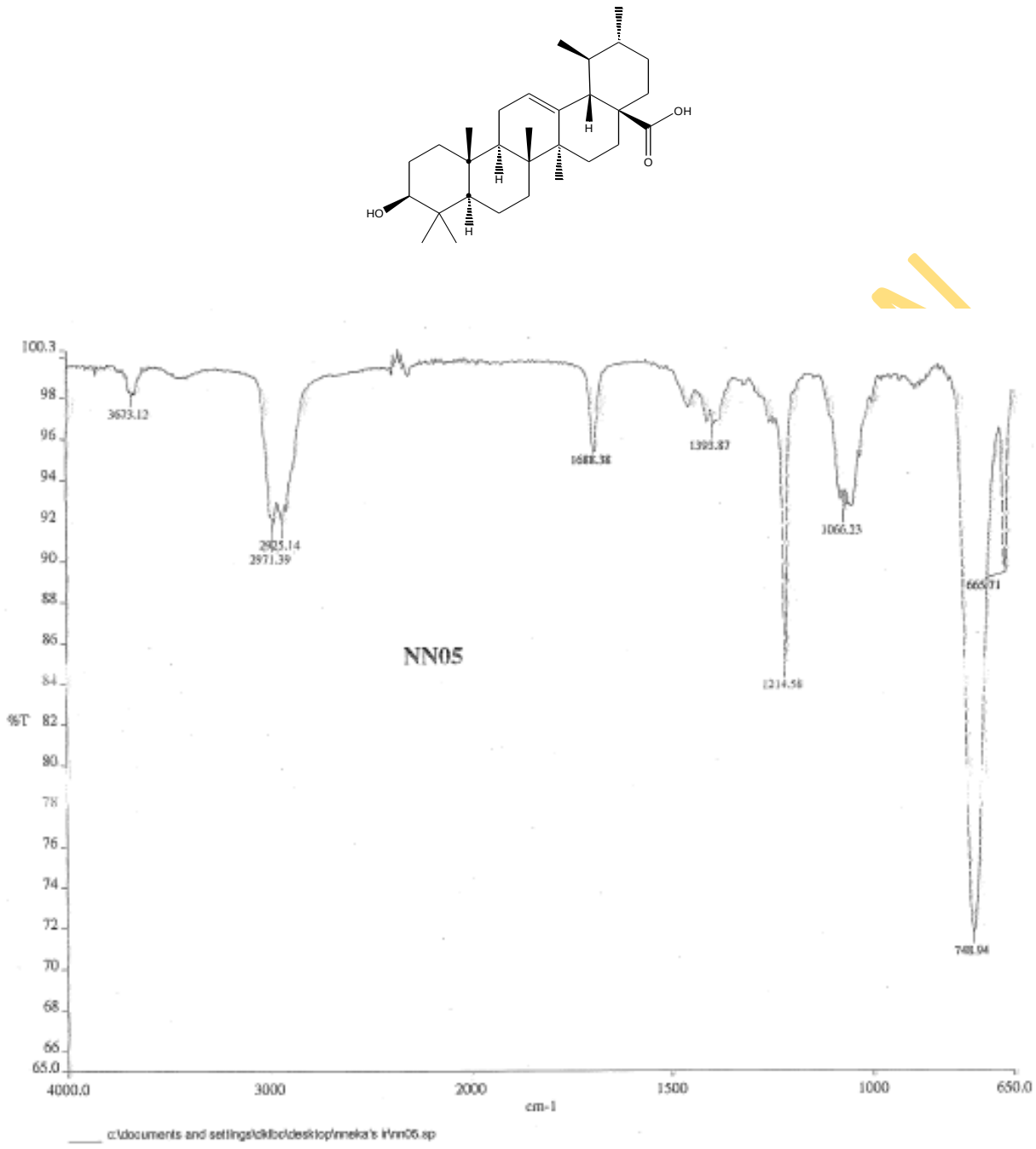

Figure 4.7. Compound NN05 (ursolic acid) IR Spectrum

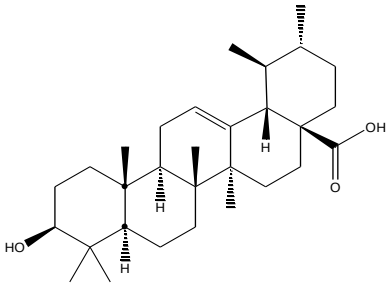

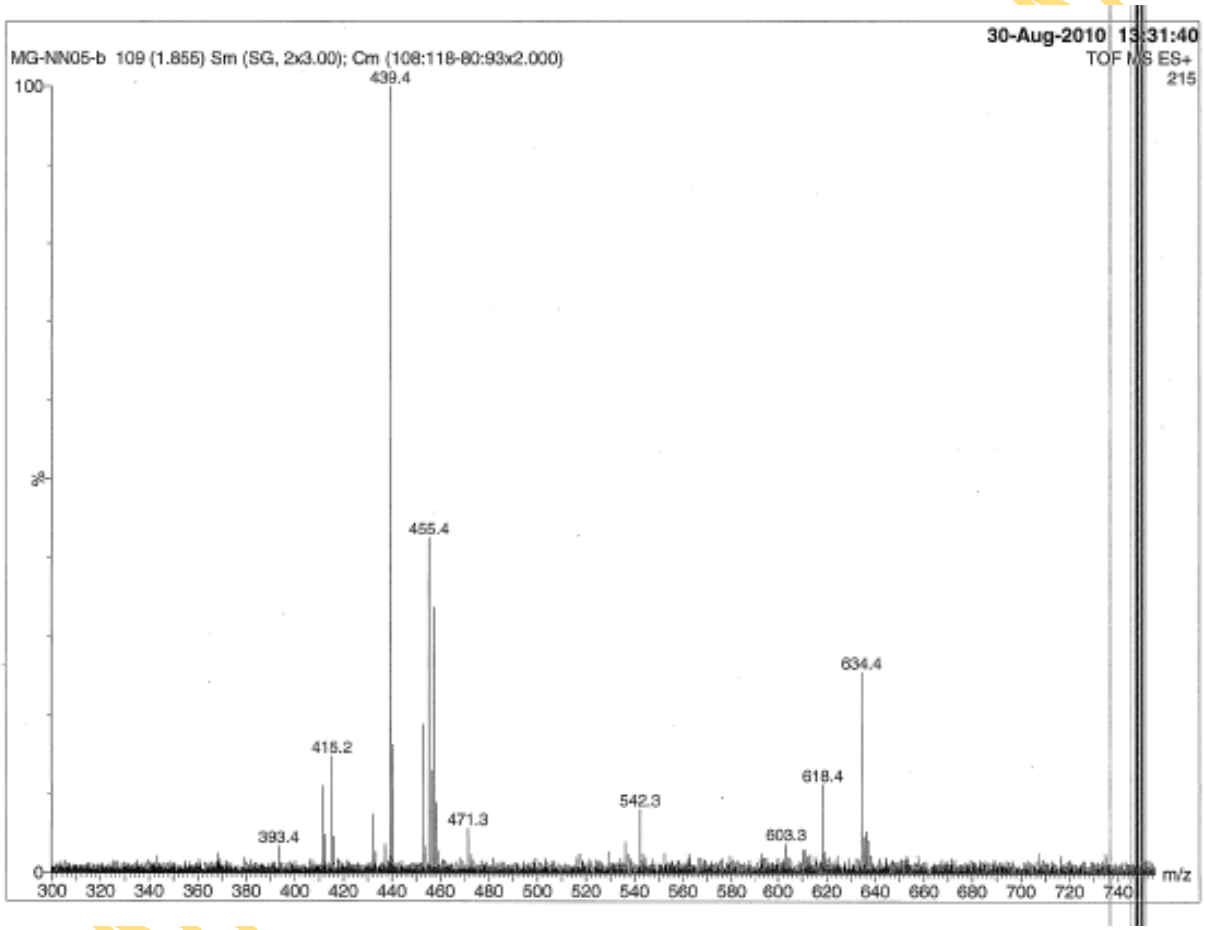

Figure 4.8. Compound NN05 (ursolic acid) ES-MS-TOF Spectrum

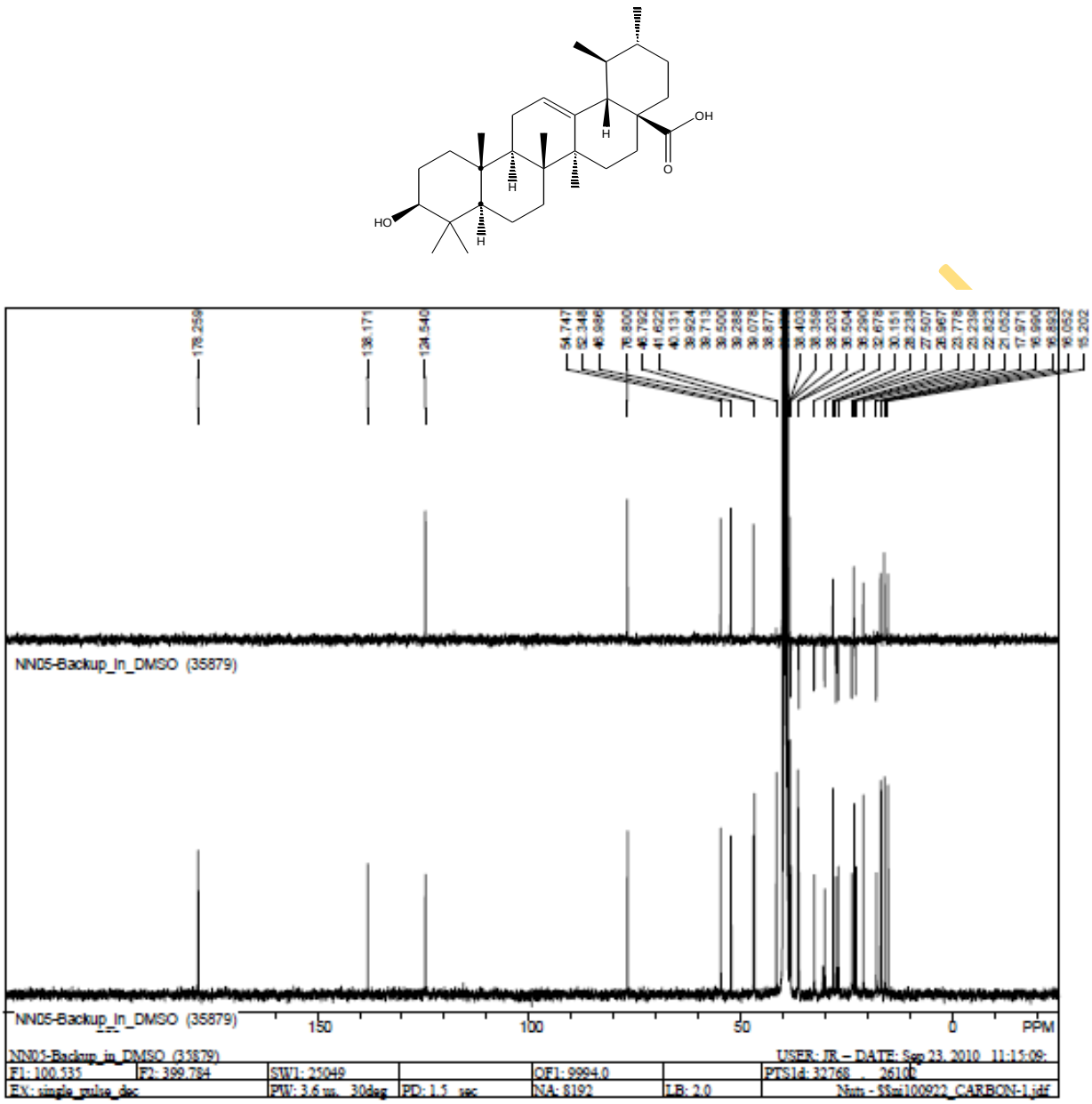

Figure 4.9. Compound NN05 (ursolic acid) 100 MHz ^{13}C and DEPT spectra in DMSO-d_6

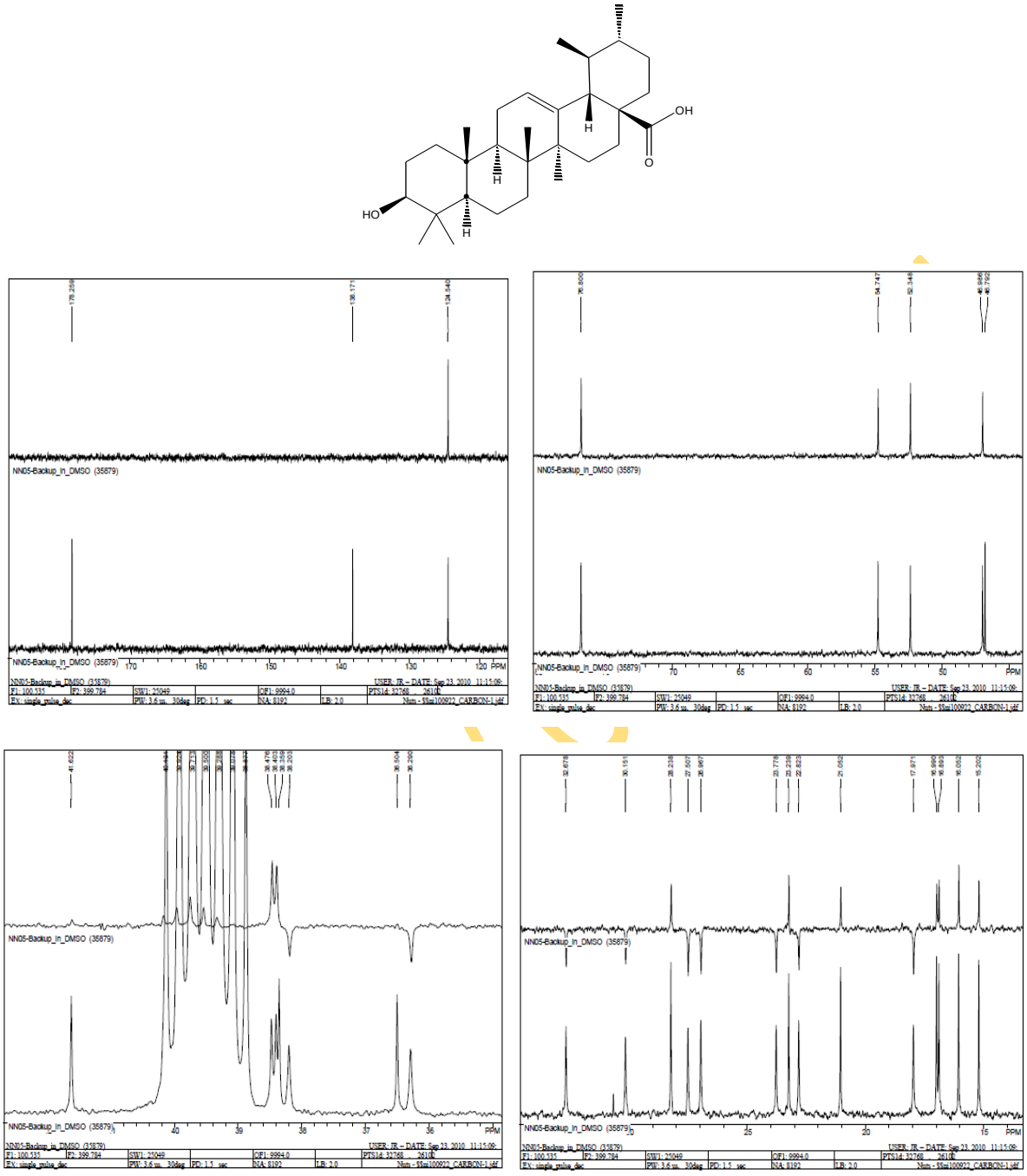

Figure 4.10. Compound NN05 (ursolic acid) 100 MHz ^{13}C and DEPT spectra in DMSO-d_6 (expanded regions)

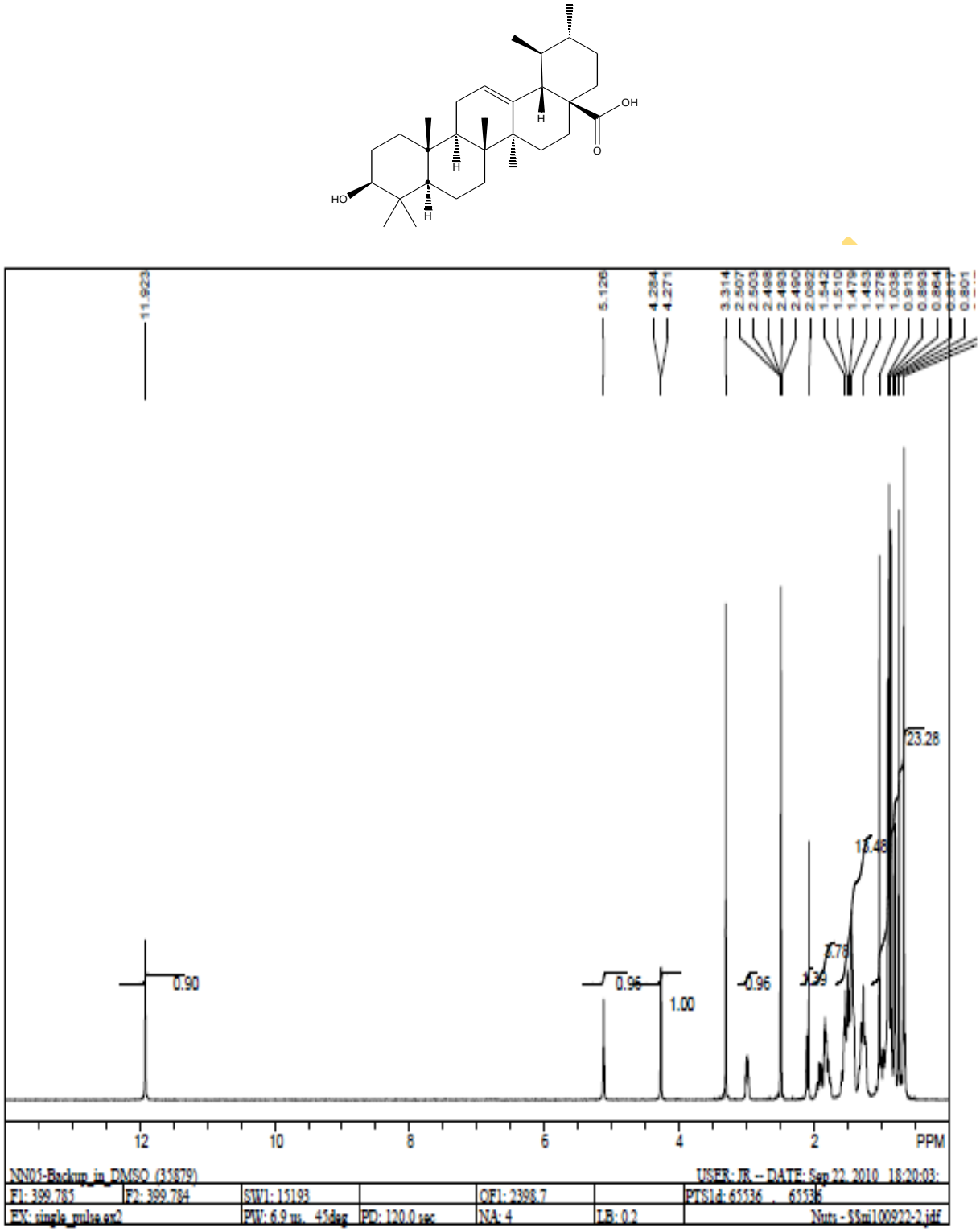

Figure 4.11. Compound NN05 (ursolic acid) 400 MHz ^{1}H spectrum in DMSO-d_6

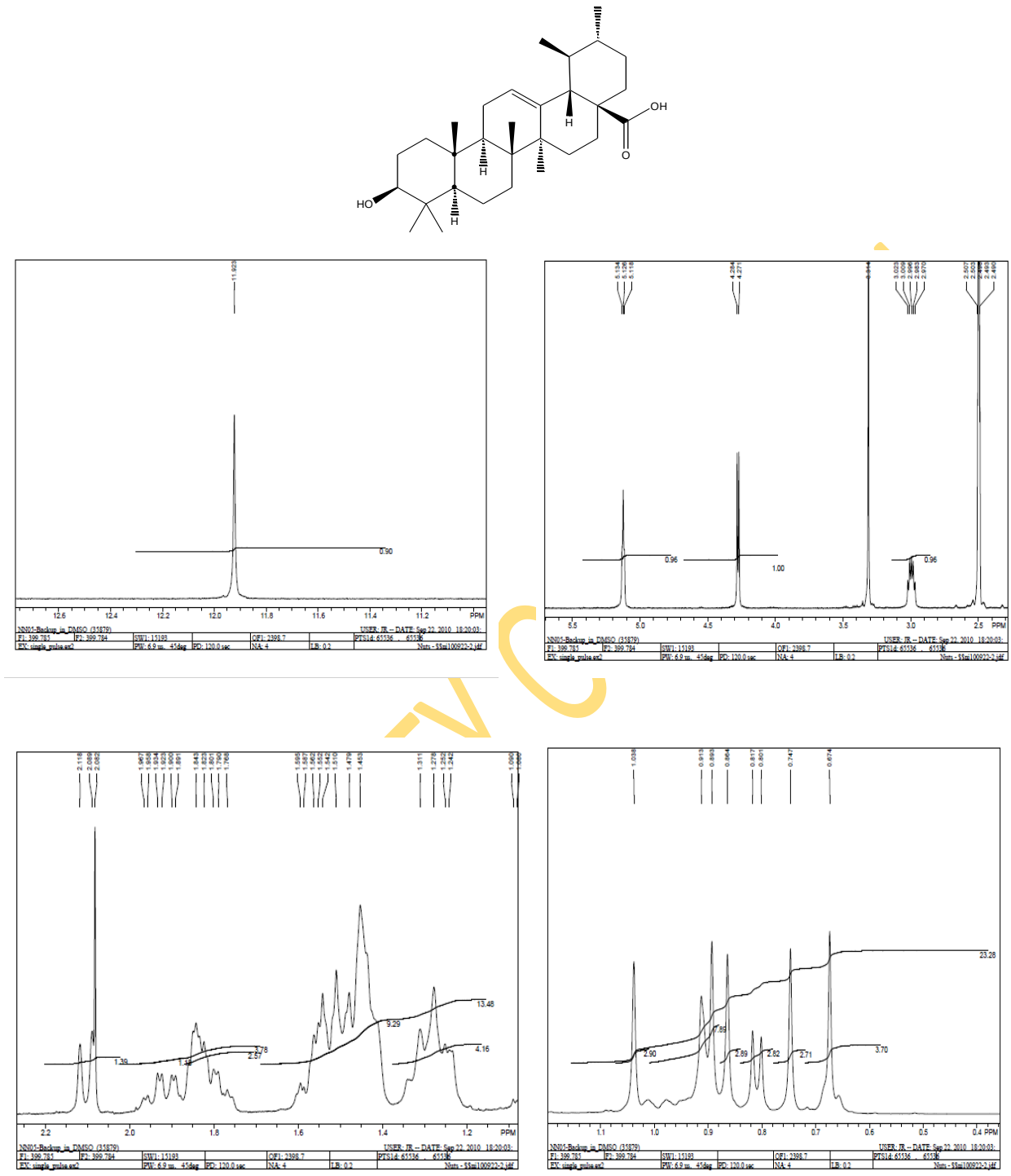

Figure 4.12. Compound NN05 (ursolic acid) 400 MHz ^{1}H spectra in DMSO-d_6 (expanded regions)

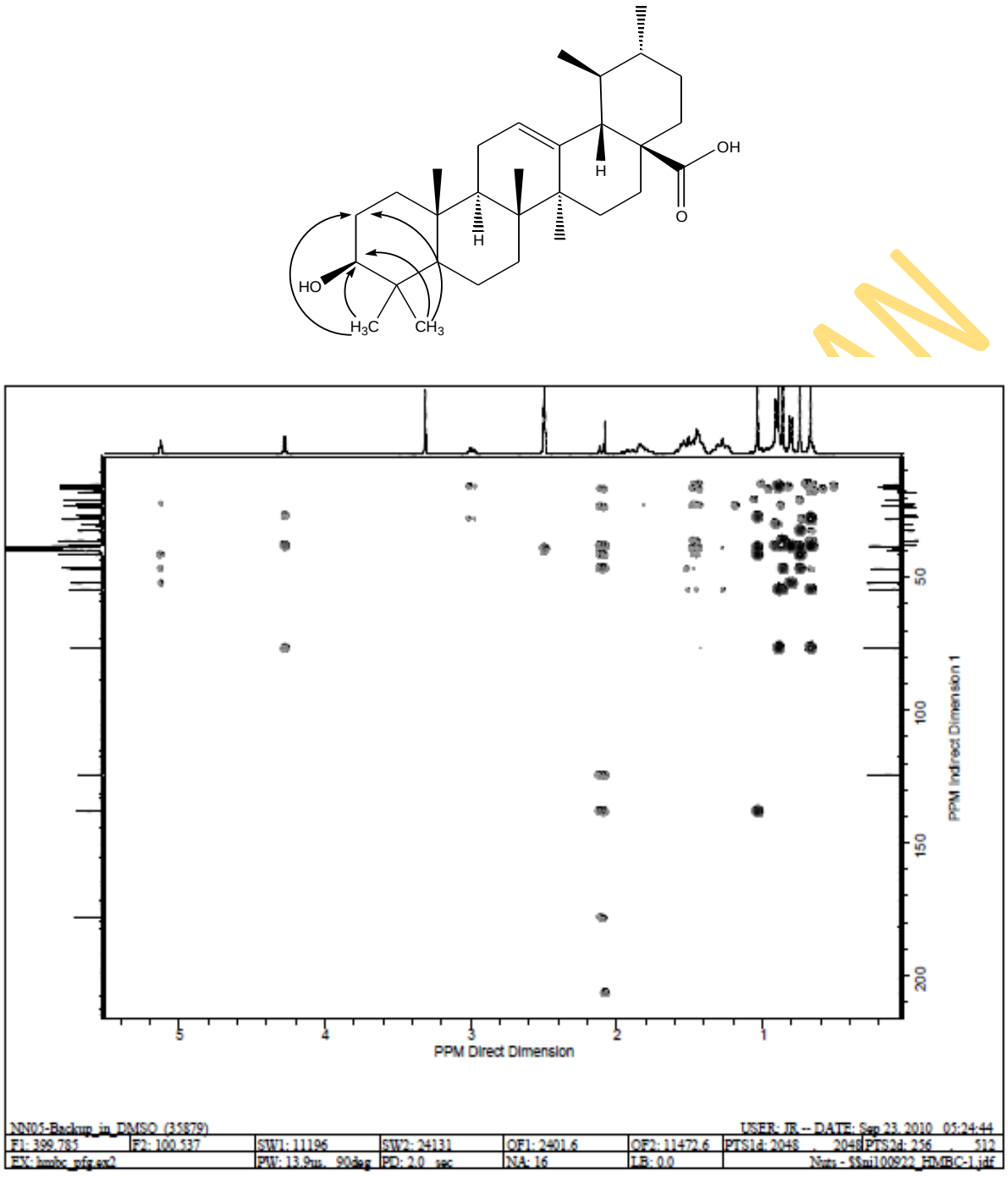

Figure 4.13. Compound NN05 (ursolic acid) 400 MHz HMBC spectrum in DMSO-d_6

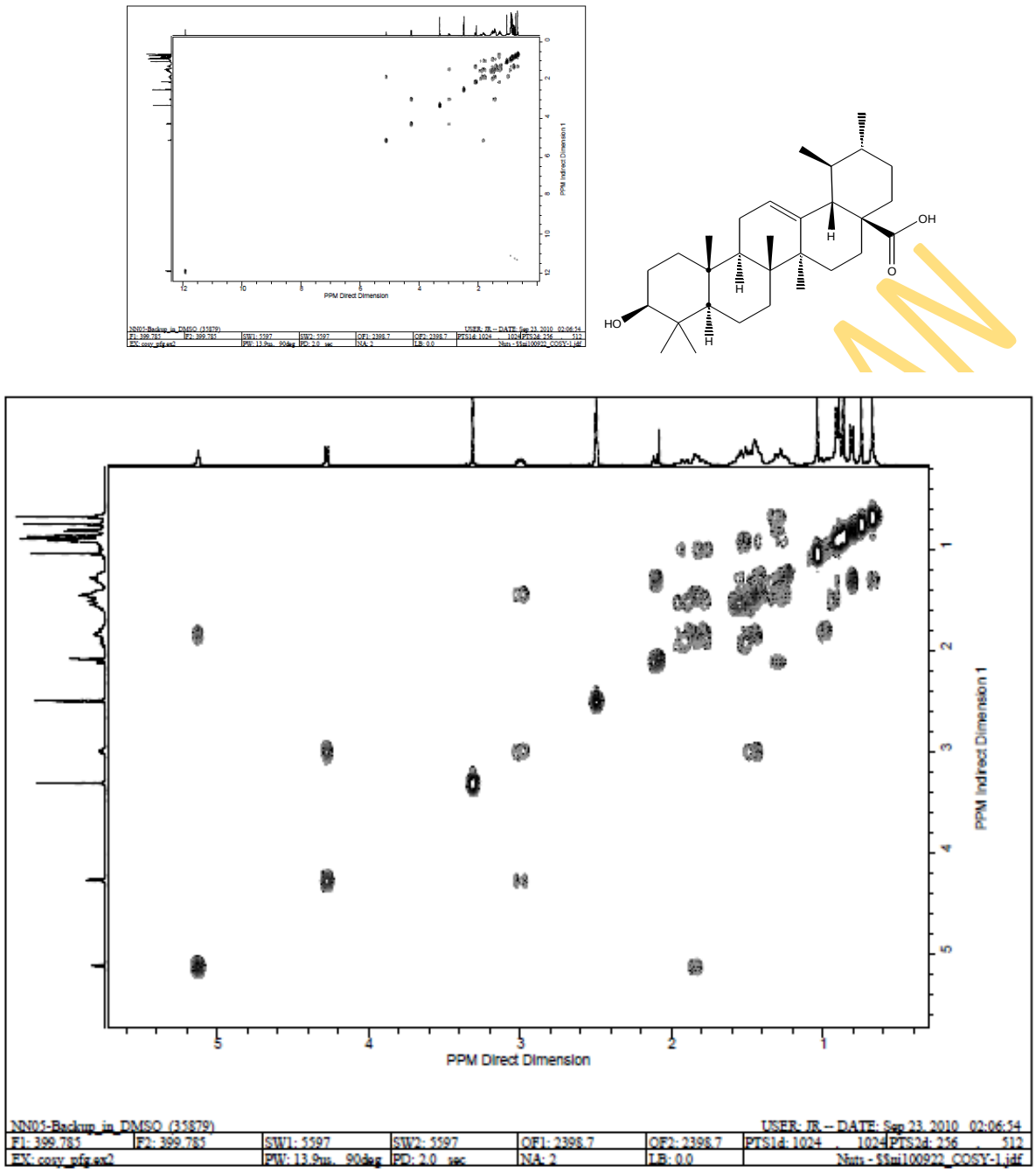

Figure 4.14. Compound NN05 (ursolic acid) 400 MHz ^{1}H- ^{1}H COSY spectrum in DMSO-d_6

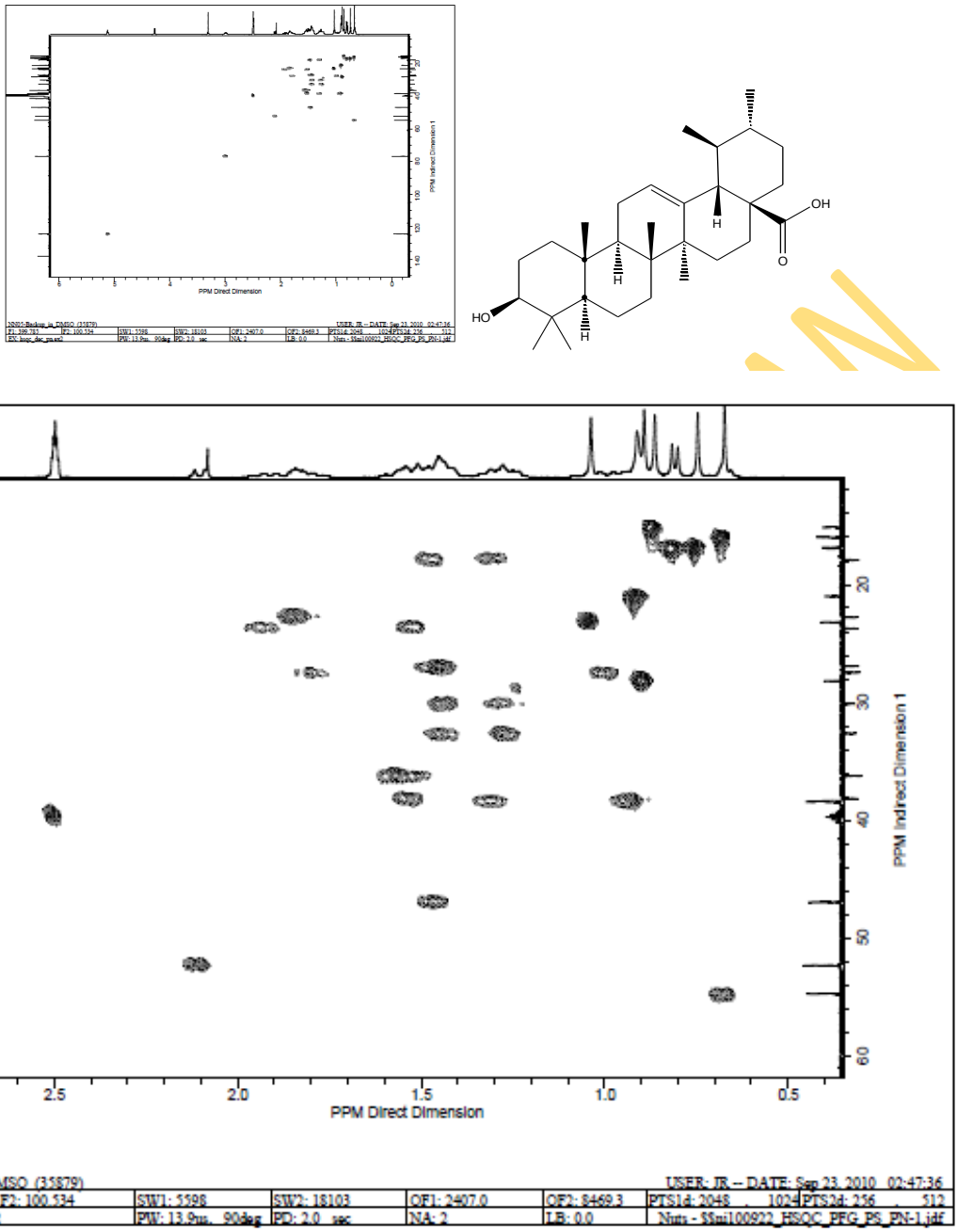

Figure 4.15. Compound NN05 (ursolic acid) 400 MHz HSQC spectrum in DMSO-d_6

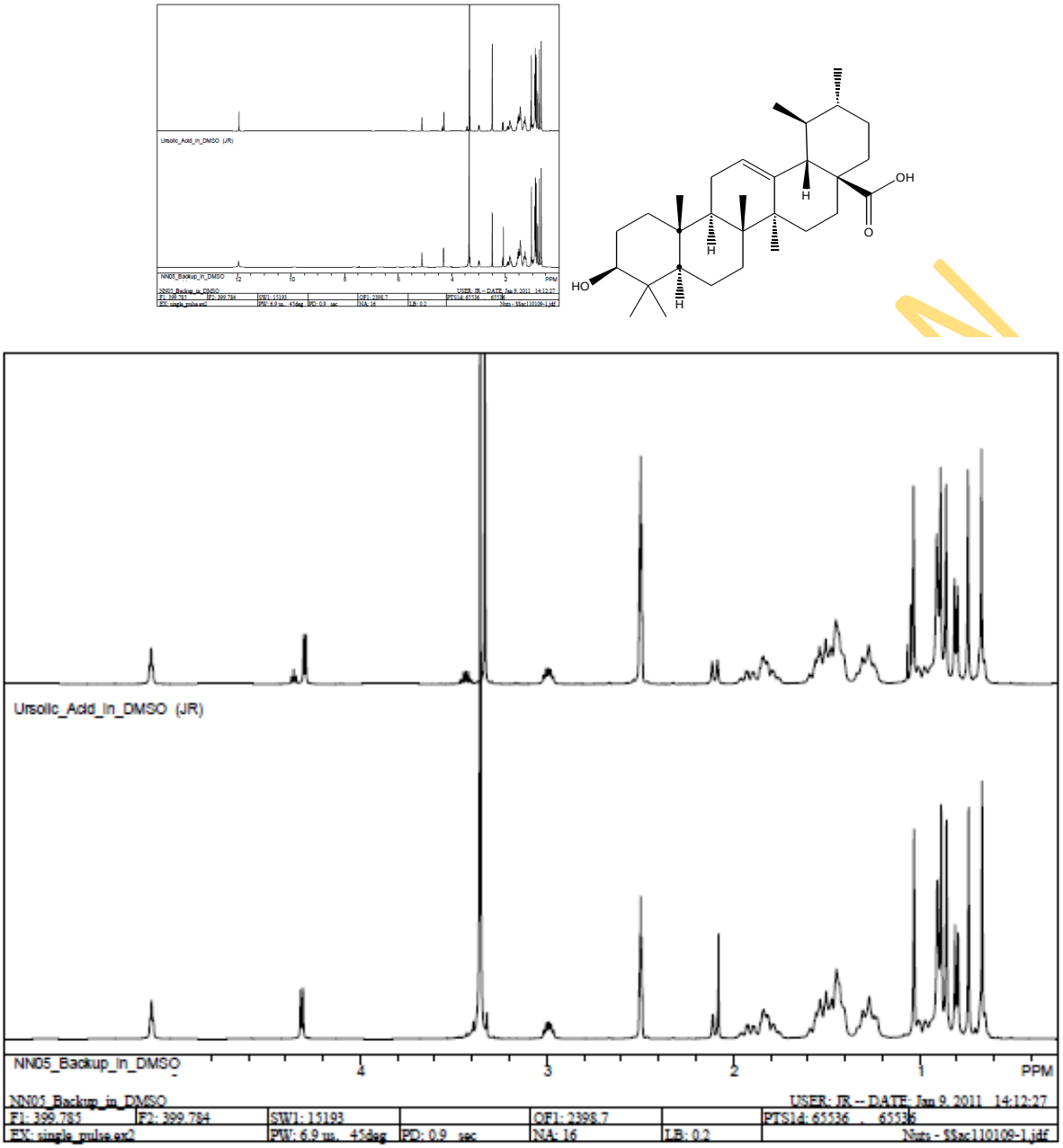

Figure 4.16. Comparative 400 MHz ^{1}H spectrum of NN05 and authentic sample (ursolic acid) in DMSO-d_6

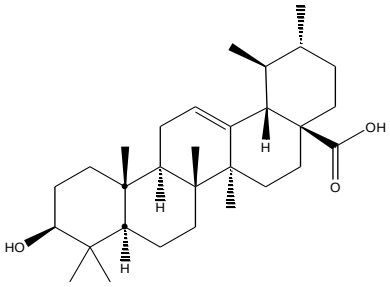

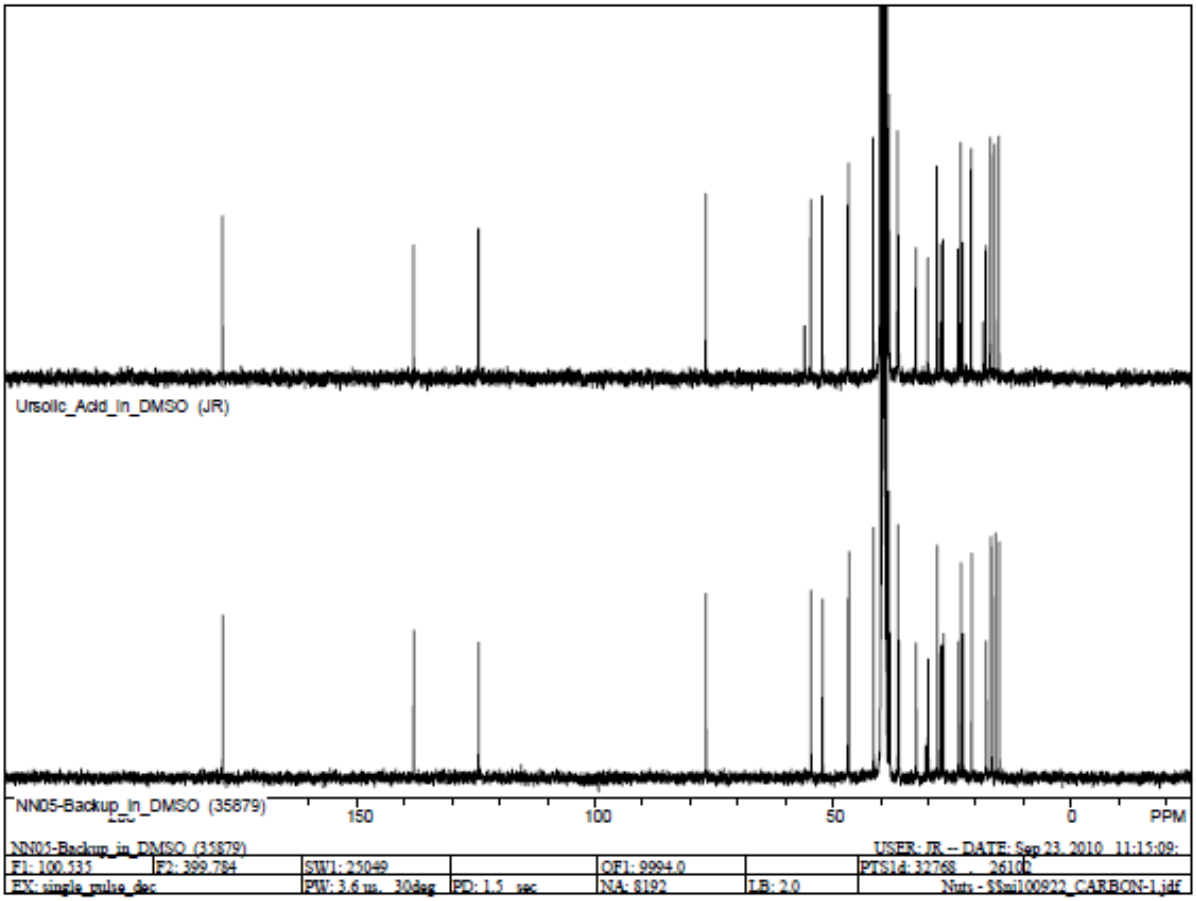

Figure 4.17. Comparative 100 MHz ^{13}C spectrum of NN05 and authentic sample (ursolic acid) in DMSO-d_6

4.3.3 Characterization of NN07

Two quasimolecular ions at *m/z* 383.1 $[M + H]^+$ and 405.1 $[M + Na]^+$ were revealed in the ESI-TOF mass spectrum (positive ion mode) of **NN07** (Fig 4.18). The molecular formula of $C_{18}H_{22}O_9$ (DBE = 8) was derived from the HRESIMS, with the $[M + H]^+$ ion at *m/z* 383.1344, supported by the ^{13}C and DEPT spectra (Figs 4.19 and 4.20) which revealed the presence of 18 carbons comprising; one methyl, 3 methylenes, 8 methines and 6 quartenary carbons. The UV spectrum exhibited absorption maxima at 218 nm and 330 nm (Fig 4.21) indicating the presence of conjugated chromophores.

The ^1H-NMR of **NN07** was run in two solvents, CD_3OD and DMSO-d_6 (Figs 4.22 – 4.24). The signals of the DMSO-d_6 spectra (Figs 4.22 and 4.23) were better resolved than that of CD_3OD (Fig 4.24), hence were used in spectral analysis. The ^1H-NMR (DMSO-d_6) spectrum of **NN07** (Figs 4.22 and 4.23) showed three aromatic protons as an ABX system at δ_H 7.01 (d, 2.0 Hz, H-2'), 6.76 (d, 8.1 Hz, H-5') and 6.95 (dd, 2.0, 8.1 Hz, H-6'). In addition, there were two olefinic protons which appeared as an AX system at δ_H 6.10 (d, 15.9 Hz, H-8') and 7.38 (d, 15.9 Hz, H-7'), characteristic of trans caffeic acid. This was supported by the ^{13}C and HSQC spectra (Figs 4.19 and 4.25, respectively) which revealed 9 resonances that were consistent with the presence of caffeic acid (Lee *et al*., 2010, Table 4.3). ^1H-^1H COSY (DMSO-d_6; Fig 4.26) also confirmed the connectivities between these protons.

Table 4.3. ^{1}H and ^{13}C NMR spectroscopic data of caffeoyl group of compound **NN07**

Position C/H Atom	**δ_H, multiplicity (*J* in Hz)**	**δ_C**	**DEPT**	**Caffeic acid (CD_3OD) Lee *et al*., (2010)**
1'		127.7	qC	127.8
2'	7.01, d (2.0)	115.16	CH	115.6
3'		149.7	qC	146.8
4'		146.9	qC	149.5
5'	6.76, d (8.1)	116.5	CH	116.5
6'	6.95, dd (2.0, 8.1)	123.0	CH	122.8
7'	7.38, d (15.9)	147.2	CH	147.0
8'	6.10, d (15.9)	115.11	CH	115.1
9'		168.3	qC	171.1

Other signals were δ_H (DMSO-d_6) 4.01 (2H, m, H-8), 5.01 (1H, m, H-3), 3.86 (1H, m, H-5), 3.56 (1H, m, H-4), 2.10 (2H, m, H-2^a, 6^a), 1.91 (1H, m, H-2^b), 1.75 (1H, m, H-6^b) and 1.12 (3H, t, H-9). The highly deshielded proton at δ_H 5.01 was indicative of a methine proton attached an acetate through oxygen. ^{1}H-^{1}H COSY (DMSO-d_6; Fig 4.25) provided more information on the connectivities between the protons:

δ_H 5.01 (1H, m, H-3) ↔ 3.56 (1H, dd, H-4)

5.01 (1H, m, H-3) ↔ 1.91(dd), 2.10 (m) (2H, H-2)

3.86 (1H, m, H-5) ↔1.75 (dd), 2.10 (m) (2H, H-6)

3.86 (1H, m, H-5) ↔ 3.56 (1H, dd, H-4)

4.01 (2H, m, H-8) ↔ 1.12 (3H, t, H-9)

With this data from ^{1}H-^{1}H COSY and more information from the ^{13}C and HSQC spectra (Figs 4.19 and 4.25, respectively), the following connectivities were deduced.

δ_H 1.75, 2.10 ($\underline{CH_2}$-COH, H-6) ↔3.86 ($\underline{CH}$-OH, H-5) ↔3.56 ($\underline{CH}$-OH, H-4) ↔5.01 ($\underline{CH}$-OH, H-3) ↔1.91, 2.10 ($\underline{CH_2}$-COH, H-2)

and δ_H 4.01 (OCH_2, H-8) ↔1.12 (CH_3, H-9)

The HMBC spectrum (Fig 4.27) also provided more information to the connectivities by revealing a common long range correlation between δ_H 7.01, 6.95 (H-2', H- 6') and δc 147.2 (C-7') confirming the caffeoyl end of the molecule. Also connectivities between δ_H 4.01 (H-8), 1.75 and 1.91 (H-6 and H-2) and δ_C 175.0 (C-7) supported the carbonyl ethyl ester substitution on C-1 of the carbocyclic group.

Unambiguous assignments were given to these carbocyclic carbons and protons and spectra was compared with the quinoyl group in literature data (Lee *et al*., 2010), as presented in Table 4.4.

Table 4.4. ^{1}H and ^{13}C NMR spectroscopic data of ethyl quinate group of compound **NN07**

C/H Atom	**δ_H, multiplicity**	**δ_C**	**DEPT**	**Quinoyl group (CD_3OD) Lee *et al.*, (2010)**
1		75.8	qC	75.8
2	2.10, 1.91, m	38.0	CH_2	38.0
3	5.01, m	72.2	CH	70.3
4	3.56, dd	72.7	CH	72.5
5	3.86, m	70.4	CH	72.1
6	2.10, 1.75, m	37.8	CH_2	37.7
7		175.0	qC	175.4
8	4.01, m	62.5	CH_2	
9	1.12, t	14.3	CH_3	

Given these data, together with biogenetic considerations, compound **NN07** was characterized as 3-caffeoyl 1-ethyl quinate (ethyl chlorogenate) (**143**).

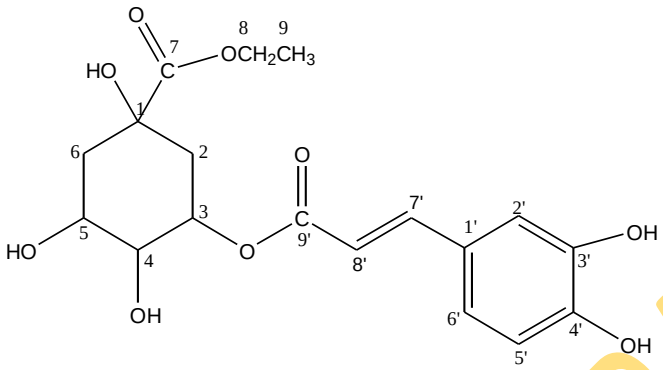

143

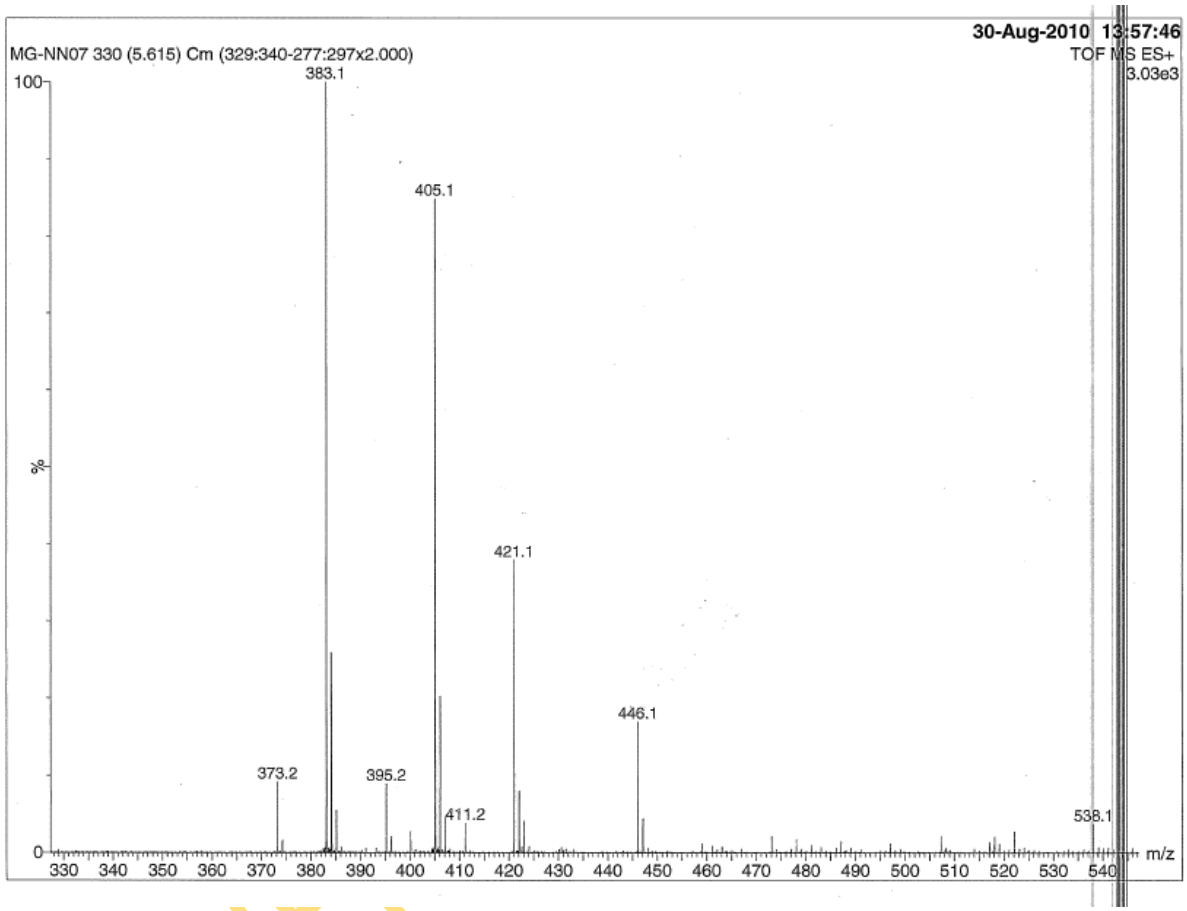

Figure 4.18. Compound NN07 (ethyl chlorogenate) ES-MS-TOF spectrum

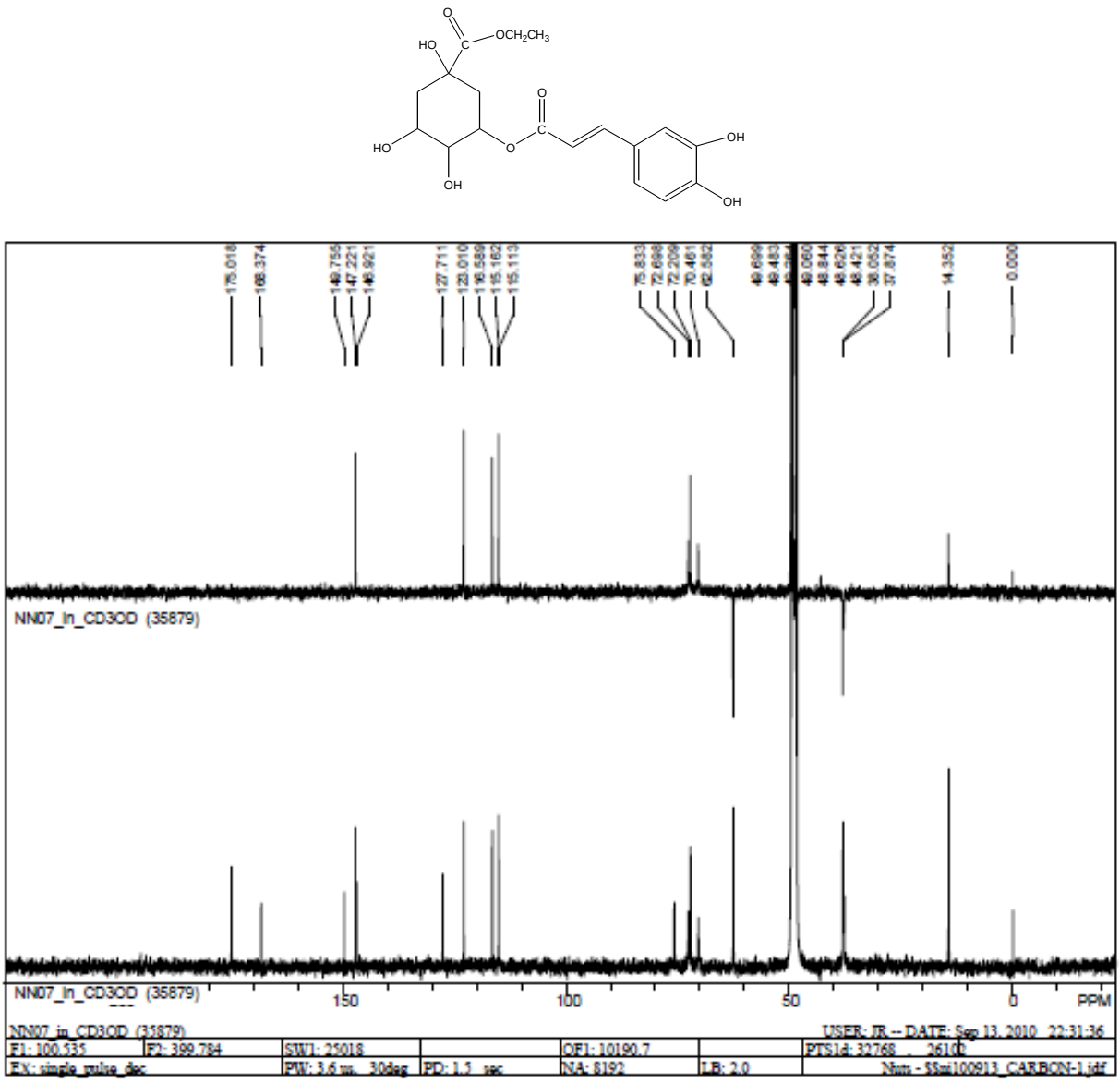

Figure 4.19. Compound NN07 (ethyl chlorogenate) 100 MHz ^{13}C and DEPT spectra in CD_3OD

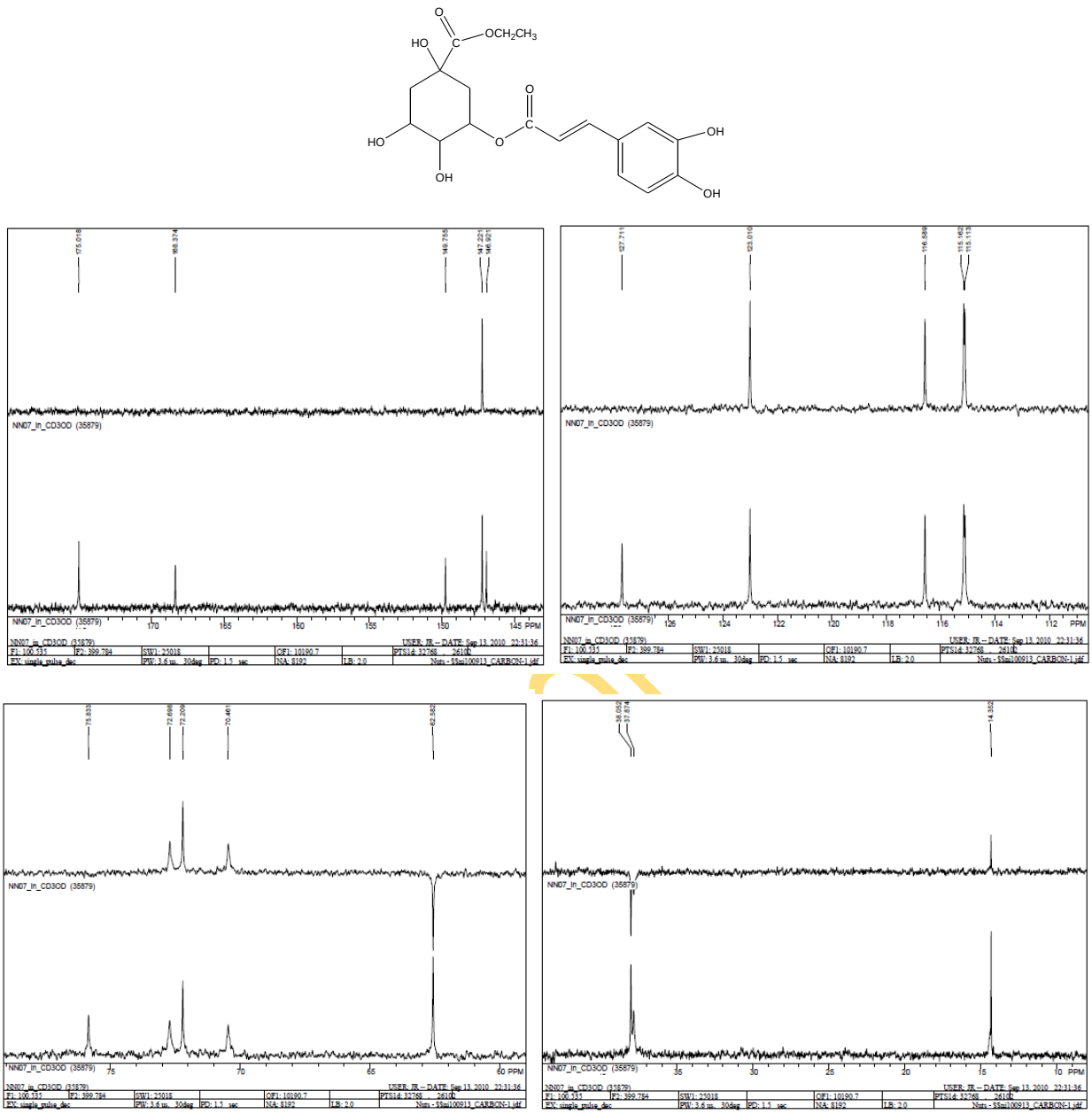

Figure 4.20. Compound NN07 (ethyl chlorogenate) 100 MHz ^{13}C and DEPT spectra in CD_3OD (expanded regions)

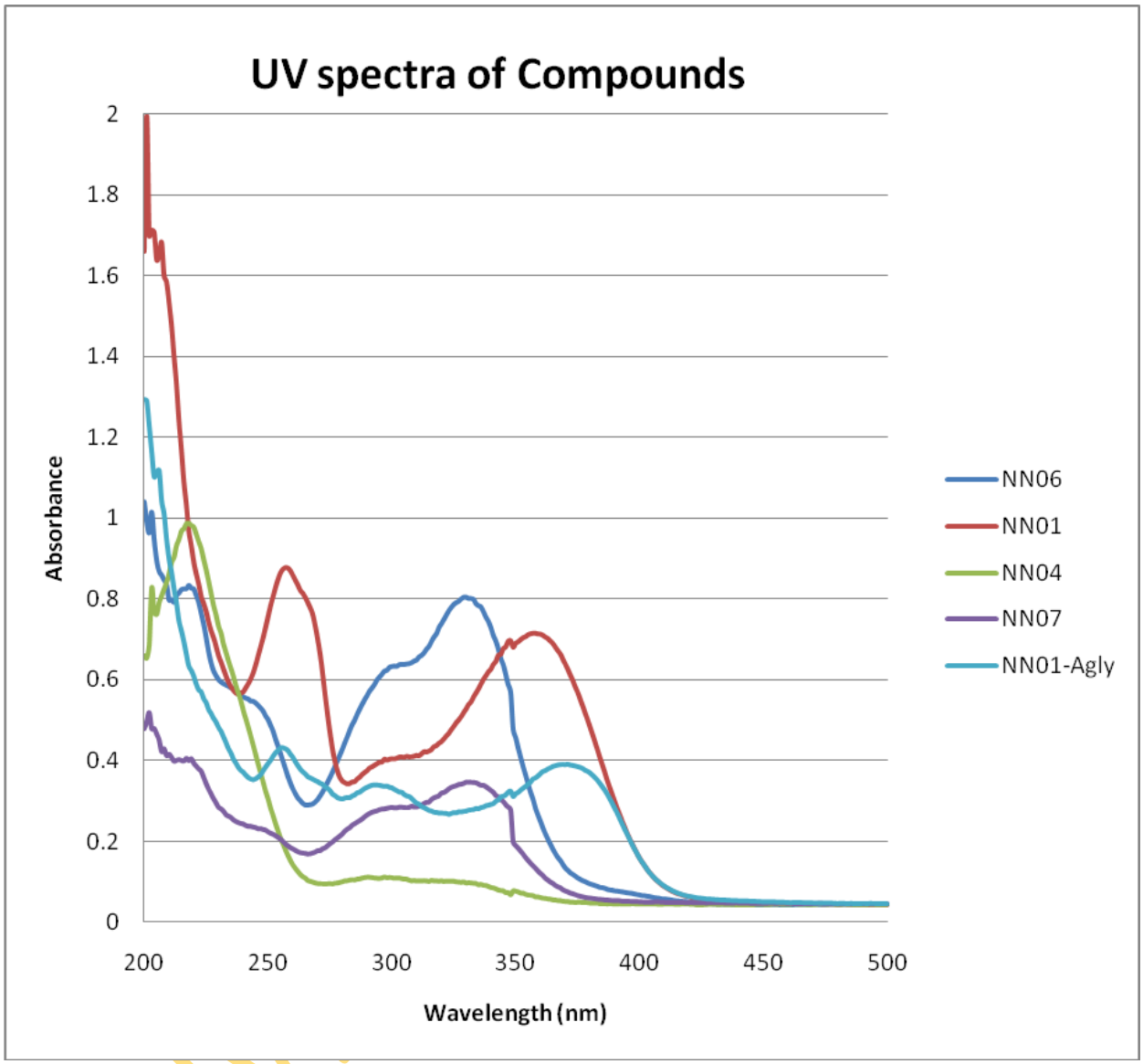

Figure 4.21. UV spectra of Compounds NN01, NN01a, NN04, NN06 and NN07

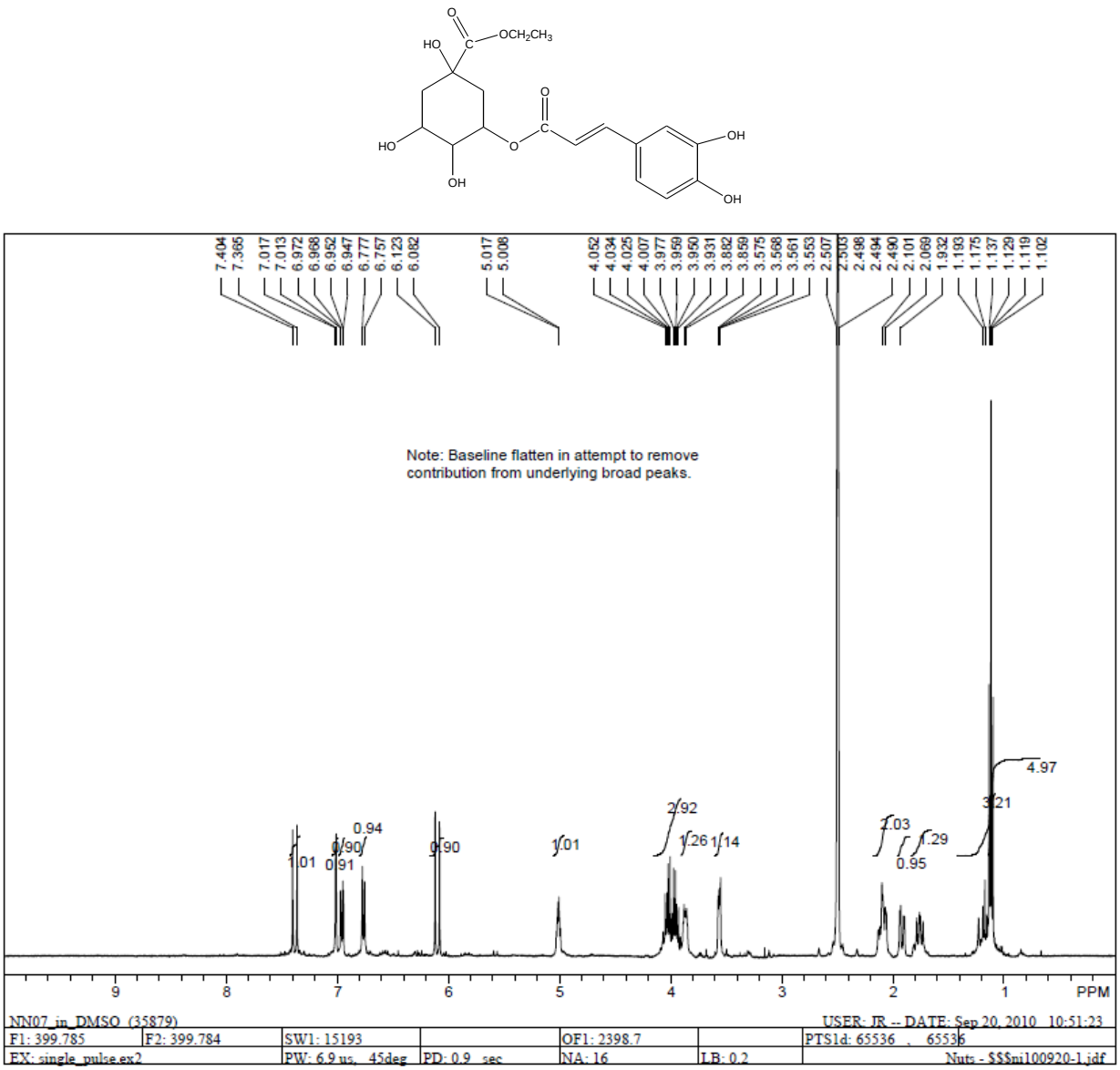

Figure 4.22. Compound NN07 (ethyl chlorogenate) 400 MHz ^{1}H spectrum in DMSO-d_6

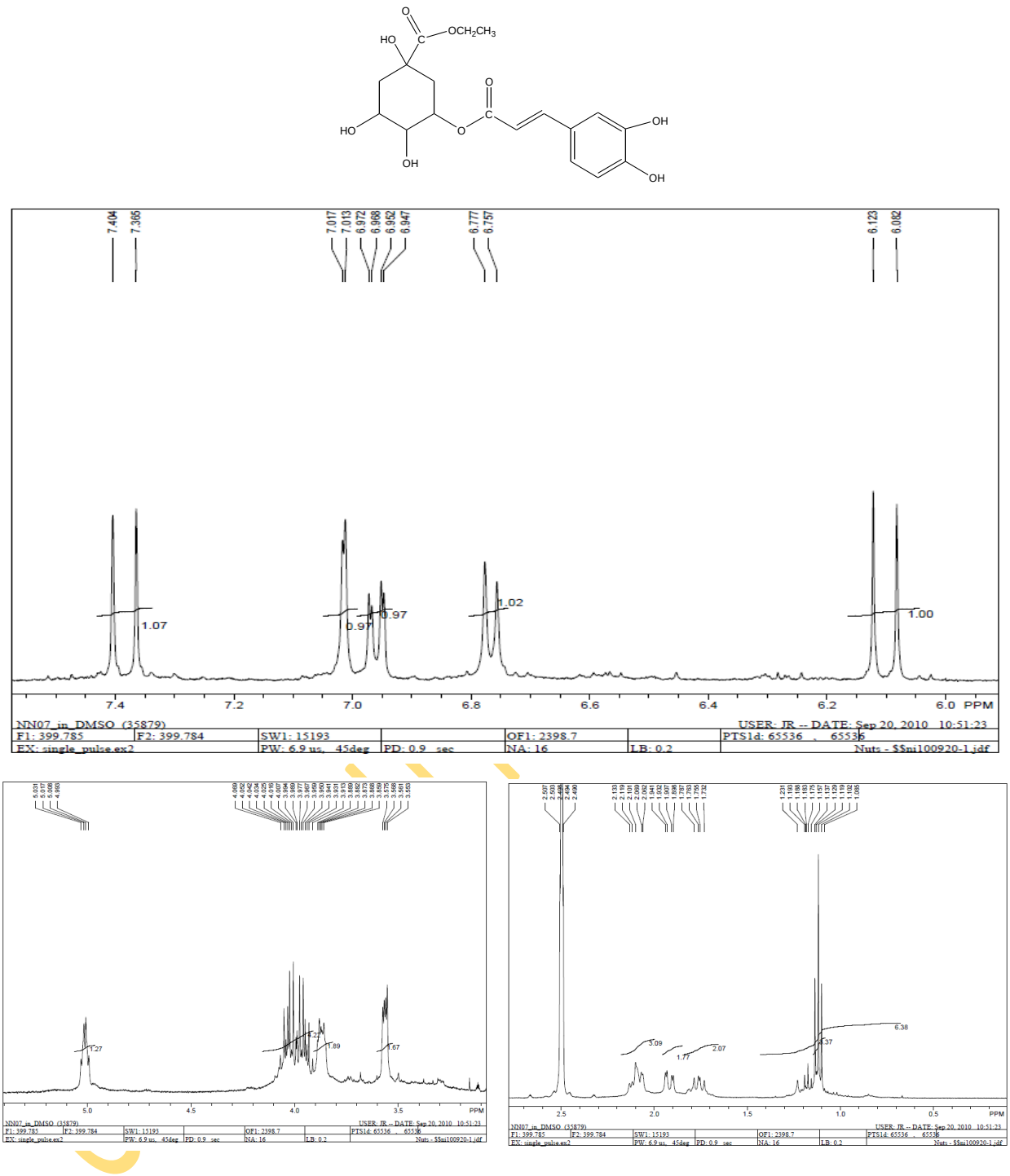

Figure 4.23. Compound NN07 (ethyl chlorogenate) 400 MHz ^{1}H spectrum in DMSO-d_6 (expanded regions)

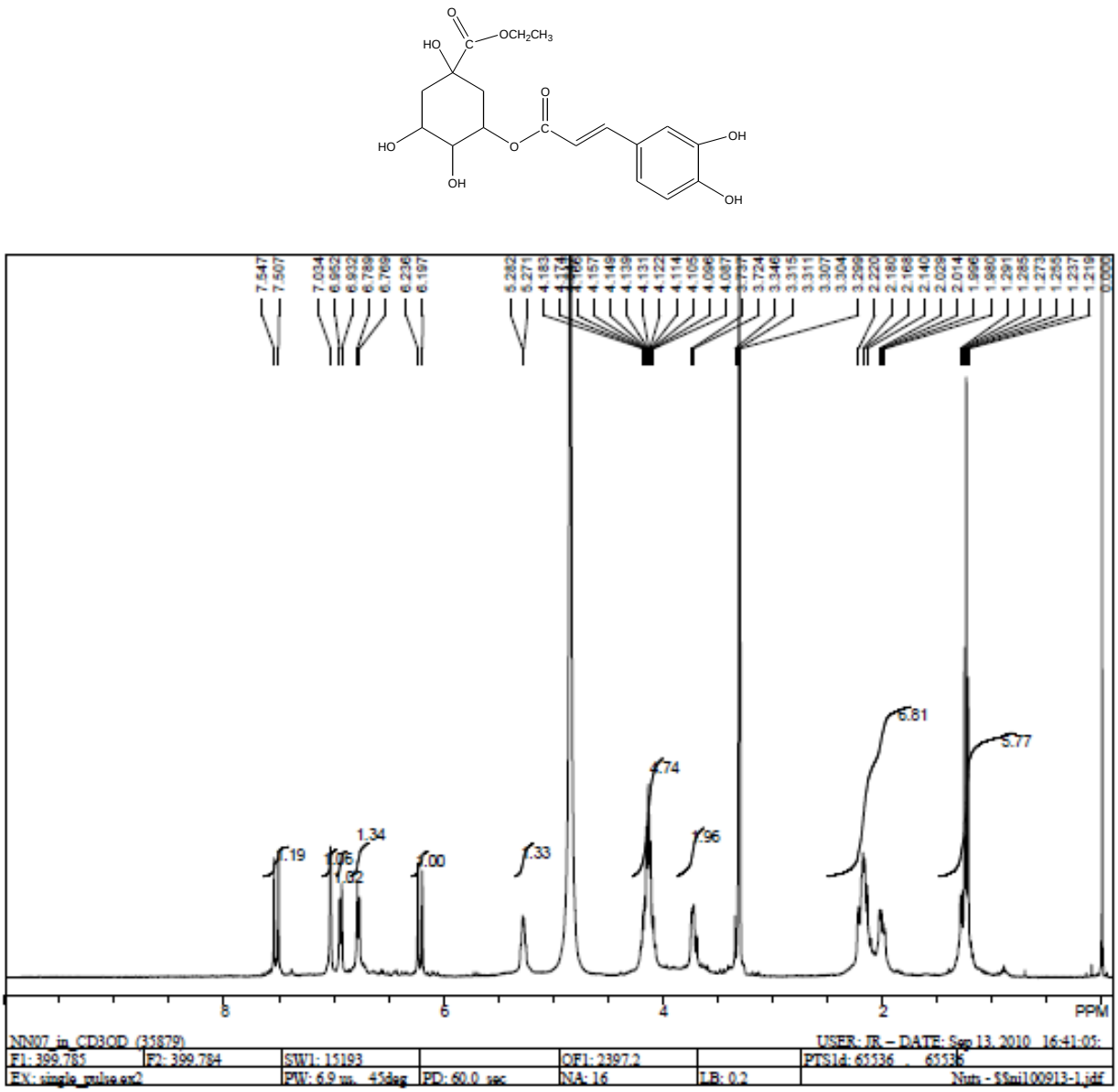

Figure 4.24. Compound NN07 (ethyl chlorogenate) 400 MHz ^{1}H spectrum in CD_3OD

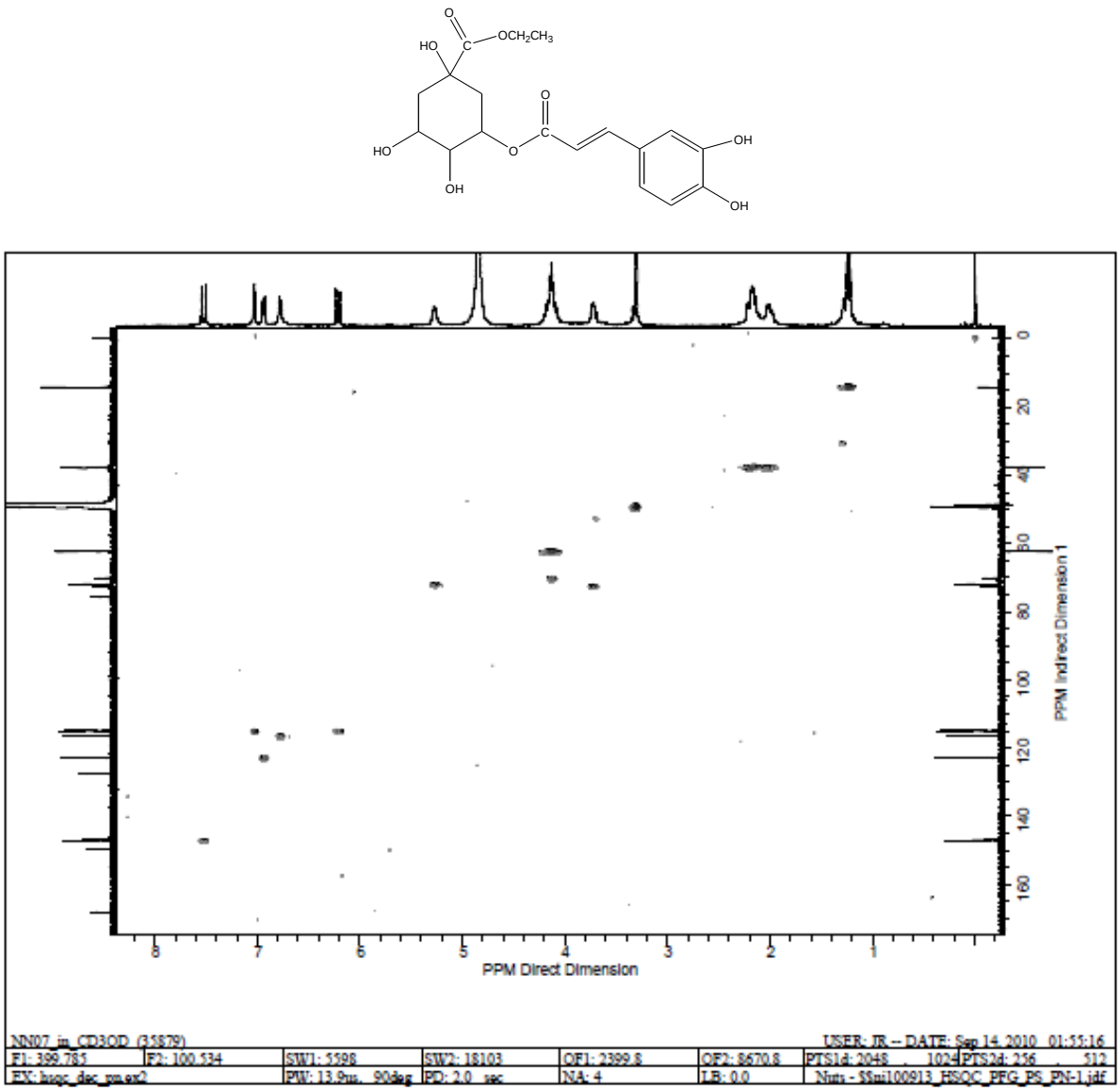

Figure 4.25. Compound NN07 (ethyl chlorogenate) 400 MHz HSQC spectrum in CD_3OD

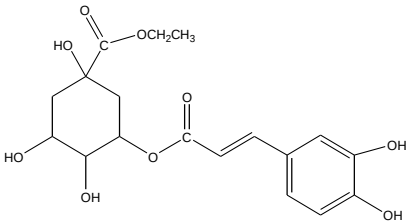

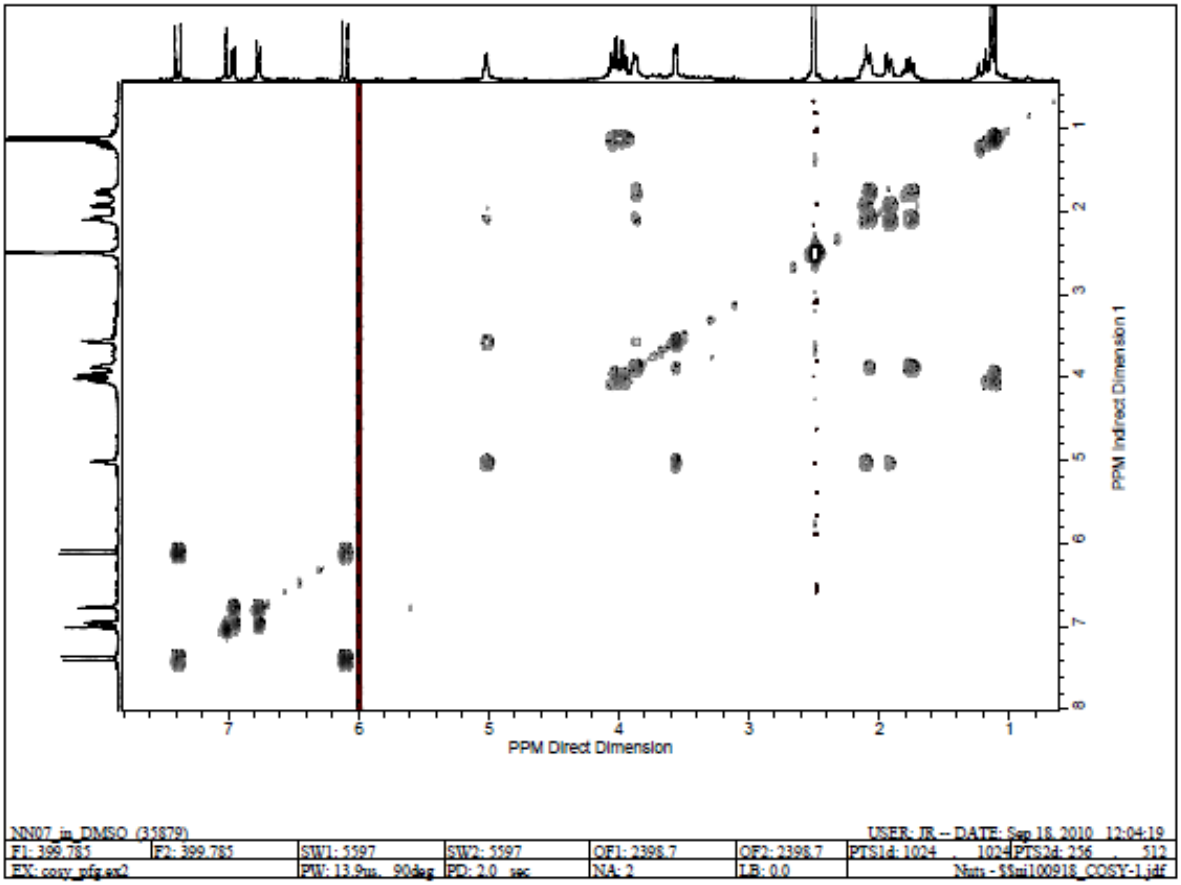

Figure 4.26. Compound NN07 (ethyl chlorogenate) 400 MHz ^{1}H- ^{1}H COSY spectrum in DMSO-d_6

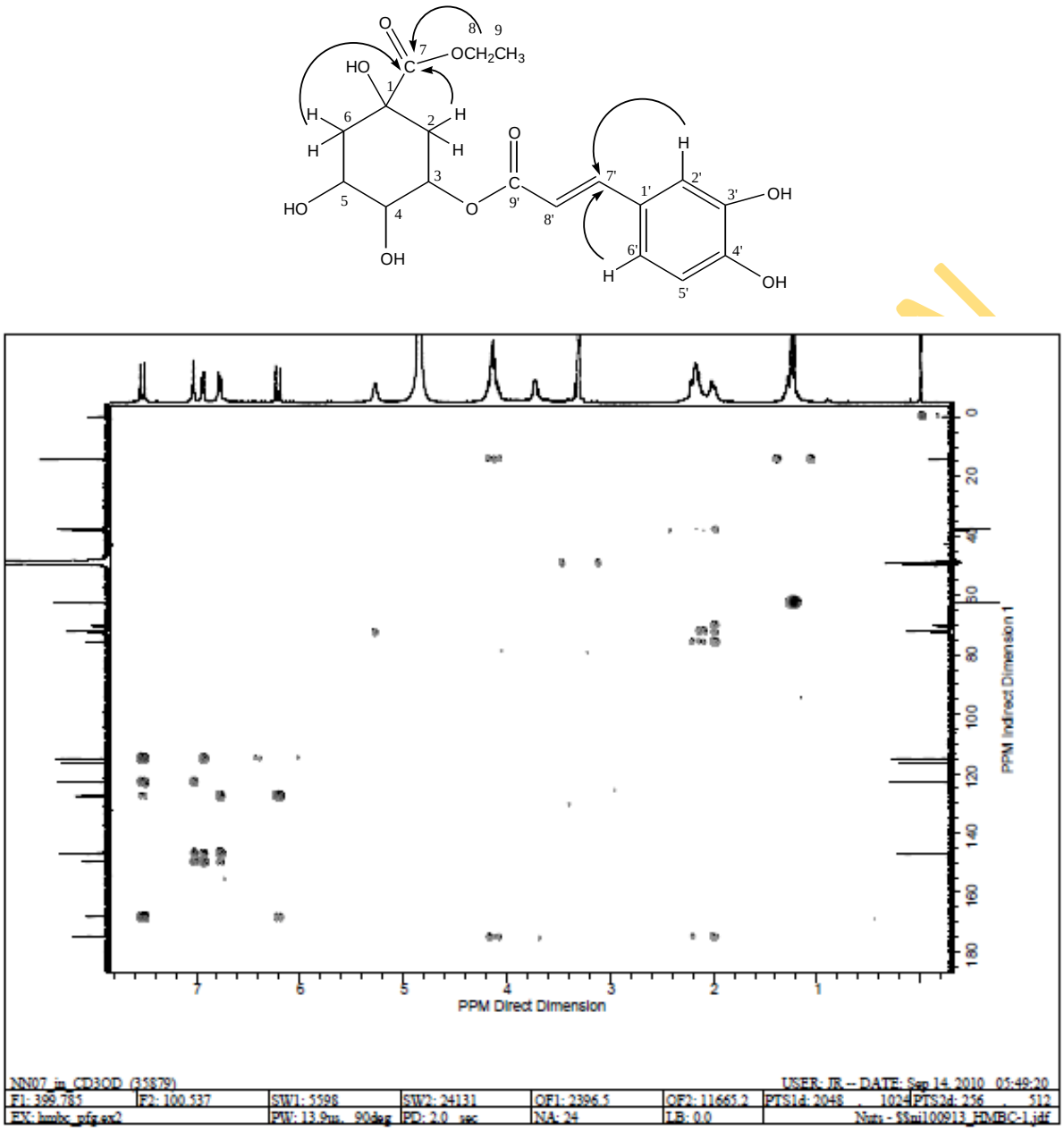

Figure 4.27. Compound NN07 (ethyl chlorogenate) 400 MHz HMBC spectrum in CD_3OD

4.3.4 Characterization of NN06

Two quasimolecular ions at *m/z* 369.1 $[M + H]^+$ and 391.1 $[M + Na]^+$ were revealed in the ESI-TOF mass spectrum (positive ion mode) of **NN06** (Fig 4.28). The molecular formula of $C_{17}H_{20}O_9$ (DBE = 8) was derived from the HRESIMS, with the $[M + H]^+$ ion at *m/z* 369.1191, supported by the ^{13}C and DEPT spectrum (Fig 4.29) which revealed the presence of 17 carbons comprising 1 methyl, 2 methylenes, 8 methines and 6 quartenary carbons. The UV spectrum exhibited absorption maxima at 218 nm and 330 nm (Fig 4.21), indicating the presence of conjugated chromophores.

The ^1H NMR (CD_3OD) spectra of **NN06** (Figs 4.30 and 4.31) were quite similar to that of **NN07** (Fig 4.24), except for the loss of the ethoxy group with protons at δ_H 1.12 (3H, t, CH_3, H-9) and 4.01 (2H, m, OCH_2, H-8) in **NN07**. This was replaced by a methoxy proton at δ_H 3.69 (3H, s, OCH_3, H-8). This was also evident in the carbon spectrum where the signals at δ_C 14.3 (C-9) and 62.5 (C-8) (in **NN07**) were lost and replaced by a signal at δ_C 53.0 (C-8). The downshift signal of this methyl group indicated that it was linked to an acetate through oxygen, thereby causing a deshielding effect. The mass spectral data of **NN06** also supported the loss of a methylene group by having an $[M + 1]^+$ of 14 units less than that of **NN07**. Information on homonuclear and heteronuclear connectivities between protons and carbons were also provided by the ^1H-^1H COSY (Fig 4.32) and HSQC spectra (Fig 4.33), respectively.

Spectral data of **NN06** was also compared with literature data (Lee *et al.*, 2010, Table 4.5). Compound **NN06** was thus identified as 3-caffeoyl-1-methyl quinate (methyl chlorogenate; **144**).

Table 4.5 ^{1}H and ^{13}C NMR spectroscopic data of compound **NN06** in CD_3OD

Position C/H Atom	**δ_H, multiplicity, (*J* in Hz)**	**δ_C**	**DEPT**	**Methyl chlorogenate (CD_3OD) Lee *et al*. (2010)**
1		75.8	qC	75.8
2	1.98-2.22, m	38	CH_2	38
3	5.27, m	72.2	CH	70.3
4	3.72, dd (3.2, 6.8)	72.7	CH	72.5
5	4.13, m	70.4	CH	72.1
6	1.98-2.22, m	37.8	CH_2	37.7
$\underline{C}OOCH_3$		175.5	qC	175.4
$COO\underline{C}H_3$	3.69, s	53.0	qC	53.0
1'		127.7	qC	127.6
2'	7.03, d (2.0)	115.18	CH	115.1
3'		149.7	qC	146.9
4'		146.9	qC	149.7
5'	6.78, d (8.1)	116.5	CH	116.5
6'	6.94, dd (2.0, 8.1)	123.0	CH	123.0
7'	7.52, d (15.9)	147.2	CH	147.2
8'	6.21, d (15.9)	115.11	CH	115.0
9'		168.3	qC	168.2

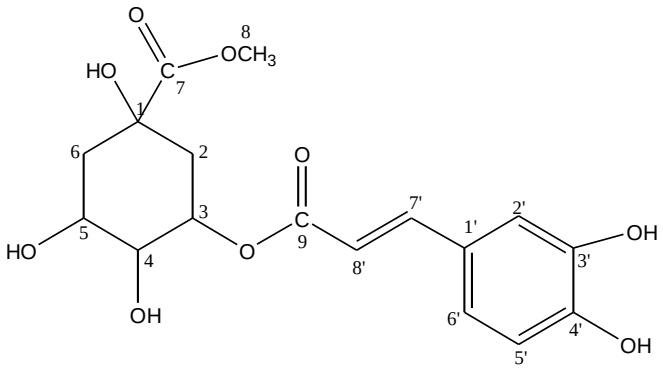

144

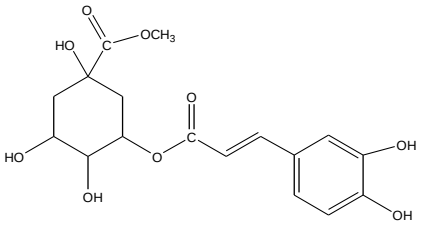

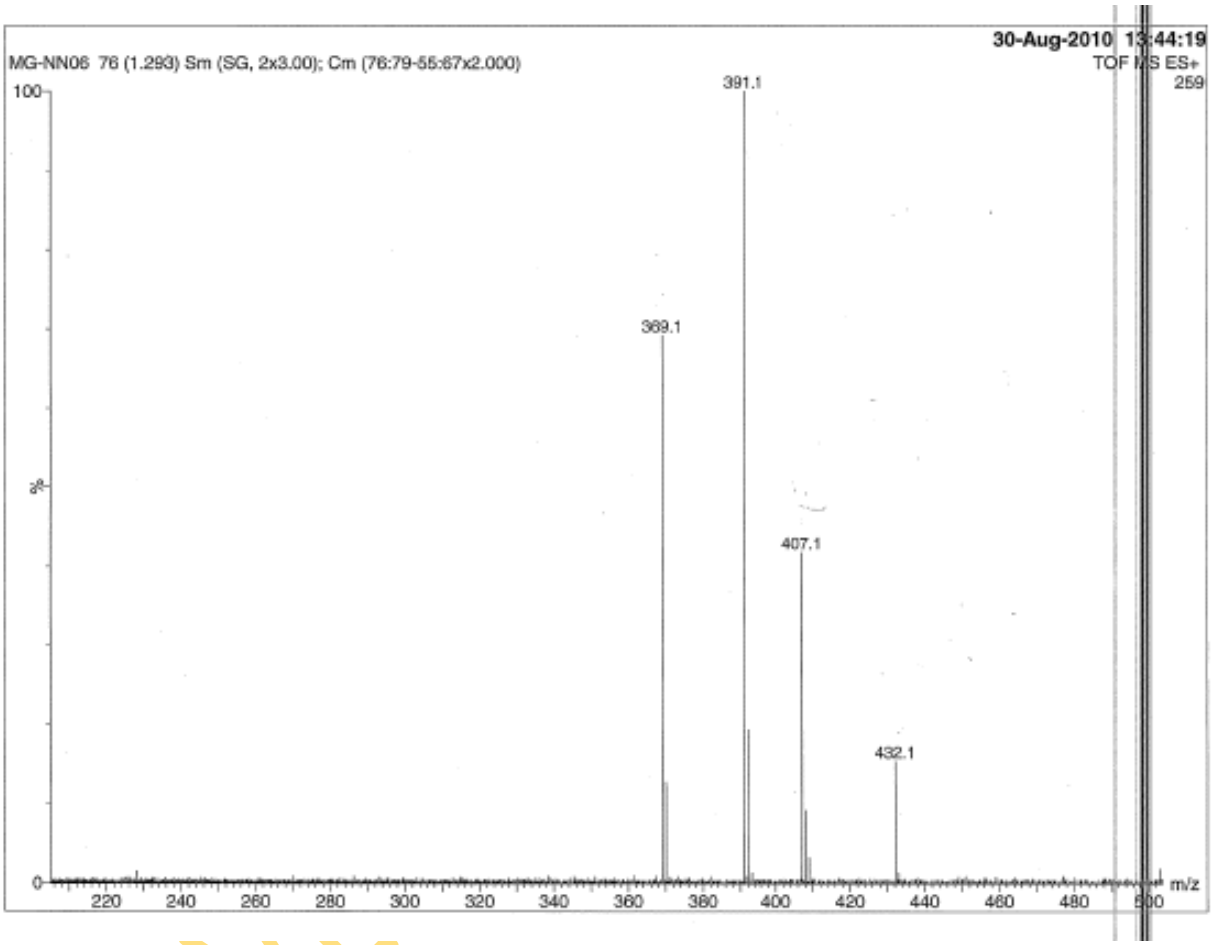

Figure 4.28. Compound NN06 (methyl chlorogenate) ES-MS-TOF spectrum

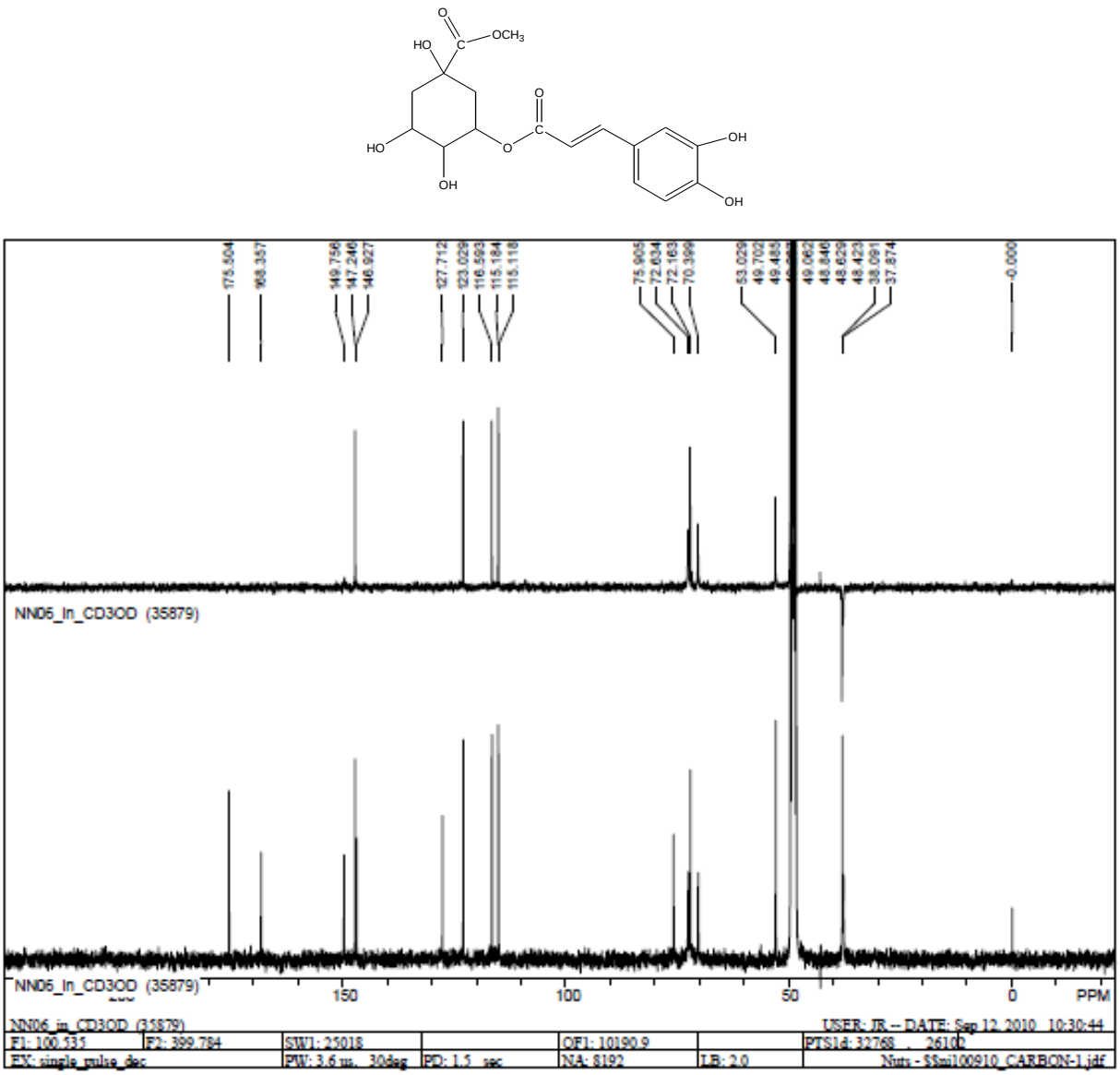

Figure 4.29. Compound NN06 (methyl chlorogenate) 100 MHz ^{13}C and DEPT spectra in CD_3OD

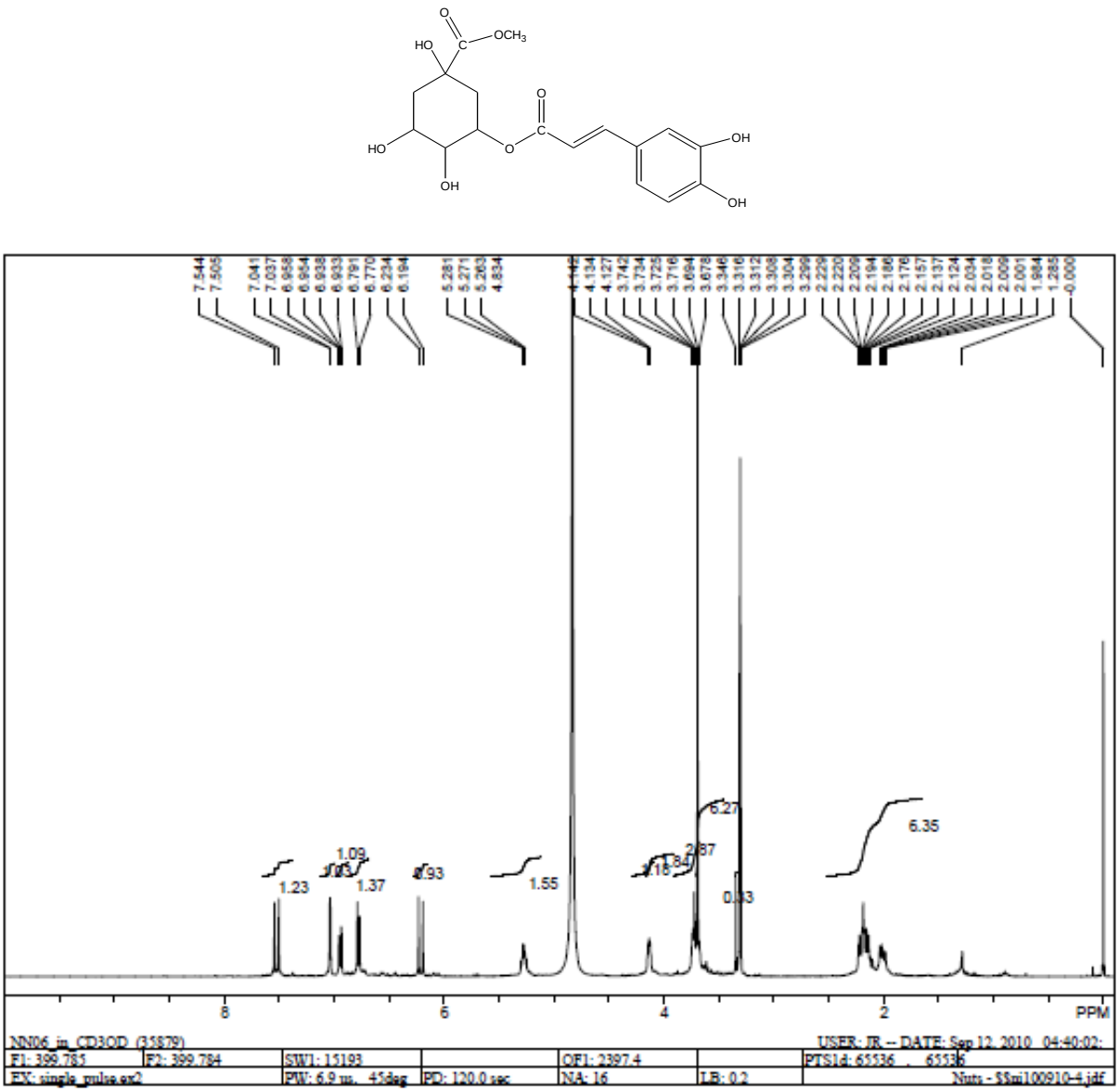

Figure 4.30. Compound NN06 (methyl chlorogenate) 400 MHz ^{1}H spectrum in CD_3OD

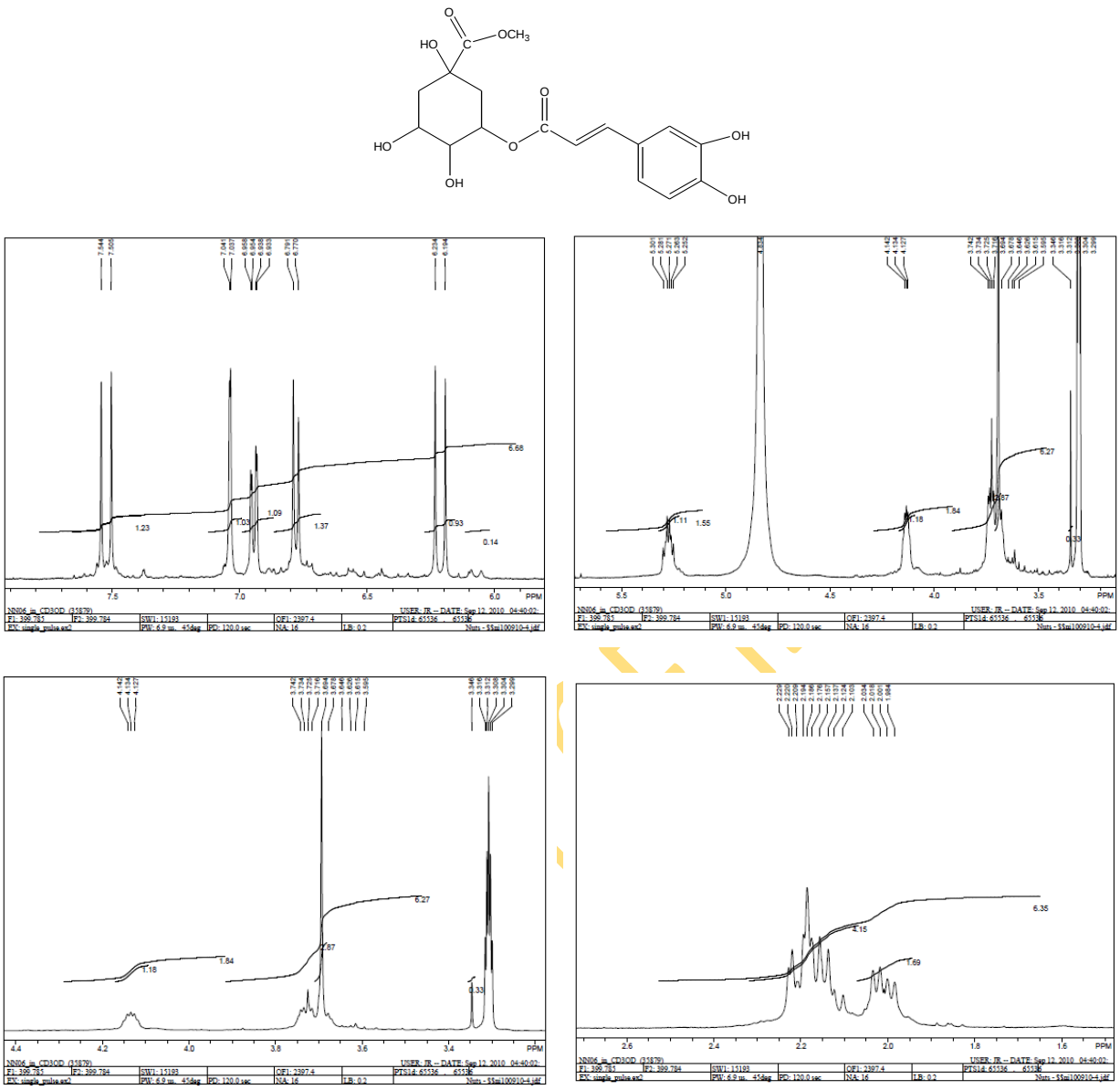

Figure 4.31. Compound NN06 (methyl chlorogenate) 400 MHz ^{1}H spectrum in CD_3OD (expanded regions)

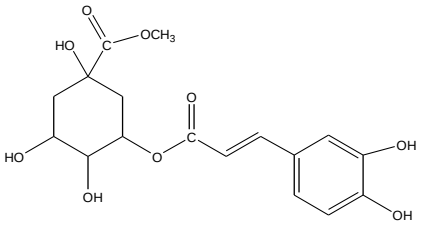

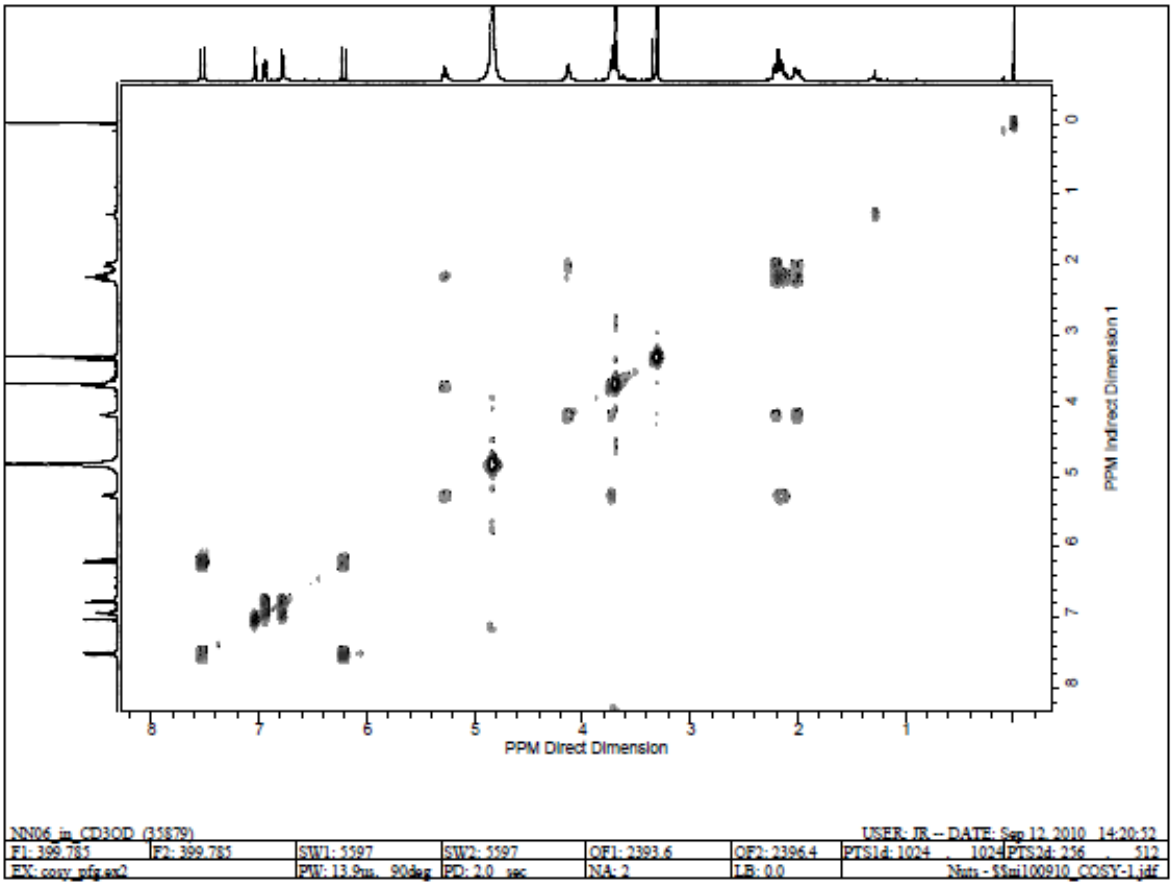

Figure 4.32. Compound NN06 (methyl chlorogenate) 400 MHz ^{1}H- ^{1}H COSY spectrum in CD_3OD

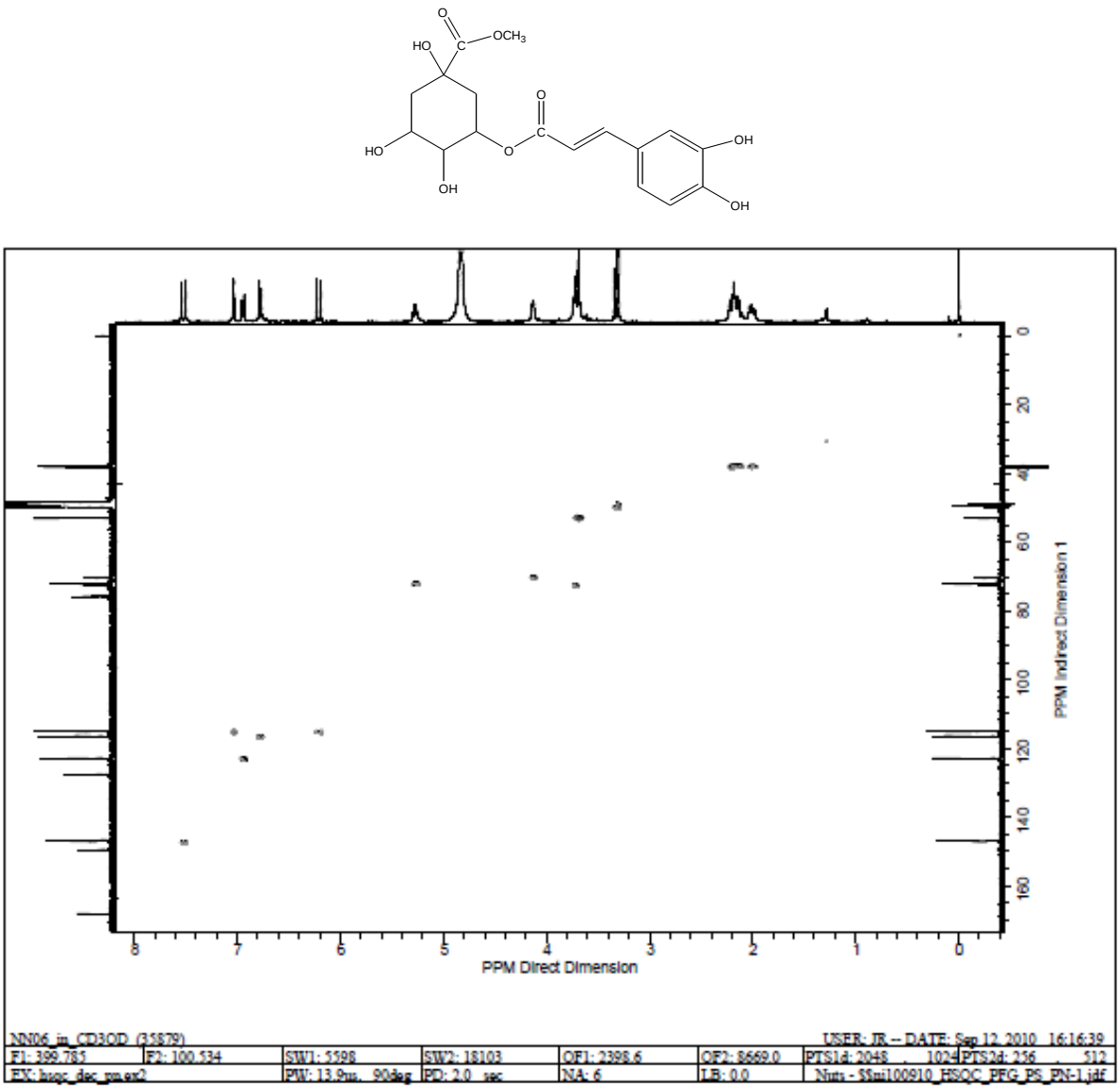

Figure 4.33. Compound NN06 (methyl chlorogenate) 400 MHz HSQC spectrum in CD_3OD

4.3.5 Characterization of NN01

The positive ion mode ESI-TOF mass spectra of **NN01** (Figs 4.34 and Fig 4.35) showed two quasimolecular ions at *m/z* 611.1 $[M + H]^+$ and 633.1 $[M + Na]^+$ and fragment ions at *m/z* 465.1 $[M + H - 146]^+$ and 449.1 $[M + H - 162]^+$. The latter two suggested the loss of glycosidic components of one deoxyhexose and one hexose. One other major fragment ion was at 303. The molecular formula of $C_{27}H_{30}O_{16}$ (DBE = 13) was derived from the HRESIMS, with the $[M + H]^+$ ion at *m/z* 611.1599, supported by the ^{13}C NMR and DEPT spectra (Figs 4.36 and 4.37).

The UV spectrum (Fig 4.21) exhibited absorption maxima at 257 nm and 358 nm that are characteristic flavone skeleton bands. The IR spectrum of **NN01** (Fig 4.38) indicated absorption bands for hydroxyl (3337 cm^{-1}), γ-pyrone carbonyl (1655 cm^{-1}) and aromatic rings (1606 cm^{-1})

In the ^1H NMR spectra (Figs 4.39 and 4.40), the presence of a 3,4, disubstituted flavonoid ring B was confirmed by three aromatic protons in an ABX pattern with signals at δ_H 7.66 (d, 2.0 Hz, H-2'), 6.85 (d, 8.0 Hz, H-5') and 7.62 (dd, 2.0, 8.0 Hz, H-6'). Furthermore, in the aromatic region, two meta- coupled doublets at δ_H 6.20 (d, 2.0 Hz, H-6) and 6.39 (d, 2.0 Hz, H-8) indicated a 5,7-disubstituted pattern for ring A. Two anomeric protons appeared at δ_H 5.11 (1H, d, 7.6 Hz, H-1") and δ_H 4.51 (1H, d, 1.6 Hz, H-1'''). The anomeric configurations were deduced from the magnitude of the homonuclear vicinal coupling constants between H-1 and H-2 of the sugar moieties, thus indicating the presence of a β-glucosyl moiety and an α-rhamnosyl moiety, respectively. The remaining glycosidic proton resonances occurred between 3.24 and 3.84 ppm, with the exception of that for a deoxyhexose methyl group at δ_H 1.12 (3H, d, 6 Hz). These data confirmed the sugars to be β-D-glucose and α-L-rhamnose.

The ^{13}C NMR and DEPT spectra (Figs 4.36 and 4.37) revealed 27 carbons comprising 1 methyl, 1 methylene, 15 methines and 10 quartenary carbons. Nine of these carbons resonated between δ_C 68.5 and 78.1 ppm indicating C-OH groups. These signals (C-OH groups), two anomeric carbon signals of the sugar moieties appearing at δ_C 104.7 and δ_C 102.4 (O-C-O), and one carbon resonance at δ_C 17.8 ppm ($\underline{C}H_3$-C), all indicated O-linked sugars. Direct homonuclear and heteronuclear connectivities were established from ^1H-^1H COSY (Fig 4.41) and HSQC (Fig 4.42) spectra. In addition to the couplings seen from the splitting pattern of protons in the ^1H spectrum, ^1H-^1H COSY showed the correlation between the anomeric proton at δ_H 5.11 (H-1") and a proton at δ_H 3.44, indicating the proton to be H-2" of the glucosyl moiety. The geminal coupling between δ_H 3.80 (dd, H-6"^{a}) and 3.38 (m, H-6"^{b}) was also observed.

The HMBC spectrum (Fig 4.43) revealed the following long range correlation signals between protons and carbons:

δ_H 7.66 (H-2'), 6.85 (H-5') ↔ δ_C 145.8 (C-3'), 149.8 (C-4'), 123.5 (C-6')

δ_H 6.39 (H-8), 6.20 (H-6) ↔ δ_C 166.0 (C-7), 105.6 (C-10)

δ_H 7.66 (H-2'), 6.39 (H-8) ↔ δ_C 159.3 (C-2)

δ_H 5.11(H-1") ↔ δ_C 135.6 (C-3)

δ_H 3.80, 3.38 (H-6") ↔ δ_C 102.4 (C-1"')

The long range correlation found between δ_C 135.6 (C-3) of the aglycone and an anomeric proton, δ_H 5.11 (H-1") confirmed the site of glycosylation of glucose at C-3 whereas that between δ_C 102.4 (C-1"') and δ_H 3.80, 3.38 (H-6")) confirmed the 1→6 interglycosidic linkage between rhamnose and glucose.

Based on the combination of data from all the NMR spectra and comparison with literature data (Lallemand and Duteil, 1977, Bello *et al*., 2011), unambiguous positions were assigned the proton and carbon NMR signals of **NN01** as shown in Table 4.6.

Table 4.6. ^{1}H and ^{13}C NMR spectroscopic data of compound **NN01** in CD_3OD

C/H Atom	**δ_H, multiplicity, *J* in Hz**	**δ_C**	**DEPT**	**δ_C rutin** (DMSO-d_6) Lallemand and Duteil (1977)	**δ_C rutin** (DMSO-d_6) Bello *et al*. (2011)
2		159.3	qC	156.9	156.4
3		135.6	qC	133.9	133.2
4		179.4	qC	178.0	177.3
5		162.9	qC	161.4	156.6
6	6.20, d (2.0)	99.9	CH	99.7	98.6
7		166.0	qC	166.3	164.0
8	6.39, d (2.0)	94.8	CH	94.8	93.6
9		158.5	qC	156.7	161.1
10		105.6	qC	104.9	103.9
1'		123.1	qC	122.0	121.1
2'	7.66, d (2.0)	117.6	CH	116.0	115.2
3'		145.8	qC	145.2	144.6
4'		149.8	qC	148.9	148.3
5'	6.85, d (8.0)	116.0	CH	117.1	116.2
6'	7.62, dd (2.0, 8.0)	123.5	CH	122.5	121.6
1"	5.11, d (7.6)	104.7	CH	102.1	101.1
2"	3.44, t (3.2)	75.7	CH	75.1	73.9
6"	3.80, dd (9.6) 3.38, m	68.5	CH_2	68.1	66.9
1'"	4.51, d (1.6)	102.4	CH	101.7	100.7
6'"	1.12, d (6)	17.8	CH_3	19.1	17.6

Acid hydrolysis of compound **NN01** with 2N conc HCl yielded **NN01a**. The positive ion mode AP-TOF mass spectrum of **NN01a** (Figs 4.44) showed a quasimolecular ion at *m/z* 303.1 $[M + H]^+$, indicating the molecular formula of $C_{15}H_{10}O_7$ (DBE = 11). The ^1H NMR of **NN01a** (Fig 4.45) showed a very close similarity to that of **NN01**, the only significant difference being the absence of the methyl protons at δ_H 1.12 and other glycosidic protons between δ_H 3.24 and 3.84. This was also evident in the ^{13}C NMR (Fig 4.46) where only the carbon resonances of the sugar moieties were absent. Comparison of **NN01** and **NN01a** showed that the carbon values of the aglycone compared well to each other except for the significant upshift of C-2 from δ_C 159.3 in **NN01** to δ_C 146.5 in **NN01a**. This may be explained as the deshielding effect and steric hinderance of sugar moiety at C-3 in **NN01** on the C ring of the aglycone. Chemical shift data of **NN01** and **NN01a** were compared with that of literature data (Lallemand and Duteil, 1977; Table 4.7) and were found quite comparable, though run in different solvents.

Table 4.7. ^{13}C NMR spectroscopic data of compound **NN01a**

C	**δ_C NN01a** (CD_3OD)	**δ_C quercetin** (DMSO-d_6) Lallemand and Duteil (1977)
2	147.5	146.5
3	136.5	135.8
4	176.5	175.9
5	161.0	161.1
6	99.5	97.8
7	166.0	164.1
8	94.5	92.9
9	156.7	156.8
10	104.0	103.1
1'	123.0	122.7
2'	116.5	114.8
3'	145.7	144.8
4'	148.1	147.3
5'	116.0	114.5
6'	121.0	120.2

NN01 was acetylated with an equal ratio of pyridine and acetic acid. This yielded a light brown solid (5 mg, **NN01b**). The positive ion mode AP-TOF mass spectrum of this compound (Fig 4.47) showed a quasimolecular ion at *m/z* 1031.2 $[M + H]^+$. This reaction proved that **NN01** was deca-acetylated showing that **NN01** had ten free hydroxyl groups of which the hydroxylic protons were replaced by acyl groups on acetylation.

Based on these data, the structures of compounds **NN01** and **NN01a** were established as quercetin 3-O-β-rutinoside (rutin; **145**) and quercetin (**146**), respectively. It was also found at the time of this write-up, that some workers recently isolated this compound from the leaves of *P. crassipes* (Bello *et al*., 2011).

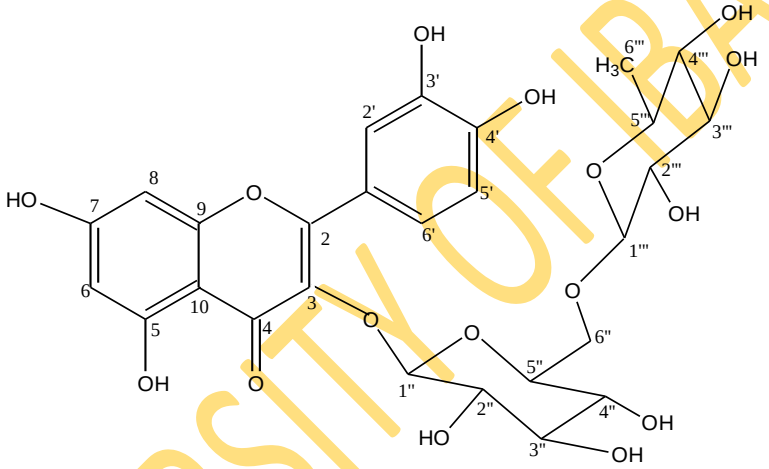

145

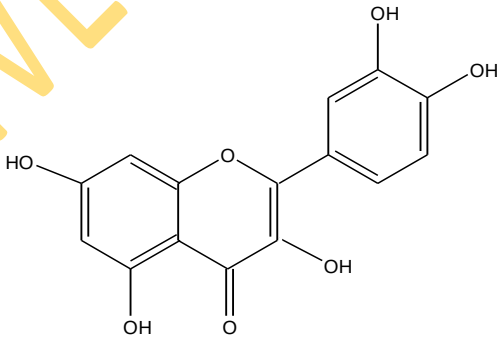

146

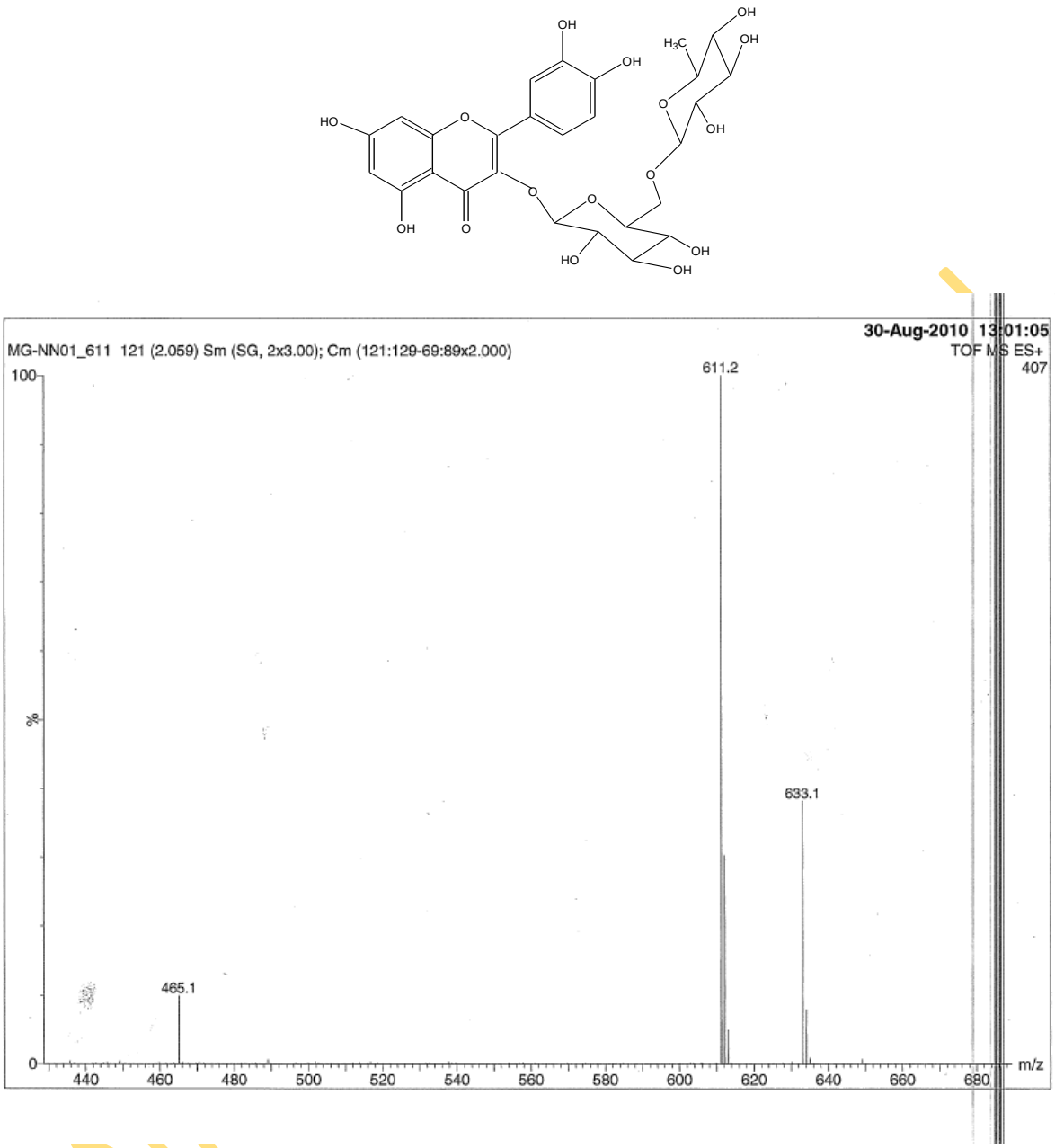

Figure 4.34. Compound NN01 (rutin) ES-MS-TOF spectrum

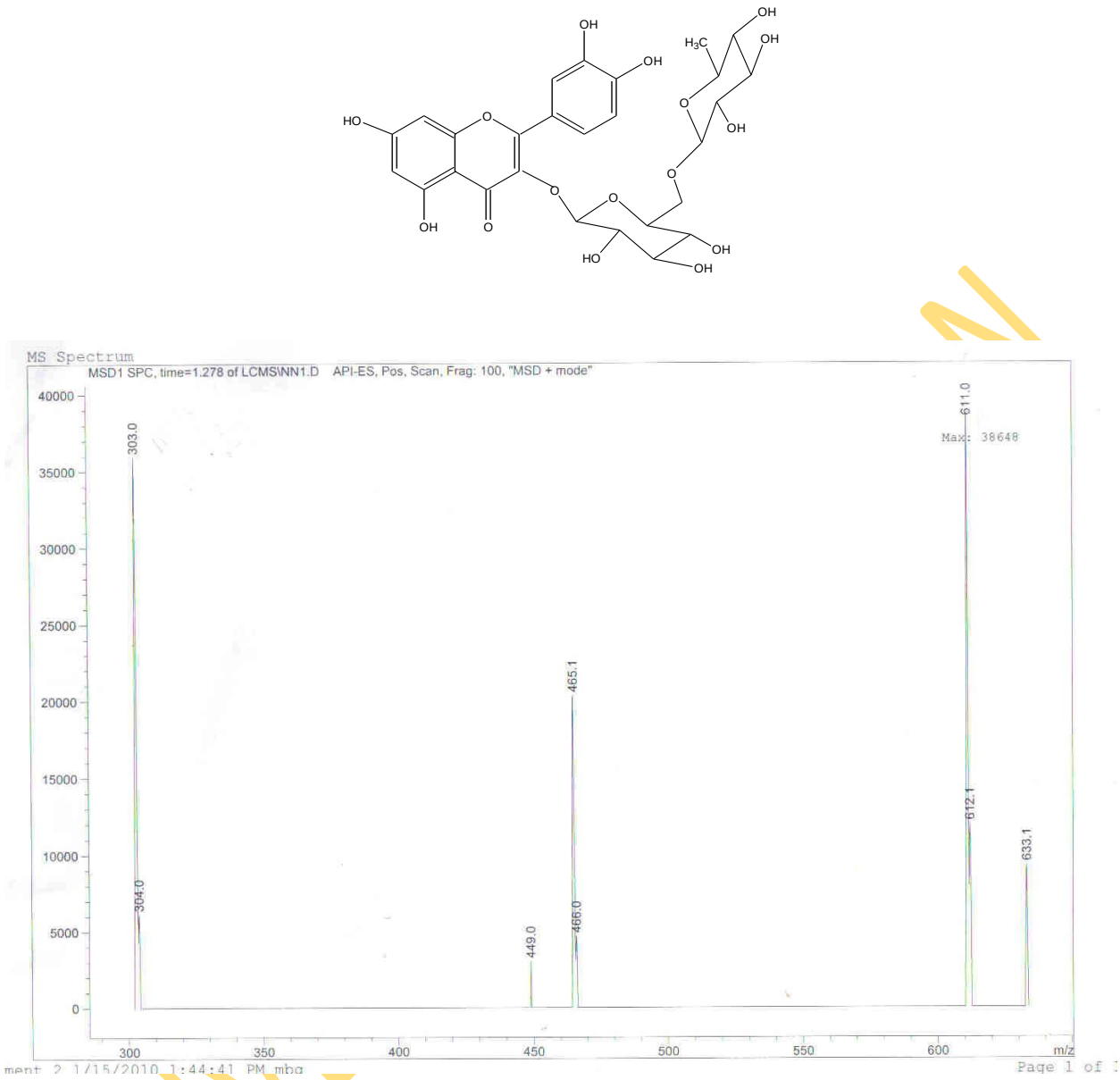

Figure 4.35. Compound NN01 (rutin) ES-MS-TOF spectrum

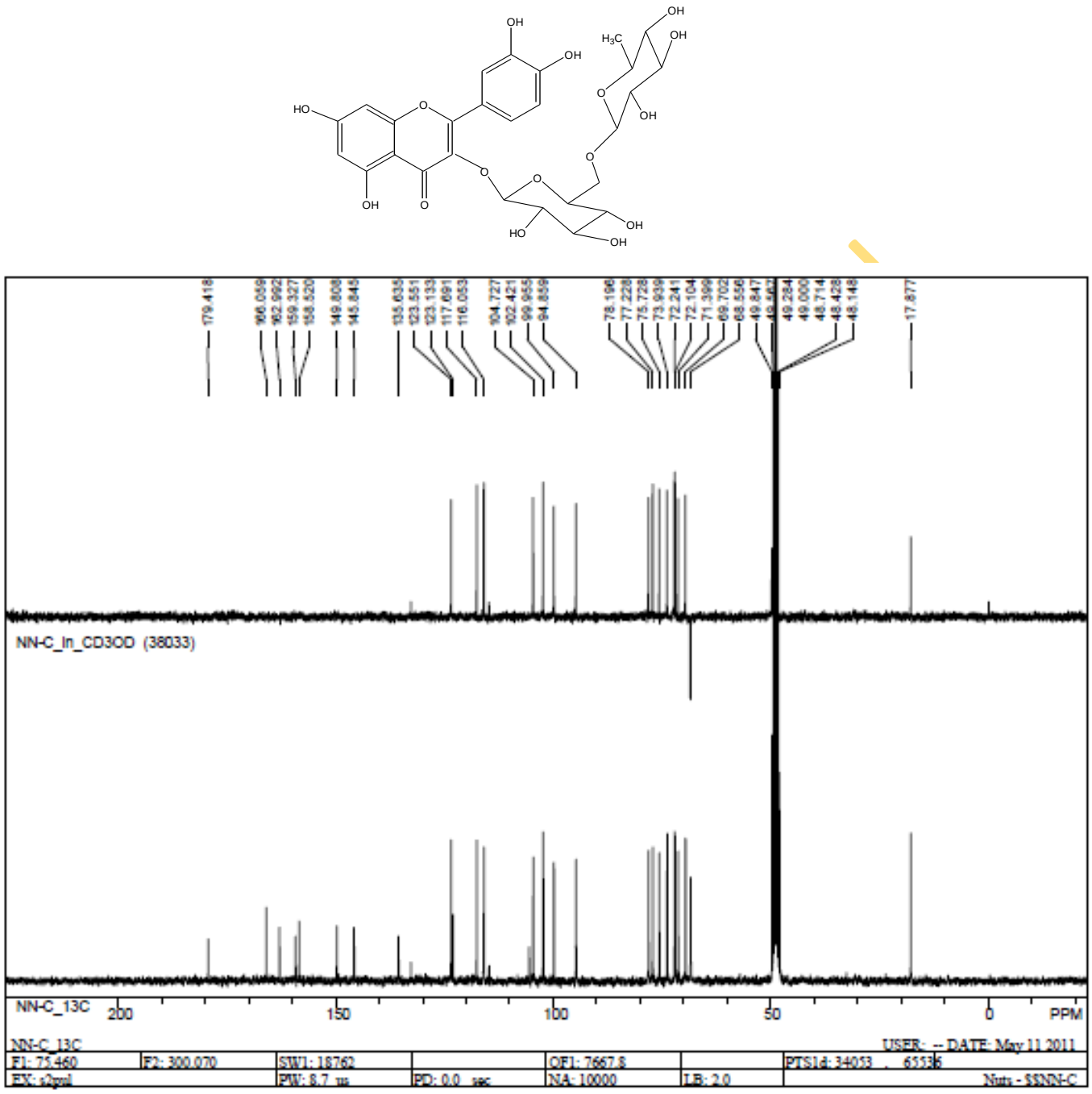

Figure 4.36. Compound NN01 (rutin) 100 MHz ^{13}C spectrum in CD_3OD

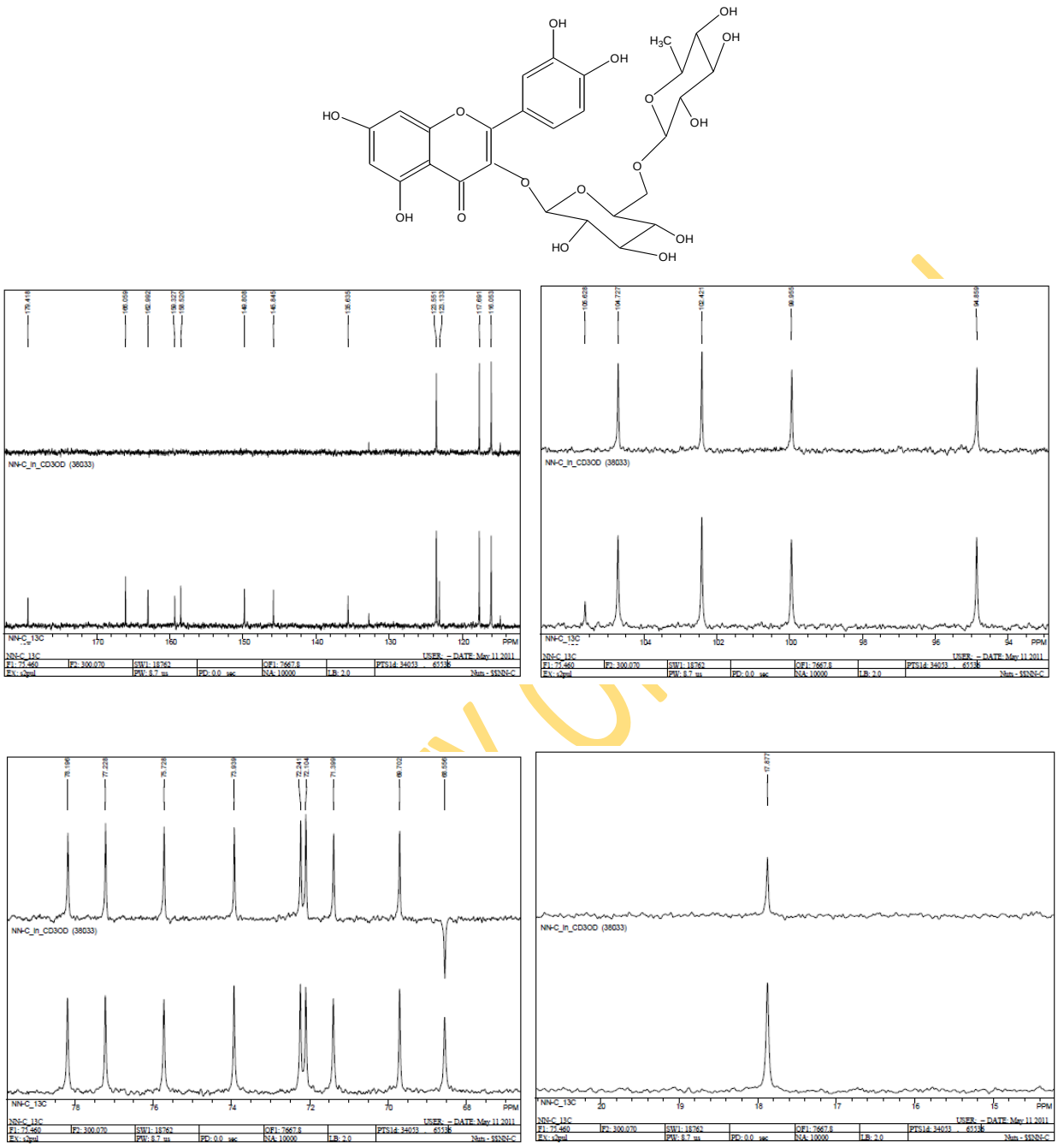

Figure 4.37. Compound NN01 (rutin) 100 MHz ^{13}C spectrum in CD_3OD (expanded regions)

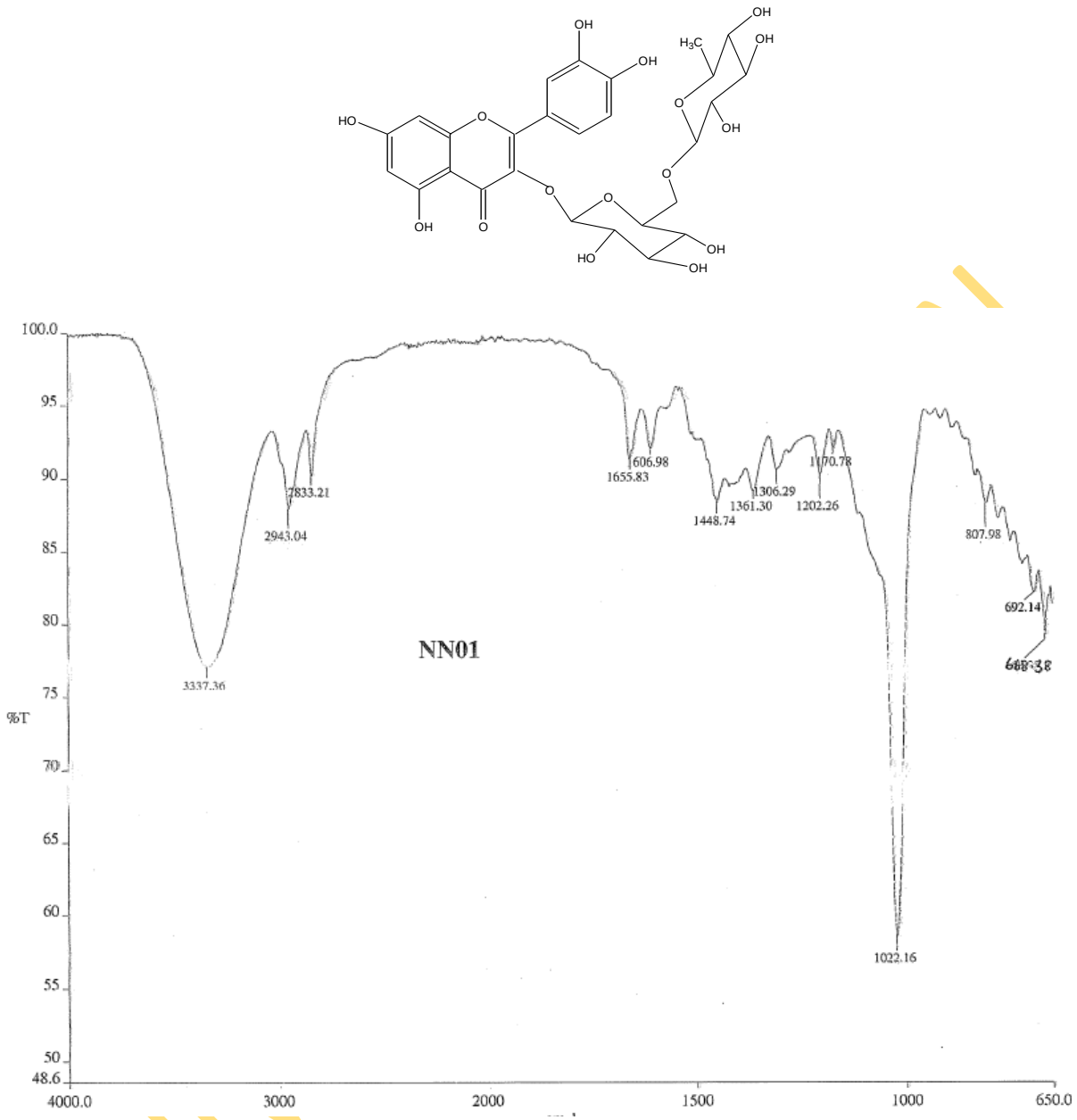

Figure 4.38. Compound NN01 (rutin) IR spectrum

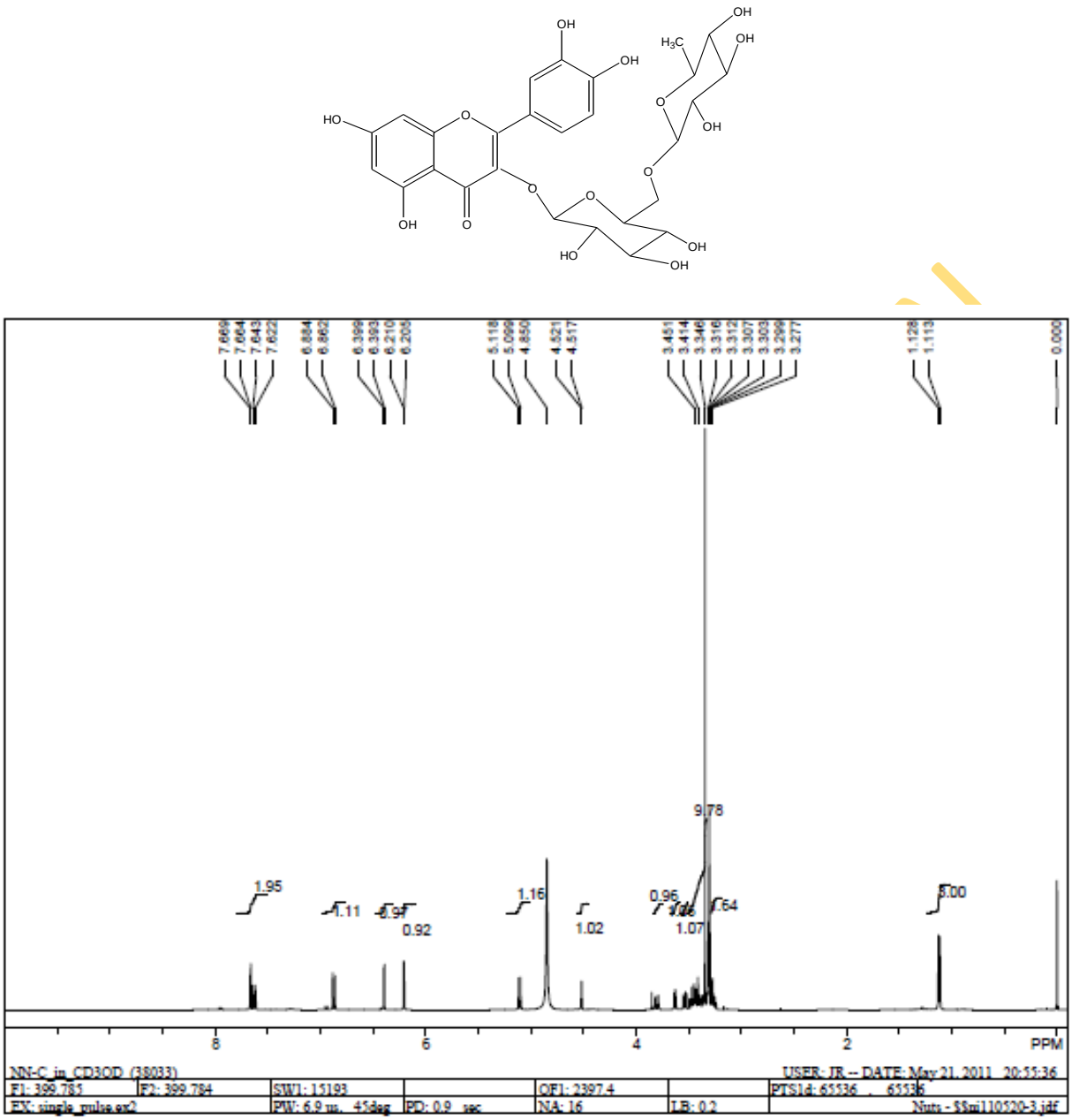

Figure 4.39. Compound NN01 (rutin) 400 MHz ^{1}H spectrum in CD_3OD

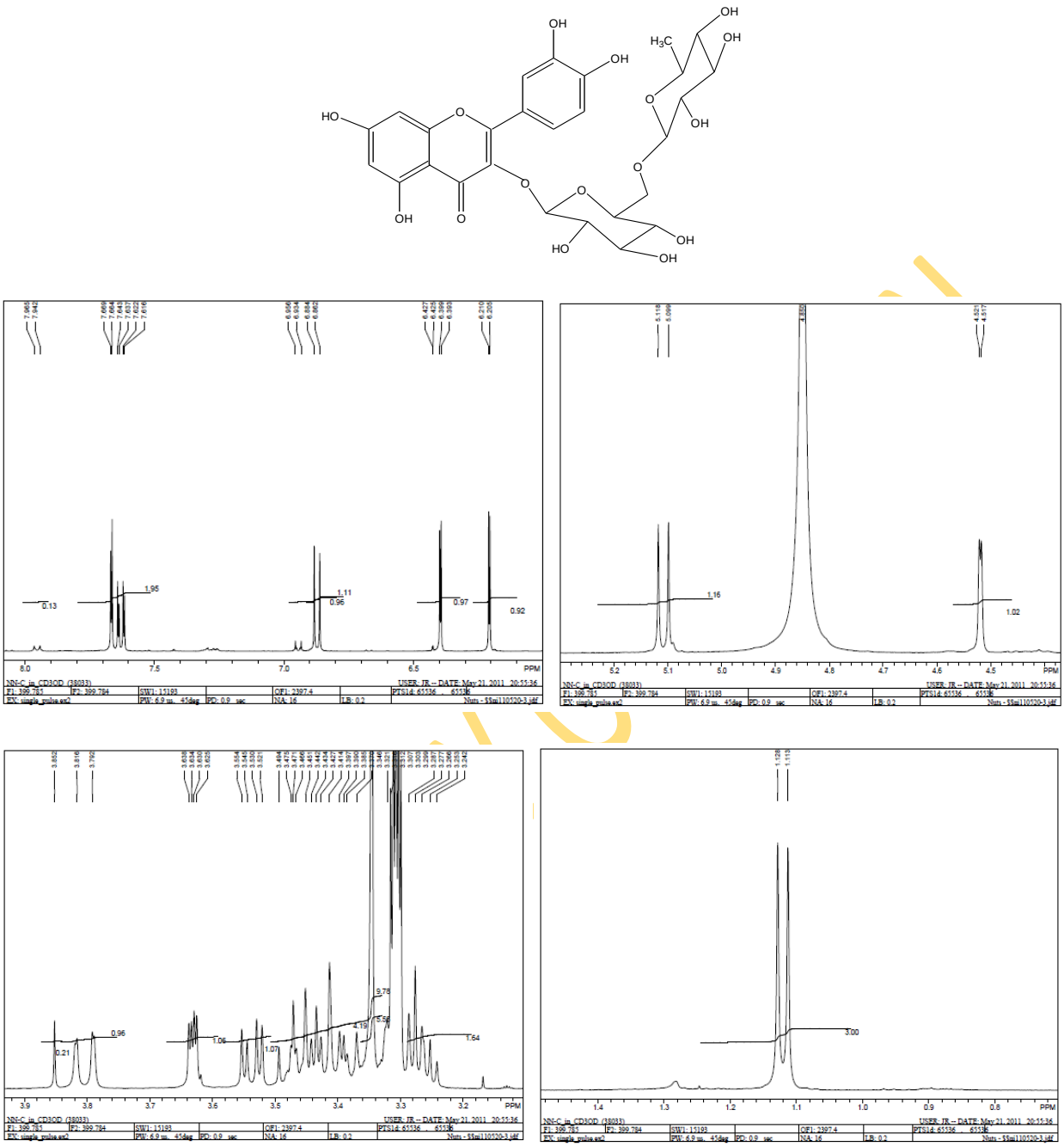

Figure 4.40. Compound NN01 (rutin) 400 MHz ^{1}H spectrum in CD_3OD (expanded regions)

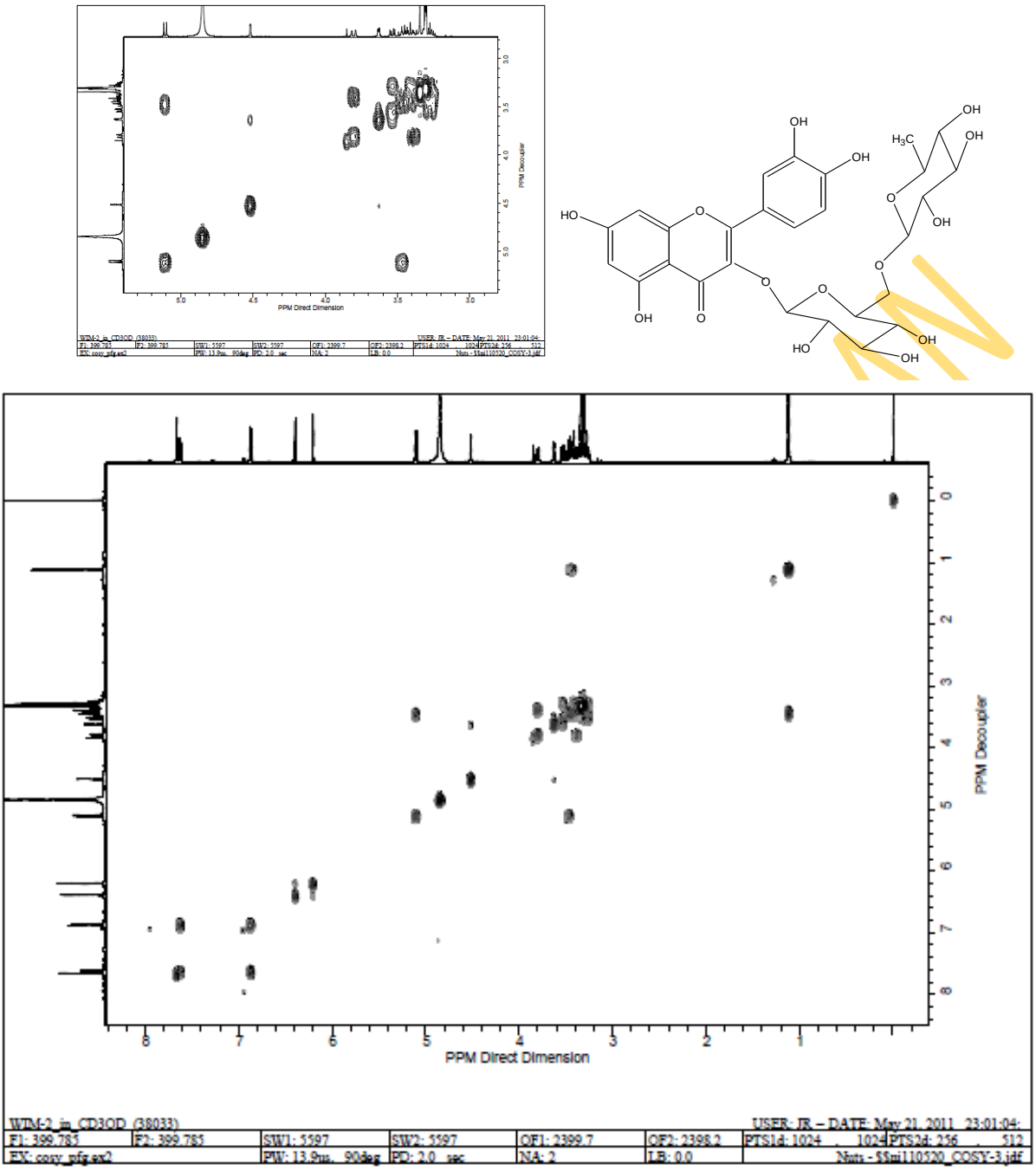

Figure 4.41. Compound NN01 (rutin) 400 MHz ^{1}H- ^{1}H COSY spectrum in CD_3OD

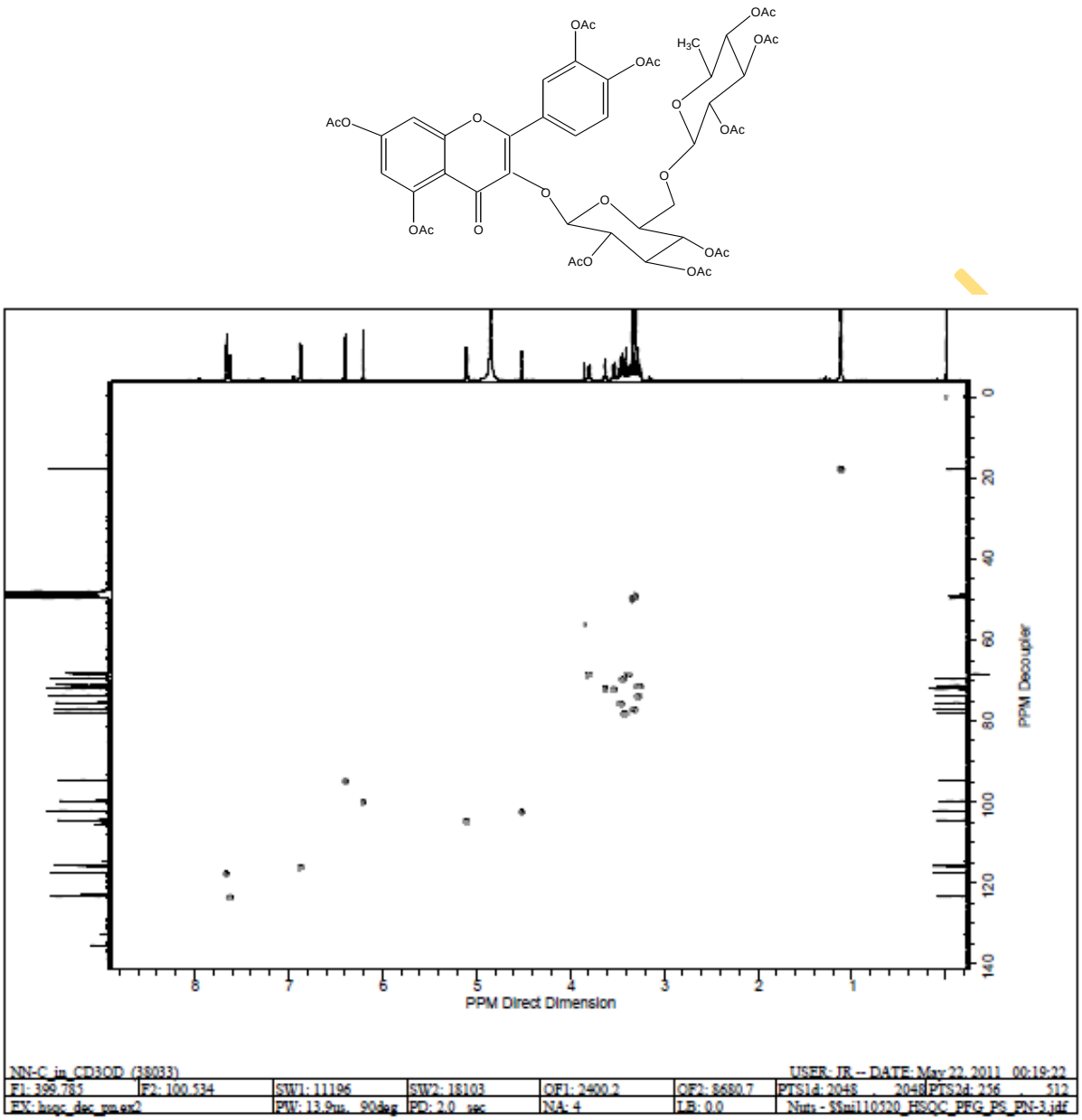

Figure 4.42. Compound NN01 (rutin) 400 MHz HSQC spectrum in CD_3OD

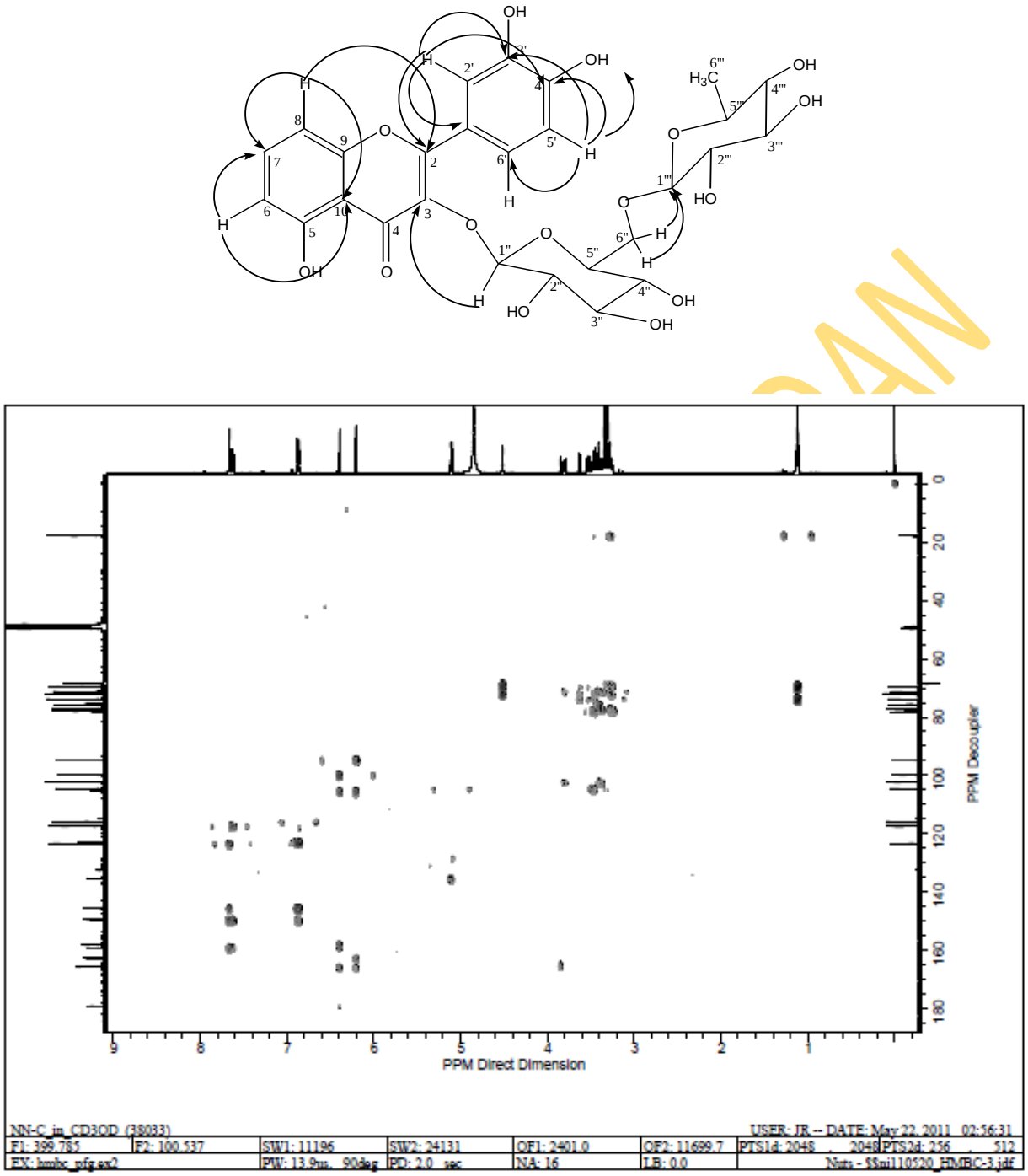

Figure 4.43. Compound NN01 (rutin) 400 MHz HMBC spectrum in CD_3OD

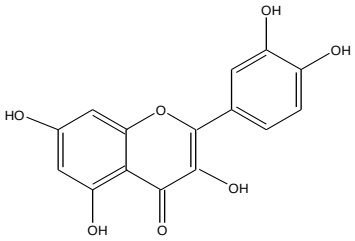

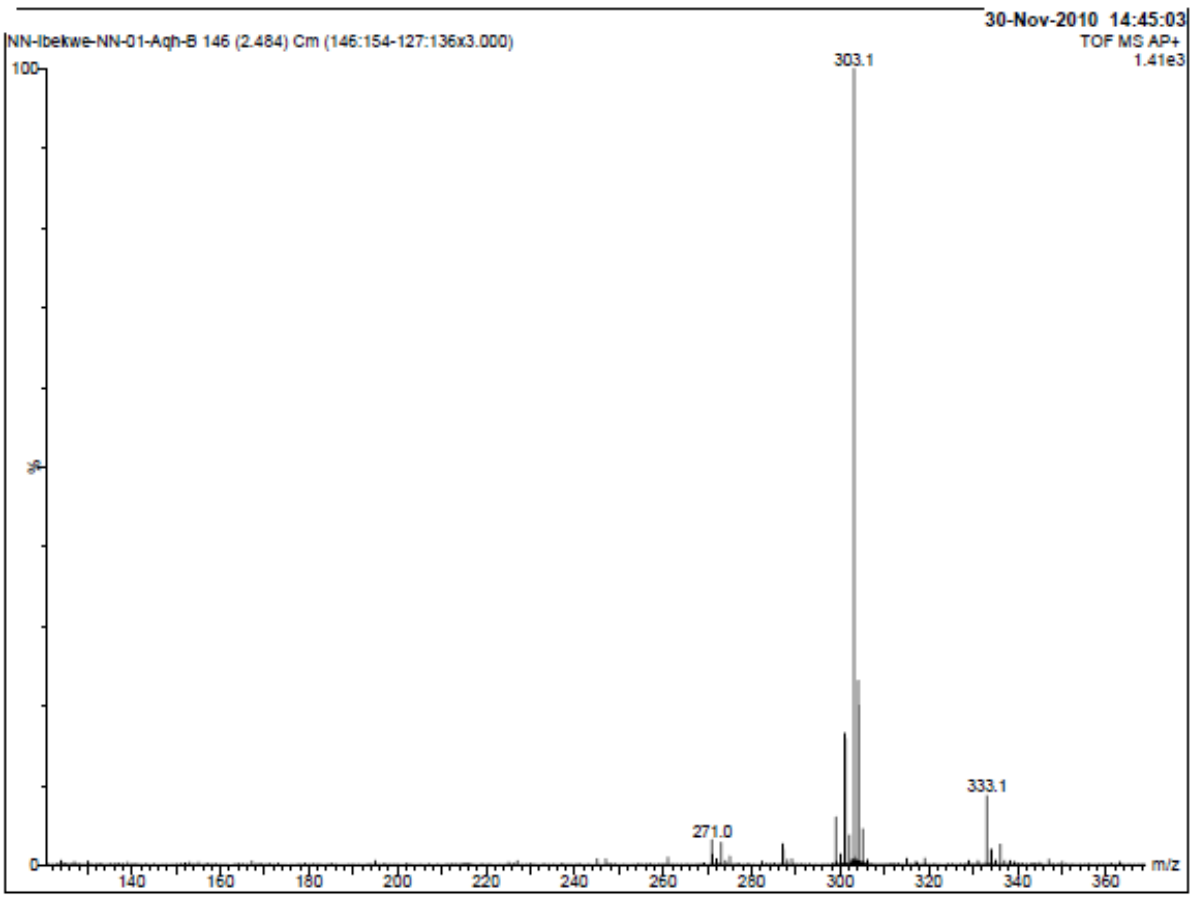

Figure 4.44. Compound NN01a (quercetin) AP-MS-TOF spectrum

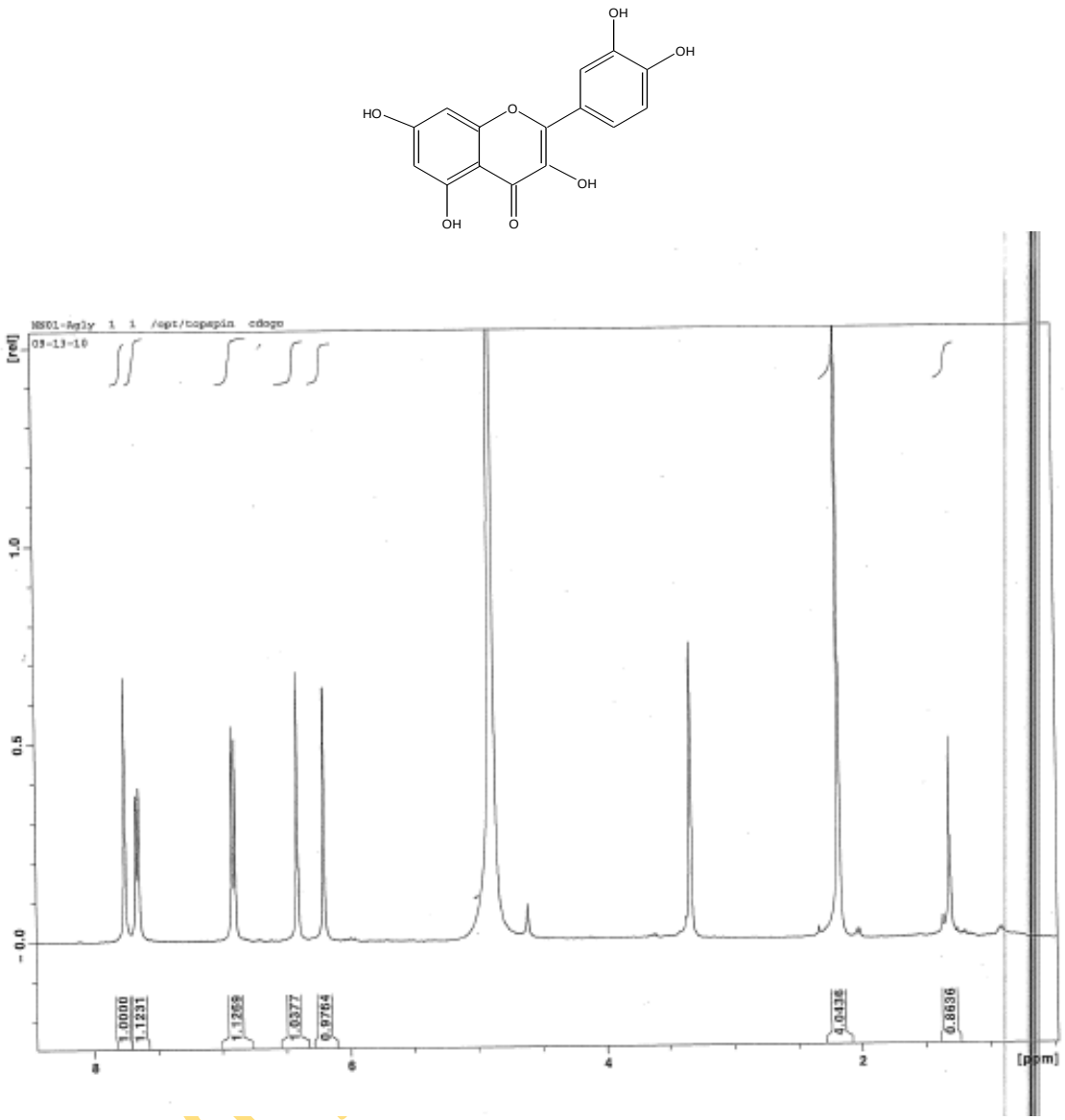

Figure 4.45. Compound NN01a (quercetin) 400 MHz ^{1}H spectrum in CD_3OD

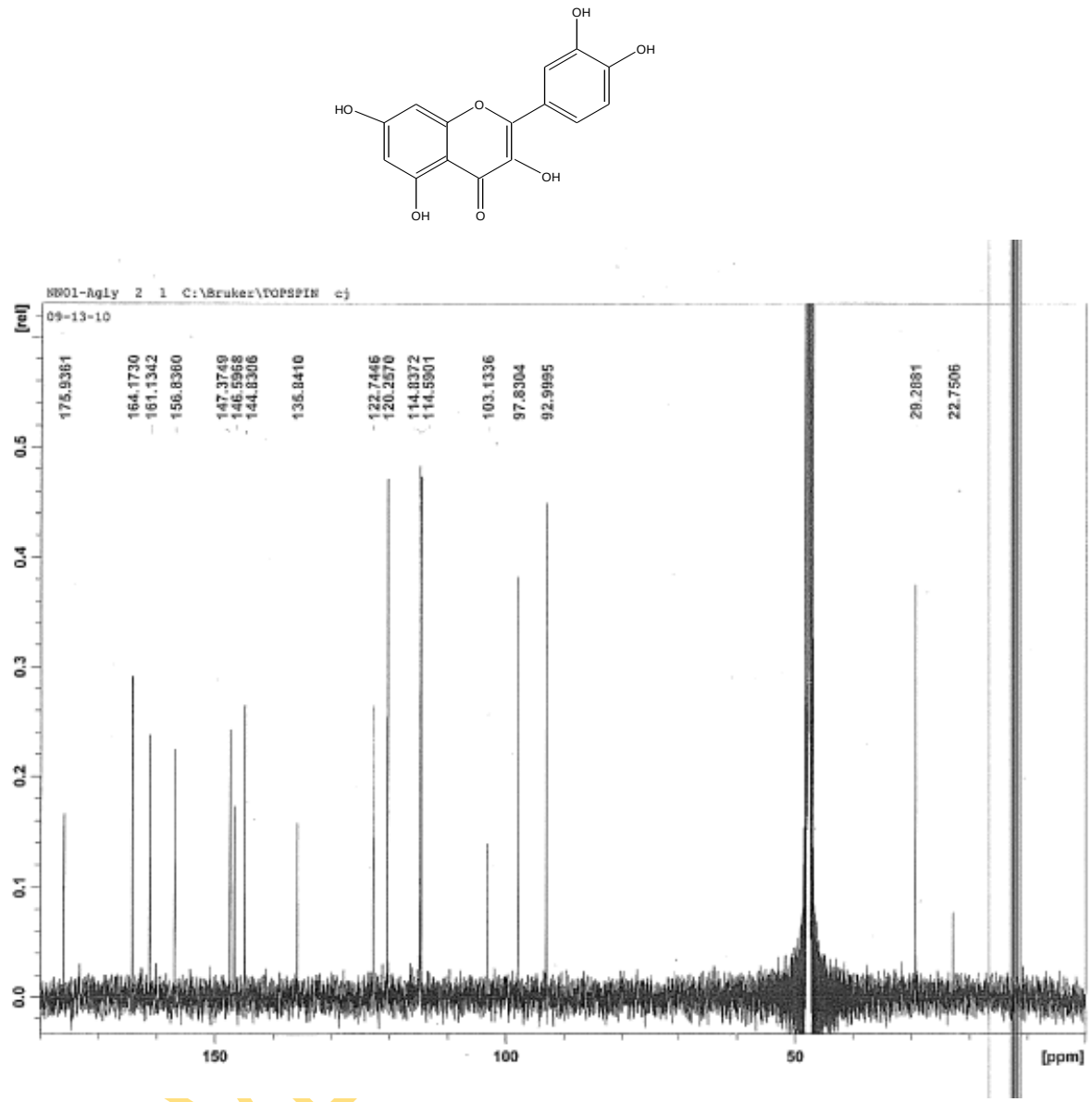

Figure 4.46. Compound NN01a (quercetin) 100 MHz ^{13}C spectrum in CD_3OD

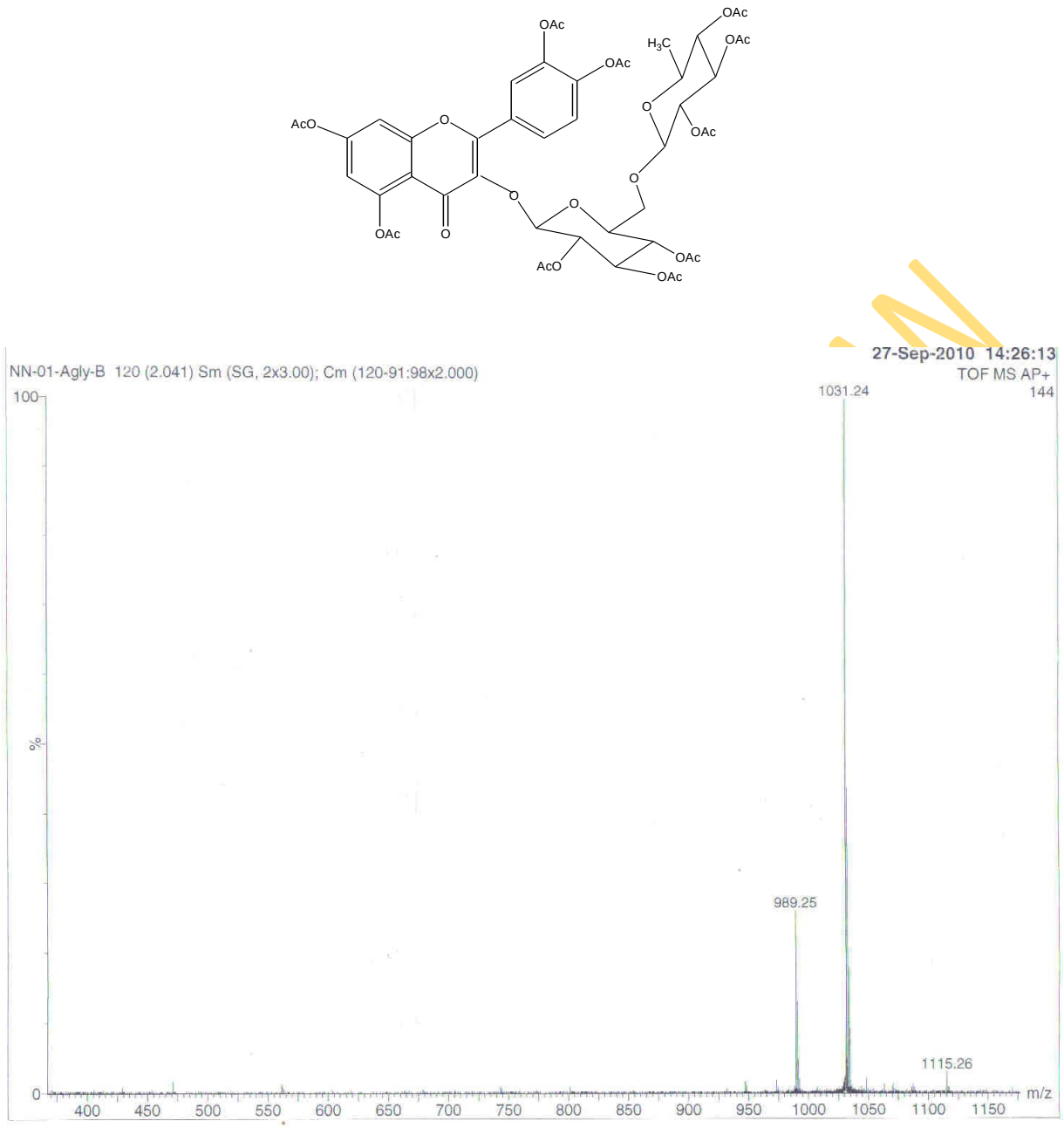

Figure 4.47. Compound NN01b (acetylated rutin) AP-MS-TOF spectrum

4.3.6 Characterization of NN04

The negative and positive ion modes ESI-TOF mass spectra of **NN04** (Figs 4.48 and 4.49) showed quasimolecular ion peaks at *m/z* 387.1 $[M - H]^-$ and 411.1 $[M + Na]^+$, respectively. The molecular formula of $C_{16}H_{20}O_{11}$ (DBE = 7) was derived from the HRESIMS, with the $[M + Na]^+$ ion at *m/z* 411.0909 supported by the ^{13}C and DEPT spectra (Figs 4.50 and 4.51) which revealed the presence of sixteen carbons comprising one methyl, two methylene, nine methine and four quartenary carbons. The negative ion mode ESI-TOF mass spectrum (Fig 4.48) showed a fragment peak at *m/z* 343.1 [*m/z* 387- 44]$^-$ representing the loss of a carboxylate ion. On the basis of the molecular formula, the degree of unsaturation was calculated as seven.

The IR spectrum (Fig 4.52) exhibited strong carbonyl (1677 cm^{-1}), olefinic (1628 cm-1) and hydroxyl (3357 cm^{-1}) stretching bands. The increase in the intensity of the olefinic (C=C) absorption was consistent with polarization brought about by conjugation with the carbonyl group (C=O). The presence of a conjugated chromophore was indicative of the UV spectrum (Fig 4.21) which showed one absorption maximum at 218 nm (λ_{max} calc = 220 nm; an α, β unsaturated carboxylic acid attached to an O-alkyl group). This further supported the presence of an an α, β unsaturated keto system as shown in the IR spectrum.

The ^1H spectra (Figs 4.53 and 4.54) displayed a highly deshielded olefinic proton of an α, β unsaturated keto system on a trisubstituted double bond. This appeared as a singlet at δ_H 7.32 (1H, s, H-3). Another trisubstituted olefinic proton resonated at δ_H 6.75 (1H, br s, H-8). The trisubstituted methine proton at δ_H 5.80 (1H, s, H-1) was suggestive of an acetal linkage. Two geminally coupled protons were observed at δ_H 2.77 (1H, m, H-6^a) and δ_H 2.38 (1H, dd, 16 Hz, 2.4 Hz, H-6^b) and were indicative of methylene protons on a saturated carbon atom. The glycosidic protons resonated between δ_H 2.94 and 4.42. An anomeric proton was observed at δ_H 4.42 (d, 7.6 Hz, H-1'), indicating the presence of a glucosyl moiety. The methylene protons of the sugar (H-6') displayed geminal coupling and showed as two doublets of a doublet at δ_H 3.65 (1H, dd, 1.6 Hz, 12 Hz, H-6'^{a}) and 3.45 (1H, dd, 4.8 Hz, 12 Hz, H-6'^{b}). A triplet was also observed at δ_H 2.94 (1H, t, 8 Hz, H-2'). Other signals were not well resolved and showed up as multiplets between δ_H 3.0 and 3.3. ^1H-^1H COSY (Fig 4.55) also revealed the direct connectivities between some protons;

δ_H 4.42 (d, 7.6 Hz, H-1') ↔ δ_H 2.94 (1H, t, 8 Hz, H-2')

δ_H 3.45 (1H, dd, 4.8 Hz, 12 Hz, H-6'^{a}) ↔ δ_H 3.65 (1H, dd, 1.6 Hz, 12 Hz, H-6'^{b})

δ_H 2.38 (1H, dd, 16 Hz, 2.4 Hz, H-6^a) ↔ δ_H 2.77 (1H, m, H-6^b)

δ_H 2.77 (1H, m, H-6^b) ↔ δ_H 3.16 (1H, H-5)

In the decoupled ^{13}C spectra (Figs 4.50 and 4.51), of the sixteen carbons observed, two were attributed to carbonyl groups (δ_C 167.7, 165.5), two to double bonds (δ_C 151.0, 145.5, 134.5, 111.2) and six to glycosidic carbons (δ_C 98.8, 76.9, 76.6, 72.9, 69.7 and 60.8). Analysis of the HSQC spectrum (Fig 4.56) allowed the assignments of each carbon resonance through the corresponding ^{13}C - ^{1}H correlation and confirmed assignments of the geminally coupled methylene protons found in the ^{1}H NMR and ^{1}H-^{1}H COSY.

In the HMBC spectrum (Fig 4.57), the following correlations were observed:

δ_H 7.32 (H-3) ↔ δ_C 32.1 (C-5), 111.2 (C-4), 167.7 (C-11)

δ_H 7.32 (H-3), 4.42 (H-1') ↔ δ_C 93.2 (C-1)

δ_H 6.75 (H-8) ↔ δ_C 32.1 (C-5), 46.3 (C-7), 165.5 (C-10)

δ_H 5.80 (H-1) ↔ δ_C 32.1 (C-5), 98.8 (C-1'), 111.2 (C-4), 134.5 (C-9), 151.0 (C-3)

Correlations between δ_H 4.42 (H-1', anomeric proton) and δ_C 93.2 (C-1) supported the acetal linkage at C-1. Full assignments of ^{1}H and ^{13}C NMR chemical shifts are as shown in Table 4.8.

Table 4.8. ^{1}H and ^{13}C NMR spectroscopic data of compound **NN04** in DMSO-d_6

C/H Atom	δ_H, multiplicity (*J* in Hz)	δ_C	DEPT
1	5.80, s	93.2	CH
3	7.32, s	151.0	CH
4		111.2	qC
5	3.16	32.1	CH
6[a]	2.38, dd (18.4, 2.4)	38.1	CH_2
6[b]	2.77, m		
7	3.16	46.3	CH
8	6.75, br s	145.5	CH
9		134.5	qC
10		165.5	qC
11		167.7	qC
1'	4.42, d (7.6)	98.8	CH
2'	2.94, t (8)	72.9	CH
3'	3.15, m	76.9*	CH
4'	3.09, m	69.7	CH
5'	3.15, m	76.6*	CH
6'[a]	3.45, dd (4.8, 12)	60.8	CH_2
6'[b]	3.65 dd (1.6, 12)		

* Assignments may be reversed

Combining these data with biogenetic considerations, the structural elucidation of **NN04** was proposed as 1-O-β-D-glucopyranosyl-7-hydroxycarbonylcyclopent-8-eno[c]pyran-3-en-4-carboxylic acid, trivially named pavetoside (**147**).

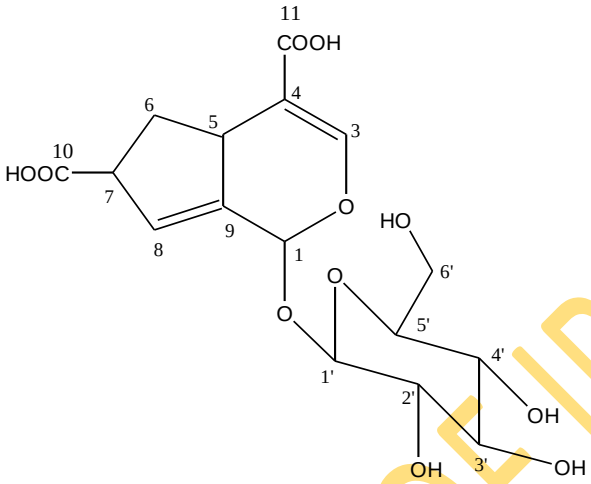

147

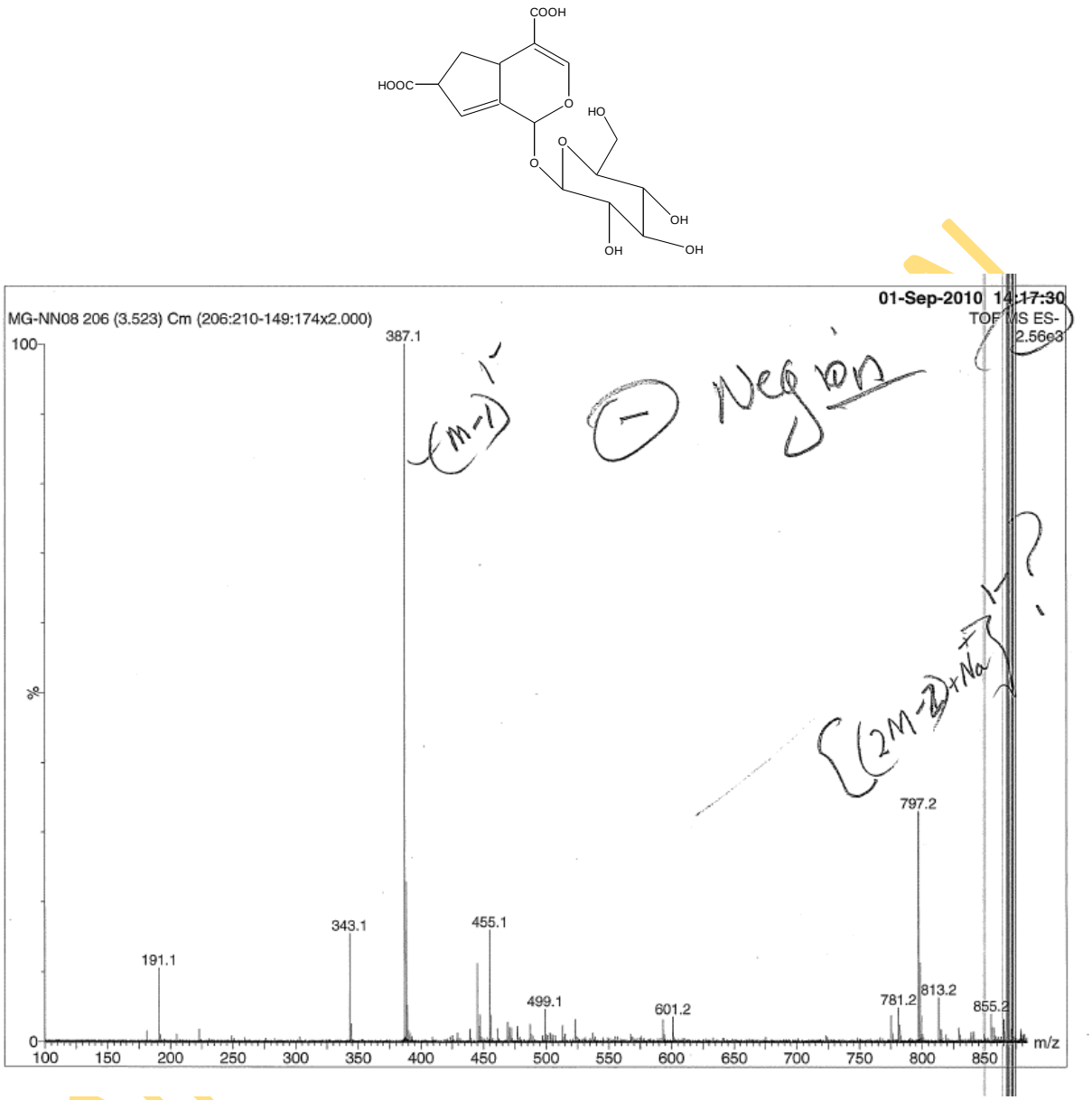

Figure 4.48. Compound NN04 (pavetoside) ESI-MS-TOF spectrum (negative ion mode)

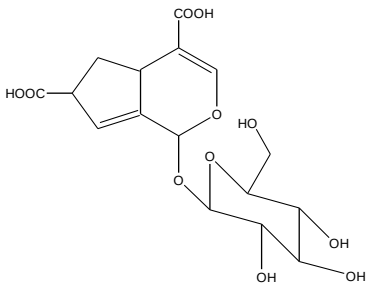

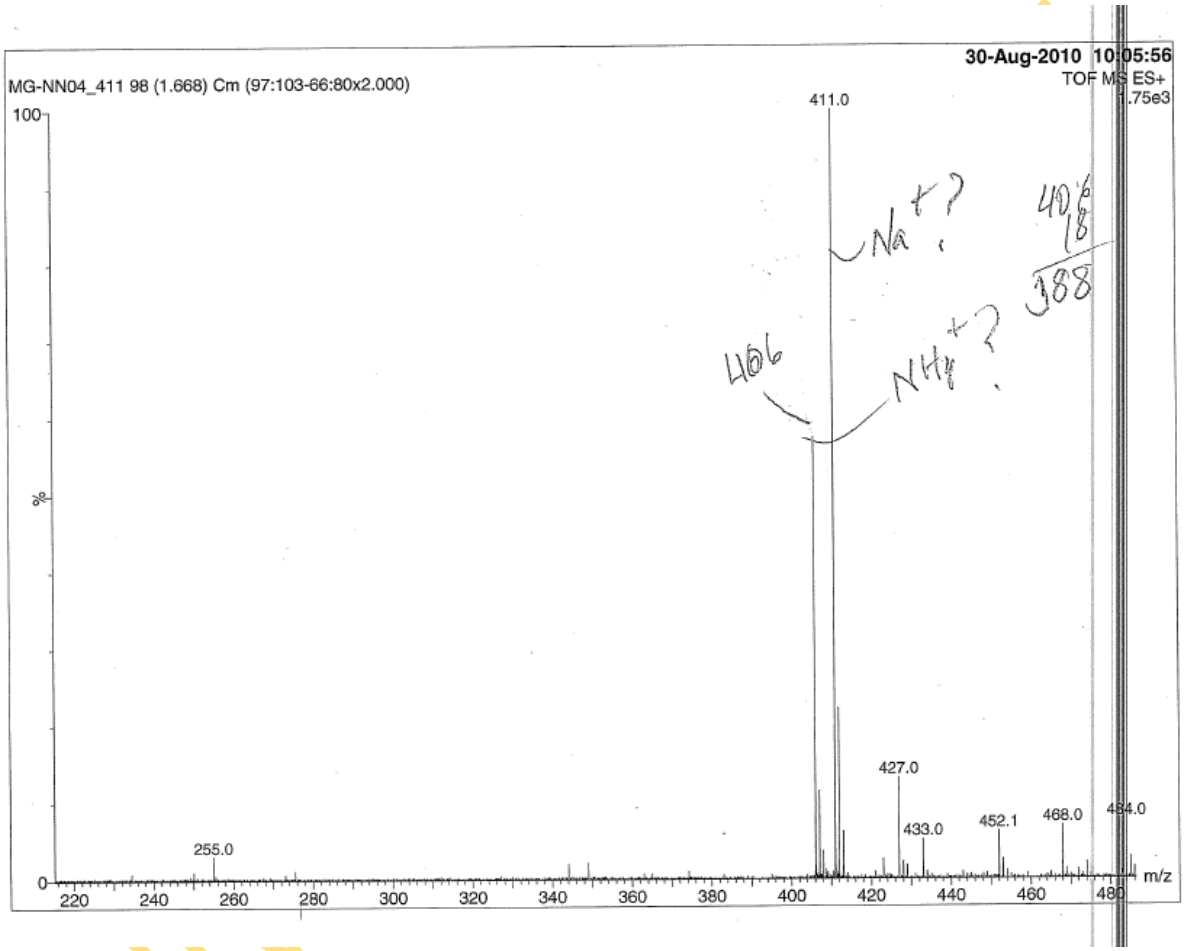

Figure 4.49. Compound NN04 (pavetoside) ESI-MS-TOF spectrum (positive ion mode)

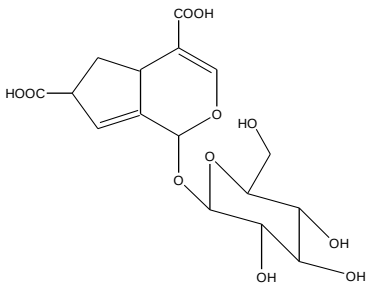

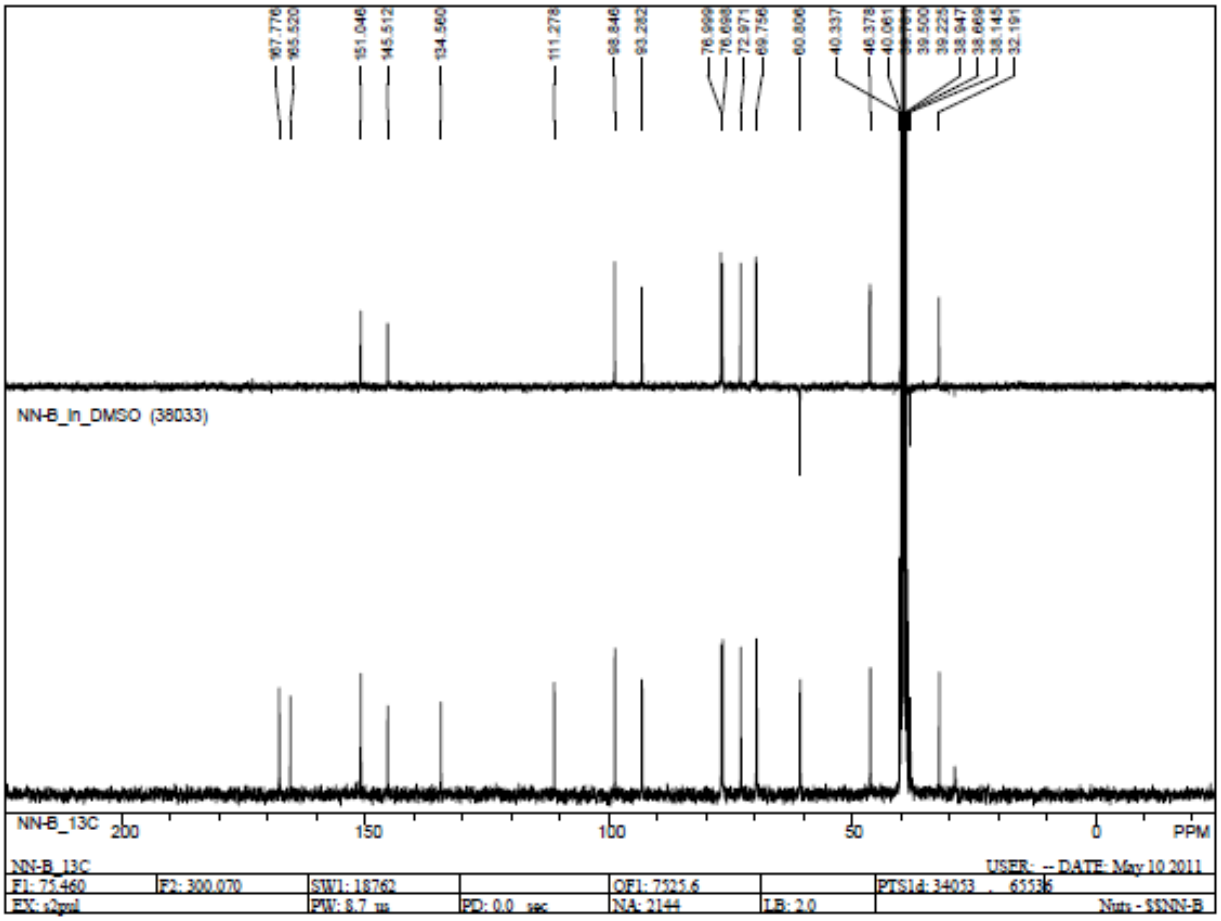

Figure 4.50. Compound NN04 (pavetoside) 100 MHz ^{13}C spectrum in DMSO-d_6

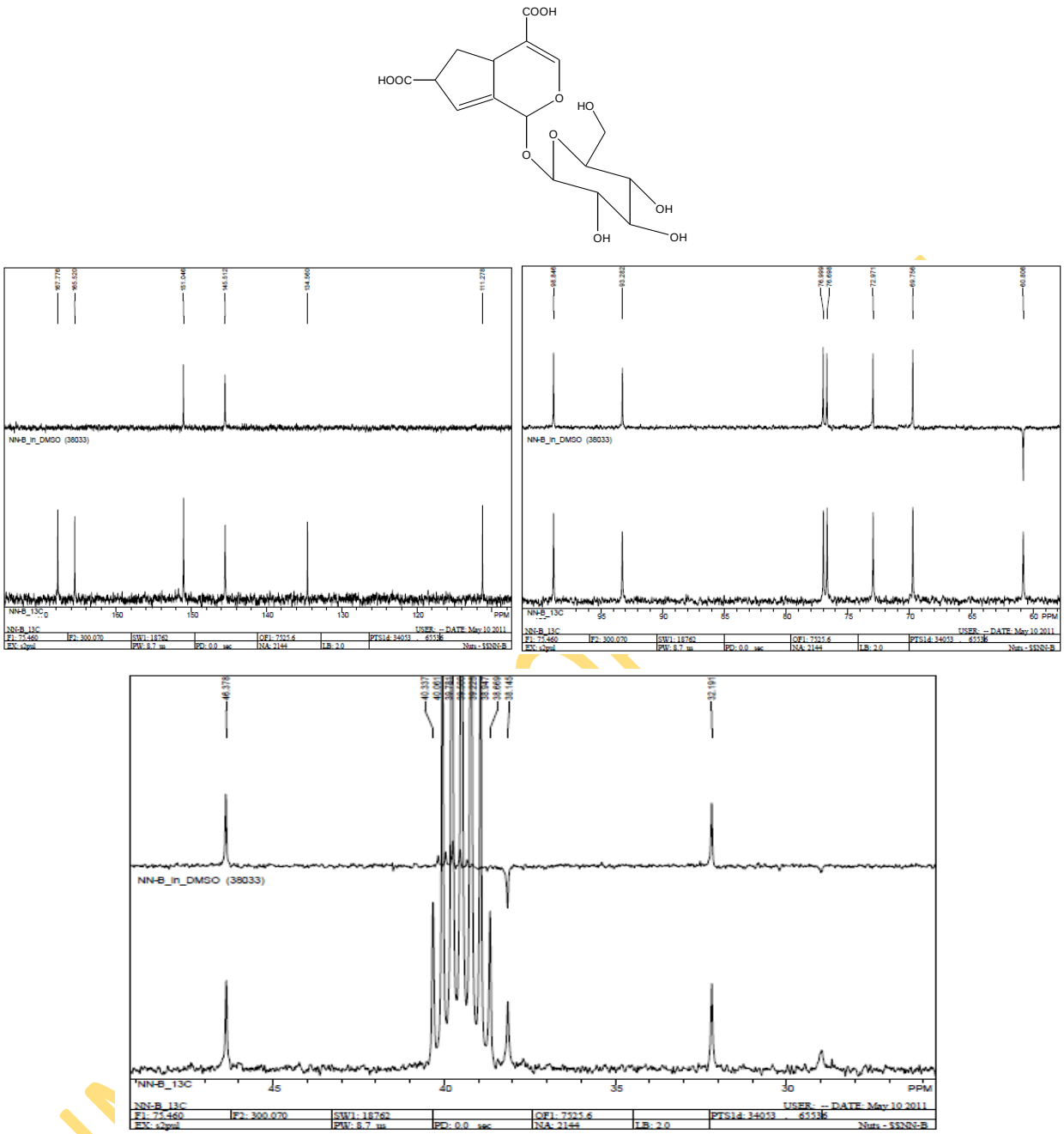

Figure 4.51. Compound NN04 (pavetoside) 100 MHz ^{13}C spectrum in DMSO-d_6 (expanded regions)

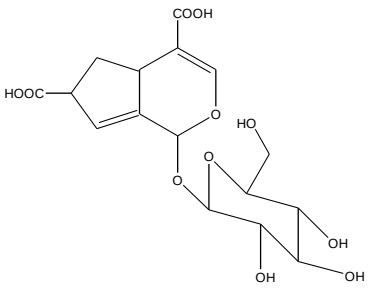

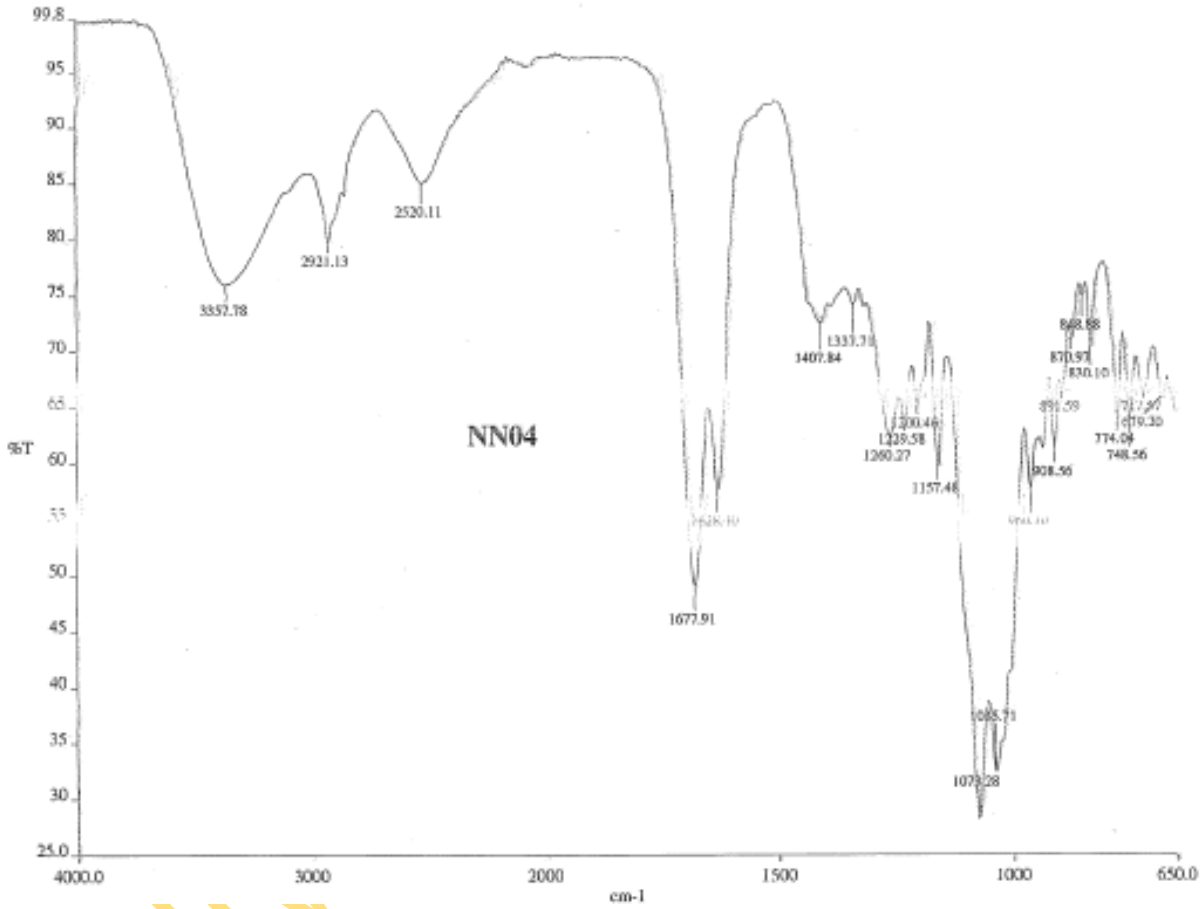

Figure 4.52. Compound NN04 (pavetoside) IR spectrum

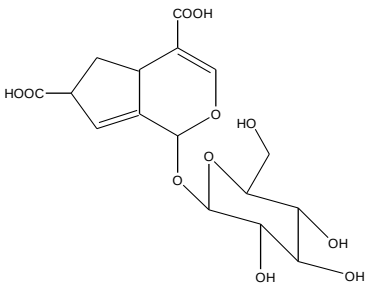

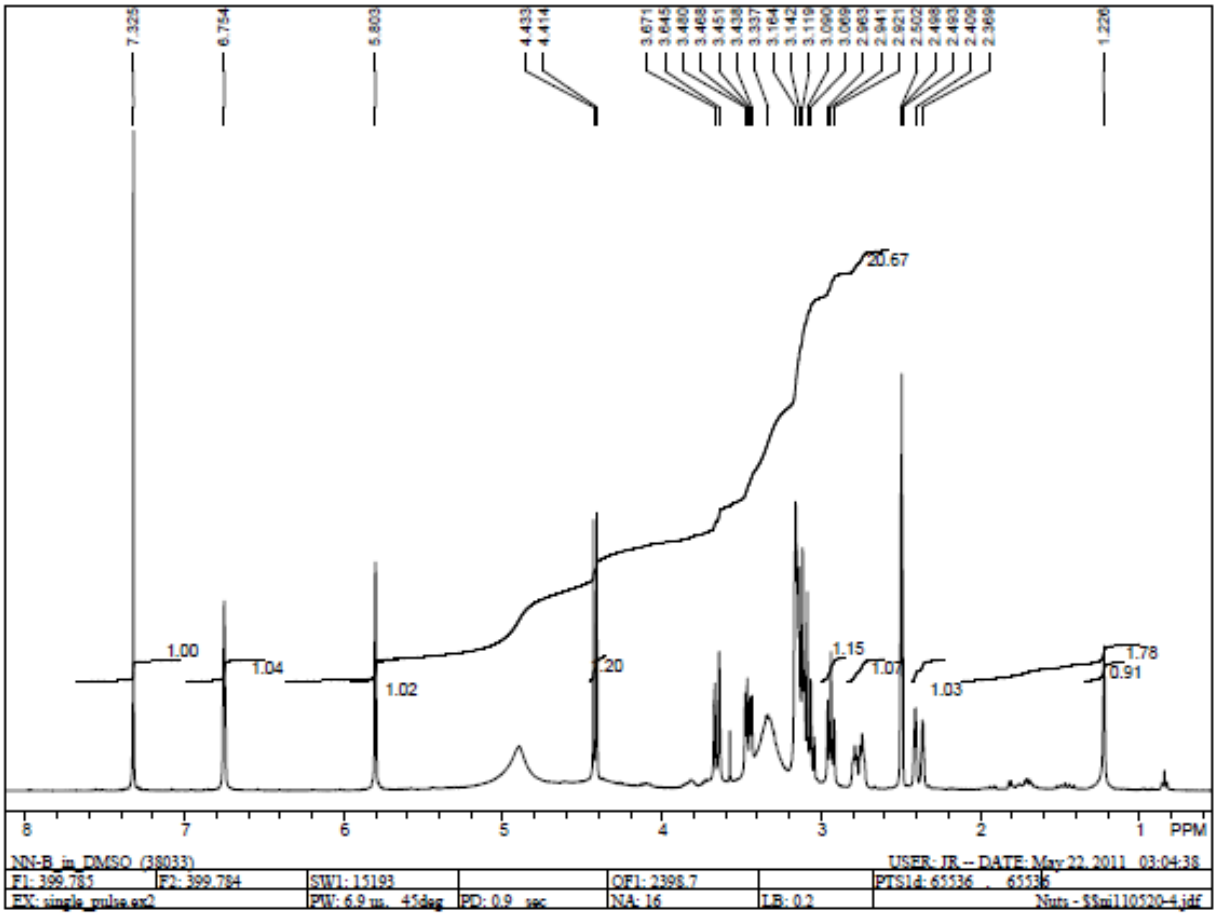

Figure 4.53. Compound NN04 (pavetoside) 400 MHz ^{1}H spectrum in DMSO-d_6

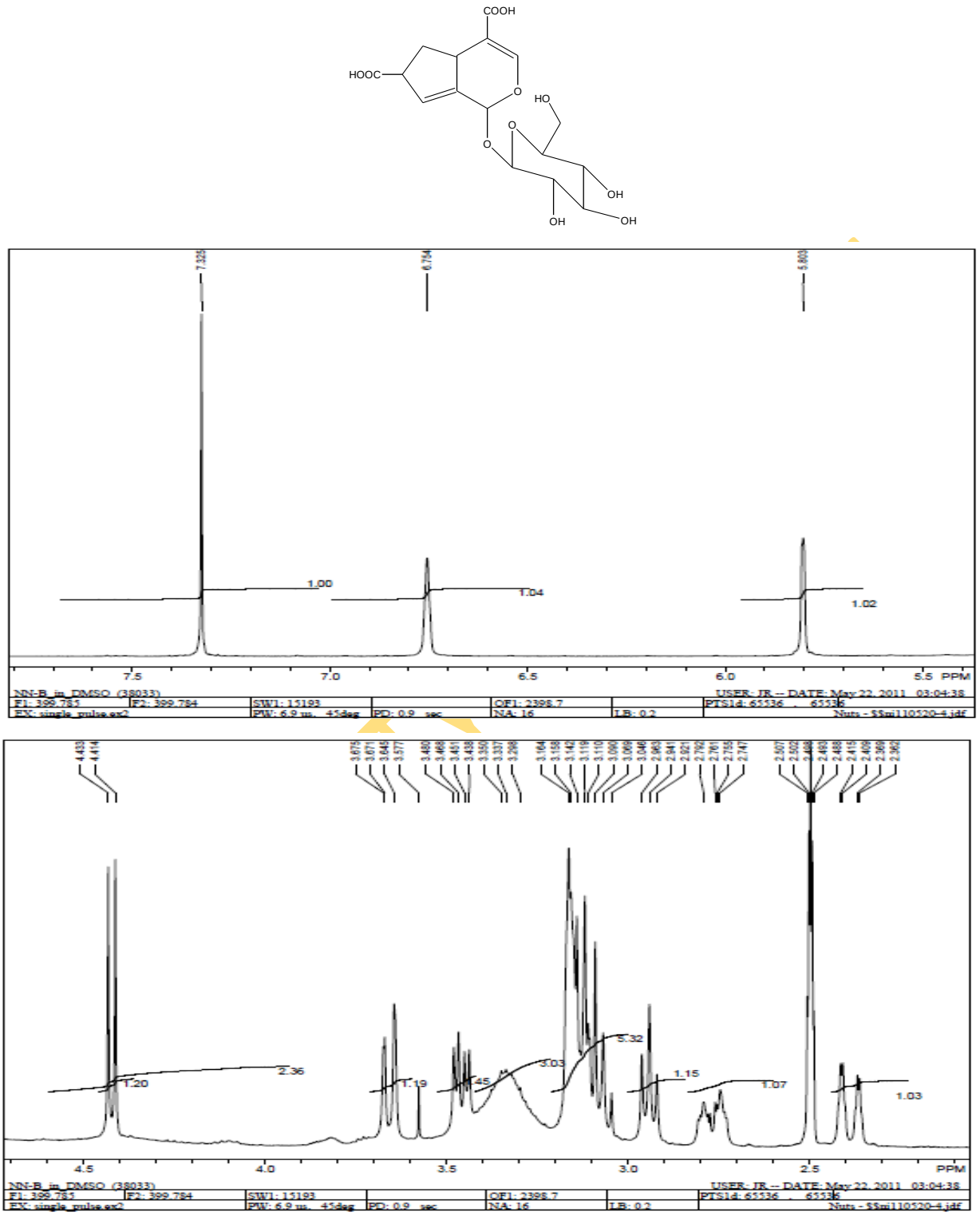

Figure 4.54. Compound NN04 (pavetoside) 400 MHz ^{1}H spectrum in DMSO-d_6 (expanded regions)

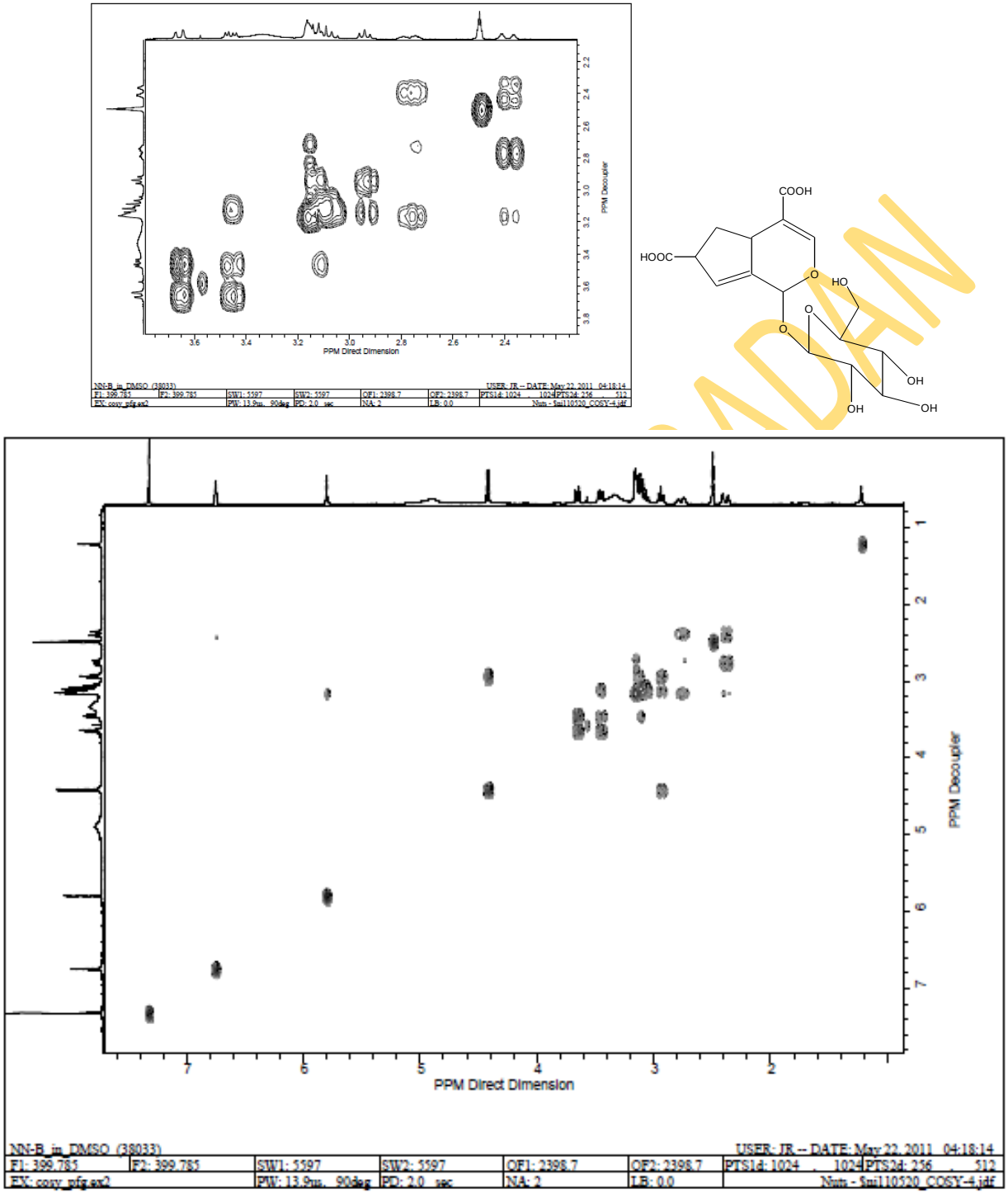

Figure 4.55. Compound NN04 (pavetoside) 400 MHz ^{1}H-^{1}H spectrum in DMSO-d_6

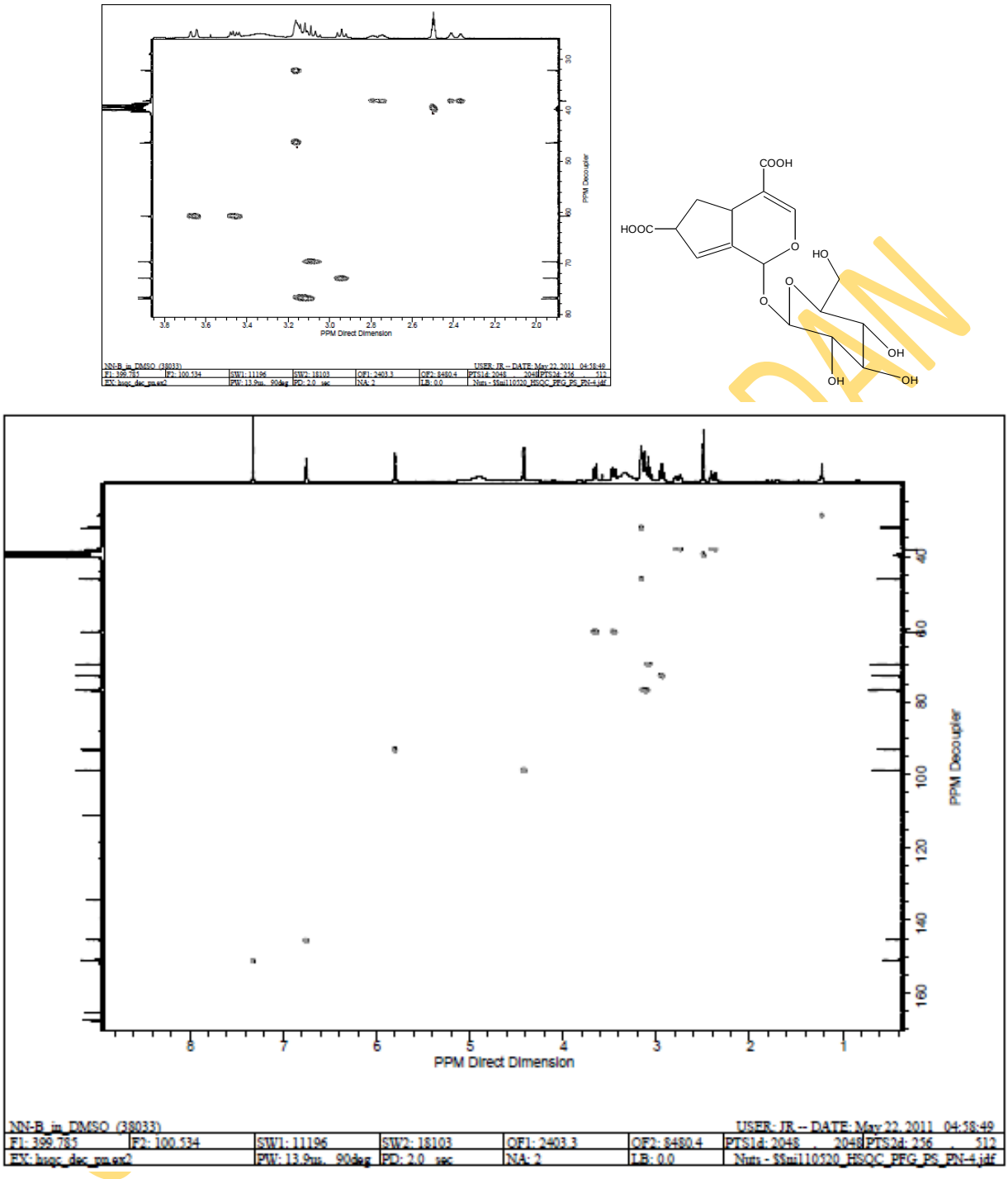

Figure 4.56. Compound NN04 (pavetoside) 400 MHz HSQC spectrum in DMSO-d_6

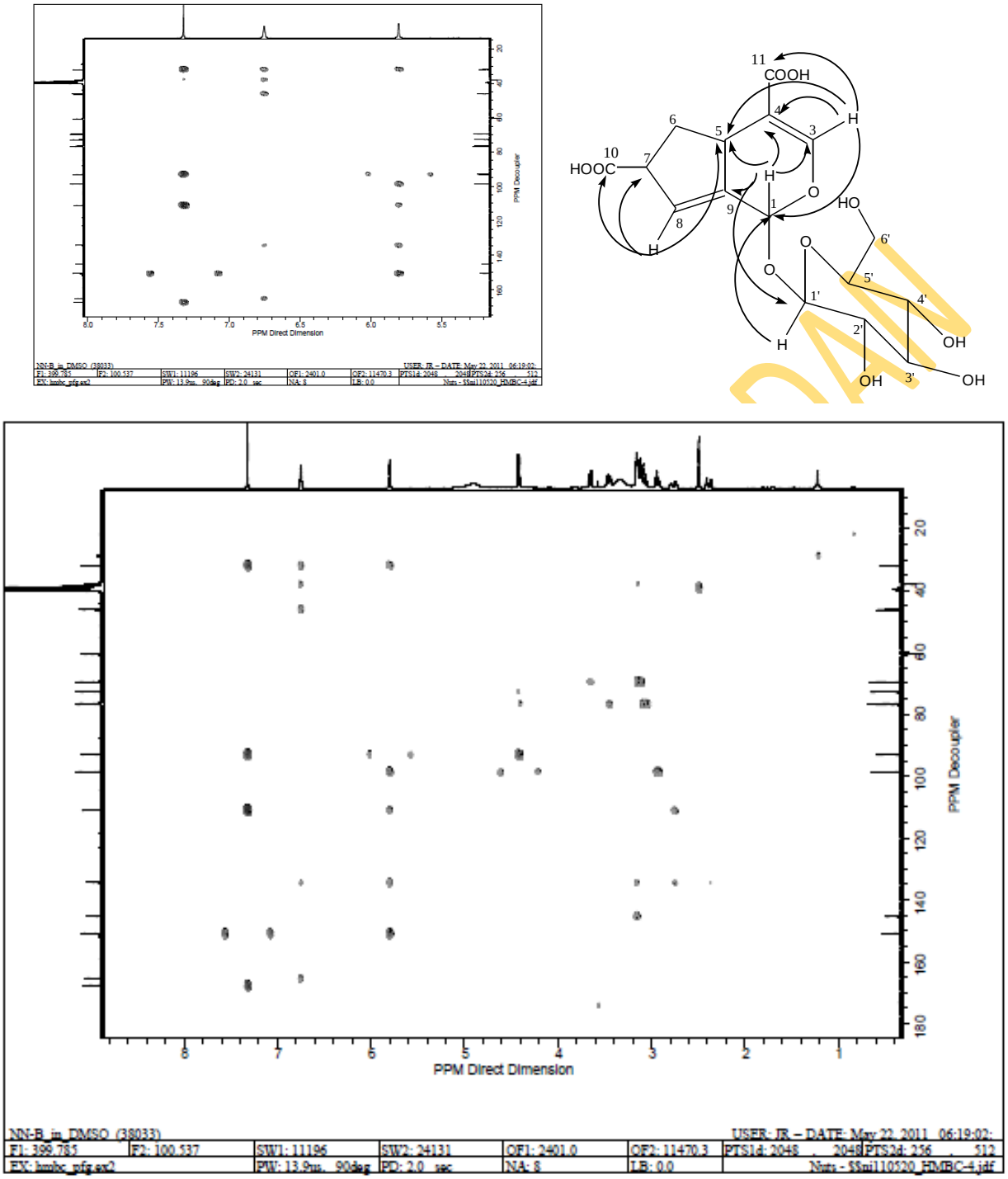

Figure 4.57. Compound NN04 (pavetoside) 400 MHz HMBC spectrum in DMSO-d_6

4.3.7 Characterization of NN02

NN02 had a melting point of 154-157^{o}C. The quasimolecular ion from the positive ion mode AP-TOF mass spectrum (Fig 4.58) was at *m/z* 183.1 $[M + 1]^+$. Other major fragments observed were *m/z* 165.1 $[M + 1 – H_2O]^+$, 147.1 $[165.1 - H_2O]^+$, 129.1 $[147.1 - H_2O]^+$, and 111 $[129.1 - H_2O]^+$. The loss of water was a clear indication of the polyhydroxyl nature of the molecule. The HRMS was calculated as *m/z* 183.0872, indicating the molecular formular to be $C_6H_{12}O_6$. The IR spectrum (Fig 4.59) showed absorption bands due to O-H (3329 cm^{-1}), C-H (2989 cm^{-1}) and C-O (1066 cm^{-1}) stretches.

The ^{1}H-NMR (D_2O) spectrum (Fig 4.60) revealed a few signals between δ_H 3.5 and 3.8. Two doublets of a doublet were observed at δ_H 3.75 (2H, dd, 2.4, 11.7 Hz, H-1, 6) and 3.56 (2H, dd, 11.7, 6 Hz, H-1, 6). A signal revealing a doublet also showed at δ_H 3.68 (2H, d, 8.6 Hz, H-2, 5). The remaining resonances were observed at δ_H 3.64 (2H, m, H-3, 4).

In the ^{13}C and DEPT (DMSO-d_6) spectra (Figs 4.61 and 4.62), 3 signals were observed; δ_C 70.8 (CH, C-2, 5), 69.2 (CH, C-3, 4) and 63.2 (CH_2, C-1, 6). This region of resonances showed that the carbons were bonded to hydroxyl groups and further supported the MS and IR data that the compound was polyhydroxylated. Another observation in the carbon spectrum was that there must be an element of symmetry in the molecule going by the number of carbon signals, thus suggesting three pairs of chemically equivalent carbon signals.

Spectral data was compared with that from literature (Hagiwara *et al*., 2005) in Table 4.9.

Table 4.9. ^{1}H and ^{13}C spectroscopic data of compound **NN02**

C/H Atom	δ_H, multiplicity (*J* in Hz)	δ_C	DEPT	D-Mannitol (D_2O) Hagiwara *et al*., (2005)
1, 6	3.75, dd (11.7, 2.4) 3.56, dd (11.7, 6)	63.2	CH_2	63.5
3, 4	3.68, d (8.6)	70.8	CH	71.1
2, 5	3.64, m	69.2	CH	69.6

The molecule was thus identified as (2R, 3R, 4R, 5R)-Hexane-1,2,3,4,5,6-hexol (D-mannitol; **148**).

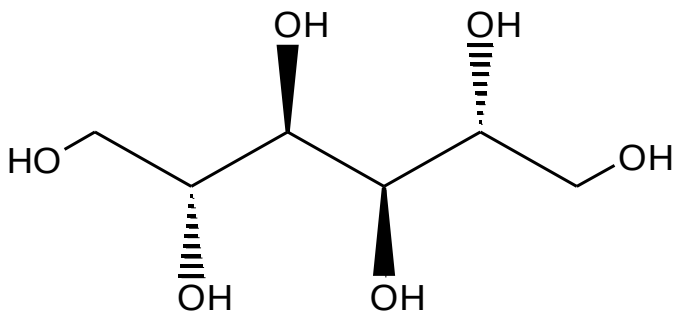

148

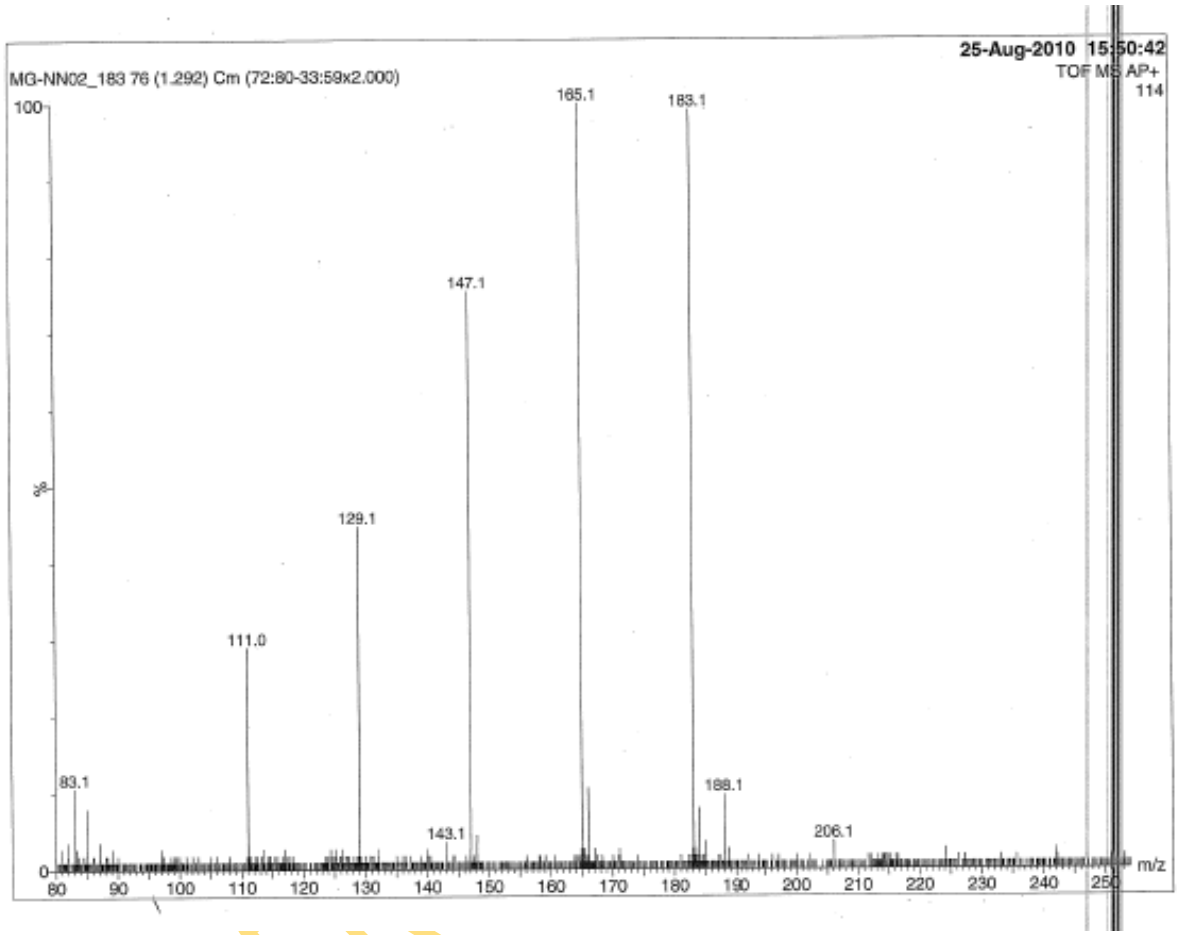

Figure 4.58. Compound NN02 (D-mannitol) AP-TOF-MS (positive ion) spectrum

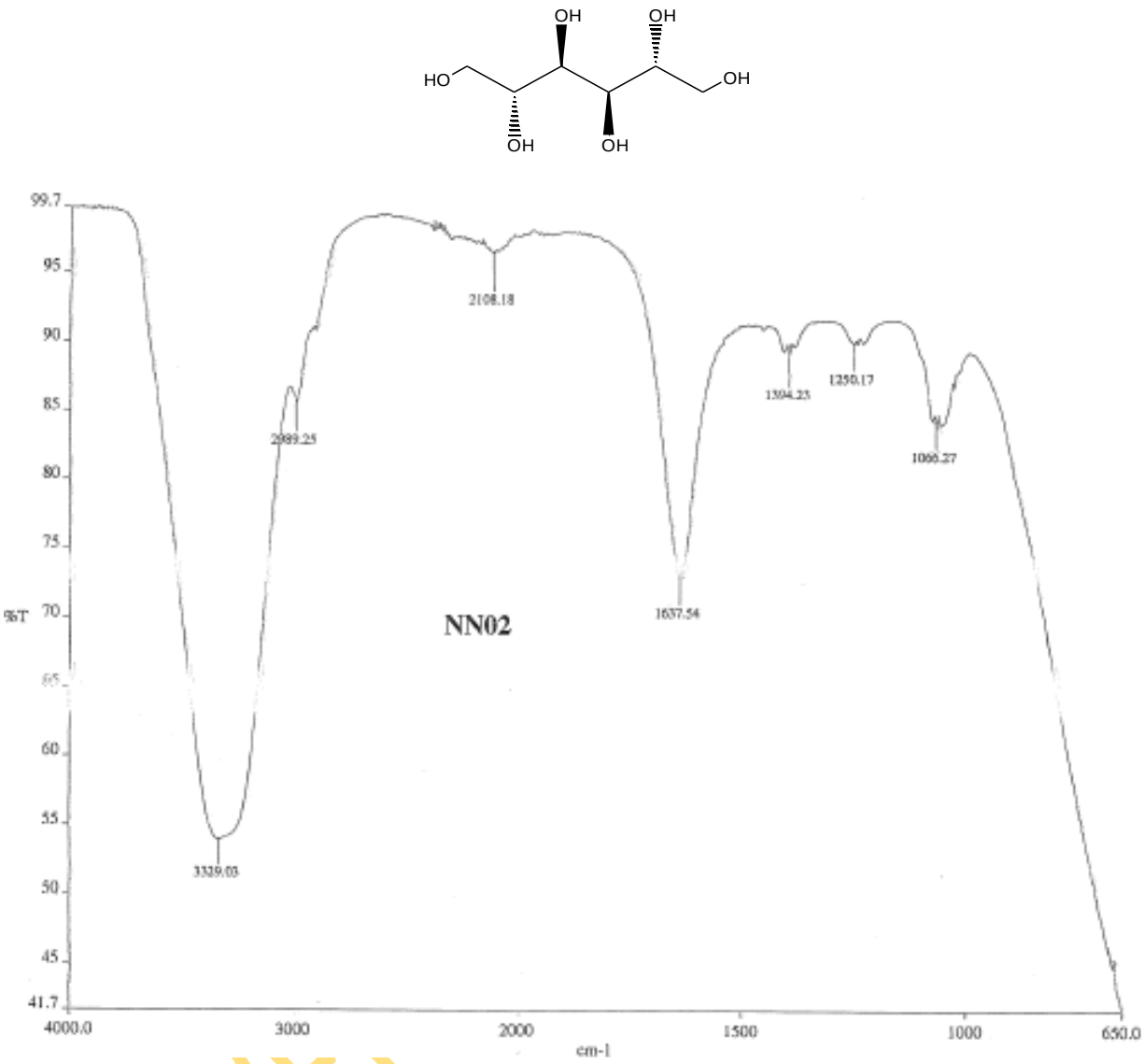

Figure 4.59. Compound NN02 (D-mannitol) IR spectrum

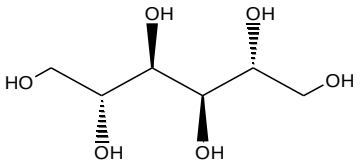

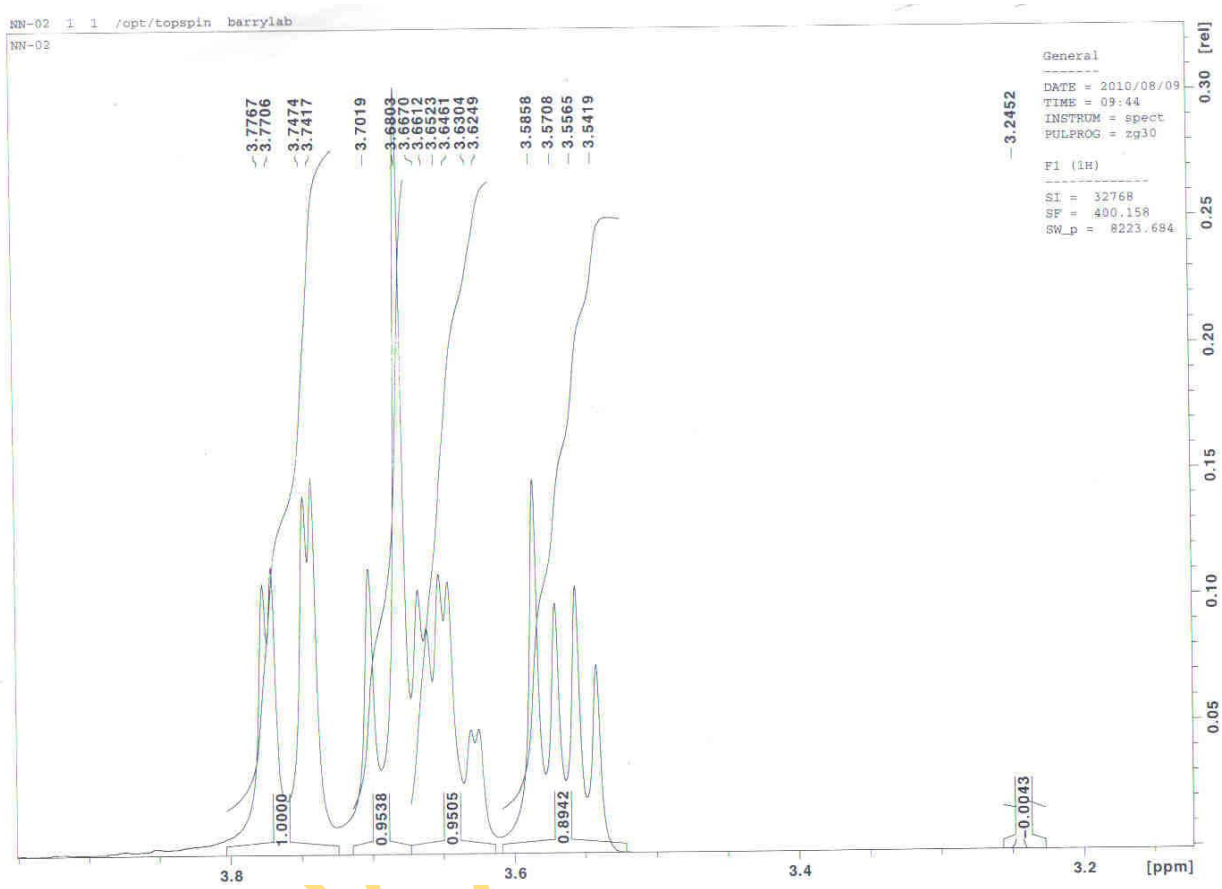

Figure 4.60. Compound NN02 (D-mannitol) 400 MHz ^{1}H spectrum in D_2O

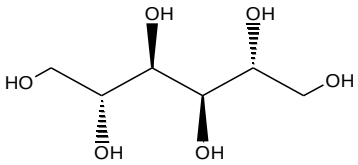

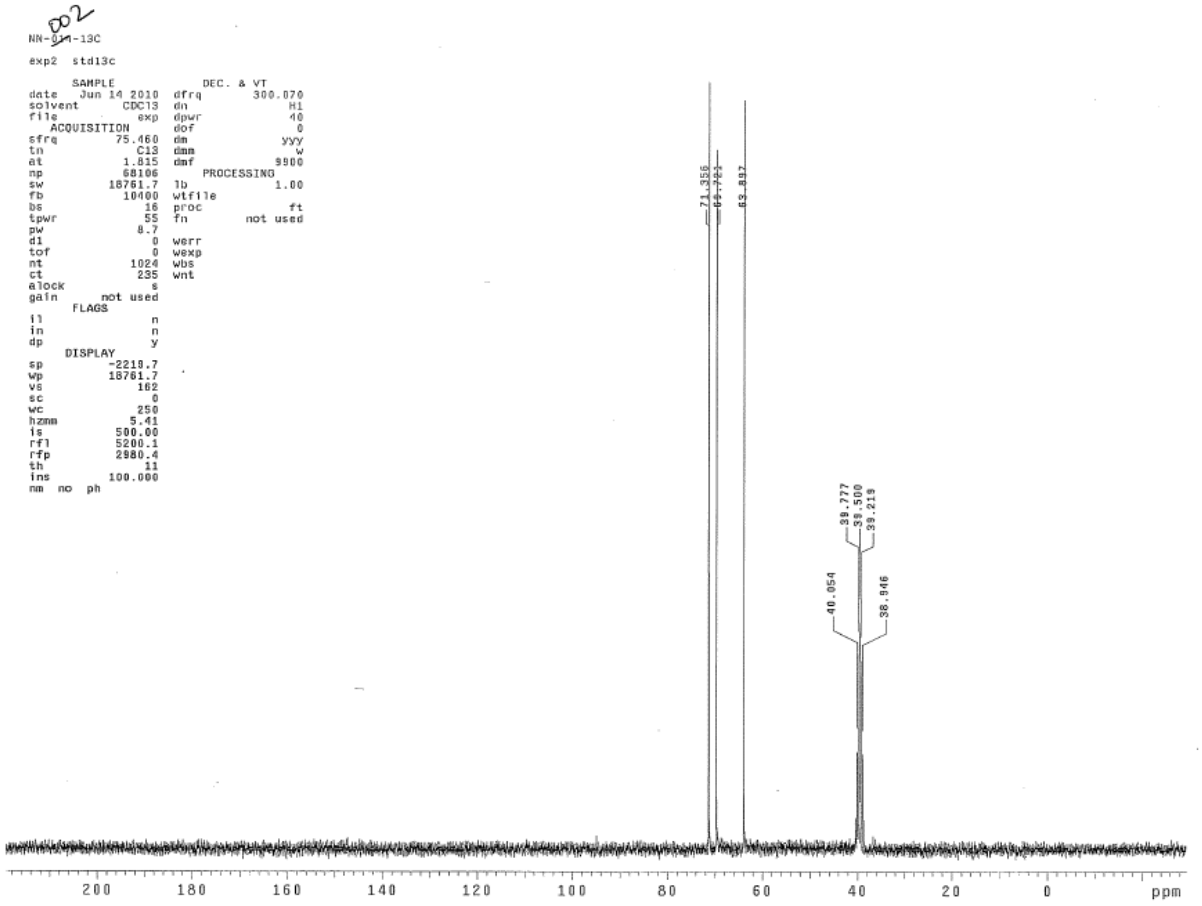

Figure 4.61. Compound NN02 (D-mannitol) 100 MHz ^{13}C spectrum in DMSO-d_6

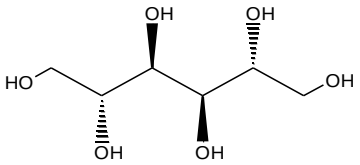

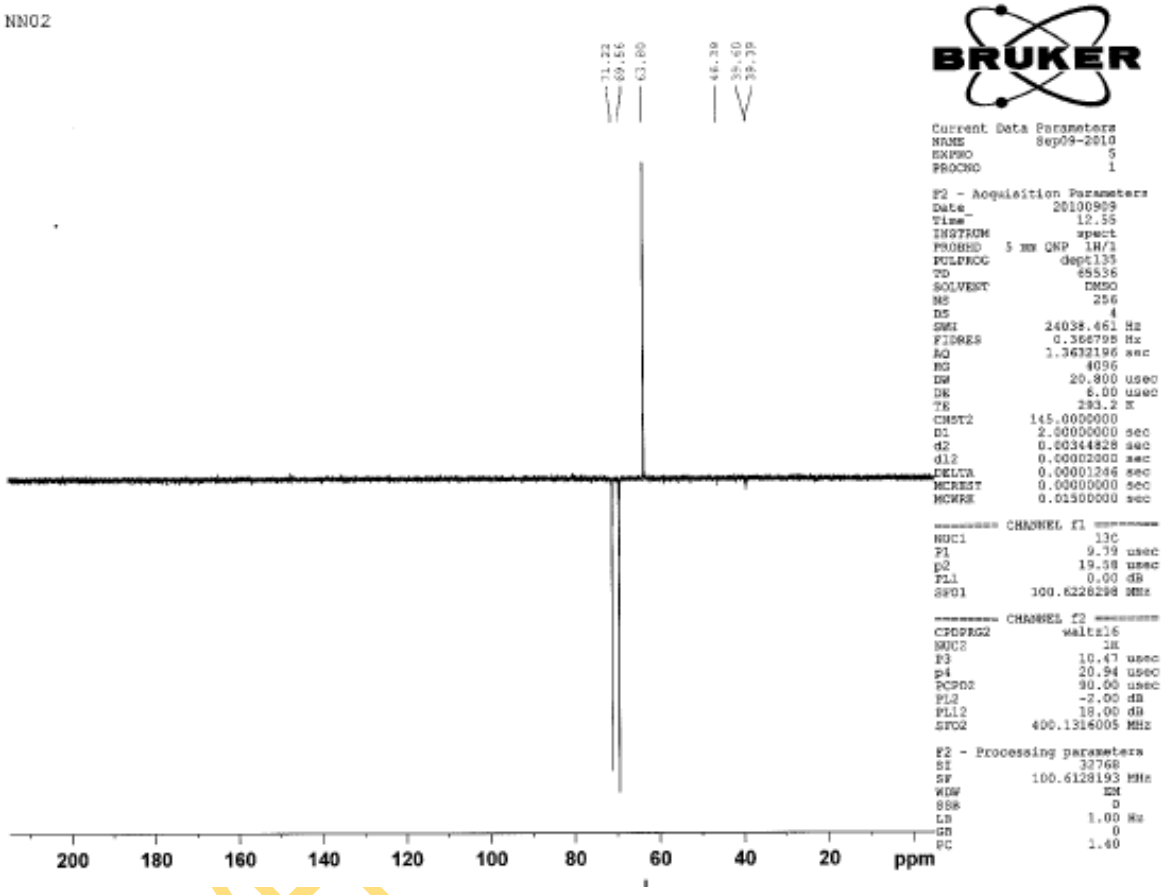

Figure 4.62. Compound NN02 (D-mannitol) 100 MHz DEPT spectrum in DMSO-d_6

4.4 Antimycobacterial Activities of Extracts/ Fractions/ Compounds

Preliminary antimycobacterial studies showed activities in the ethyl acetate and methanol extracts with MICs of 250 µg/mL and 521µg/mL respectively. Bio-assay of fractions of the active extracts employing the Broth Microdilution Method (BMM) showed that for the ethyl acetate extract, the best antimycobacterial activity at 500 µg/mL, was eluted with 10% methanol in ethyl acetate. In the methanol extract, the activities were distributed across the various fractions eluted between 5% ethyl acetate in hexane to 100% ethyl acetate with MICs ≤ 900 µg/mL (Table 4.10).

All isolated compounds with final concentrations of 200 µg/mL (GFPMA) and 400 µg/mL (BMM) were screened against *M. tuberculosis* (Table 4.11). **NN05**, **NN06**, **NN07** were found active at 200, 100 and 50 µg/mL respectively. Compounds **NN06** and **NN07** are methyl chlorogenate and ethyl chlorogenate, respectively, while **NN05** is ursolic acid.

Table 4.10. Antimycobacterial activities of active fractions against *M. tuberculosis* $H_{37}Rv$

Extract	Fractions	MIC (µg/ mL)	Mobile phase
EtOAc	14	500	10% MeOH in EtOAc
CH_3OH	1	250	5- 10% EtOAc in Hex
"	3	325	10% EtOAc in Hex
"	4	200	30% EtOAc in Hex
"	8	900	100% EtOAc

Table 4.11. Antimycobacterial activity of compounds against *M. tuberculosis* $H_{37}Rv$

Compound	**GFPMA**	**BMM**
	MIC in µg/mL	**MIC in µg/mL**
NN01	NA	NA
NN01a	NA	NA
NN02	NA	NA
NN03	NA	NA
NN04	NA	NA
NN05	NA	200
NN06	200	100
NN07	100	50

NA = Not Active (at the concentration tested)

Ursolic acid (**120**) and its analogue, 24-hydoxyursolic acid have previously been reported as anti mycobacterial agents from *Valeriana laxiflora* (Gu *et al*., 2004) and *Leyssera gnaphaloides* (Bamuamba *et al*., 2008). Some pentacyclic tritepenes with substituents in C-3 and C-17, such as oleanolic acid, oleanonic acid, and 3-epioleanolic acid inhibited the growth of *M. tuberculosis* H_{37}Rv with MIC values of 50, 16, and 16 µg/mL, respectively (Caldwell *et al*., 2000). It has been reported that the presence of hydroxyl or keto groups in A or B rings, and a carboxylic group in D/E rings, gave the molecule a moderate antimycobacterial activity (Watcher *et al*., 1999; Caldwell *et al*., 2000). These authors also suggested that the mechanism of action of such triterpenoids depended on the lipophilicity of the compounds that allowed a rapid penetration across the lipid-rich mycobacterial cell wall. In their review paper, Ducati *et al.* (2006) also stated that lipophilic molecules should be able to easily cross the mycobacterium membrane, dissolving in the hydrocarbon interior of the lipid bilayer, though factors such as low fluidity of the mycolic acid leaflet and the bilayer's uncommon thickness may result in reduction of this process. The chemoprotective properties and in particular, the antitumour activities of ursolic acid have also been reported (Ovesna *et al*, 2004).

The antimycobacterial activities of ethyl chlorogenate (**143**) and methyl chlorogenate (**144**) have not been reported hitherto. Interestingly, the bioactive chlorogenate esters are structurally similar, but for the length of the alkyl group on the ester substituent. Ethyl chlorogenate, being less polar was shown to be more active (50 µg/mL) than methyl chlorogenate (100 µg/mL). This may be explained to be due to the easier permeability of the cell wall of *M. tuberculosis* which is lipophilic in nature. Methyl chlorogenate has been recently reported for its antioxidant activities (Ao *et al*., 2010; Lin *et al*., 2011). The isolation of both chlorogenate esters have also been reported from *Ericybe hainanesis* (Song *et al*., 2010).

β-Sitosterol (**142**), rutin (**145**), quercetin (**146**), pavetoside (**147**) and mannitol (**148**) were found not have any significant activities against *M. tuberculosis*. Extensive literature search did not reveal any of these compounds to have shown any previous antituberculosis activities.

β-Sitosterol (**142**) is an ubiquitous constituent of many plants, but its antimycobacterial activities have not been reported. Four sterols structurally related to β-sitosterol were isolated from *Thalia multiflora* (Gutierrez-Lugo *et al*., 2005), and exhibited activities against *M. tuberculosis* H_{37}Rv. These compounds, stigmast-5-en-3β-ol-7-one (**128**), stigmast-4-ene-6β-ol-3-one (**129**), stigmasta-5,22-dien-3β-ol-7-one (**130**) and stigmasta-4,22-dien-6β-ol-3-one (**131**) were found

active with MIC values of 1.98, 4.2, 1.0 and 2.2 µg/mL, respectively. The authors attributed the activities to the presence of α, β unsaturated ketone either on ring A or B, in addition to being lipophilic**.**

Quercetin (**146**), the aglycone of rutin (**145**), is a molecule reputed for its antioxidant properties. In this study, it was not found active against *M. tuberculosis* neither was the glycoside, rutin. Pharmacological properties which include antioxidant, antiinflamatory and antidepressant activities have rather been observed in rutin (Kessler *et al*., 2003; Guardia *et al*., 2001; Machado *et al*., 2008). It may be worth mentioning that rhamnose, a deoxyhexose, forms part of the cell wall of *M. tuberculosis*, and as such, as part of the glycoside of quercetin, may only enhance the growth of the bacterium, rather than inhibiting it.

Pavetoside (**147**), a monoterpene iridoid glucoside, was not active against *M. tuberculosis*. Studies on the bioactivity of iridoids revealed these compounds to have a wide range of bioactivities; cardiovascular, antihepatoxic, choleretic, hypoglycemic and hypolipidemic, anti-inflammatory, antiplasmodic, antitumor, antiviral, immunomodulator and purgative activities (Dinda *et al*., 2007). No antimycobacterial activities have been reported from this class of compounds.

D-mannitol (**148**), a simple sugar was also not found active against *M. tuberculosis*. Studies carried out on this compound showed it to rather have antihypertensive activities (Hagiwara *et al*., 2005).

CHAPTER FIVE

CONCLUSIONS AND RECOMMENDATIONS

The search for new antituberculosis agents led to the selection of a Nigerian ethnomedicinal plant, *Pavetta crassipes* (leaves), a plant claimed to be effective in the treatment of tuberculosis and tuberculosis related symptoms in Northern Nigeria. *In vitro* screening against *M. tuberculosis* employing the microbroth dilution and the green fluorescent protein microplate assay techniques, were carried out on the extracts, fractions and compounds of the leaves of *P. crassipes*. The results showed that the antituberculosis activities of *P. crassipes* leaves was attributed to an ursane type triterpene acid, ursolic acid and two chlorogenate esters, methyl chlorogenate and ethyl chlorogenate with MICs of 200, 100 and 50 µg/mL, respectively. This is the first report of the antimycobacterial activities of these compounds from this plant. More interestingly, this is also the first report of chlorogenate esters as antimycobacterial agents. This group of phenolics may represent promising antimycobacterial agents and should be investigated further as potential leads in the drug discovery of antituberculosis agents.

The antimycobacterial activities of the leaves of *P. crassipes* is relevant and it would be interesting to explore the potentials of the active compounds; ursolic acid and the chlorogenate esters as drug templates by carrying out structural activity relationship (SAR) studies to synthesize new derivatives which may be highly specific to treat the disease. Cytotoxicity studies should also be carried out on these active compounds to preclude non-specific activities.

Seven structurally diverse compounds were isolated, characterized and phytochemically identified from the leaves of *P. crassipes*. These compounds were characterized as β-sitosterol, ursolic acid, ethyl chlorogenate, methyl chlorogenate, rutin, pavetoside and D-mannitol. Isolation of these compounds was achieved through a combination of chromatographic procedures while different spectral techniques were used in characterizing the compounds.

This is the first detailed study on the phytochemistry of this plant. One of the compounds, pavetoside, a monoterpene iridoid glucoside, is a novel compound isolated for the first time. Literature searches carried out have reported the isolation of its regioisomer, Erinoside, from

Erinus alpinus (Taskova *et al*., 2005). This adds a new knowledge to science and to the database of natural products.

Chemotaxonomically, the present study on the phytochemistry of *P. crassipes* is important as some of the isolated compounds may be useful as markers of the Rubiaceae family. Compounds such as iridoids, triterpene acids, chlorogenic acid derivatives and flavonoids have been reported from other members of the Rubiaceae family, such as *Adina racemosa*, *Galium verum, Galium tortumense, Saprosma scortechinii*, *Morinda citrifolia* and *Asperula arvensis* (Itoh *et al*., 2003; Demirezer *et al*., 2006; Guvenalp *et al*., 2006; Ling *et al*., 2002; Sang *et al*., 2001; Guvenalp and Demirezer, 2005). An extensive literature search carried out did not reveal much information on the phytochemistry of plants in the *Pavetta* genus. It is therefore recommended that more investigations should be carried out on other species comprising this genus.

In conclusion, this study provides some scientific basis and a biological explanation for the ethnomedicinal use of *Pavetta crassipes* as a traditional antituberculosis remedy, through a combination of indigenous knowledge and natural products chemistry.

REFERENCES

Abubakar, M.S., Musa, A.M., Ahmed, A. and Hussaini, I.M. 2007. The perception and practice of traditional medicine in the treatment of cancers and inflammations by the Hausa and Fulani tribes of Northern Nigeria. *Journal of Ethnopharmacology* 111: 625- 629.

Adams, M., Wube, A.A., Bucar, F., Bauer, R., Kunert, O. and Haslinger, E.J.G. 2005. Quinolone alkaloids from *Evodia rutaecarpa*: a potent new group of antimycobacterial compounds. *International Journal of Antimicrobial Agents* 26: 262.

Adeleye, I.A., Onubogu, C.C., Ayolabi, C.I., Isawumi, A.O. and Nshiogu, M.E. 2008. Screening of crude extracts of twelve medicinal plants and "wonder-cure" concoction used in Nigeria unorthodox medicine for activity against *Mycobacterium tuberculosis* isolated from tuberculosis patients sputum. *African Journal of Biotechnology* 7.18: 3182-3187.

Agraval, S.S. and Paridhavi, M. 2007. *Herbal Drug Technology*. India: University Press Limited.

Agrawal, D.K., Saikai, D., Tiwari, R., Ojha, S., Shanker, K., Kumar, J.K., Gupta, A.K., Tandon, S., Negi, A.S. and Khanuja, S.P.S. 2008. Demethoxycurcumin and its semisynthetic analogues as antitubercular agents. *Planta Medica* 74: 1828-1831.

Alasbahi, R. and Melzig, M.F. 2008. Screening of some Yemeni medicinal plants for inhibitory activity against peptidases. *Pharmazie* 63.1: 86-88.

Amos, S., Akah, P.A., Binda, L., Enwerem, N.M., Ogundaini, A., Wambebe, C., Hussaini, I.M. and Gamaniel, K.S. 2003. Hypotensive activity of the ethanol extract of *Pavetta crassipes* leaves. *Biological and Pharmaceutical Bulletin* 26: 1674-1680.

Amos, S., Okwuasaba, F.K., Gamaniel, K., Akah, P. and Wambebe, C. 1998. Inhibitory effects of the aqueous extract of *Pavetta crassipes* leaves on gastrointestinal and uterine smooth muscle preparations isolated from rabbits, guinea pigs and rats. *Journal of Ethnopharmacology* 61: 209-213.

Andrews, J.M. 2001. Determination of minimum inhibitory concentrations. *Journal of Antimicrobial Chemotherapy* 48: 5-16.

Ao, C., Higa, T., Ming, H., Ding, Y. and Tawata. S. 2010. Isolation and identification of antioxidant and hyaluronidase inhibitory compounds from *Ficus microcarpa* L. fil. Bark. *Journal of Enzyme Inhibition and Medicinal Chemistry* 25.3: 406-413.

Asres, K., Bucar, F., Edelsbrunner, S., Kartnig, T., Höger, G. and Thiel, W. 2001. Investigations on antimycobacterial activity of some Ethiopian medicinal plants. *Phytotherapy Research* 15.4: 323-326.

Balandrin, M.F., Kinghorn, A.D. and Farnsworth, N.R. 1993. Plant derived natural products in drug discovery and development: an overview. *Human Medicinal Agents from Plants*. A.D. Kinghorn and M.F. Balandrin Eds. ACS symposium series 534. Washington D.C: American Chemical Society. 2-12.

Balde, A.M., Claeys, M., Pieters, A., Wrayt, V. and Vlietinck, A.J. 1991a. Ferulic acid esters from stem bark of *Pavetta owariensis*. *Phytochemistry* 30.3: 1024-1026.

Balde, A.M., De Bruyne, T., Pietiers, L, Claeys, M., Berghe, D.V. and Vlietinck, A. 1993. Proanthocyanidins from stem bark of *Pavetta owariensis*, 3.[(1)] NMR study of acetylated trimeric proanthocyanidins possessing a doubly linked structure.[(2)] *Journal of Natural Products* 56.7: 1078-1088.

Balde, A.M., Pietiers, L.A., Kolodziej, H., Claeys, M. and Vlietinck, A.J. 1991b. A-type proanthocyanidins from stem bark of *Pavetta owariensis*. *Phytochemistry* 30.1: 337-342.

Balde, A.M., Van Marck, E.A., Kestens, L., Gigase, P.L. and Vlietinck, A.J. 1989. Schistosomicidal effects of *Pavetta owariensis* and *Harrisonia abyssinica* in mice infected with *Schistosoma mansoni*. *Planta Medica* 55.1: 41-43.

Balde, E.S., Megalizzi, V., Traore, M.S., Cos, P., Maes, L., Decaestecker, C., Pieters, L. and Balde, A.M. 2010. *In vitro* antiprotozoal, antimicrobial and antitumor activity of *Pavetta crassipes* K. Schum leaf extracts. *Journal of Ethnopharmacology* 130: 529- 535.

Bamuamba, K., Gammon, D.W., Meyers, P., Dijoux-Franca, M.G. and Scott, G. 2008. Anti-mycobacterial activity of five plant species used as traditional medicines in the Western Cape Province (South Africa). *Journal of Ethnopharmacology* 117.2: 385-390.

Bello, I.A., Ndukwe, G.I., Audu, O.T and Habila, J.D. 2011. A bioactive flavonoid from *Pavetta crassipes* K.Schum. *Organic and Medicinal Chemistry Letters* 1.14, doi: 10.1186/2191-2858-1-14.

Bishai, W.R. 2000. Rekindling old controversy on elusive lair of latent tuberculosis. *Lancet* 356: 2113-2114.

Bloom, B.R. and Murray, C.J.L. 1992. Tuberculosis: commentary on a reemergent killer. *Science* 257: 1055-1064.

Bremekamp, C.E.B. 1939. A monograph of the genus Pavetta L: Additions and Emendations. *Repertorium novarum specierum regni vegetabilis* 47: 12-28.

Bridson, D.M. 2003. Pavetta. *Flora Zambesiaca*. G.V. Pope. Royal Botanic Gardens, Kew. vol. 5.3, 543-598.

Burkill, H.M. 1997. *The useful plants of West Tropical Africa*. Royal Botanic Gardens, Kew. vol 4, 588-589.

Caldwell, C.G., Franzblau, S.G., Suarez, E. and Timmermann, B.N. 2000. Oleanane triterpenes from *Junellia tridens*. *Journal of Natural Products* 63.12: 1611-1614.

Cantrell, C.L., Franzblau, S.G. and Fischer N.H. 2001. Antimycobacterial plant terpenoids. *Planta Medica* 67.8: 685-694.

Cantrell, C.L., Rajab, M.S., Franzblau, S.G., Fronczek, F.R. and Fischer, N.H. 1999. Antimycobacterial ergosterol-5,8-endoperoxide from *Ajuga remota*. *Planta Medica* 65.8: 732-734.

Case, R.J., Wang, Y., Franzblau, S.G., Soejarto, D.D., Matainaho, L., Piskaut, P. and Pauli, G.F. 2007. Advanced applications of counter-current chromatography in the isolation of antituberculosis constituents from *Dracaena angustifolia*. *Journal of Chromatography A* 1151: 169-174.

Center for Disease Control. 2006. *Emergence of Mycobacterium tuberculosis with extensive resistance to second-line drugs worldwide, 2000-2004*. 55.11: 301-305. Retrieved Nov, 2006 from http://www.cdc.gov/mmwr/preview/mmwrhtml/mm5511a2.htm.

Chen, F.C., Peng, C.F., Tsai, I.L. and Chen, I.S. 2005. Antitubercular constituents from the stem wood of *Cinnamomum kotoense*. *Journal of Natural Products* 68: 1318-1323.

Chen, J., Lin, W., Shieh, P., Chen, I., Peng, C. and Sung, P. 2010. A new long chain alkene and antituberculosis constituents from the leaves of *Pourthiaea lucida*. *Chemistry & Biodiversity* 7: 717-721.

Chhabria, M., Jani, M. and Patel, S. 2009. New frontiers in the therapy of tuberculosis: fighting with the global menance. *Mini-Reviews in Medicinal Chemistry* 9: 401-430.

Chokchaisiri, R., Suaisom, C., Sriphota, S., Chindaduang, A., Chuprajob, T. and Suksamrarn, A. 2009. Bioactive flavonoids of the flowers of *Butea monosperma*. *Chemical and Pharmaceutical Bulletin* 57.4: 428-432.

Clarkson, C., Madikane, E.V., Hansen, S.H., Smith, P.J. and Jaroszewski, J.W. 2007. HPLC-SPE-NMR characterization of sequisterpenes in an antimycobacterial fraction from *Warburgia salutaris*. *Planta Medica* 73: 578-584.

Clayden, J., Greeves, N., Warren, S. and Wothers, P. 2001. *Organic Chemistry*. New York: Oxford University Press.

Coban, A.Y., Birinci, A., Ekinci, B. and Durupinar, B. 2004. Drug susceptibility testing of *Mycobacterium tuberculosis* by the broth microdilution method with 7H9 broth. *Memorias do Instituto Oswaldo Cruz* 99.1: 111-113.

Cogne, A.L., Queiroz, E.F., Wolfender, J-L., Marston, A., Mavi, S. and Hostettmann, K. 2003. On-line identification of unstable catalpol derivatives from *Jamesbrittenia fodina* by LC-MS and LC-NMR. *Phytochemical Analysis* 14.2: 67-73.

Collins, L.A., Terreto, M.N. and Franzblau, S.G. 1998. Green fluorescent protein reporter microplate assay for high-throughput screening of compounds against *Mycobacterium tuberculosis*. *Antimicrobial Agents and Chemotherapy* 42: 344-347.

Connolly, J.D. and Hill, R.A. 2007. Triterpenoids. *Natural Product Reports* 24: 465-486.

Copp, B.R. 2003. Antimycobacterial natural products. *Natural Product Reports* 20: 535–557.

Copp, B.R. and Norrie Pearce, A. 2007. Natural product growth inhibitors of *Mycobacterium tuberculosis*. *Natural Product Reports* 24: 278–297.

Corbett, E.L., Marston, B., Churchyard, G.J. and De Cock, K.M. 2006. Tuberculosis in sub-Saharan Africa: opportunities, challenges, and change in the era of antiretroviral treatment. *Lancet* 367: 926-937.

Coy, E.D., Cuca, L.E. and Sefkow, M. 2009. Macrophyllin-Type Bicyclo[3,2,1] octanoid neolignans from the leaves of *Pleurothyrium cinerium*. *Journal of Natural Products* 72: 1245-1248.

Cragg, G.M. and Newman, D.J. 2005. Biodiversity; continuing sources of novel drug leads. *Pure and Applied Chemistry* 77: 7-24.

Cragg, G.M., Newman, D.J. and Snader, K.M. 1997. Natural products in drug discovery and development. *Journal of Natural Products* 60: 52-60.

Daniel, T.M., Bates, J.H. and Downes, K.A. 1994. History of Tuberculosis. *Tuberculosis: Pathogenesis, Protection and Control*. B.R. Bloom. Ed. Washington D.C: American Society for Microbiology. 13-24.

Davies, P.D.O. 1999. *Multi-drug resistant tuberculosis*. Retrieved February, 2009 from http://www.priory.com/cmol/TBMultid.htm.

De Cock, K.M. and Chaisson, R.E. 1999. Will DOTS do it? A reappraisal of tuberculosis control in countries with high rates of HIV infection. *International Journal of Tuberculosis and Lung Disease* 3: 457-465.

Demirezer, L.O., Gurbuz, F., Guvenalp, Z., Stroch, K. and Zeeck, A. 2006. Iridoids, flavonoids and monoterpene glycosides from *Galium verum* subsp. verum. *Turkish Journal of Chemistry* 30: 525-534.

Deng, S., Wang, Y., Inui, T., Chen, S.N., Farnsworth, N.R., Cho, S., Franzblau, S.G. and Pauli, G.F. 2008. Anti-TB polyynes from the roots of *Angelica sinensis*. *Phytotherapy Research* 22.7: 878-882.

Dewick, P.M., 2009. *Medicinal natural products: A biosynthetic approach*. 3rd ed. United Kingdom: Wiley.

Dinda, B., Debnath, S. and Harigaya, Y. 2007. Naturally occurring iridoids. A review, Part 1. *Chemical and Pharmaceutical Bulletin* 55.2: 159-222.

Ducati, R.G., Ruffino-Netto, A., Basso, L.A. and Santos, D.S. 2006. The resumption of consumption - A review on tuberculosis. *Memorias do Instituto Oswaldo Cruz* 101.7: 697- 714.

Dye, C. 2006. Global epidemiology of tuberculosis. *Lancet* 367: 938-940.

Dye, C., Scheele, S., Dolin, P., Pathania, V. and Raviglione, M.C. 1999. Global burden of tuberculosis: estimated incidence, prevalence, and mortality by country. *Journal of the American Medical Association* 282: 677–686.

Dye, C., Watt, C.J., Bleed, D.M., Hosseini, S.M. and Raviglione, M.C. 2005. Evolution of tuberculosis control and prospects for reducing tuberculosis incidence, prevalence, and deaths globally. *Journal of the American Medical Association* 293.22: 2767-2775.

El Sayed, K.A., Hamann, M.T., Abd El-Rahman, H.A. and Zaghloul, A.M. 1996. New pyrrole alkaloids from *Solanum sodomaeum*. *Journal of Natural Products* 61.6: 848-850.

ElSohly, H.N., Danner, S., Li, X.C., Nimrod, A.C. and Clark, A.M. 1999. New antimycobacterial saponin from *Colubrina retusa*. *Journal of Natural Products* 62.9: 1341-1342.

Fabricant, D.S. and Farnsworth, N.R. 2001. The value of plants used in traditional medicine for drug discovery. *Environmental Health Perspectives* 109: 69-75.

Farnsworth, N.R. 1995. An old source for new drugs. *Pharmaceutical Technology* Aug: 14-15.

Farnsworth, N.R., Akerele, O., Bingel, A.S., Soejarto, D.D. and Guo, Z. 1985. Medicinal plants in therapy. *Bulletin of the World Health Organisation*. 63.6: 965-981.

Ferrari, J., Terreaux, C., Wolfender, J-L. and Hostettmann, K. 2000. Stop flow time-slice LC-NMR and LC-MS^n of *Gnidia involucrata*: a rational approach for a rapid chemical screening. *Chimia* 54: 406.

Forget, E.J. and Menzies, D. 2006. Adverse reactions to first-line antituberculosis drugs. *Expert Opinion on Drug Safety* 5.2: 231-249.

Friis-Møller, A., Chen, M., Fuursted, K., Christensen, S.B. and Kharazmi, A. 2002. *In vitro* antimycobacterial and antilegionella activity of licochalcone A from Chinese licorice roots. *Planta Medica* 68: 416-419.

Fu, S., Arráez-Roman, D., Segura-Carretero, A., Menéndez, J.A., Menéndez-Gutierrez, M.P., Micol, V. and Fernández-Gutierréz, A. 2010. Qualitative screening of phenolic compounds in olive leaf extracts by hyphenated liquid chromatography and preliminary evaluation of cytotoxic activity against human breast cancer cells. *Analytical and Bioanalytical Chemistry* 397: 643-654.

Gautam, R., Saklani, A. and Jachak, S.M. 2007. Indian medicinal plants as a source of antimycobacterial agents. *Journal of Ethnopharmacology* 110.2: 200-234.

Geismann T.A. and Crout D.H.T. 1969. *Background and Character of Natural Products Chemistry*. California: Freeman, Cooper R Company.

Gentry, E.J., Jampani, H.B., Keshavarz-Shokri, A., Morton, M.D., van der Velde, D., Telikepalli, H., Mitscher, L.A., Shawar, R., Humble, D. and Baker, W. 1998. Antitubercular natural products: berberine from the roots of commercial *Hydrastis canadensis* powder. Isolation of inactive 8-oxotetrahydrothalifendine, canadine, beta-hydrastine, and two new quinic acid esters, hycandinic acid esters-1 and -2. *Journal of Natural Products* 61: 1187-1193.

Gordien, A.Y., Gray, A.I., Franzblau, S.G. and Seidel, V. 2009. Antimycobacterial terpenoids from *Juniperus communis* L. (Cuppressaceae). *Journal of Ethnopharmacology* 126: 500-505.

Graham, J.G., Zhang, H., Pendland, S.L., Santarsiero, B.D., Mesecar, A.D., Cabieses, F. and Farnsworth, N.R. 2004. Antimycobacterial naphthopyrones from *Senna obliqua*. *Journal of Natural Products* 67: 225-227.

Gu, J.Q., Wang, Y., Franzblau, S.G., Montenegro, G., Yang, D. and Timmermann, B.N. 2004. Antitubercular constituents of *Valeriana laxiflora*. *Planta Medica* 70: 509-514.

Guardia, T., Rotelli, A.E., Juarez, A.O and Pelzer, L.E. 2001. Anti-inflamatory properties of plant flavonoids. Effects of rutin, quercetin and heperidin on adjuvant arthritis in rats. *II Farmaco* 56.9: 683-687

Gutierrez-Lugo, M., Wang, Y., Franzblau, S.G., Suarez, E. and Timmermann, B.N. 2005. Antitubercular sterols from *Thalia multiflora* Horkel ex Koernicke. *Phytotherapy Research* 19: 876-880.

Guvenalp, Z and Demirezer, L.O. 2005. Flavonol glycosides from *Asperula arvensis* L. *Turkish Journal of Chemistry* 29: 163-169.

Guvenalp, Z., Kilic, N., Kazaz, C., Kaya, Y. and Demirezer, L.O. 2006. Chemical constituents of *Galium tortumense. Turkish Journal of Chemistry* 30: 515-523.

Hagiwara, S., Takahashi, M., Shen, Y., Kaihou, S., Tomiyama, T., Yazawa, M., Tamai, Y., Sin, Y., Kazusaka, A. and Terazawa, M. 2005. A phytochemical in the edible Tamogi-take mushroom (*Pleurotus cornucopiae*), D-Mannitol, inhibits ACE activity and lowers the blood pressure of spontaneously hypertensive rats. *Bioscience Biotechnology and Biochemistry* 69.8: 1603-1605.

Hay, L., Schultz, R.A. and Schutte, P.J. 2008. Cardiotoxic effects of pavetamine extracted from *Pavetta harborii* in the rat. *Onderstepoort Journal of Veterinary Research* 75.3: 249-253.

Heifets, L. 1997. Mycobacteriology laboratory. *Clinics in Chest Medicine* 18.1: 35-53.

Hernández-Pando, R., Jeyanathan, M., Mengistu, G., Aguilar, D., Orozco, H., Harboe, M., Rook, G.A.W. and Bjune, G. 2000. Persistence of DNA from *Mycobacterium tuberculosis* in superficially normal lung tissue during latent infection. *Lancet* 356: 2133–2137.

Hiserodt, R.D., Franzblau, S.G. and Rosen, R.T. 1998. Isolation of 6-, 8-, and 10-gingerol from ginger rhizome by HPLC and preliminary evaluation of inhibition of *Mycobacterium avium* and *Mycobacterium tuberculosis*. *Journal of Agricultural and Food Chemistry* 46.7: 2504-2508.

Hostettmann, K., Wolfender, J.-L. and Rodriguez, S. 1997. Rapid detection and subsequent isolation of bioactive constituents of crude plant extracts. *Planta Medica* 63: 2-10.

Hu, J.F., Garo, E, Yoo, H.D., Cremin, P.A., Zeng, L. and Goering, M.G. 2005. Application of capillary-scale NMR for the structure determination of phytochemicals. *Phytochemical Analysis* 16: 127–133.

Inui, T., Wang, Y., Deng, S., Smith, D.C., Franzblau, S.G. and Pauli, G.F. 2007. Counter-current chromatography based analysis of synergy in an antituberculosis ethnobotanical. *Journal of Chromatography A* 1151: 211-215.

Itoh, A., Fujii, K., Tomatsu, S., Takao, C., Tanahashi, T., Nagakura, N. and Chen, C. 2003. Six secoridoid glucosides from *Adina racemosa*. *Journal of Natural Products* 66, 1212-1216.

Jiménez-Arellanes, A., Meckes, M., Torres, J. and Luna-Herrera, J. 2007. Antimycobacterial triterpenoids from *Lantana hispida* (Verbenaceae). *Journal of Ethnopharmacology* 111: 202-205.

Kessler M., Ubeaud, G and Jing, L. 2003. Anti- and pro-oxidant activity of rutin and quercetin derivatives. *Journal of Pharmacy and Pharmacology* 55.1: 131-142.

Kobaisy, M., Abramowski, Z., Lermer, L., Saxena, G., Hancock, R.E., Towers, G.H., Doxsee, D. and Stokes, R.W. 1997. Antimycobacterial polyynes of Devil's Club (*Oplopanax horridus*), a North American native medicinal plant. *Journal of Natural Products* 60.11: 1210-1213.

Koyama, S., Yamaguchi, Y., Tanaka, S. and Motoyoshiya, J. 1997. A new substance (Yoshixol) with an interesting antibiotic mechanism from wood oil of Japanese traditional tree (Kiso-Hinoki), *Chamaecyparis obtusa*. *General Pharmacology* 28.5: 797-804.

Lall, N. and Meyer, J.J.M. 1999. *In vitro* inhibition of drug-resistant and drug-sensitive strains of *Mycobacterium tuberculosis* by ethnobotanically selected South African plants. *Journal of Ethnopharmacology* 66: 347–354.

Lallemand, J.Y. and Duteil, M. 1977. ^{13}C NMR spectra of quercetin and rutin. *Organic Magnetic Resonance* 9.3: 179-180.

Lambert, M., Wolfender, J.-L., Stærk, D., Christensen, S. B., Hostettmann, K. and Jaroszewski, J.W. 2007. Identification of natural products using HPLC-SPE combined with CapNMR. *Analytical Chemistry* 79: 727- 735.

Lee, E.J., Kim, J.S., Kim, H.P., Lee, J-H. and Kang, S.S. 2010. Phenolic constituents from the flower buds of *Lonicera japonica* and their 5-lipoxygenase inhibitory activities. *Food Chemistry* 120: 134-139.

Lee, S., Kim, K.S., Shim, S.H, Park, Y.M. and Kim, B-K. 2003. Constituents from the non-polar fraction of *Artemisia apiacea*. *Archives of Pharmacal Research* 26.11: 902-905.

Lekphrom, R., Kanokmedhakul, S. and Kanokmedhakul, K. 2009. Bioactive styryllactones and alkaloids from flowers of *Goniothalamus laoticus*. *Journal of Ethnopharmacology* 125: 47-50.

León-Rivera, I., Mirón-López, G., Molina-Salinas, G.M., Herrera-Ruiz, M., Estrada-Soto, S., Gutiérrez, M., Alonso-Cortez, D., Navarrete-Vázquez, G., Ríos, M.Y. and Said-Fernández, S. 2008. Tyrianthinic acids from *Ipomoea tyrianthina* and their antimycobacterial activity, cytotoxicity, and effects on the central nervous system. *Journal of Natural Products* 71: 1686-1691.

Limmatvapirat, C., Sirisopanaporn, S. and Kittakoop, P. 2004. Antitubercular and antiplasmodial constituents of *Abrus precatorius*. *Planta Medica* 70: 276-278.

Lin, Y-L., Lu, C-K., Huang, Y-J. and Chen, H-J. 2011. Antioxidative caffeoylquinic acids and flavonoids from *Hamerocallis fulva* flowers. *Journal of Agricultural and Food Chemistry* 59: 8789-8796.

Ling, S-K., Komorita, A., Tanaka, T., Fujioka, T., Mihashi, K. and Kouno, I. 2002. Iridoids and anthroquinones from the Malaysian medicinal plant, *Saprosma scortechinii* (Rubiaceae). *Chemical and Pharmaceutical Bulletin* 50.8: 1035-1040.

Lu, T., Cantrell, C.L., Robbs, S.L., Franzblau, S.G. and Fischer, N.H. 1998. Antimycobacterial matricaria esters and lactones from *Astereae* species. *Planta Medica* 64: 665-667.

Ma, C., Case, R.J., Wang, Y., Zhang, H.J., Tan, G.T., Hung, N.V., Cuong, N.M., Franzblau S.G., Soejarto, D.D., Fong, H.H. and Pauli, G.F. 2005. Antituberculosis constituents from the stem bark of *Micromelum hirsutum*. *Planta Medica* 71: 261-267.

Machado, D.G., Beltio, L.E.B., Cunha, M.P, Santos, A.R.S, Pizzolalti, M.G., Brighente, I.M.C and Rodrigues, A-L.S. (2008). Antidepressant-like effect of rutin isolated from the ethanolic extract from *Schinus molle* L. in mice: evidence for the involvement of the serotonergic and noradrenergic systems. *European Journal of Pharmacology* 587.1-3: 163-168.

Mandal, S.C., Lakshmi, S.M., Ashok Kumar, C.K., Sur, T.K. and Boominathan, R. 2003. Evaluation of anti-inflammatory potential of *Pavetta indica* Linn. leaf extract (Family: Rubiaceae) in rats. *Phytotherapy Research* 17: 817- 820.

Mann, A., Amupitan, J.O., Oyewale, A.O., Okogun, J.I., Ibrahim, K., Oladosu, P., Lawson, L., Olajide, I. and Nnamdi, A. 2008. Evaluation of *in vitro* antimycobacterial activity of Nigerian plants used for treatment of respiratory diseases. *African Journal of Biotechnology* 7.11: 1630-1636.

Mata, R., Morales I., P´erez, O., Rivero-Cruz, I., Acevedo, L., Enriquez-Mendoza, I., Bye, R., Franzblau, S. and Timmermann, B. 2004. Antimycobacterial compounds from *Piper sanctum*. *Journal of Natural Products* 67: 1961-1968.

Mcgaw, L.J., Lall, N., Hlokwe, T.M., Michel, A.L., Meyer, J.J.M. and Eloff, J.N. 2008b. Purified compounds and extracts from Euclea species with antimycobacterial activity against *Mycobacterium bovis* and fast growing mycobacteria. *Biological and Pharmaceutical Bulletin* 31.7: 1429- 1433.

Mcgaw, L.J., Lall, N., Meyer, J.J.M. and Eloff, J.N. 2008a. The potential of South African plants against *Mycobacterium* infections. *Journal of Ethnopharmacology* 119: 482-500.

Microsoft Encarta Encyclopedia, 2006. *Nigeria*. Retrieved November, 2006 from http://encarta.msn.com/encnet/refpages/RefArticle.aspx?refid=761557915

Mitscher, L. A. and Baker, W.R. 1998a. Tuberculosis: a search for novel therapy starting with natural products. *Medicinal Research Reviews* 18.6: 363-374.

Mitscher, L. A. and Baker, W.R. 1998b. A search for novel chemotherapy against tuberculosis amongst natural products. *Pure and Applied Chemistry* 70.2: 365-371.

Moco, S., Bino, R.J., Vorst, O., Verhoeven, H.A., de Groot, J., van Beek T.A., Vervoort, J. and de Vos, C.H. 2006. A liquid chromatography-mass spectrometry-based metabolome database for tomato. *Plant Physiology* 141. 4: 1205-1218.

Murillo, J.I., Encarnación-Dimayuga, R., Malmstrøm, J., Christophersen, C. and Franzblau, S.G. 2003. Antimycobacterial flavones from *Haplopappus sonorensis*. *Fitoterapia* 74: 226-230.

Murray, J.F. 2004. A Century of Tuberculosis. *American Journal of Respiratory and Critical Care Medicine* 169: 1181-1186.

Namdaung, U., Aroonrerk, N., Suksamrarn, S., Danwisetkanjana, K., Saenboonrueng, J., Arjchomphu, W. and Suksamran, A. 2006. Bioactive constituents of the root bark of *Artocarpus rigidus* subsp. *rigidus*. *Chemical and Pharmaceutical Bulletin* 54.10: 1433-1436.

Newman, D.J., Cragg, G.M. and Snader, K.M. 2003. Natural products as sources of new drugs over the period 1981- 2002. *Journal of Natural Products* 66: 1022- 1037.

Newton S.M., Lau C and Wright C.W. 2000. A review of antimycobacterial natural products. *Phytotherapy Research* 14: 303–322.

O'Neill, M.J. and Lewis, J.A. 1993. The renaissance of plant research in the pharmaceutical industry. *Human Medicinal Agents from Plants*. A.D. Kinghorn and M.F. Balandrin Eds. ACS symposium series 534. Washington D.C: American Chemical Society. 48-55.

Okunade, L., Elvin-Lewis, M.P. and Lewis, W.H. 2004. Natural antimycobacterial metabolites: current status. *Phytochemistry* 65: 1017– 1032.

Okunade, L., Hufford, C.D., Richardson, M.D., Peterson, J.R. and Clark, A.M. 1994. Antimicrobial properties of alkaloids from *Xanthorhiza simplicissima*. *Journal of Pharmaceutical Sciences* 83: 404-406.

Ovesna, Z., Vachalkova, A., Horvathova, K. and Tothova, D. 2004. Pentacyclic triterpenoid acids: new chemoprotective compounds. Minireview. *Neoplasma* 51: 327-333.

Pattamadilok, D. and Suttisri, R. 2008. Seco-terpenoids and other constituents from *Elateriospermum tapos*. *Journal of Natural Products* 71: 292-294.

Pauli, G.F., Case, R.J., Inui, T., Wang, Y., Cho, S., Fischer, N.H. and Franzblau, S.G. 2005. New perspectives on natural products in TB drug research. *Life Sciences* 78: 485 – 494.

Peloquin, C. and Ebert, S. 1999. Tuberculosis. *Pharmacotherapy: A Pathophysiologic Approach*. Fourth ed. J. Dipiro. Ed. New York: McGraw-Hill. 1717-1736.

Politi, M., Sanogo, R., Ndjoko, K., Guilet, D., Wolfender, J.-L., Hostettmann, K. and Morelli, I. 2004. HPLC-UV/PAD and HPLC-MS^n analyses of leaf and root extracts of *Vismia guineensis* and isolation and identification of two new bianthrones. *Phytochemical Analysis* 15: 355- 364.

Queiroz, E.F., Wolfender, J.-L. and Hostettmann, K. 2009. Modern approaches in the search for new lead antiparasitic compounds from higher plants. *Current Drug Targets* 10: 202-211.

Rajab, M.S., Cantrell, C.L., Franzblau, S.G. and Fischer, N.H. 1998. Antimycobacterial activity of (E)-phytol and derivatives: a preliminary structure-activity study. *Planta Medica* 64: 2-4.

Rangkaew, N., Suttisri, R., Moriyasu, M. and Kawanishi, K. 2009. A new acyclic diterpene acid and bioactive compounds from *Knema glauca*. *Archives of Pharmacal Research* 32.5: 685-692.

Rivero-Cruz, I., Acevedo, L., Guerrero, J.A., Mart´ınez, S., Bye, R., Pereda-Miranda, R., Franzblau, S., Timmermann, B.N. and Mata, R. 2005. Antimycobacterial agents from selected Mexican medicinal plants. *Journal of Pharmacy and Pharmacology* 57: 1117-1126.

Rodriguez, S., Wolfender, J-C., Hakizamungu, E. and Hostettman, K. 1995. An antifungal naphtoquinone, xanthones and secoiridoids from *Swertia calycina*. *Planta Medica* 61: 362- 364.

Rohdich, F., Hecht, S., Bacher, A. and Eisenreich, W. 2003. Deoxyxylulose phosphate pathway of isoprenoid biosynthesis. Discovery and functions of *ispDEFGH* genes and their cognate enzymes. *Pure and Applied Chemistry* 75: 393-405.

Rugutt, J.K., Henry III, C.W., Franzblau, S.G. and Warner, I.M. 1999. NMR and molecular mechanics study of pyrethrins I and II**.** *Journal of Agricultural and Food Chemistry* 47: 3402-3410.

Saludes, J.P., Garson, M.J., Franzblau, S.G. and Aguinaldo, A.M. 2002. Antitubercular constituents from the hexane fraction of *Morinda citrifolia* Linn. (Rubiaceae). *Phytotherapy Research* 16: 683-685.

Sang, S., Cheng, X., Zhu, N., Stark, R.E., Badmaev, V., Ghai, G., Rosen, R.T. and Ho, C-T. 2001. Flavonol glycosides and novel iridoid glycoside from the leaves of Morinda citrifolia. *Journal of Agricultural and Food Chemistry* 49: 4478-4481.

Sanon, S., Ollivier, E., Azas, N., Mahiou, V., Gasquet, M., Ouattara, C.T., Nebie, I., Traore, A.S., Esposito, F., Balansard, G., Timon-David, P. and Fumoux, F. 2003. Ethnobotanical survey and *in vitro* antiplasmodial activity of plants used in traditional medicine in Burkina Faso. *Journal of Ethnopharmacology* 86: 143-147.

Schaller, F., Wolfender, J.L., Hostettmen, K. and Mavi, S. 2001. New antifungal "quinine methide" diterpenes from *Bobgunnia madagascariensis* and study of their interconversion by LC/NMR. *Helvetica Chimica Acta* 84: 222-229.

Seebacher, W., Simic, N., Weis, R., Saf, R. and Kunert, O. 2003. Complete assignments of ^{1}H and ^{13}C NMR resonances of oleanolic acid, 18α-oleanolic acid, ursolic acid and their 11-oxo derivatives. *Magnetic Resonance in Chemistry* 41: 636-638.

Song, S., Li, Y., Feng, Z., Jiang, J. and Zhang, P. 2010. Hepatoprotective constituents from the roots and stems of *Ericybe hainanesis*. *Journal of Natural Products* 73: 177-184.

Sunthitikawinsakul, A., Kongkathip, N., Kongkathip, B., Phonnakhu, S., Daly, J.W., Spande, T.F., Nimit, Y. and Rochanaruangrai, S. 2003. Coumarins and carbazoles from *Clausena*

excavata exhibited antimycobacterial and antifungal activities. *Planta Medica* 69. 2: 155-157.

Sutthivaiyakit, S., Thongnak, O., Lhinhatrakool, T., Yodchun, O., Srimark, R., Dowtaisong, P. and Chuankamnerdkarn, M. 2009. Cytotoxic and antimycobacterial prenylated flavonoids from the roots of *Eriosema chinens*e. *Journal of Natural Products* 72: 1092-1096.

Tabanca, N., Bedir, E., Ferreira, D., Slade, D., Wedge, D.E., Jacob, M.R., Khan, S.I., Kirimer, N., Baser, K.H.C. and Khan, I.A. 2005. Bioactive constituents from Turkish *Pimpinella* species. *Chemistry and Biodiversity* 2: 221-232.

Tasdemir, D., Brun, R., Franzblau, S.G., Sezgin, Y. and Çalis, I. 2008. Evaluation of antiprotozoal and antimycobacterial activities of the resin glycosides and the other metabolites of *Scrophularia cryptophila*. *Phytomedicine* 15: 209-215.

Taskova, R.M., Gotfredsen, C.H. and Jensen, S.R. 2005. Chemotaxonomic markers in Digitalideae (Plantaginaceae). *Phytochemistry* 66: 1440-1447.

Tripathi, R.P., Tewari, N., Dwivedi, N. and Tiwari, V.K. 2005. Fighting tuberculosis: an old disease with new challenges. *Medicinal Research Reviews* 25: 93–131.

Ulubelen, A., Topcu, G. and Johansson, C.B. 1997. Norditerpenoids and diterpenoids from *Salvia multicaulis* with antituberculous activity. *Journal of Natural Products* 60: 1275-1280.

Van Wyk, P. 1974. *Trees of the Kruger National Park*. Purnell, Cape Town, vol. 2, 584.

Vongvanich, N., Kittakoop, P., Charoenchai, P., Intamas, S., Danwisetkanjana, K. and Thebtaranonth, Y. 2005. Combretastatins D-3 and D-4, new macrocyclic lactones from *Getonia floribunda*. *Planta Medica* 71: 191-193.

Wächter, G.A., Valcic, S., Flagg, M.L., Franzblau, S.G., Montenegro, G., Suarez, E. and Timmermann, B.N. 1999. Antitubercular activity of pentacyclic triterpenoids from plants of Argentina and Chile. *Phytomedicine* 6.5: 341-345.

Waffo, K., Azebaze, G.A., Nkengfack, A.E., Fomum, Z.T., Meyer, M., Bodo, B. and van Heerden, F.R. 2000. Indicanines B and C, two isoflavonoid derivatives from the root bark of *Erythrina indica*. *Phytochemistry* 53: 981-985.

Wambugu, S.N., Mathiu, P.M., Gakuya, D.W., Kanui, T.I., Kabasa, J.D. and Kiama, S.G. 2011. Medicinal plants used in the management of chronic joint pains in Machakos and Makueni counties, Kenya. *Journal of Ethnopharmacology* 137.2: 945-955.

Wang, J., Dai, H., Wei, Y., Zhu, H., Yan, Y., Wang, Y., Long, C., Zhong, H., Zhang, L. and Cheng, Y. 2010. Antituberculosis agents and an inhibitor of the para-aminobenzoic acid biosynthetic pathway from *Hydnocarpus anthelminthica* seeds. *Chemistry and Biodiversity* 7: 2046-2052.

Weigenand, O., Hussein, A.A., Lall, N. and Meyer, J.J.M. 2004. Antibacterial activity of naphthoquinones and triterpenoids from *Euclea natalensis* root bark. *Journal of Natural Products* 67: 1936-1938.

Woldemichael, G.M., Gutierrez-Lugo, M.T., Franzblau, S.G., Wang, Y., Suarez, E. and Timmermann, B.N. 2004. *Mycobacterium tuberculosis* growth inhibition by constituents of *Sapium haematospermum*. *Journal of Natural Products* 67.4: 598-603.

Wolfender, J.-L. 2009. HPLC in natural product analysis: The detection issue. *Planta Medica* 75: 719-734.

Wolfender, J.-L., Ndjoko, K. and Hostettmann, K. 2003. Liquid chromatography with ultraviolet absorbance-mass spectrometric detection and with nuclear magnetic resonance spectroscopy: a powerful combination for the on-line structural investigation of plant metabolites. *Journal of Chromatography A* 1000: 437- 455.

Wolfender, J.-L., Ndjoko, K. and Hostettmann, K. 2001. The potential of LC-NMR in phytochemical analysis. *Phytochemical Analysis* 12: 2-22.

Wolfender, J.-L., Queiroz, E.F. and Hostettmann, K. 2005. Phytochemistry in the microgram domain – a LC-NMR perspective. *Magnetic Resonance in Chemistry* 43: 697-709.

World Health Organisation. 1996. *Tuberculosis: Directly observed treatment short course*. Retrieved November, 2006 from http://www.who.int/tb/dots/dotsplus/faq/en/index.html.

World Health Organisation. 2004. *TB/HIV: A clinical manual*. 2nd ed. Retrieved February, 2009 from http://whqlibdoc.who.int/publications/2004/9241546344.pdf.

World Health Organisation. 2006. *Tuberculosis*. Retrieved November 2006 from http://www.who.int/mediacentre/factsheets/fs104/en/print.html.

World Health Organisation. 2008. *Global tuberculosis control*. 129-132. Retrieved February 2009 from http://www.who.int/globalatlas/predefinedReports/TB/PDF_Files/nga.pdf.

Zgoda, J.R., Freyer, A.J., Killmer, L.B. and Porter, J.R. 2001. Polyacetylene carboxylic acids from *Mitrephora celebica*. *Journal of Natural Products* 64.10: 1348-1349.